UNIVERSITY OF BELGRADE

FACULTY OF MECHANICAL ENGINEERING

Mohammed Saleh Mohammed, M.Sc.

EXERGOECONOMIC ANALYSIS AND OPTIMIZATION OF COMBINED CYCLE POWER PLANTS WITH COMPLEX CONFIGURATION

Doctoral Dissertation

Belgrade, 2015

УНИВЕРЗИТЕТ У БЕОГРАДУ

МАШИНСКИ ФАКУЛТЕТ

Mohammed Saleh Mohammed, M.Sc.

Ексергоекономска анализа и оптимизација комбинованих постројења гасне и парне турбине комплексне конфигурације

Докторска дисертација

Београд, 2015

COMMITTEE

Prof. dr. Milan Petrović, University of Belgrade - Faculty of Mechanical Engineering, mentor

Prof. dr. Zoran Stefanović, University of Belgrade - Faculty of Mechanical Engineering

Prof. dr. Dragan Tucaković, University of Belgrade -Faculty of Mechanical Engineering

Prof. dr. Mirko Komatina, University of Belgrade, Faculty of Mechanical Engineering

ACKNOWLEDGEMENTS

I have been waiting this day since I started writing the paper. I would like to express my sincere thanks and gratitude to my supervisor, professor dr. Milan Petrović for his valuable and continuous advice, wholeheartedness, and assistance throughout the duration of this work.

I would also like to extend my sincere gratitude to Professor dr. Zoran Stefanović for his contributions and advices.

I would also like to take this opportunity to thank my mother, my brothers, and my sisters, who are all surely proud of me today.

Special thanks to the staff, students, and friends that I have met during my research work – especially those in the Mechanical Engineering Department.

Lastly but most importantly, I want to express my gratitude to my wife, my lovely daughters, and sons - each of whom gave me support, encouragement, love in my life, and made this thesis possible.

Above all, I am very much grateful to almighty Allah for giving me courage and good health for completing the venture.

Mohammed Saleh Mohammed

EXERGOECONOMIC ANALYSIS AND OPTIMIZATION OF COMBINED CYCLE POWER PLANTS WITH COMPLEX CONFIGURATION

Abstract

The objective of the presented research work is to develop an exergoeconomic optimization method in order to predict the cost effectiveness of a combined cycle gas turbine (CCGT) power plant and suggest ways of improving the cost effectiveness from both thermodynamic and economic points of view. The exergy analysis (second law analysis) is used for providing information about the losses qualitatively as well as quantitatively along with their locations. Exergetic (thermodynamic) optimization improves the performance of a system by reducing the exergetic inefficiencies (exergy destruction and exergy losses) and increasing exergetic efficiency. This improvement, however, is accompanied by an increase in capital investment of the system. Hence, a combined cycle power plant should be optimized from both thermodynamic and economic points of view.

The exergoeconomic analysis provides a complete diagnosis of the performance of the combined cycle power plant, both in exergetic and in monetary values. In the exergoeconomic analysis, the principle of exergy costing is used to assign monetary costs to all energy streams, as well as to assign the exergy destruction incurred within each component of a plant. All this important information can then be used for the system improvements and optimization.

In this regard, exergoeconomic optimization is a better tool as it combines the thermodynamic analysis with the economic principles. Here, appropriate costs are assigned to the thermodynamic inefficiencies of the system components, which add to the hidden cost. For maximum exergoeconomic efficiencies, these costs have to be minimized. Therefore, it is necessary to correlate the exergy with cost value. These can be carried out through exergoeconomic analysis.

The system considered in this thesis is a triple pressure combined cycle power plant. For this system, an energetic, economic, and exergoeconomic analyses are performed to predict thermodynamic, economic and thermoeconomic parameters of the system. This system is exergoeconomically optimized to reduce the specific total cost of

the products, which leads to a reduction in the investment cost, and to an increase in the power output and efficiency. In addition, two more optimization methods were developed: the first one (used as the reference) was based on a thermoeconomic analysis with production cost of electricity as an objective function, and the second was based on the exergetic and economic analysis with a total cost rate as an objective function. To test the effectiveness of the optimization methods, a fourth optimization method applying MIDACO software was used.

The optimal values of the most influential variables are obtained by minimizing the objective functions while satisfying a group of constraints. A selected procedure of the best optimum point is introduced and a final optimum design point is then determined. The design variables are high, intermediate, and low steam pressure in the pressure drums and three pressure levels of pinch point temperatures (PP), low intermediate, and high. The effects of design variables on the objective function and production cost are investigated in detail.

Three-comparison analyses were performed: the first one was between the initial case and the results of the previously mentioned optimization methods. The second was made between the optimization cases where the pinch points are assumed to be the same for all evaporators, and another one having different pinch points for every pressure level. The third comparison was made between the simple optimization methods and the optimization method using MIDACO software.

The optimization results demonstrate that all three optimization methods can improve the thermodynamic and economic performance, but with different values. Exergoeconomic optimization method is the most effective method for designing and operating a system with high efficiency and low investment cost.

Key words: combined cycle, heat recovery steam generator, exergy, thermodynamic optimization, exergoeconomic optimization.

Scientific field:
Technical science, Mechanical engineering, Thermal power engineering

Narrow scientific field:
Thermal power engineering

UDC number: 621.311.26:519.863(043.3)

Ексергоекономска анализа и оптимизација комбинованих постројења гасне и парне турбине комплексне конфигурације

Апстракт

Циљ рада је развој методе за ексергоекономску анализу у циљу предвиђања исплативости примене комбинованог гасно-парног циклуса у термоелектранамаи рад и унапређења постојећих решења са термодинамичког и економиског становишта. Ексергетска анализа термодинамичког циклуса (анализа по другом закону термодинамике) коришћена је због добијања информација о местима настајања губитака и њиховим квалитативним и квантитативним карактеристикама. Ексергетска (термодинамичка) оптимизација користи се за побољшање перформанси система смањењем ексергетске неефекасности (деструкције, односно, губитка ексергије у систему) и унапређњење искоришћења почетне енергије. Могућа побољшања су, међутим, праћена повећаним капиталним улагањима. Стога, комбиновано термоенергетско постројење са гасном и парном турбином треба да буде оптимизовано и са термодинамичког и са економског становишта.

Ексергоекономска анализа пружа комплетну дијагностику преформанси термоелектране са комбинованим циклусом у ексергетским и у новчаним вредностима. У ексергоекономској анализи користи се принцип цене ексергије како би се појединим токовима енергије доделила монетарна вредност и како би деструкција ексергије у појединим компонентама постројења била вреднована као новчани губитак. Овако добијене информације се потом могу користити за оптимизацију и унапређење система.

У том смислу, ексергоекономска оптимизација представља бољи алат јер комбинује термодинамичку анализу са економским принципима. У овом истраживању, одговарајући трошкови додељују термодинамичким неефикасностима компоненти система који доприносе скривеним трошковима. За достизање максималне ексергоекономске ефикасности ови трошкови морају бити сведени на минимум. Због тога је неопходно да се доведе у везу ексергија са трошковима. Ово се може постићи ексергоекономском анализом.

Систем разматран у овом раду је комбиновано термоенергетско постројење са гасном и парном турбином са комплексном топлотном шемом (на три нивоа притисака). За овај систем, енергетска, економска и ексергоекономска анализа се врше да би се предвидели термодинамички, економски и термоекономски параметри система. Овај систем се оптимизује ексергоекономски да би се смањила специфична укупна цена производене енергије, што опет води и ка смањењу инвестиционих трошкова, као и

повећању електричне снаге и економичности електране. Поред тога, развијене су још две методе оптимизације: прва (коришћена као референтна) је била заснована на термоекономској анализи са производном ценом електричне енергије као циљном функцијом, док је друга била заснована на ексергијској и економској анализи са укупним трошкима као циљном функцијом. Да би се тестирала ефикасност метода оптимизације, коришћена је четврта метода оптимизације применом MIDACO софтвера.

Оптималне вредности најутицајнијих променљивих су добијене минимизирањем циљних функција уз задовољење дефинисаних ограничења. Одабран је поступак тражења оптимума и онда су одређене оптималне пројектоване вредности појединих параметара. Променљиве које су предмет оптимизације су високи, средњи и ниски притисак свеже паре и вредности температурске разлике између продуката сагоревања на излазу из испаривача и температуре испаравања паре (pinch point PP) на сва три нивоа притиска. Утицаји вредности појединих пројектних променљивих на циљне функције и трошкове производње су детаљно истражени.

Три упоредне анализе су спроведене: прва је била поређење између резултата добијених за иницијалне вредности претходно поменутих параметара и резултата са пареметрима добијеним методом оптимизације. Друга анализа је проучавала разлику између случаја оптимизације где је претпостављено да су вредности pinch point PP исте за све испариваче и случаја где су дефинисане различите вредности pinch point PP за сваки ниво притиска. Треће поређење је направљено између резултата добијених применом једноставног модела оптимизације који је развио аутор и резуклтата оптимизације добијених применом комерцијалног оптимизационог софтвера.

Резултати оптимизације показују да све три методе оптимизације могу да побољшају термодинамичке и економске перформансе, али са различитим вредностима. Ексергоекономски метод оптимизације је најефикаснији за пројектовање термоенергетског постројења са високом степеном корисности и ниском инвестиционим трошковима.

Кључне речи: комбиновани циклус, котао утилизатор, ексергија, термодинамичка оптимизација, екергоекономска оптимизација

Научна област:

Техничке науке, Машинство, Термоенергетика

Ужа научна област:

Термоенергетика (Топлотне турбомашине и термоенергетска постројења)

УДК број: 621.311.26:519.863(043.3)

TABLE OF CONTENTS

LIST OF FIGURES

LIST OF TABLES

Nomenclature

A	Heat transfer area	m^2
C	Cost	$
C_a	Amortization cost	$/year
$CCPP$	Combined Cycle Power Plants	-
cfu	Price of fuel	$·kW/h
cp	Heat capacity at constant pressure	kJ/kg·K
$\dot{e}$	specific exergy	kJ/kg
$\dot{E}$	Exergy	kJ
$\dot{E}_D$	Exergy destruction	kJ
$\dot{E}_p$	exergy production	kJ
g	Gravity acceleration	kg·m/s^2
GT	Gas Turbine	-
h	Specific enthalpy	kJ/kg
H	Enthalpy	kJ
HI	Low heating value of the fuel	kJ/kg
HR	Heat rate	kJ/kg
$HRSG$	Heat Recovery Steam Generator	-
k	Specific heat ratio	-
LHV	Low heating value	kJ/kg
$\dot{m}$	Mass flow rate	kg/s
$_o$	Ambient	-
p	Pressure	bar
P_G	Power	[MW]
PP	Pinch point	K or ^{o}C
$\dot{Q}$	Heat transfer	kW
Q	Heat supplied or rejected	kJ
q	Specific heat supplied or rejected	kJ/kg
r_p	pressure ratio	-
S	Entropy	kJ/K
s	specific entropy	kJ/kg·K
S_{gen}	Entropy generation	kJ
ST	steam turbine	kW
T	temperature	K or ^{o}C
TIT	Inlet temperature of the gas turbine	K
v	specific volume	m^3/kg
V	velocity	m/s
$\dot{W}$	Work rate	kW

W	Work output	kJ
w	Specific work output	kJ/kg
z	Height	m

Greek Symbols

η	Efficiency	
γ	Density	Kg/m^3
β	Exergy factor	
ε	Simple exergy efficiency	
ε_{tr}	Efficiency with transiting exergy	
Ψ	Rational efficiency	

Subscripts

CCGT	Combined cycle gas turbine
CH	Chemical
CV	control volume
e	outlet
evap	Evaporation
F	Fuel
GT	Gas turbine
HP	High pressure
i	Inlet
IP	Intermediate pressure
LOSS	Losses
LP	Low pressure
net	Net
out	Outlet
PH	Physical
pr	Production
surr	Surrounding
sys	system
th	Thermal

Superscripts

ΔT	Temperature difference
ΔP	Pressure difference

1 Introduction

Optimization of energy conversion systems becomes more important due to limitations of fossil fuels and the environmental impact during their use. The usage of energy is found everywhere in a variety of applications from heating and cooling to nuclear power plants. For decades, the response to the ever-growing need for electric generation capacity was to build a new steam power plant, one not very different from the previous one.

The energy conversion engineer is faced with a variety of issues today: emerging technologies, changing social and technological climate in which a diversity of approaches is likely to be accepted.

Some important characteristics of new power initiatives are low capital and operating costs, ability to operate with a variety of fuels and with high tolerance to fuel variability, short construction time, low emission of pollutants, marketable or at least inert and easily disposable waste products, and high efficiency, maintainability, finance ability, and reliability.

Another key problem facing the energy conversion engineer is the finiteness of natural resources critically important for human beings (such as natural gas and oil) in the world and ever-increasing energy demands by developing countries.. Perhaps future power plants should utilize coal and nuclear energy to save the natural gas and petroleum for industrial feed stocks and other more critical future needs. On the other hand, serious problems exist with respect to utilization of natural resources. Much of the readily available coal has unacceptably high sulfur, which significantly degrades the environment when released from power plant stacks in untreated combustion products. The well-known problem of acid rain has been attributed to emissions from coal-burning power plants.

In addition, there are economic problems. As it becomes harder to exploit fossil fuels a deposit in the world, the price of energy is increasing, coupled with higher demand due to increased technology implementation and population. Moreover, replacement energies (renewable energies) are economically less efficient than fossil fuels.

Increasingly, the new alternative solutions may take the form of repowering the old plant to increase efficiency, reaching pollution standards, and minimizing the financial impact of meeting new power demands. The improvement of the efficiency of power plants that use conventional cycles is usually evolutionary in nature, by virtue of high temperature limitations and advances in materials. Hence, only gradual improvements in efficiency can be expected. On the other hand, significant improvements in efficiency can sometimes be obtained by combining conventional cycles in appropriate ways. Such power plants are referred to as combined-cycle plants. It is evident from the study of the Rankin and Brayton cycles, and in fact, all heat engines, that the rejection of large amounts of thermal energy to the surroundings accompanies the production of useful power. This heat rejection cannot be eliminated, but it can be reduced by improving the thermal efficiency of the cycle.

Due to the mentioned problems, it becomes increasingly important to understand the mechanisms that degrade energy and resources. Moreover, developing systematic approaches is important for improving the design of energy systems and reducing the impact on the environment; in this regard successive energy crises have stimulated the study of finding more efficient ways for the use of the available energy in fuels. This means that the optimization of power generation systems becomes one of the most important subjects in the energy-engineering field. Recent thermoeconomic analysis and optimization of thermal systems became the key solution in providing a better system in both optimal energy consumption and optimal system configuration.

Classical thermodynamics provides the concept of energy, energy transfer by heat and work, energy balance, entropy and entropy balance and calculations of thermodynamic properties at equilibrium. The second law of thermodynamics enhances an energy balance by calculating the true thermodynamic value of an energy carrier and real thermodynamic inefficiencies and losses from the process and system. Exergy is the maximum useful work attainable from an energy carrier under the given environmental conditions. The exergy of an energy carrier is a thermodynamic property that depends on both the state of the carrier being considered and the state of the environment. It expresses the maximum capability of the energy carrier to cause changes. Thus, exergy is closely related to the economic value of the carrier because users pay the potential of

energy to cause changes. When costs are assigned to energy carriers, exergy should serve as a basis in the costing process.

Conventionally, first law analysis gives only energy utilization scenario in terms of conservation of energy. However, it cannot provide the information regarding the losses both qualitatively and quantitatively, and cannot find the location of these losses. These limitations force us to perform exergy analysis based on second law of thermodynamics. Exergy is not a conserved property but some of it is destroyed in the real process. Exergy analysis gives a uniform base for comparison of various thermodynamic processes. This analysis proves the information regarding losses that include their location qualitatively and quantitatively. This information can be used for further improvement in the design and operation of the system. By locating the exergy destruction, the system performance can be improved by improving the exergetic efficiency of the component and the system.

The term "thermoeconomic" was formally used to indicate an appropriate combination of exergetic and economic analysis in which the cost was assigned to the exergy (not the energy) content of an energy carrier (exergy costing), in parallel. However, the term "thermoeconomic analysis" was used by others to report conventional thermodynamic analyses based only on the first law of thermodynamics and economic analyses, conducted separately from the thermodynamic ones and without the consideration of exergy or exergy costing. However, "thermos", is a derivative of the Greek word for heat and it is used in most major languages. Thus, thermoeconomic does not imply exergy costing or exergy economics, but a combination of heat and economics.

Along with the thermodynamic analysis, economic analysis gives the information regarding fixed cost e.g. investment cost, running cost, operating and maintenance cost. In most of the cases, the overall cost of the system will increase with the increase in the system exergetic efficiency and capacity. Thus, thermodynamic improvement in a system is accompanied by an increase in the economic cost. Therefore, the system should be optimized between these two conflicting requirements. In this regard, thermoeconomic analysis evolved and joined thermodynamic and economic parameters to one common platform and now combines thermodynamic

analysis with economic analysis. As discussed above, exergy analysis is preferred for thermodynamic analysis; the newly evolved field is called exergoeconomic analysis.

The exergoeconomic methods help in the system improvement using thermodynamic as well as economic points of view, by simultaneous modeling of thermodynamic and economic aspects of the system and its components. These methods are based on optimization techniques, which search for all possible solutions for the optimum design and operation of the system and its components. Just like the exergoeconomic analysis, exergoeconomic optimization combines thermodynamic and economic aspects. For thermodynamic optimization based on exergetic consideration, the exergy destruction method is identified as a methodology.

In exergoeconomic, a system and its components are thermodynamically based on exergy as well as economically analyzed to formulate an objective function, which would satisfy the thermodynamic and the economic objectives of the system simultaneously. The thermodynamic objective is to maximize the exergetic efficiencies of the components and the system, while the economic objective is to minimize the investment cost, operation, and maintenance cost of the system. Thus, the objective of thermoeconomic is to obtain the compromise between these two competing objectives. In this methodology, appropriate costs are assigned to the thermodynamic inefficiencies of the system components through some meaningful fuel-product definition. For maximum exergetic efficiencies, these costs need to be minimized.

1.1 The Aim of the Thesis

The scope and purpose of this research is to develop effective methodology to achieve thermoeconomic optimizations of CCGT power plants. Therefore, the aim of the work is to improve the thermoeconomic performance of the power plant by means of proposing an exergoeconomic optimization method. With the help of this method, it would be possible to:

a) Predict the cost effectiveness of a combined cycle gas turbine (CCGT) power plant.
b) Provide information about the exergy destruction and exergy losses along with their location.
c) Predict the highest exergy destructor components of the system.

d) Suggest ways of improving the cost effectiveness from both thermodynamic and economic points of view.

e) Find the optimal realistic values of operating parameters, which gives the maximum possible power output, efficiency, and annual cash flow. Additionally, is would be possible to calculate minimum possible exergy destructions, cost per unit of generated electricity, and purchase investment cost.

1.2 Outline of the Thesis

The thesis is divided into seven chapters. In this chapter, the general concept of exergoeconomic optimization is introduced. The importance of the optimization and the objective of the study are briefly discussed.

Chapter 2 presents an extensive review of literature covering topics related to this study, about exergy analysis and optimization and exergoeconomic analysis and optimization.

Chapter 3 is an overview of combined cycle gas turbine power plant system. The main emphasis is given to combined cycle thermodynamic and its main components.

Chapter 4 deals with the theoretical background of exergy, exergy analysis, and exergoeconomic optimization, with the expressions and equations used in the mathematical model. It also explains the optimization technique used in this paper.

Chapter 5 is the base plants modeling chapter and it contains a detailed description of the plant, and energy exergy economic analysis. It presents the mathematical procedure of the solution for the optimization problem.

Chapter 6 presents the results of each step of the methodology. In addition, it discusses the effect of the operating parameter on the performance parameters. The comparisons between the cases were also presented.

Chapter 7 concludes the study results.

2 Literature Survey and Status of Investigation

In order to have an idea of the present methodology development in the area of performance and optimization of combined cycle gas turbine power plant, a brief survey of available literature was made. However, this chapter is concerned with a review of literature on optimization performed on various thermal systems. In general, some authors focus on the gas turbine operating parameters (topping cycle), others optimize the steam plant (bottoming cycle) on the basis of a given gas turbine, whereas others propose appropriate optimization methods for the whole combined cycle power plant. Furthermore, the optimization can be analyzed from a thermodynamic point of view, according to the first and/or second law analysis, or using a thermoeconomic or environmental-economic strategy (Kaviri et al [1], Ahmadi and Dincer [2], Boyano et al [3] and Petrakopoulou et al [4]). From the point of view of optimization methodology, there are many types of analyses. In this work, the review will highlight most common methodology: the exergy destruction method, and the exergoeconomic method.

2.1 Review of Analysis and Optimization of Topping Cycle

2.1.1 Thermodynamic Analysis and Optimization

The gas turbine operating parameters which influence the combined cycle gas turbine performance are; ambient conditions, compressor pressure ratio, and turbine inlet temperature.

2.1.1.1 The Effect of Ambient Conditions

One of the factors that affect gas turbine performance is the ambient conditions, mainly ambient temperature, atmospheric pressure, and the relative humidity of air. These parameters affect the generated electric power and the heat-rate during operation. The location of power plant plays a major role on its performance. The atmospheric air, which enters the compressor, becomes hotter after compression and it is directed to a combustion chamber. Several authors reported the effect of ambient temperature: Ibrahim et al [5], Ameri and Hejazi [6], Boonnasa et al [7] and Hosseini et al [8].

Ameri and Hejazi [6] observed that the variation in the ambient temperature causes a loss of 20% of the rated capacity of the 170 gas turbine units in Iran. They studied five gas turbines, where the difference between the ambient temperature and the ISO conditions was on average 11.8 °C. They found that for each 1 °C increase in ambient temperature, the power output was decreased by 0.74%, and they suggested cooling the compressor's intake-air temperature to improve the gas turbine cycle efficiency.

Hosseini et al [8] indicated that the gas turbine compressor is designed for constant air volume flow, which makes the electric power output dependent on the ambient temperature through the specific mass flow rate. They added that the increase in the ambient temperature also decreases the compressor's output pressure, which reduces the gas turbine cycle efficiency, while the increase in the air density reduces the gas turbine's heat rate and increases its specific fuel consumption. They stated that for each 1°C increase in the ambient air temperature, the electric power output of the gas turbine decreases by 0.5% to 0.9%, and by 0.27% for a combined cycle.

2.1.1.2 Effect of Compressor Pressure Ratio

The properties of air entering combustion chamber depend upon the compressor pressure ratio studied by: Ibrahim et al [5], Ibrahim and Rahman [9], and Khaliq and Kaushik [10].

Ibrahim and Rahman [9] performed a parametric thermodynamic analysis of a combined cycle gas turbine. They investigated the effect of operating parameters, compression ratio, gas-turbine peak temperature ratio, isentropic compressor and efficiency and air fuel ratio on the overall plant performance. Their results show that the compression ratios, air to fuel ratio as well as the isentropic efficiencies are strongly influenced by the overall thermal efficiency of the combined cycle gas turbine power plant. The overall thermal efficiency increases with compression ratio as well as isentropic compressor and turbine efficiency. However, the variation of overall thermal efficiency is minor at the lower compression ratio while it is very significant at the higher compression ratio for both isentropic compressor and turbine efficiency. The overall efficiencies for combined cycle gas turbine are much higher than the efficiencies of gas turbine plants. Efficiency quoted range is about 61%. In addition, the overall

thermal efficiency increases and total power output decreases linearly with the increase of the compression ratio with constant turbine inlet temperature. The peak overall efficiency occurs at the higher compression ratio with the higher cycle peak temperature ratio as well as higher isentropic compressor and turbine efficiencies.

2.1.1.3 Effect of Turbine Inlet Temperature

The turbine inlet temperature (TIT) plays an important role on the performance of combined cycle. The maximum value of TIT is fixed due to the metallurgical problem of turbine blade cooling. Research in this area was done by:

Sanjay [11] stated that the parameter that affects cycle performance most is the turbine inlet temperature TIT. The TIT should be kept on the higher side, because at lower values, the exergy destruction is higher.

Khaliq and Kaushik [10] and **Khaliq** [12] reported in their detailed analyses that the exergy destruction in the combustion chamber increases with the cycle temperature ratio, and the second-law efficiency of the primary combustor behaves in reverse from the second-law analysis. Increasing the maximum cycle temperature gives a significant improvement in both efficiency and specific work-output. The study also concludes that the efficiency reduces rapidly with a reduction in the TIT.

2.1.2 Thermoeconomic Optimization

If the sole objective of a CCGT design were to maximize the thermodynamic efficiency, its total cost would be very high. Therefore, the design of a modern power plant means a product with a low investment cost and high efficiency. Thermoeconomic analysis represents a very important tool for the thermal systems designer to determine the optimal configuration for a new system or plan changes in an existing. The thermoeconomic study was very important in order to get a compromise between plant efficiency and costs.

Kaviri et al [13] show that increase in the compressor pressure ratio decreases the cost of exergy destruction. The reason is that by increasing the compressor ratio, the outlet temperature increases as well. Therefore, the temperature difference decreases. Because the cost of exergy destruction is a direct function of exergy destruction, it leads to a decrease in the cost of exergy destruction. As the compression ratio increases, the air exiting the compressors is hotter, therefore less fuel is required (lowering the air fuel

ratio) to reach the desired turbine inlet temperature in a fixed gas flow to the gas turbine. The work required in the compressor and the power output of the gas turbine steadily increases with compression ratio, and then causes decreases in the exhaust gases temperature. This lower gas temperature causes less steam to be produced in the HRSG, therefore lowering the outputs of the steam cycle. It is noticed that the total power output increases with compression ratio. However, the variation of the total power output is minor at the lower compression ratio while it is significant at the higher compression ratio for all gas turbine configurations.

2.2 Review of Analysis and Optimization of Bottoming Cycle

2.2.1 Thermodynamic Analysis and Optimization

The efficiency of steam power plants can be improved by increasing the live steam and reheat-steam parameters, and by introducing high-efficiency, low-loss turbine blade geometries. The first goal, to increase the steam parameters, is primarily achieved by choosing appropriate materials for the components operating under live-steam and reheat-steam conditions while retaining the proven designs. Collaborative European programs have led to the development and qualification of steels with much improved creep properties at temperatures of up to 600 °C, appropriate for the manufacture of key components. At the same time, optimization of the blade profiles and geometries allowed further major improvements in operating efficiency. The achievable improvements in efficiency is about 0.5% per 10 °C live steam and reheat (RH) temperature increase, and 0.2 % per 10 bar pressure increase. Second important part of the bottoming cycle is the heat recovery steam turbine (HRSG), its design and optimization affects to a large extent influence the efficiency and the cost of the whole plant.

Mohagheghi and Shayegan [14] performed the thermodynamic optimization of design variables and heat exchangers layout in a heat recovery steam generator HRSG for combined cycle gas turbine CCGT using a genetic algorithm. Their method was introduced for modeling the steam cycle in advanced combined cycles by organizing the non-linear equations and their simultaneous used solutions with numerical methods. In addition to the optimization of design variables of the recovery boiler, they performed the distribution of heat exchangers among different sections and optimized their layouts

in HRSGs. A standard gas turbine was assumed, and then outlet gas stream conditions (mass flow rate, temperature, and chemical composition of gas stream) were considered as the inlet parameters for the recovery boiler model. From the optimization process maximum output power from a steam cycle for different HRSGs was then analyzed.

Bracco and Silvia [15] studied a combined cycle power plant with a single level heat recovery steam generator HRSG. They developed a mathematical model to determine the optimal steam pressure values in the HRSG according to different objective functions (in the HRSG for a given gas turbine). Their work reports numerical results for the combined cycle power plant considering four different gas turbines. The optimization approach was focused on the study of the heat transfer between the steam and the exhaust gas in the HRSG, based on an exergetic analysis. They present the comparison among different objective functions that refer to the HRSG specifically or to the whole bottoming cycle. In their mathematical model, they considered the presence of specific constraints for the operating parameters of the power plant, the most important constraints that were considered refer to the steam quality at the turbine outlet, the HRSG outlet exhaust gas temperature and the steam turbine blade height. In their work, a parametric analysis was also performed to evaluate the influence of the gas temperature at the HRSG inlet and the pinch point temperature difference on the considered objective functions.

Woudstra et al [16] performed the thermodynamic evaluation of combined cycle plants with the same gas turbine and different steam bottoming cycles. The evaluation showed that the increasing the number of pressure levels of steam generation will reduce the losses due to heat transfer in the HRSG, but also the exergy loss due to the exhaust of flue gas to the stack. Among the investigated configurations for bottoming cycle, triple pressure reheat was the best option from exergy point of view.

Mansouri et al [17] investigated the effect of pressure levels of steam generation at heat recovery steam generator HRSG on the energetic and exergetic efficiency of HRSG, bottoming cycle and combined cycle power plants , as well as the effect of HRSG (heat recovery steam generator) pressure levels on exergy destruction at HRSG and other main components of the bottoming cycle. Their result show that an increase in pressure levels of steam generation at HRSG leads to an increase in the exergy efficiency of HRSG and CCPP increase respectively. In addition, an increase in

pressure levels at HRSG decreases the exergy destruction due to heat transfer in HRSG: the exergetic efficiency of HRSG increases with an increase in pressure levels of steam generation and adding reheat to the cycle.

Xiang and Chen [76] considered a combined cycle with three-pressure HRSG, equipped with the GE PG9351FA gas turbine. They maximized the combined cycle efficiency through the optimization of the HRSG operating parameters by minimizing exergy losses. Moreover, they highlighted the influence of the HRSG inlet gas temperature on the bottoming cycle efficiency. They studied the influence of HRSG inlet gas temperature on the steam bottoming cycle efficiency. Their result shows that increasing the HRSG inlet temperature has less improvement to steam cycle efficiency when it is over 590ºC.

2.2.2 Thermoeconomic Optimization

As we mentioned, the combined cycle gas turbine power plants are thermodynamically attractive. Thermodynamics plays an important role in selection of the type of power plan Kamate and Gangavati [18], but thermodynamics is not the only criterion for decision. Other factors, such as price, environmental impact, fuel availability are also important Kehlihofer [19]. The most important part of a CCPP is the heat recovery steam generator. Therefore, the optimal design of HRSG in CCPPs is an important subject due to the increase in fuel prices and decrease in fossil fuel resources.

Alus and Petrović [20] performed an optimization of a triple pressure CCGT. The objective of their work was developing a new system for optimization of parameters for CCGT with triple-pressure heat recovery steam generator. The objective of the thermodynamic optimization is to enhance the efficiency of the CCGT and to maximize the power production in the steam cycle (steam turbine gross power). Improvement of the efficiency of the CCGT plants was achieved through optimization of the operating parameters: temperature difference between the gas and steam pinch point (PP) and the steam pressure in the HRSG. The aim of the thermoeconomic optimization was to minimize the production costs per unit of the generated electricity, optimization was to minimize the production cost of electricity in the CCGT power plant based on energetic and economic analysis.

Casarosa et al [21] minimized the total cost of the exergy losses of the HRSG for a combined cycle using the Simplex method. The objective function was defined as the total installed cost of the HRSG and the cost of the increased fuel consumption when the area of the HRSG was reduced.

Ahmadi and Dincer [22] performed the thermodynamic analysis and thermoeconomic optimization of a dual pressure combined cycle power plant with a supplementary firing unit. They conducted an exergy and exergoeconomic analyses for the power plant. The design parameters of this study were compressor pressure ratio, compressor isentropic efficiency, gas turbine isentropic efficiency, gas turbine inlet temperature, duct burner mass flow rate, high pressure stream, low pressure stream, high pressure main steam temperature, low pressure steam temperature, high pressure pinch point temperature difference, low pressure pinch point temperature difference, condenser pressure, steam turbine isentropic efficiency, and pump isentropic efficiency. They introduced an objective function, a new objective function, representing the total cost of the plant (in terms of dollar per second) defined as the sum of the operating cost related to the fuel consumption and the capital investment for equipment purchase and maintenance costs. The optimum key variables were obtained by minimizing the objective function using a generic algorithm. The optimum design parameters obtained for the plant showed a trade-off between the thermodynamic and economic optimal designs. The sensitivity analysis was also performed. Two factors were considered: unit cost of fuel, and net output power of the combined cycle power plant. They concluded that by increasing the fuel price, the optimized decision variables in the thermoeconomic design tend to reach those of the thermodynamic optimum design.

Behbahani-nia et al [23] presented an exergy based thermoeconomic method, which was applied to find the optimum values of design parameters for a single pressure HRSG in combined cycle power plants. The design variables optimized in this work were pinch point and gas side velocity. Optimization was performed by being based on two different objective functions. The first function was the thermodynamic(the summation of exergy loss due to an outflow of hot gas escaping from the HRSG through stack, and exergy destruction due to internal irreversibility inside the HRSG). The second function was a thermoeconomic objective function (the summation of exergy loss and destruction in terms of expenses including the cost of fuel and

electricity, and the capital cost of HRSG). They investigated the effects of pinch point and gas-side velocity on the components of objective functions. The study concluded that a considerable amount of exergy is destroyed due to gas pressure drop, especially when pinch point is very close to zero.

Sanjay [11] investigated the effect of HRSG configuration on exergy destruction of bottoming cycle components and concluded that the distribution of exergy destruction is sensitive to a type of bottoming cycle configuration. He found that the best utilization of heat energy in bottoming steam cycle is exhibited in the case of triple pressure reheat configuration. In all bottoming cycle components (HRSG, Steam turbine, and Condenser), it was observed that component-wise exergy destruction is lower in reheated configuration with respect to the same configuration without reheat.

Ghazi et al [24] carried out a thermo-economic modeling and optimization method to obtain the optimum values of design parameters (high and low drum pressures, steam mass flow rates, high pressure and low pressure pinch point temperature differences, and the duct burner fuel consumption flow rate) for a dual pressure HRSG. They performed the complete sensitivity analysis of changes in inlet gas temperature entering the HRSG and exergy unit cost. Total cost per unit of produced steam exergy was defined as the objective function. They found that at higher inlet gas enthalpy the required heat transfer surface area (capital cost) increases.

Hajabdollahi et al [25] modeled an HRSG with a typical geometry and a number of pressure levels used at CCPPs, and developed a thermodynamic model and thermoeconomic optimization. They conducted exergoeconomic analysis and multi-optimization of an HRSG through energy and exergy, and compared their results with data provided from a power plant situated near the Caspian Sea in Iran. They introduced a new objective function (the total cost per unit of steam produced exergy). Then, optimum design parameters were selected when objective function was minimized while HRSG exergy efficiency was maximized. Authors summarized that an increase in high and low-pressure drums increases exergy efficiency, while an increase in pinch point decreases exergy efficiency. Additionally, an increase in the HRSG inlet gas enthalpy results in an increase of the exergy efficiency.

Naemi et al [26] developed the thermodynamic model of a dual pressure HRSG coupled with a heavy-duty gas turbine. They investigated thermodynamic and

thermoeconomic analyses to achieve the optimum operating parameters of a dual pressure heat recovery steam generator, and computed exergy waste and exergy destruction for different pinch points. They discussed the effects of non-dimensional parameters on the HRSG performance. They also investigated optimum design of HRSG regarding financial considerations, and performed a sensitivity analysis.

Najjar [27] described that the efficiency of a gas turbine engine is relatively low at design point and it deteriorates further at part load and at off-design high ambient temperatures. His work comprises of the study of adding an inlet air pre cooler driven by the tail-end heat recovered from the engine exhaust gases. A heat recovery boiler was used to partly recover the exhaust heat. The performance of this combined system, namely power, efficiency, and specific fuel consumption was studied and compared with the simple cycle. The variables in this parametric study were mainly compressor pressure ratio, turbine inlet temperature, and ambient temperature. Results show that the combined system achieves gains in power. The performance of the combined system showed less sensitivity to variations in operating variables. Thermo economic evaluation shows that the combined system is viable.

2.3 Review of Optimization of whole CCGT

One of these alternative methods is optimizing the combined cycle, which has been the subject of many investigations. Some investigators focused on optimizing the thermal performance: Franco and Casarosa [30], Valdes and Rapun [31], Bassily [32], and Bassily [33]; whereas other investigators optimized an objective function of the net revenue or total cost: Valdés et al [29], and Casarosa et al [21].

Tyagi and Khan [28] studied the effects of gas turbine exhaust temperature, stack temperature and ambient temperature on the overall efficiency of combine cycle power plant keeping the gas turbine efficiency as well as steam turbine efficiency constant. They concluded that the stack temperature should be minimum and gas turbine exhaust temperature should be maximum. Out of these three variables i.e. turbine exhaust temperature, stack temperature and ambient temperature, the dominating factor of increasing the overall efficiency of the combine cycle power plant is the stack temperature.

Valdés et al [29] showed a possible way to achieve a thermoeconomic optimization of combined cycle gas turbine power plants. The optimization was done by using a genetic algorithm, tuned by applying it to a single pressure CCGT power plant. Once tuned, the optimization algorithm was used to evaluate more complex plants, with two and three pressure levels in the heat recovery steam generator. The variables considered for the optimization were the thermodynamic parameters that established the configuration of the HRSG. Two different objective functions were proposed: one minimizes the cost of production per unit of output and the other maximizes the annual cash flow. The results obtained with both functions were compared in order to find the better optimization strategy. The results show that it is possible to find an optimum for each design parameter. This optimum depends on the selected optimization strategy.

Bassily [32] presented the effects of varying the inlet temperature of the gas turbine and PP on the performance of a dual pressure reheat combined cycle. He also modeled some feasible techniques to reduce the irreversibility of the HRSG of both cycles, and showed that optimizing or reducing the irreversibility of these cycles could increase their efficiencies by 2–3%. Applying gas reheat increases the generated power and average temperature at which heat is supplied, whereas applying gas recuperation takes advantage of the increased gas temperature at the outlet of the GT to enhance cycle efficiency. For gas-reheat gas-recuperated combined cycles, recuperated heat exchangers fabricated from stainless steel have to be used to withstand these conditions. He compared the optimized results with the regularly designed triple pressure reheat combined cycle Bassily [33].

Boonnasa et al [7] studied the performance improvement of an existing combined cycle power plant located in Bangkok that consisted of two gas turbines (110.76MW each), and one 115.14MW steam turbine in ISO conditions. The plant used an absorption chiller to cool one of the two gas turbine's intake-air to 15°C, in addition to having a thermal energy storage tank that stored the sensible heat of the chilled water to meet the varying daily cooling load. Low-pressure steam from a heat recovery steam generator was used to drive the absorption chiller needed to meet a maximum load of 7049.58kW with the help of the thermal heat storage. As a result, the power output of the cooled gas turbine increased by 10%, improving the CCPP total power output by 6.24%. Economically, the study found that due to the low initial investment cost of

retrofitting the absorption chiller the internal rate of return was 40%, and the payback period was just 3.81 years. However, the authors also reported a reduction by 2.85% in the steam turbine power output, which was due to powering the absorption chiller directly from the HRSG unit steam that was powering the steam turbine. This reduction in the steam turbine power output could have been avoided if they had used a boiler that utilized the waste heat energy from the stack after the HRSG unit.

2.4 Exergy and Exergoeconomic Methods

Exergoeconomics or thermoeconomic is the branch of engineering that appropriately combines, at the level of system components, thermodynamic evaluations based on an exergy analysis with economic principles. This technique was first used in 1930s and for designing efficient energy conversion systems or optimizing such systems. It combines the second law of thermodynamics through exergy with economics and economic principles. Various exergoeconomic methodologies were developed over the last 20 years. They include the Average Costing (AVCO), the Last In- First Out (LIFO), the Specific Exergy Costing (SPECO), the Exergetic Costing (EXCO) Lozano and Valero [34], the Thermo-functional Analysis (TFA), and the Engineering Functional Analysis (EFA) methods Lazzaretto and Tsatsaronis [35]. With understanding of the combination of irreversibilities and economics, the cost of exergy destroyed in a plant's component becomes measurable, and such information is not obtainable with conventional energy analysis. Exergoeconomics, therefore, provides the plant designer and/or operator with information critical to the plant as costs due to thermodynamic inefficiencies are identified and evaluated and, therefore, can be reduced, creating opportunities for the optimization of the system, at either the design phase or the operational phase.

Exergetic and thermoeconomic analyses studies together with cost analysis were performed by Kwak et al [36] for each component of a 500-MW combine cycle plant. With the computer program developed, they were able to determine the production costs of the power plants, such as gas- and steam-turbine plants and gas-turbine cogeneration plants.

2.4.1 Exergy Analysis

Fiasch and Giampaolo [37] investigated an exergy analysis of the semi-closed gas turbine combined cycle. They concluded that combustion, heat recovery steam generator, water injection/mixing, and water recovery system are the main sources of the losses, representing globally more than 80% of the overall exergy destruction.

Cihan et al [38] carried out energy and exergy analyses for a combined cycle located in Turkey, and suggested modifications to decrease the exergy destruction in CCPPs. Their results showed that combustion chambers, gas turbines, and HRSGs are the main sources of irreversibilities, representing over 85% of the overall exergy losses.

Mousafarash and Ameri [39] their study consist of exergy analysis of a typical GT power plant, analysis of system performance at different ambient temperatures and partial loads, and exergo-economic analysis of the gas turbine power plant. The results of their study reveal that the highest exergy destruction occurs in the combustion chamber, where the large temperature difference is the major source of the irreversibility. In addition, the effects of the gas turbine load variations and ambient temperature were investigated to see how system performance changes: the gas turbine was significantly affected by the ambient temperature, which led to a decrease in net power output. The results of the load variation of the gas turbine showed that a reduction in gas turbine load resulted in a decrease in the exergy efficiency of the cycle as well as all the components. They conducted an exergo-economic analysis to determine the cost of exergy destruction in each component and to determine the cost of fuel. The results show that combustion chamber has the largest cost of exergy destruction.

Butcher and Reddy [40] carried out exergy analysis for waste heat recovery based power generation system. The performance of the waste heat recovery power generation systems based on second law analysis was investigated for various operating conditions. The temperature profiles across the heat recovery steam generator (HRSG), network output, second law efficiency, and entropy generation number were simulated for various operating conditions. The variation in specific heat with exhaust gas composition and temperature were accounted in the analysis and results. The effect of pinch point on the performance of HRSG, entropy generation rate and second law efficiency were also investigated. The researchers found that the second law efficiency

of the HRSG and power generation system decreases with increasing pinch point. The first and second law efficiency of the power generation system varies with exhaust gas composition and with oxygen content in the gas. The results contribute further information about the role of gas composition, specific heat and pinch point influence on the performance of a waste heat recovery based power generation system (based on first and second law of thermodynamics).

2.4.2 Exergy Destruction Method

Kamate and Gangavati [18] analyzed cogeneration power plants in sugar industries through exergy destruction method for various steam inlet condition. The result shows that, at optimal steam inlet conditions of 61 bar and 475 C, the backpressure steam turbine cogeneration plant perform with energy and exergy efficiency of 0.863 and 0.307, while the condensing steam turbine plant perform with energy and exergy efficiency of 0.682 and 0.26, respectively. Boiler is the least efficient component and turbine is the most efficient component of the plant.

Aljundi [41] studied energy and exergy analysis of a steam power plant in Jordan using exergy destruction method. A component wise modeling and a detailed break-up of energy and exergy losses estimated the performance of the plant. The modeling shows that the thermal efficiency (26%) is low compared to modern power plants, because this efficiency was not based on the specific heat input to the steam; rather, it was based on the lower heating value of the fuel to incorporate the losses occurring in the furnace-boiler system due to energy lost with hot gases, incomplete combustion, etc. It was also observed that the maximum exergy destruction is in boiler and maximum exergy loss in condenser.

Abusoglu and Kanoglu [42] applied the exergy destruction method to the diesel engine powered cogeneration systems generating electricity and steam. They defined the fuel and product in terms of exergy flow for each component of the system and then calculated the exergetic efficiency of them. It was observed that the total exergy destruction in the engine was mostly due to the highly irreversible combustion process in the engine, heat losses from engine, and friction.

2.4.3 Exergoeconomic Analysis and Optimization Method

Exergoeconomic methods can be classified in two groups: algebraic and calculus methods.

Algebraic methods use algebraic balance equations, always require auxiliary cost equations for each component, focus essentially on the cost formation process, and determine average costs. Many researchers have conducted algebraic methods for thermal system optimization: Lozano and Valero [34], Kim et al [46], Kwon et al [47], Tsatsaronis [51] and Vieira et al [75].

Lazzaretto and Tsatsaronis [35] proposed a methodology for defining and calculating exergetic efficiencies and exergy related costs in thermal systems. It was based on the SPECO. Separate forms of exergy and costs associated with these exergy streams were used to define exergetic efficiencies in a detailed manner. It was concluded that the SPECO was a powerful approach to express the validation of the calculated cost values.

Kanoglu et al [43] developed methodology for calculating exergy flows, cost formation, and allocation within high temperature steam electrolysis system. They used specific exergy costing methodology while applying exergetic fuel and product approaches to obtain the cost balance equations. They examined exergy efficiency, exergy destruction rates, exergy loss–exergy destruction ratio, capital investment, operating, maintenance costs, and exergoeconomic factor. The capital investment cost, the operating and maintenance costs, and the total cost of the system were calculated as 422.2, 2.04 and 424.3 €/kWh, respectively. The cost distribution among the components was also determined. The exergetic costs of the steam were 0.000509, 0.000544 and 0.000574 €/kWh at the outdoor temperatures of 25 °C, 11°C and −1°C, respectively.

Orhan and Dincer [44] studied the minimization cost of a copper–chlorine (Cu-Cl) thermo-chemical cycle for hydrogen production. The specific exergy costing method was used to determine changes in design parameters of the cycle, which could improve the cost effectiveness of overall system. It was found that the cost rate of the exergy destruction took the values between $1 and $15 per kg hydrogen. The exergoeconomic factors were calculated between 0.5 and 0.02.

Kim et al [46] introduced modified productive structure analysis (MOPSA) method where an exergy costing method is used without flow-stream cost calculations.

For the entire system a set of equations for the unit exergy costs are obtained by assigning a unit exergy cost for the cost balance equation for each component.

Kwon et al [47] compared specific exergy cost method and modified productive structure analysis methods by applying them to the CGAM problem.

Calculus methods are built on differential equations. These methods are generally based on the Lagrange multipliers technique and are considered subjective with regard to the mathematical description of the function of each component in the system. A particular difficulty in the application of calculus methods to complex systems is the fact that the Lagrange multipliers vary from iteration to iteration when component thermoeconomic isolation is not achieved. This problem has led to the development of the Thermoeconomic Functional Analysis (TFA) Frangopoulos [53].

Calculus method use differential equations, such that the system cost flows are obtained in conjunction with optimization procedures based on the method of Lagrange multipliers, and determine marginal costs El-Sayed and Gaggioli [49], and Gaggioli and El-Sayed [50].

3 Thermodynamic Principle of Combined Cycle Power Plant and Description of its Main Components

3.1 Introduction

First generations of combined-cycle power generation systems installed during the 1950s and early 1960s included conventional-fired boilers. These systems were adaptations of conventional steam plants with the gas turbine exhaust gas serving as combustion air for the boiler. The efficiency of this type of combined cycle was approximately 5–6% higher than that of a similar conventional steam plant. These systems could economically utilize bare tubes in the boiler because of the high mean temperature difference between the combustion products and the water/steam. The second generation, which combined cycle system with finned tube boilers, entered service in1959. During the 1960s, the application of the heat recovery type of combined-cycle systems became more prevalent. Its initial application was in power and heat applications where its power-to-heat ratio was more favorable. In addition, a small number of the heat recovery type combined cycles were installed in utility power generation applications during the 1960s. The application of these systems in the 1970s and 1980s established the heat recovery feed water heating combined cycle as a mature technology for base load and mid-range service [45].

By 1970, there were a number of plants in operation. Throughout the 1980s, the technology developed with larger gas turbines and the introduction of pre-mixed combustion for low NO_2 emissions. Around 1990 the net plant efficiency of combined cycles passed 50% (LHV). Throughout the 1990s, a large number of combined cycle power plants were built, and many of them in base load operation. Around 1995 a new generation of large gas turbines came to the market, bringing the block size of combined cycle power output to 350-400MW and efficiency up to 57-58% [78]. As of 2011, the power output was increased to about 570MW and efficiency close to 61% [79].

Table 3-1 shows the energy utilization for a typical combined cycle plant. The gas turbine may typically convert 36% of the fuel energy into power, leaving 63% as heat passed to the HRSG from the exhaust of the gas turbine (typical mechanical electrical and heat losses in the GT account for 1%).

Table 3-1: Typical modern day combined cycle performance [48]

COMBINED CYCLE PERFORMANCE				
	% OF FUEL INPUT			
Fuel Input LHV	**100**			
Gas Turbine Power	36			
Gas Turbine Losses	1			
Gas Turbine Exhaust Heat	**63**			
Stack Loss		22		
Input to Steam		**41**		
Steam Turbine Power			19	
Steam Turbine Losses			1	
Heat to Condenser			**21**	
Gross Electric Power				**55**
Auxiliaries Power				2
Total Net Power and Efficiency				**53**

The HRSG captures approximately two thirds of the gas turbine exhaust heat with the remaining third being lost in the exit stack. Finally, 19% of the fuel input is converted into power via the steam turbine with 1% lost in the turbine and 21% of the fuel energy lost in the spent steam, which is sent to the condenser. The combined gross power of gas and steam turbines equates to 55% (LHV) of the fuel energy. Plant auxiliary accounts for ~2% of the fuel input finally leaving 53% as net output combined cycle efficiency. Therefore, the main justification for utilizing HRSGs within utility power plants lays in the clear benefit from superposition of the gas turbine Brayton cycle over the steam turbine Rankin cycle Figure 3-1 which results in an enhanced overall thermal efficiency [48].

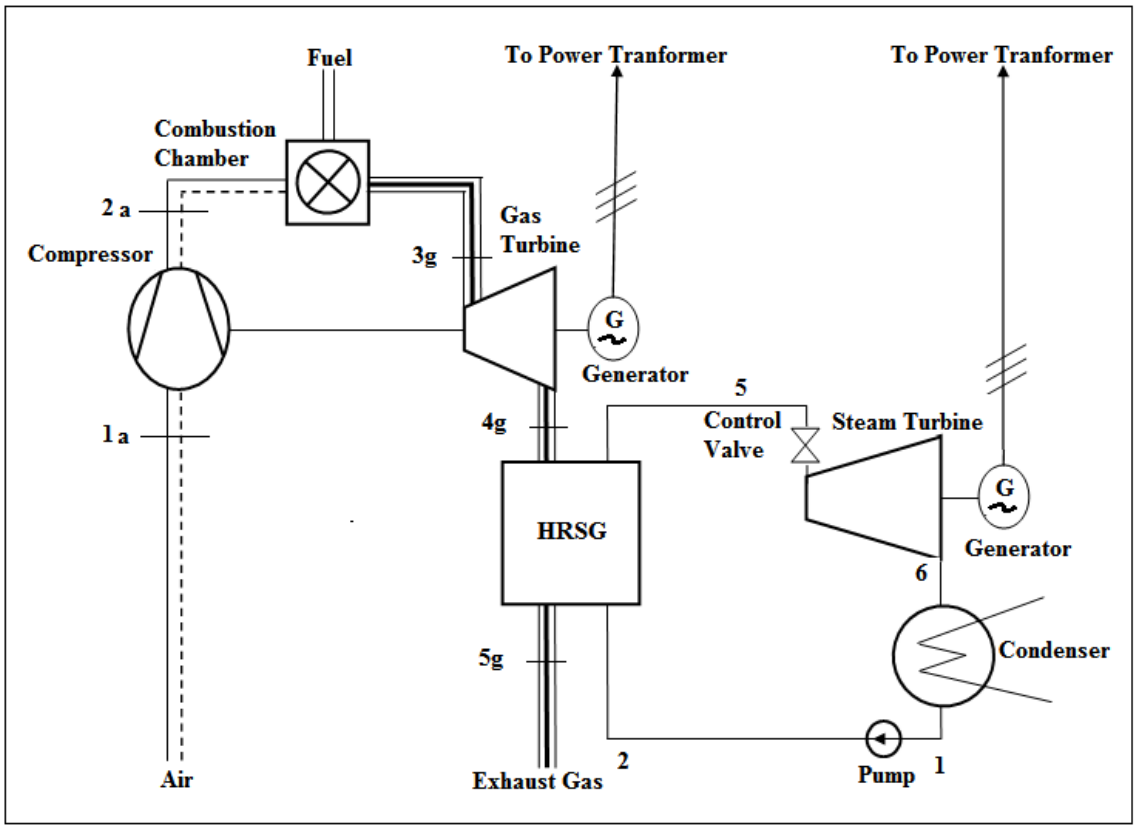

Figure 3-1 Schematic combined cycle gas turbine topping cycle and bottoming cycle

3.2 Gas Turbine

A gas turbine is a machine delivering mechanical power or thrust. It does this using a gaseous working fluid. The mechanical power generated can be used by, for example, an industrial device. The outgoing gaseous fluid can be used to generate thrust or to generate electricity. In the gas turbine, there is a continuous flow of the working fluid. This working fluid is initially compressed in the compressor. It is then heated in the combustion chamber. Finally, it goes through the turbine as seen in Figure 3-2. The turbine converts the energy of the gas into mechanical work. Part of this work is used to drive the compressor. The remainder, the "useful power", is used as the output shaft power to turn an energy conversion device, such as an electrical generator [82]. In the electricity generation field, the gas turbine can be employed as a stand-alone unit or with combined cycle power plants. Electricity generating gas turbines are usually open cycle operated. The gas turbine performance depends on the performance of its components i.e. compressor, combustion chamber, and turbine.

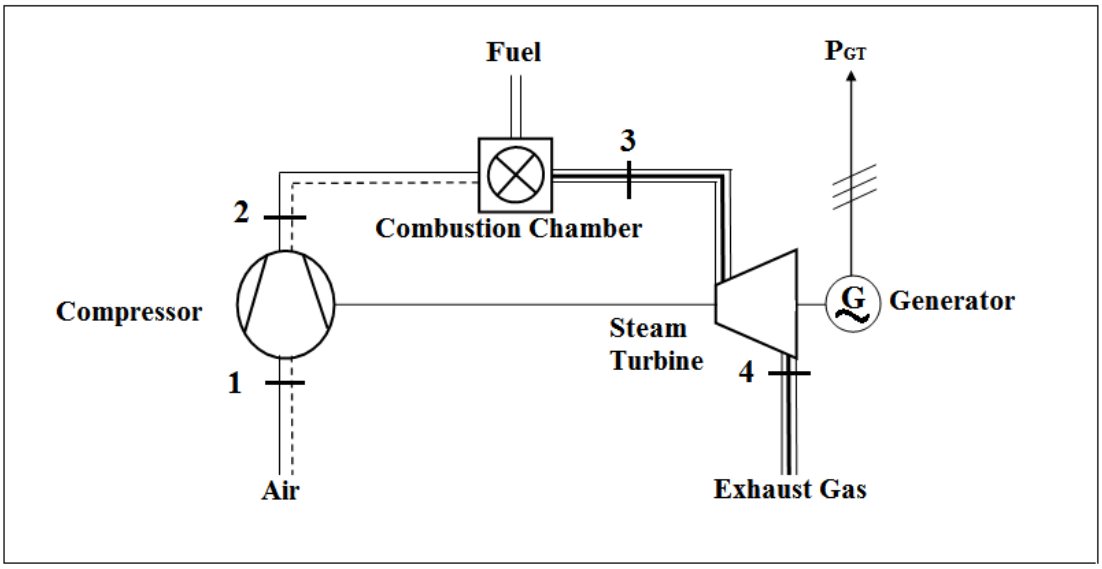

Figure 3-2: The schematic gas turbine

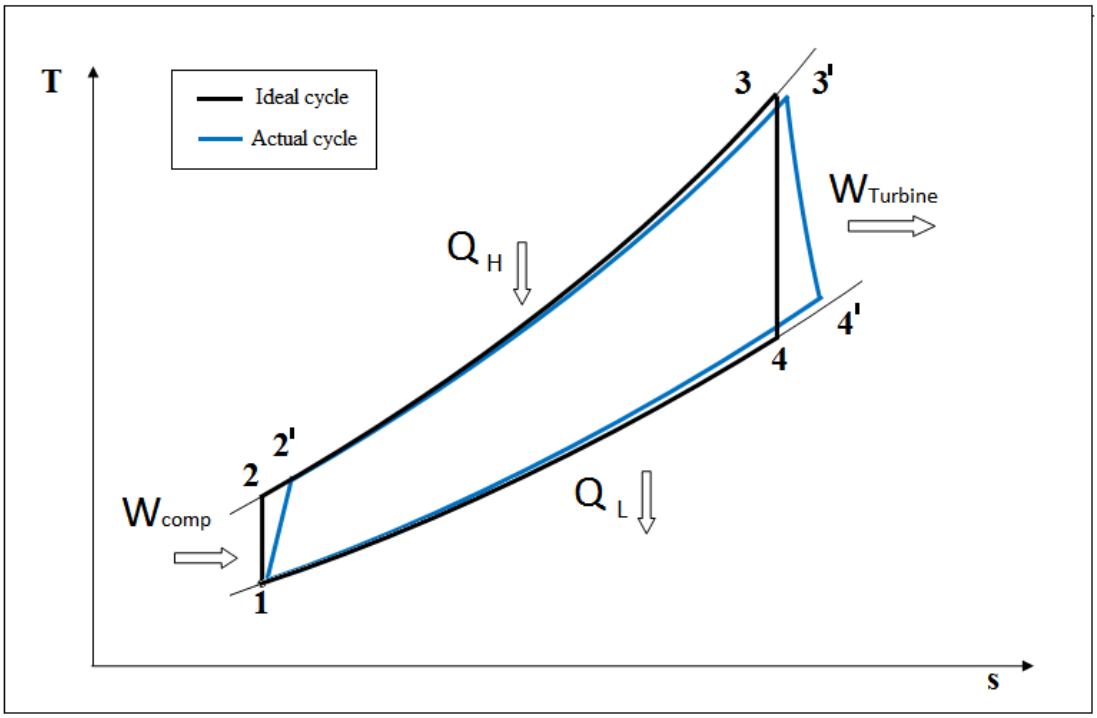

Figure 3-3: Brayton cycle

The thermodynamic cycle of a gas turbine is known as the Brayton cycle. Gas turbines usually operate on an open cycle. As seen in Figure 3-3, the air is first compressed in the compressor, the air drawn at ambient conditions into the compressor intake, where the compressor pressurizes the air up to p_2, increasing both pressure and temperature at the expenses of using compression work (W_{comp}) which is supplied by

the turbine itself. The high-pressure air proceeds into the combustion chamber, where the fuel is burned at a constant pressure. This added heat ($\dot{Q}_H$) raises the temperature from T_2 to the turbine inlet temperature (highest cycle temperature) T_3. The resulting high temperature gases then enter the turbine, where they expand to the atmospheric pressure while producing power ($W_{Turbine}$) enough to drive the compressor and produce net shaft work (W). Finally, heat ($\dot{Q}_L$) is rejected to the environment. Most of the gas turbines in electricity generation use axial flow compressors [83].

The exhaust gases leaving the turbine are thrown out (not re-circulates), causing the cycle to be classified as an open cycle. The Compression ratio and turbine inlet temperature are important parameters.

3.3 Steam Turbine

Steam turbine is an excellent prime mover to convert heat energy of steam to mechanical energy. It is one of the well-known prime movers, such as gasoline engines, diesel engines, gas turbines, jet engines, etc. All steam engines, whether turbines or not, are designed to extract energy from high-pressure steam and convert it into motion by allowing the steam to expand. For the turbine designs, steam allowed to expand gradually through more than one set of blades, for attaining much higher efficiencies compared to a single step expansion [84]. The steam expands through successive rings of moving blades on a shaft and fixed blades in a casing, producing purely rotary movement. When coupled with an electric generator, steam turbine is one of the most important means of producing bulk electric power in the world. The modern steam turbine may have three stages. The high-pressure section has small blades. They are small because the incoming steam has very high energy at very high temperature. After the steam passes through the high-pressure section (Figure 3-4,) it is sent back to the boiler to be reheated. The steam is then sent to the next section of the turbine, called the intermediate pressure section. The blades here are larger than those in the high-pressure section. After passing through this section, the steam is sent to the low-pressure section of the turbine. Because most of the energy was previously removed from the steam, the blades here are the largest in the turbine. The steam exits the turbine through the bottom, where it is condensed back into water. From there it is sent back to the boiler, to be made into steam again. The steam turbine is often used in a combined heat and

power generation process where the turbine drives a machine at the same time: steam extracted from the machine is used to supply district heating and/or process steam networks [83].

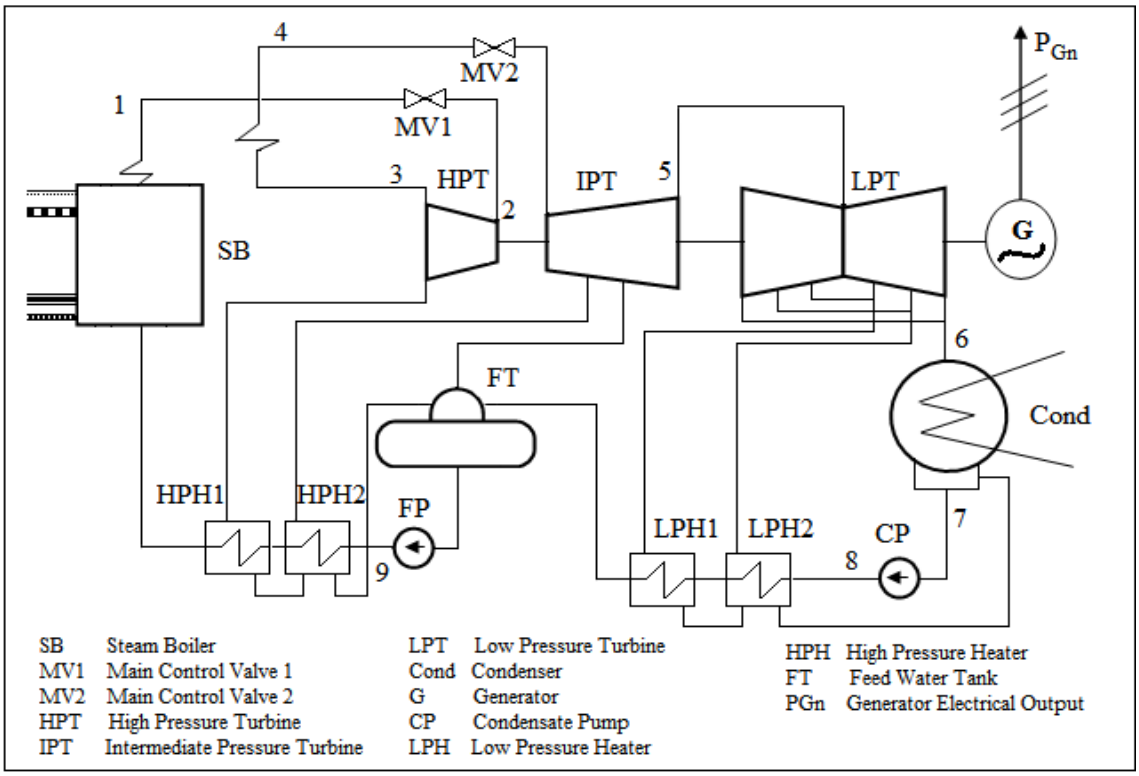

Figure 3-4 Schematic steam turbine [87]

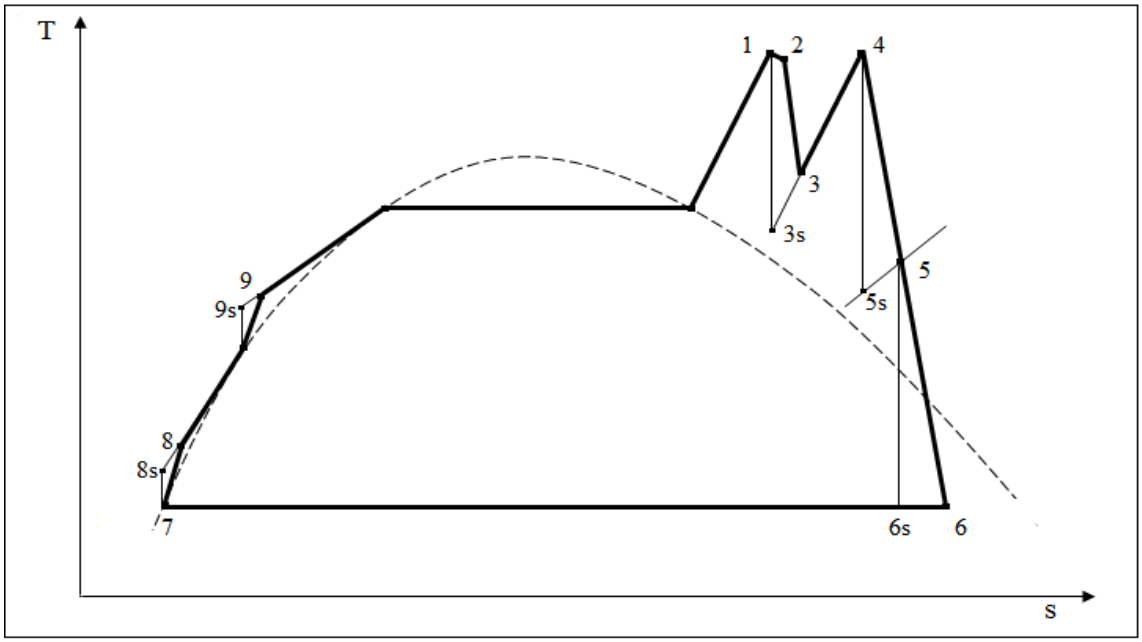

Figure 3-5 Rankin cycle [87]

A single unit of steam turbine can develop power ranging from 1 MW to 1000 MW. The thermal efficiency of modern steam power plant above 120 MW is as high as 38% to 40% [51]. Water (steam) is the working fluid for most vapor power cycles. Water works over a broad range of temperatures and pressures, has a large heat capacity, and it is stable, safe, and very environmentally friendly. The energy sources used to generate steam include gas, coal, oil, and nuclear sources.

Steam Turbine Capacity: the capacities of small turbines and coupled generators vary from 500 to 7500 kW, whereas large turbo alternators have capacity varying from 10 to 90 MW. Very large size units have capacities up to 500 MW. Generating units of 200 MW capacity are becoming quite common. The steam consumption by steam turbines depends on steam pressure and temperature at the inlet, exhaust pressure number of bleeding stages etc. The steam consumption of large steam turbines is about 3.5 to 5 kg per kWh [77].

Steam Turbine Performance: Turbine performance is expressed by the following factors:

a) The steam flow process through the unit-expansion line or condition curve
b) The steam flow rate through the unit
c) Thermal efficiency
d) The losses such as: exhaust, mechanical, generator and radiation

Mechanical losses include bearing losses, oil pump losses, and generator bearing losses. Generator losses include electrical and mechanical losses. Exhaust losses include the kinetic energy of the steam as it leaves the last stage and the pressure drop from the exit of last stage to the condenser stage. For successful operation of a steam turbine, it is desirable to supply steam at constant pressure and temperature. Steam pressure can be easily regulated by means of safety valve fitted on the boiler.

The most commonly used vapor power cycle is the Rankin cycle. Even though a description of the Rankin cycle can be found in any engineering thermodynamics textbook, it is briefly covered here. The simple Rankin cycle, shown in Figure 3-5 consists of four steps. The working fluid is pumped to a high pressure and circulated through the boiler. The fluid is boiled at a constant pressure in the boiler after which the high-pressure vapor produced is expanded through a turbine, thus extracting work from

it. The vapor exiting the turbine is condensed in a condenser by rejecting heat to a cooling fluid.

Several modifications to the Rankin cycle are used to achieve better efficiencies. These include superheating, reheating and regeneration. Many of the impracticalities associated with the Carnot cycle can be eliminated by superheating the steam in the boiler and condensing it completely in the condenser, as shown schematically on a T-s diagram in Figure 3-5.

The cycle that results is the Rankin cycle, which is the ideal cycle for vapor power plants. The ideal Rankin cycle does not involve any internal irreversibility and consists of the following four processes: isentropic compression in a pump, constant pressure heat addition in a boiler, isentropic expansion in a turbine, and constant pressure heat rejection in a condenser. All four components of the Rankin cycle are steady-state steady-flow devices. The potential and kinetic energy effects can be neglected. The boiler and the condenser do not involve any work, and the pump and the turbine are assumed to be isentropic [84].

3.4 Heat Recovery Steam Generator

In the current technology, the most efficient energy conversion systems to produce electrical and thermal energy are the combined cycle power plants. In a typical CCPP, exhaust heat from the gas turbine GT is recovered in a heat recovery steam generator to generate steam in the steam cycle. HRSG performance has a large impact on the overall performance of a combined-cycle power plant. Steam generated in HRSG with different pressure levels depend on the design. HRSG consist of three heat exchanger packages (economizer, evaporator, and superheater) Figure 3-6. Combustion gases enter superheater, evaporator, and economizer package respectively. The heat recovery from gas side to the water-steam is achieved in three steps:

In the economizer, the feed water is heated to temperature close to its saturation temperature.

In the evaporator, the water evaporates at a constant temperature and pressure and becomes saturated steam.

In the superheater, the high value heat from the exhaust is used for superheating the steam generated in the evaporator. Superheated steam is fed to the steam turbine.

Classification of HRSG: Heat recovery steam generator can be classified according to:

a. The generated steam pressure; single pressure Figure 3-6, duel pressure Figure 3-7, and triple pressure Figure 3-8

b. The type of circulation system being used Figure 3-9:

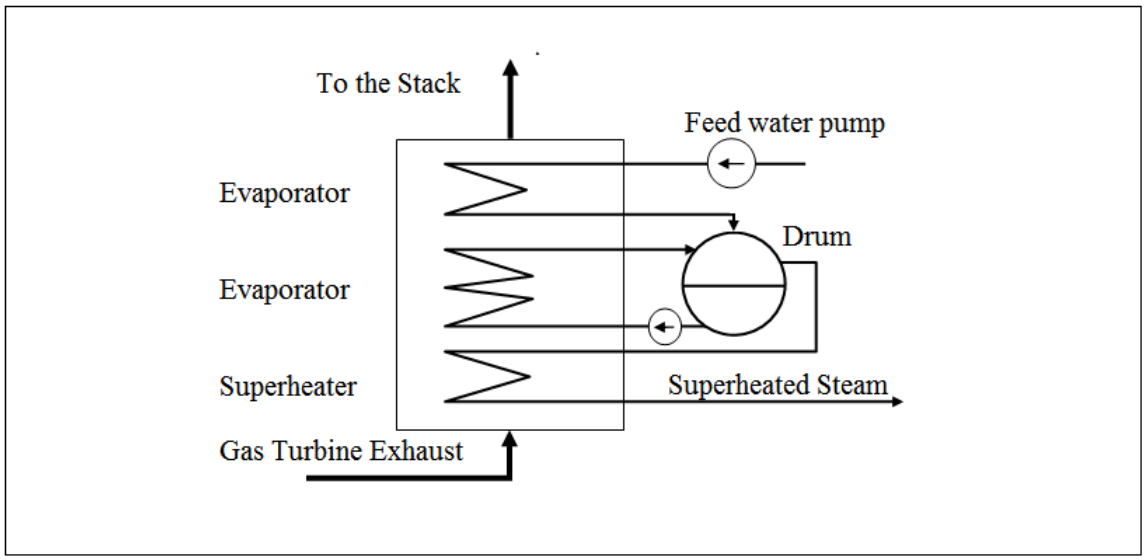

Figure 3-6 Single pressure HRSG

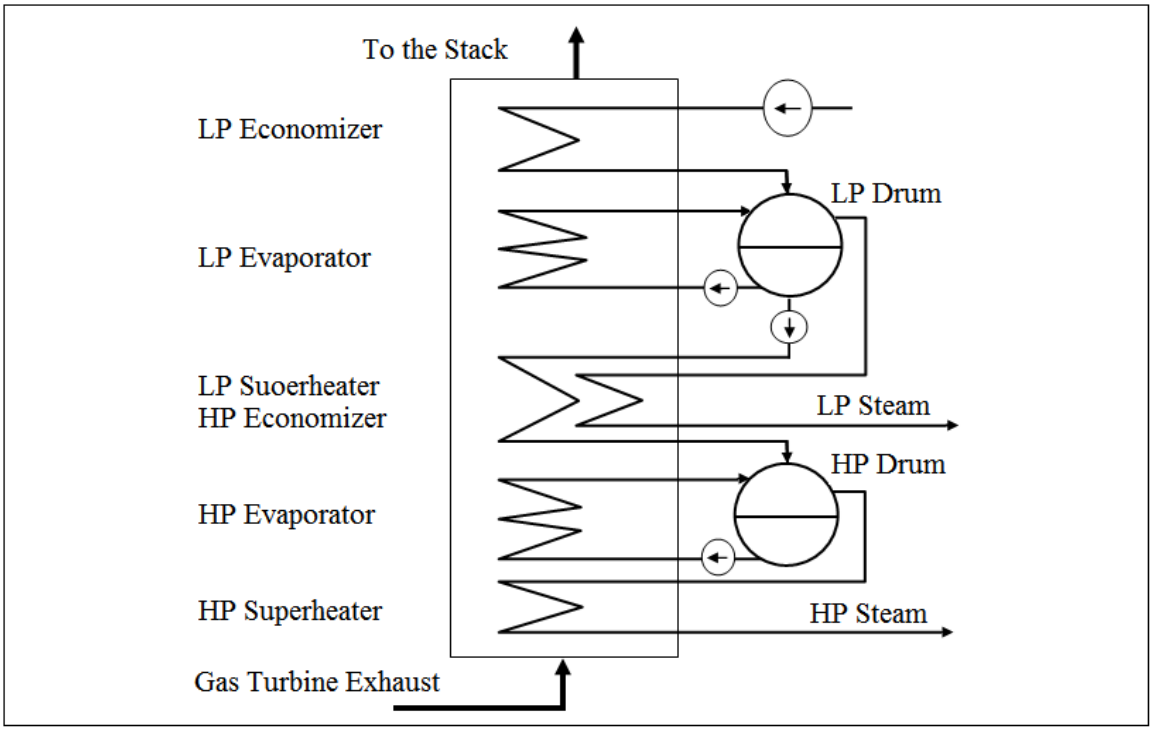

Figure 3-7 Duel pressure HRSG

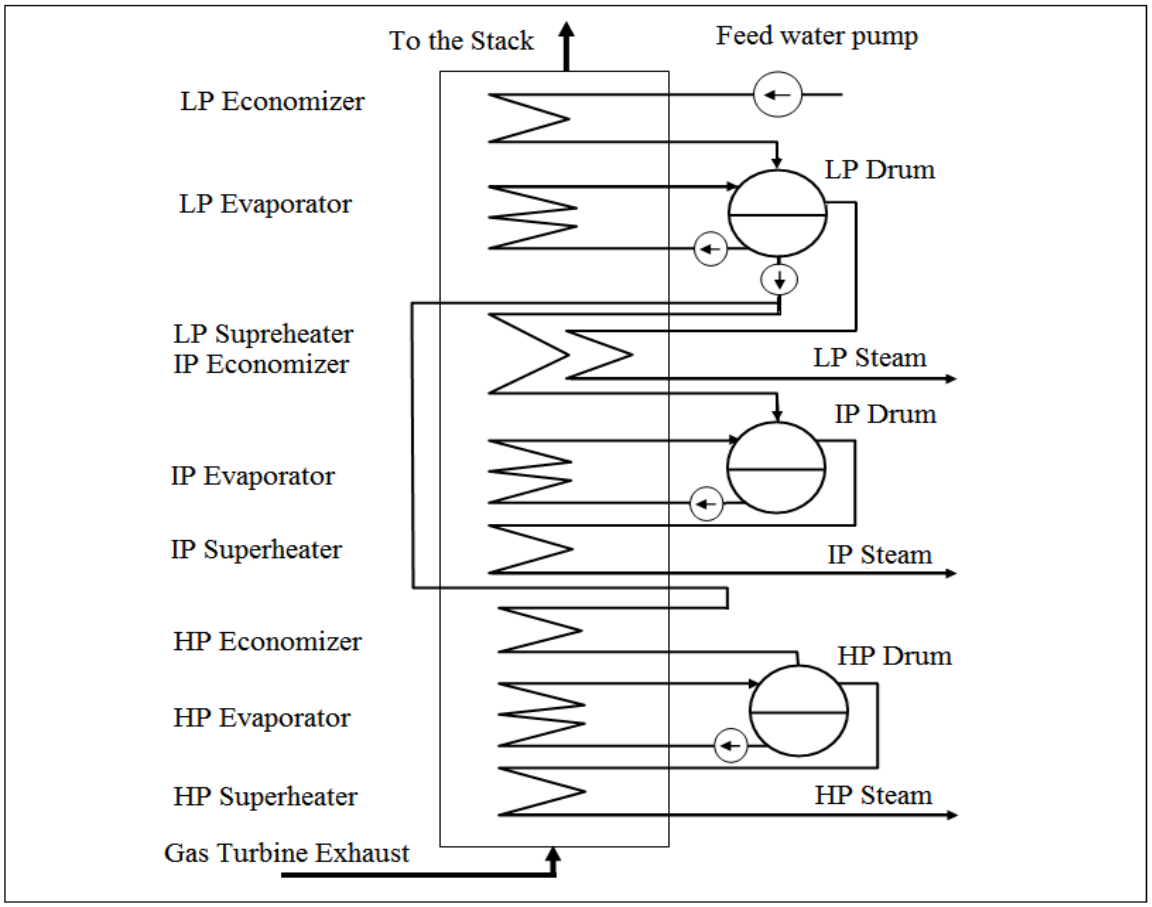

Figure 3-8 Triple pressure HRSG

Natural circulation typically consists of vertical tubes and horizontal flow arrangement.

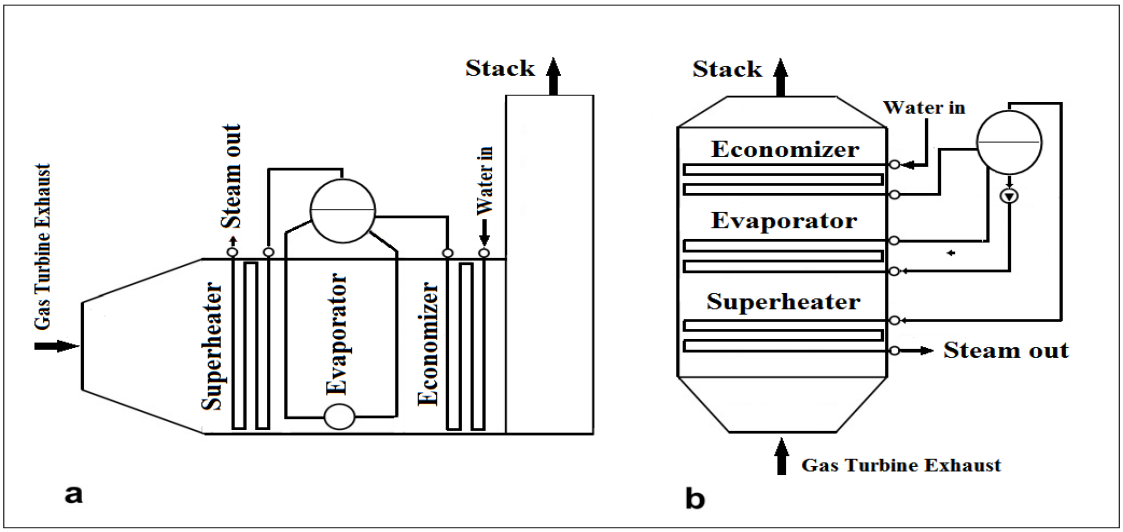

Figure 3-9 HRSG (a) Natural circulation, (b) Forced circulation

Circulation maintained by the density differences between cold water in lower chamber and hot steam-water mixture in evaporator tubes are shown in Figure 3-9a.

Forced circulation; HRSGs are characterized by horizontal tubes with vertical gas flow and use pumps to circulate steam-water mixture (Figure 3-9b).

3.4.1 Important HRSG Performance and Design Parameters

3.4.1.1 HRSG Main Design Parameters

In general, when designing of any gas turbine HRSG the following parameters should be considered:

a) Pinch point temperature: pinch point temperature is the difference between the saturation temperature of water and the gas temperature of the gas leaving the evaporator (Figure 3-10).

b) Economizer approach temperatures (approach point): the approach point is the difference between the temperature of saturated steam and the temperature of the water entering the evaporator (Figure 3-10). Selection of these two variables also affects the size of the superheater, the evaporator, and the economizer. The smaller temperature difference means that the surface area required to produce the same heat transfer will be much greater. The direct consequence is that more material is used and hence capital cost is higher.

c) Steam pressure and temperature are the outlet parameters from HRSG supplied to the steam turbine. These parameters are selected to provide an economical design.

d) Superheater approach temperatures: the difference between the superheating steam temperature in the superheater and gas turbine outlet temperature.

e) Stack outlet temperatures: the temperature of the gases that leave the HRSG to the atmosphere (Figure 3-10).

f) Allowable backpressure. The HRSG cross sectional area significantly influences the gas turbine backpressure. Smaller, more compact HRSGs require higher gas turbine backpressures to drive through the flue gas, however, while the size reduction may reduce HRSG cost, the requirement

to provide a higher pressure at the turbine exit has a detrimental effect on gas turbine efficiency. The typical values of gas turbine back-pressures are 2.5 to 3.7 kPa in most units [80].

3.4.1.2 T-Q Diagram of HRSG

The T-Q diagram shows profiles for the heat transfer process between exhaust gas and water/steam, using temperature on the ordinate axis and heat transferred on the abscissa axis.

The use of T-Q diagram is crucial in understanding and designing combined cycles. Figure 3-10 shows the T-Q diagram for a single-pressure combined cycle. The smallest temperature difference in the HRSG is called the pinch-point, and it is located on the cold side of the evaporator. The upper line, with an almost constant slope, represents the temperature profile of the flue-gas, and the lower line represents the temperature of the water/steam. The HRSG of a single-pressure combined cycle consists of three different sections.

First section HRSG: starting at the lowest temperature, the first section is called the economizer, and is the place where liquid water is heated to the saturation temperature. To avoid evaporation, which could cause steam blockage that may result in "water hammering" in the economizer, the outlet temperature is always kept a few degrees below the saturated state. This temperature difference is called the approach point.

Second section: is the evaporator, in which the water is evaporated at constant temperature.

Third section HRSG is the superheater where the evaporated steam is superheated.

The relation between temperature and heat can be described by:

$$\dot{Q} = \dot{m} c_p \Delta T \tag{3-1}$$

This equation (3-1) is valid when the working medium does not undergo a phase transition. In the HRSG, a phase transition from water to steam occurs in the evaporator [54], which means that equation (3-2) must be replaced by:

$$\dot{Q} = \dot{m} \Delta h_{evap} \tag{3-2}$$

where $\dot{Q}$ the energy is transferred and Δh_{evap} is the evaporation enthalpy. If equation (3-1) is rearranged it can be seen that the slope of the line in the T-Q diagram is

inversely proportional to the mass flow and the specific heat. From equation (3-2) it can be understood that the term $\dot{m}\Delta h_{evap}$ is the length of the evaporation line. These relations are central for the analysis of combined cycle power plants.

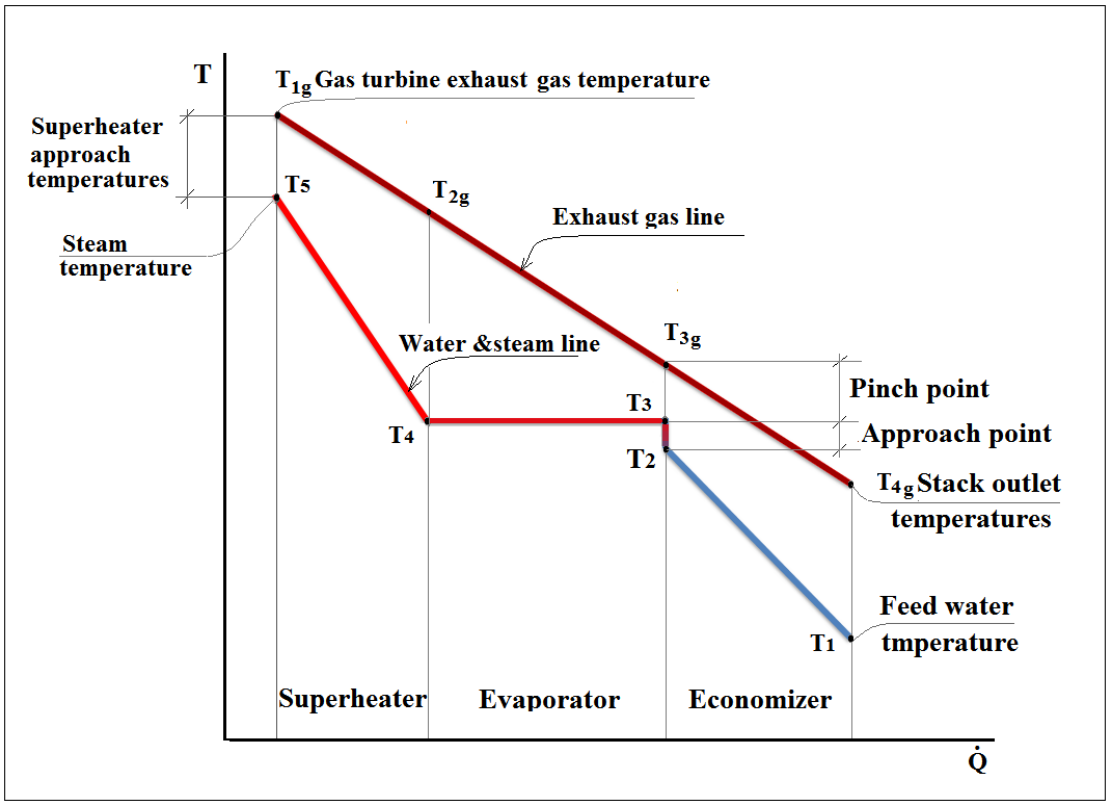

Figure 3-10: T-Q Diagram for a single pressure HRSG

At the beginning of this section it was mentioned that the HRSG should be designed taking both the first and second laws of thermodynamics into consideration. The first law implies that as much heat as possible should be recovered from the flue-gas. The second law, which also embodies a very important factor in the HRSG design, states that the potential or exergy of the flue-gas energy should be utilized as efficiently as possible. In other words, as small amount of entropy as possible should be generated through the process. To evaluate this, an exergy analysis of the system can be performed, which will quantify the deficiencies of the process. If the temperature difference throughout the T-Q diagram is minimized, the process generates a minimum amount of entropy generation (exergy destruction). More details can be found in Section 4.2.4. A reversible or perfect process is one that can return both the system and the surroundings to their initial conditions with no network input. A reversible process will never occur in reality. However, for a heat exchanger, the process is reversible if

there is no temperature difference between the hot and the cold sides. Thus, the irreversibility increases with increasing temperature difference.

Considering the first and second laws of thermodynamics when designing a HRSG means a compromise between the following [54]:

- As much energy as possible should be recovered, i.e., the T-Q diagram should be extended as far as possible along the x-axis
- The temperature difference, i.e. the area between the lines in the T-Q diagram, should be minimized.

3.4.1.3 Dew Point of Exhaust Gas and Water

There are two types of dew points to consider for a HRSG: sulphur dew point and water dew point.

The sulphur dew point must be considered for sulphur-containing fuels. Normally natural gas contains so little sulphur that the dew point is far below any exhaust gas temperatures [78], some authors use (65 °C) as a lower limit for exhaust gas temperature [33]. For oil and solid fuels, depending on the sulphur content, the dew point is typically in the range 100-165 °C [46].

The stack temperature has to be kept above the sulphur dew point temperature in order to avoid corrosion on metal surfaces in the HRSG and stack. The significance of the water dew point is that a liquid phase is formed, which contains acid components. These components may contain sulphur acid (H_2SO_4) or nitric acid (HNO_3). The latter is formed from NO or NO_2 originating from the combustion. The presence of water may cause corrosion.

The water dew point of gas turbine exhaust gas is typically around 40 °C. It is rare that bulk exhaust temperatures become even close to that in power plants. A typical exhaust gas stack temperature in a high-efficiency plant is about 80-100 °C. Even if the bulk exhaust temperature is above the dew point, it may be below the dew point near a cold surface. In order to avoid condensation of water at the tube wall surface, a rule of thumb within the industry is to require the $HRSG$ feed water to enter with a minimum temperature of 60 °C. This means that some kind of preheating is normally required from the condenser temperature up this minimum [78].

Corrosion may also be avoided by using stainless steel, or coating the tubes with a non-corroding material. Both of these options are very expensive in *HRSG* , so the preheating option is preferred.

3.5 Combined Cycle Power Plant

Conventional combined cycle power plant consists of the combination of Brayton and Rankin cycle forming one of the most efficient cycles used for power generation today (Figure 3-11). In the Brayton Cycle, there is the gas turbine cycle, also called the topping cycle and the Rankin Cycle is the steam turbine cycle, also described as bottoming cycle. Thermal efficiency of the combined cycle plants given in Figure 3-1 is somewhat higher today and exceeds 60% [79].

Gas-turbine cycles typically operate at considerably higher temperatures than steam cycles. The maximum fluid temperature at the turbine inlet is about 620°C for modern steam power plants, but over 1425°C for gas-turbine power plants. It is over 1500°C at the burner exit of turbojet engines. The use of higher temperatures in gas turbines was made possible by recent developments in cooling the turbine blades and coating the blades with high temperature resistant materials such as ceramics.

Because of the higher average temperature at which heat is supplied, gas-turbine cycles have a greater potential for higher thermal efficiencies. However, the gas-turbine cycles have one inherent disadvantage: the gas leaves the gas turbine at very high temperatures (usually above 500°C), which erases any potential gains in the thermal efficiency. The situation can be improved somewhat by using regeneration, but the improvement is limited. It makes engineering sense to take advantage of the very desirable characteristics of the gas-turbine cycle at high temperatures and to use the high temperature exhaust gases as the energy source for the bottoming cycle such as a steam power cycle.

The result is a combined gas–steam cycle, as shown in Figure 3-1. In this cycle, energy is recovered from the exhaust gases by transferring it to the steam in a heat exchanger that serves as the boiler. In general, one (or more) gas turbine is needed to supply sufficient heat to the steam. In addition, the steam cycle may involve regeneration as well as reheating. Energy for the reheating process can be supplied by burning some additional fuel in the oxygen-rich exhaust gases. The gas turbine flue gas

temperature is within the range 450-650 °C. The energy contained in the flue gas is an amount of the fuel energy that is not converted to power by the gas turbine. This energy is used to raise steam and to produce power by the steam turbine. Depending upon the type of HRSG the flue gas temperature is reduced to 80-200 °C, where the lower value is typical for large modern combined cycle burning a fuel with no or very little sulfur. The steam is produced with a temperature in the range 450-560 °C, and a pressure in the range 30-170 bar. Steam may be produced at multiple pressure levels. The use of super-critical steam pressure (>220.64 bar) was suggested by Bolland [78]. Super-critical steam pressure gives the combined cycle potentially higher efficiency, but it depends on size of the steam turbine and dependence of pressure on the steam turbine efficiency.

The cycle operating at the higher temperatures is called the topping cycle, while the cycle reutilizing the energy flux is the bottoming cycle. The Combined Cycle Gas Turbine power plant uses the Brayton cycle as the topping cycle while the Ranking cycle acts as the bottoming cycle.

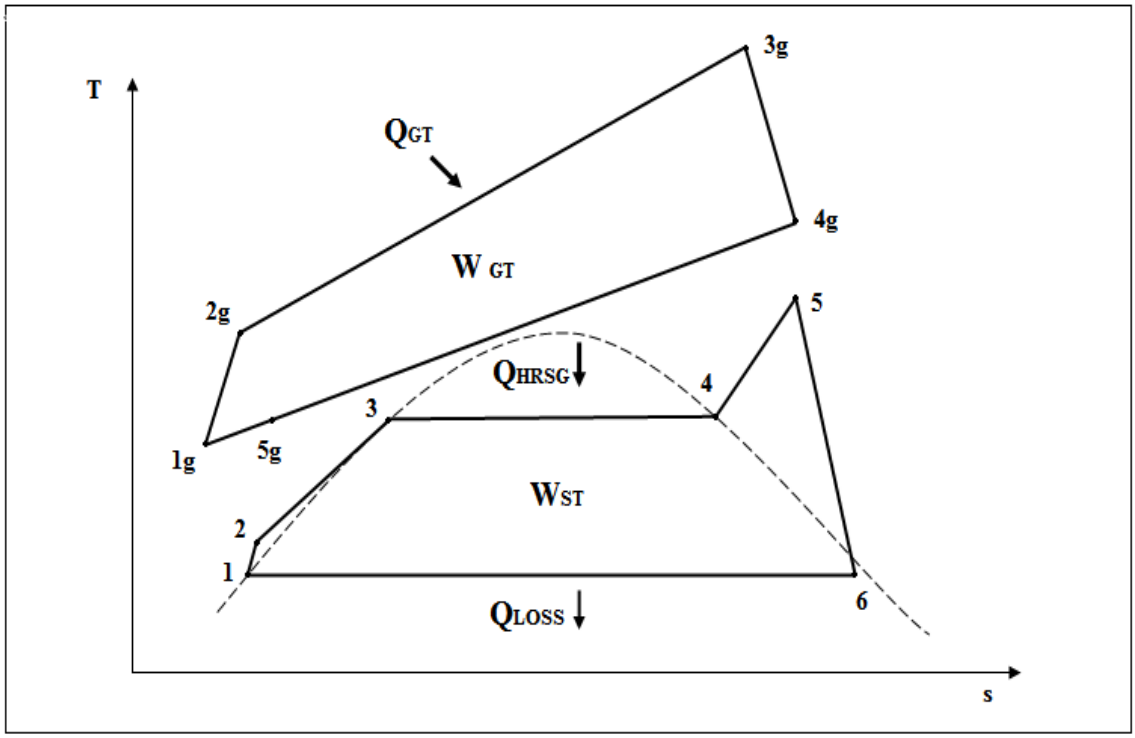

Figure 3-11 T-s diagram of the combined cycle gas turbine CCGT process

4 Exergoeconomic Analysis and Optimization - Background

This chapter provides a fundamental background for the development of exergoeconomic optimization, with the governing equations necessary to achieve the optimization purposes. The exergoeconomic optimization technique consists of the following steps.

4.1 Energy Analysis

An energy analysis is based on the first law of thermodynamics. The first law of thermodynamics is more commonly known as the law of energy conservation. The first law of thermodynamics indicates that energy can neither be created nor destroyed, and it can only change from one form to another. This law defines internal energy as a state function, and provides a formal statement of the conservation of energy. The most common energy systems, such as power generation and refrigeration systems, are open systems (systems in which mass flows through the various components). The typical components of power and refrigeration systems are boilers, turbines, evaporators etc., all of which have inlets and outlets. The expression of the first law of thermodynamics for open systems is:

$$\begin{bmatrix}\text{Rate of Internal}\\ \text{Energy Change}\\ \text{within Control Volume}\end{bmatrix}=\begin{bmatrix}\text{Net Rate}\\ \text{of Heat}\\ \text{Addition}\end{bmatrix}-\begin{bmatrix}\text{Net Rate}\\ \text{of}\\ \text{work out}\end{bmatrix}+\begin{bmatrix}\text{Rate of}\\ \text{Energy Addition}\\ \text{with Mass}\end{bmatrix}+\begin{bmatrix}\text{Rate of}\\ \text{Energy Removal}\\ \text{with Mass}\end{bmatrix} \quad (4\text{-}1)$$

The mathematical equation for the first law of thermodynamics for an open system, or any component in an open system, is:

$$\left(\frac{dE}{dtr}\right)_{CV}=\dot{Q}-\dot{W}_{CV}+\sum\dot{m}_i\left(h_i+\frac{1}{2}V^2+gz_i\right)-\sum m_e\left(h_e+\frac{1}{2}V_e+gz_e\right) \quad (4\text{-}2)$$

where $\left(\frac{dE}{dtr}\right)_{CV}$ is the time rate of change of the total energy stored within the given control volume, $\dot{Q}$ is the net rate of heat addition, $\dot{w}_{CV}$ is the net rate of the non-flow work out; and $\sum\dot{m}\left(h+\frac{1}{2}V^2+gz\right)$ is the rate of the energy h is the specific enthalpy, $\frac{1}{2}V^2$ is the specific kinetic energy, and gz is the specific potential energy addition or

removal due to mass flowing ($\dot{m}$) into (i) or out of (e) the given control volume. For almost every typical component in an energy system, the velocity and height differences for the working fluid flows can be ignored, so that the rates of energy addition and removal are only associated with the enthalpy, such that:

$$\begin{bmatrix} \text{Rate of Energy} \\ \text{Addition with Mass} \end{bmatrix} = m_i h_i \tag{4-3}$$

$$\begin{bmatrix} \text{Rate of Energy} \\ \text{Removal with Mass} \end{bmatrix} = m_e h_e \tag{4-4}$$

An energy analysis is commonly used in evaluating the performance of a component or a system, and can be used to determine the first law efficiency (η_{th}) for a power production cycle.

However, an energy balance provides no information about the direction in which processes can spontaneously occur and/or the reversibility of the thermodynamic processes. The first law cannot provide information about the inability of any thermodynamic process to convert heat fully into mechanical work, or any insight into why mixtures cannot spontaneously separate themselves [56].

4.2 Exergy Analysis

Exergy can be defined briefly as: the maximum theoretical work obtained from a system when this system is brought from a state to equilibrium with the environment while interacting only with the environment. The state of a system is defined by temperature, pressure, and composition. In addition, exergy is the minimum theoretical work needed to bring the system from equilibrium with the environment to the given state. This means that exergy is a measure of the departure of the state of a system from the state of the environment. This makes exergy an attribute of both the system and environment together. The definition of exergy will not be complete, however, until we define the reference environment.

Exergy analysis is a method that uses the conservation of mass and conservation of energy principles together with the second law of thermodynamics for the analysis, design, and improvement of energy systems. The exergy method is a useful tool for furthering the goal of more efficient energy-resource use, for it enables the locations, types, and true magnitudes of wastes and losses to be determined.

4.2.1 Exergy of a System

The total exergy is that exergy that can be extracted through heat and work processes, hence,

$$\Delta \dot{E}_{system} = \Delta \dot{E}_{heat} - \Delta \dot{E}_{work} \tag{4-5}$$

Exergy associated with work transfer: from the definition of the work, that equivalent of a given form of energy as a measure of its exergy, clearly work is equivalent to exergy in every respect. Thus, exergy transfer can be specified both in magnitude and in direction by the work transfer to which it corresponds [59].

$$\Delta \dot{E}_{work} = W + \int p_0 dV \tag{4-6}$$

Exergy associated with heat transfer: assuming a uniform temperature distribution in a thermal energy reservoir, the exergy transfer rate, $\Delta \dot{E}_{work}$ connected with the heat transfer rate Q, can be calculated by the following formula [60]:

$$\Delta \dot{E}_{heat} = (1 - \frac{T_0}{T})\dot{Q} , \tag{4-7}$$

substituting equation (4-6) and (4-7) in equation (4-5),

$$\Delta \dot{E}_{system} = (Q - T_o \int dS) - (W - \int p_o dV) \tag{4-8}$$

and rearranging

$$\Delta \dot{E}_{system} = Q - W - T_o \int dS + \int p_o dV . \tag{4-9}$$

Introducing the first law:

$$\Delta E = Q - W \tag{4-10}$$

eliminates Q and W yielding,

$$\Delta \dot{E}_{system} = \Delta E - T_o \int dS + \int p_o dV \tag{4-11}$$

expanding

$$\Delta \dot{E} = \Delta U - T_o \int dS + \int p_o dV + m \frac{1}{2} V^2 + mgz \tag{4-12}$$

Integrating the above between the state of the system and the dead state yields,

$$\dot{E} = U - U_o - T_o (S - S_o) + p_o (V - V_o) + m \frac{1}{2} V^2 + mgz , \tag{4-13}$$

equation (4-13) can be expressed on unit-of-mass basis,

$$\dot{e} = (u - u_o) + p_o (v - v_o) - T_o (s - s_o) + \frac{1}{2} V^2 + gz , \tag{4-14}$$

here V is the velocity of the system relative to the reference frame of the environment and z is the height of the system relative to the reference frame of the environment (where $z_o = 0$ usually the ground).

4.2.2 Exergy Component

The total exergy of a system $\dot{E}$ can be divided into four components: physical exergy $\dot{E}_{PH}$, kinetic exergy $\dot{E}_{KN}$, potential exergy $\dot{E}_{PT}$, and chemical exergy $\dot{E}_{CH}$,

$$\dot{E} = \dot{E}_{PH} + \dot{E}_{KN} + \dot{E}_{PT} + \dot{E}_{CH} \tag{4-15}$$

$$\dot{e} = \dot{e}_{PH} + \dot{e}_{KN} + \dot{e}_{PT} + \dot{e}_{CH} \tag{4-16}$$

equation (4-15) can be expressed on unit-of-mass basis.

4.2.2.1 Kinetic Exergy

Kinetic exergy $\dot{e}_{KN}$ is equal to kinetic energy calculated with the velocity of movement with respect to the environment.

$$\dot{e}_{KN} = \frac{1}{2}V^2 \tag{4-17}$$

4.2.2.2 Potential Exergy

Potential exergy $\dot{e}_{PT}$ is determined with potential energy with respect to zero level connected to the environment. Since potential energy must take into account all the forces affecting the examined matter and environment, it means that, besides the environment force, one should also take into account the force generated by the pressures of the environment components. Assuming that the acceleration of gravity does not vary with height, potential energy can be calculated from the following:

$$\dot{e}_{PT} = gz - g\int_o^h \gamma_o dh \tag{4-18}$$

where g, h and γ_o are gravity acceleration, height of matter center with respect to zero level and environment density respectively.

4.2.2.3 Physical Exergy

Physical exergy represents a part of the exergy that appears due to the difference in temperature and pressure of the observed matter and the temperature and pressure of the environment (T_o, p_o). It is naturally divisible into two components.

Thermal component $e_{PH}^{\Delta T}$, is the component resulting from the temperature difference between the stream and the environment,

$$e_{PH}^{\Delta T} = cp\left[(T - T_o) - T_o \ln\frac{T}{T_o}\right], \tag{4-19}$$

where T, T_o and cp signify temperatures of the given gas, temperatures of the environment and specific thermal capacity.

Pressure component $e_{PH}^{\Delta p}$, the component resulting from the pressure difference between the stream and the environment [59].

$$e_{PH}^{\Delta p} = (h - h_o) + T_o (s - s_o) \tag{4-20}$$

4.2.2.4 Chemical Exergy

In determining physical exergy, the final state of stream is the environmental state. Now, this state will be the initial state in the reversible processes that are used to determine the chemical exergy of this material stream. According to the definition of exergy, the final state to which the substance will be reduced is the standard dead state. Thus, chemical exergy is defined as the maximum work obtainable when the substance under consideration is brought from environmental state to the standard dead state by process involving heat transfer and exchange of substances only with the environment [59].

To determine a substance's chemical exergy, we need to define a reference environment in terms of its temperature T_o, pressure p_o, and chemical composition. In some reference-environment models, substances present in atmosphere, the hydrosphere, and the upper part of the crust of the earth, at pressure p_o and temperature T_o, forms the basis of a reference environment. In some models, these substances are allowed to react with each other hypothetically and allowed to reach a stable state with a minimum Gibbs energy, at sea level, at rest without other force fields [59].

The general form of chemical exergy equation of mixture can be written as

$$\dot{e}_{CH} = \sum x_n (\dot{e}_o)_n + \bar{R} T_o \sum x_n \ln x_n \tag{4-21}$$

$$\dot{e}_o = T_o \ln\frac{p_o}{p_{oo}} \tag{4-22}$$

here, x_n is the mole fraction of the k_{th} gas in the mixture, $\dot{e}_o$ is the chemical exergy of reference substances, $\bar{R}$ is the universal gas constant and p_{oo} is partial pressure of the gaseous reference substance.

Equation for the fuel specific exergy $\dot{e}_{CH,fuel}$ given as:

$$\dot{e}_{CH,fuel} = \beta(LHV) \tag{4-23}$$

and the exergy factor β is given by [59],

$$\beta = 1.0437 + 0.1882\left(\frac{h}{c}\right) + 0.0610\left(\frac{o}{c}\right) + 0.0401\left(\frac{n}{c}\right) \tag{4-24}$$

where c, h, o and n are the mass fractions of C, H, O and N respectively.

4.2.3 Exergy Balance

By combining the first and second law of thermodynamics, the mathematical equation of an exergy balance is [61],

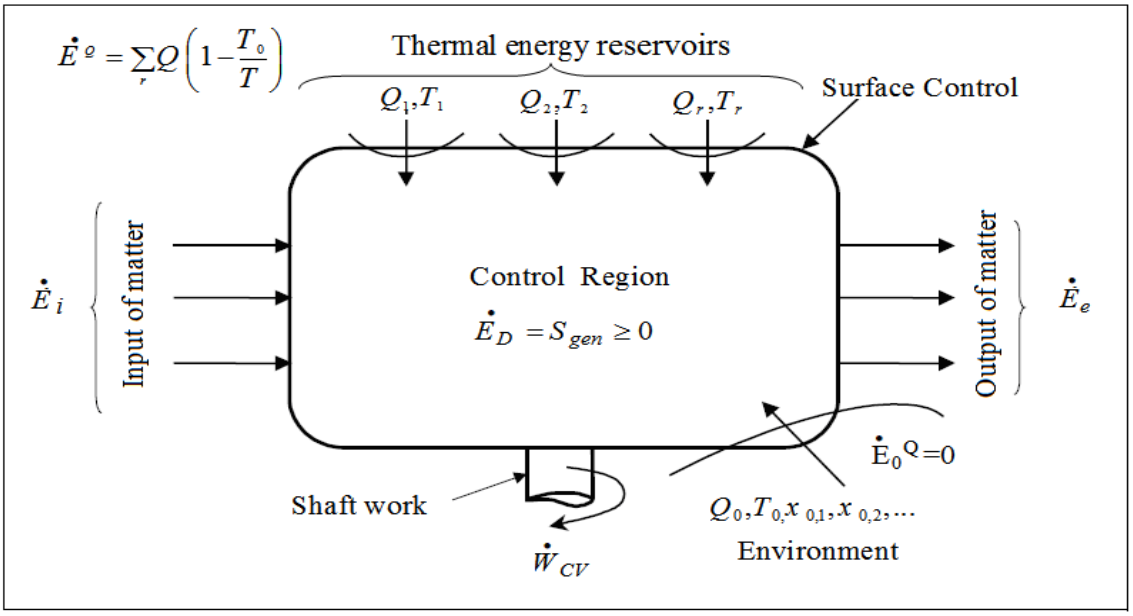

Figure 4-1: Steady state process in an open control region [59]

An expression of an exergy analysis for an open system is:

$$\begin{bmatrix}\text{Rate of}\\ \text{Exergy change}\\ \text{within}\\ \text{Control}\\ \text{Volume}\end{bmatrix} = \begin{bmatrix}\text{Net}\\ \text{Exergy}\\ \text{Transfer}\\ \text{by Heat}\end{bmatrix} + \begin{bmatrix}\text{Net}\\ \text{Exergy}\\ \text{Transfer}\\ \text{by Work}\end{bmatrix} - \begin{bmatrix}\text{Rate of}\\ \text{Exergy}\\ \text{Addition}\\ \text{with Mass}\end{bmatrix} + \begin{bmatrix}\text{Rate of}\\ \text{Exergy}\\ \text{Removal}\\ \text{with Mass}\end{bmatrix} + \begin{bmatrix}\text{Exergy}\\ \text{Destruction}\\ \text{within}\\ \text{control}\\ \text{Volume}\end{bmatrix} \tag{4-25}$$

$$\left(\frac{d\dot{E}}{dt}\right)_{CV} = \sum_j (1-\frac{T_o}{T_j})\dot{Q}_j - W_{CV} + \sum m_i \dot{e}_i - \sum m_e \dot{e}_e - \dot{E}_D \qquad (4\text{-}26)$$

where $\left(\frac{d\dot{E}}{dt}\right)_{CV}$ is the time rate of change of the exergy stored within the control volume, $\sum_j (1-\frac{T_o}{T_j})\dot{Q}$ is the net exergy change due to heat transfer, T_j is the temperature at j^{th} control volume boundary (where the heat is crossing into the control volume at that boundary); W_{CV} is the net exergy transfer due to non-flow work out of the control volume; $\sum m\dot{e}$ is the exergy addition (i) or removal (e) due to mass flow; and $\dot{E}_D = T_o S_{gen}$ is the exergy destruction within the control volume.

4.2.4 Exergy Wastes (Exergy Destructions and Exergy Losses)

The thermal system under consideration for analysis is supplied with some input (fuel exergy $\dot{E}_F$) derived from energy source. This input transfers into some exergy output (product exergy $\dot{E}_P$). For a real process the exergy input always exceeds the exergy output, and this unbalance is due to waste in exergy; it is useful to differentiate between types of exergy wastes in order to study where irreversibilities occur. Two kinds of exergy wastes can be distinguished: internal and external [60].

External exergy wastes (exergy losses $\dot{E}_{loss}$) represent the remaining exergy contents of losses and emissions that are dissipated or removed from the production and embody, thus unused (exergy remaining non-utilized output) .

Internal exergy wastes (exergy destruction $\dot{E}_D$) correspond to the wastes of quality due to internal inefficiencies within the process, it is the direct result of the irreversibility's in a system. These internal irreversibilities may be of technical nature due to technical inefficiencies within the plant, e.g. friction or lack of insulation, or they may be of a structural nature. Structural exergy destruction $\dot{E}_D$ is determined by the principle and design of the system. Whereas technical exergy destruction $\dot{E}_D$ can be reduced through optimization, structural waste can be reduced only by redesigning the system.

The exergy loss is associated with the design engineer's decision not to further use the exergy of a stream in a given system (unused exergy, i.e. exergy flow to the environment). Both represent exergy waste, but irreversibilities have by definition, no exergy and no environment effects. The exergy destruction is related to the entropy generation equation.

$$\dot{E}_{loss} = \dot{E}_{out} - \dot{E}_P \tag{4-27}$$

$$\dot{E}_D = \dot{E}_{in} - \dot{E}_{out} \tag{4-28}$$

$$\dot{E}_{waste} = \dot{E}_D + \dot{E}_{loss} \tag{4-29}$$

For the exergy analysis, it is necessary to define product and fuel for each component and for overall system. The product is defined according to the purpose of owning and operating the component under consideration and fuel represent the resources consumed in generating the product. Fuel and product are expressed in terms of exergy. Exergy destruction is the amount of exergy lost due to irreversibilities and cannot be used anywhere. The exergy losses is the amount of exergy that is lost from the system under consideration, but can be useful to other system.

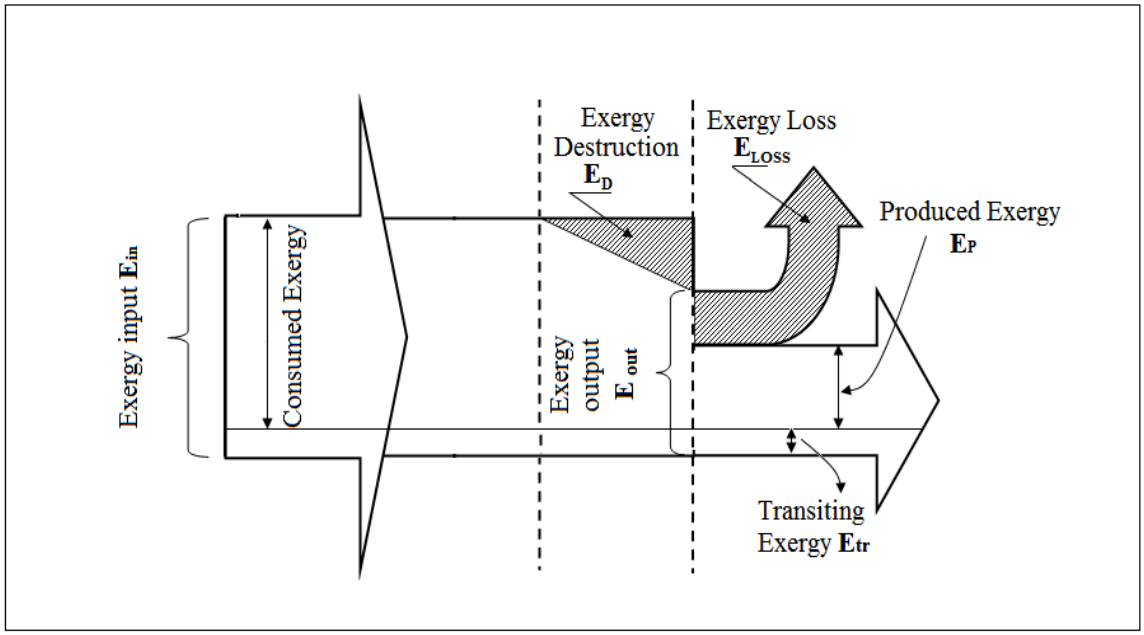

Figure 4-2: Graphical presentation of overall exergy balance [88]

The exergy destruction can be calculated from equation (4-26), the exergy destruction equation for any control volume at steady state with negligible kinetic and potential energy changes can be written as in equation (4-30).

$$\dot{E}_D = \sum_j (1 - \frac{T_o}{T_j})\dot{Q}_j - W_{CV} + \sum \dot{E}_i - \sum \dot{E}_e \quad (4\text{-}30)$$

An exergy balance, by definition, only exists for reversible processes. Thus, for real processes, i.e. irreversible processes, exergy is never in balance, because the total exergy input always exceeds the total exergy output, i.e. $\dot{E}_{in} > \dot{E}_{out}$. Hence, it is misleading to talk about an exergy balance for real processes.

By calculating the exergy waste, i.e. destruction and loss, we can visualize possible process improvements. In general, when the exergy loss is high, we should consider improving this part first. However, this approach is not always appropriate. The reason is that every part of the system depends on each other and an improvement in one part may cause increased losses in other parts, so that the total losses in the modified process may be equal or even larger than in the original process configuration. Therefore, the problem needs a more carefully approach, which we will discuss below [63].

The rate of exergy destruction in a system component can be compared to the exergy rate of the fuel provided to the overall system $\dot{E}_{F,TOT}$, giving the exergy destruction ratio:

$$y_D = \frac{\dot{E}_D}{\dot{E}_{F,TOT}} \quad (4\text{-}31)$$

The component exergy destruction rate can be compared to the total exergy destruction rate within the system $\dot{E}x_{D,TOT}$ giving the ratio:

$$y^*_D = \frac{\dot{E}_D}{\dot{E}_{D,TOT}} \quad (4\text{-}32)$$

The exergy loss ratio is defined similarly by comparing the exergy loss to the exergy of the fuel provided to the overall system.

$$y_{Loss} = \frac{\dot{E}_{Loss}}{\dot{E}_{F,TOT}} \quad (4\text{-}33)$$

4.2.5 Exergy Efficiency

Exergy efficiencies can be used for various purposes. An obvious application is to use them for assessing, analyzing, and optimizing processes and systems. Exergy efficiencies are particularly valuable in analyzing and optimizing systems. An exergy

analysis usually includes a detailed calculation of the exergy values of process flows and the exergy waste in the system. Such a calculation shows the places in the system where waste occur. In the analysis, the question that has to be answered is how the exergy losses can be avoided or limited. Based on the absolute value of exergy loss, it is usually difficult to assess whether an exergy waste in an apparatus is unnecessarily large. An exergy efficiency in which the exergy loss is compared with the added or transferred exergy gives a better picture of the quality of the processes in the apparatus, and thus gives a better impression of whether exergy waste can be reduced.

The calculation of exergy efficiency can be a rather difficult subject due to the lack of standardization and ambiguity of some terms found in the literature.

Two main classes of exergy efficiencies definitions will be presented next, universal exergy efficiency and functional exergy efficiency, and several authors have provided these definitions [62].

4.2.5.1 Universal Exergy Efficiency

Universal exergy efficiency is defined as a ratio of gross exergy output to gross exergy input Figure 4-3. There are two main classes of universal exergy efficiencies reported in the literatures. The first is simple efficiency and the second is the efficiency with transiting exergy [89].

- Simple Efficiency

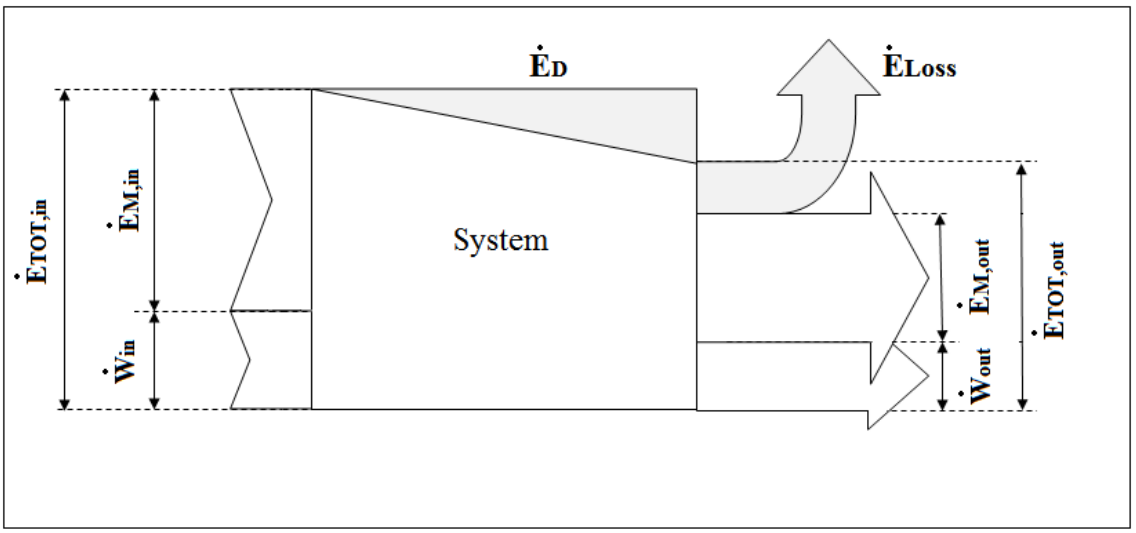

Figure 4-3 Simple exergy efficiency [89]

Because of its simplicity, it is a generally applicable definition for exergy efficiency. This form of efficiency is based on the exergy balance to express all exergy input as used exergy, and all exergy output as utilized exergy equation (4-29). Therefore, the exergy efficiency ε becomes [62]:

$$\varepsilon = \frac{\dot{E}_{out}}{\dot{E}_{in}} = 1 - \frac{\dot{E}_D}{\dot{E}_{in}} \tag{4-34}$$

However, this efficiency does not always provide an adequate characterization of the thermodynamic efficiency of processes, such as heat transfer, separation, expansion etc.

There is often a part of the output exergy which is unused, i.e. an exergy loss $\dot{E}_{loss}$ to the environment; moreover, the exergy efficiency ε_1 becomes

$$\varepsilon_1 = \frac{\dot{E}_{out} - \dot{E}_{loss}}{\dot{E}_{in}} = \varepsilon - \frac{\dot{E}_{loss}}{\dot{E}_{in}} \tag{4-35}$$

- Efficiency with Transiting Exergy

Efficiency with transiting exergy ε_{tr} is seen as an improvement of the simple efficiency. The untransformed components are here subtracted from the incoming and the outgoing components (Figure 4-2). The efficiency will be defined by:

$$\varepsilon_{tr} = \frac{\dot{E}_{out} - \dot{E}_{tr}}{\dot{E}_{in} - \dot{E}_{tr}} \tag{4-36}$$

where $\dot{E}_{tr}$ is the transiting exergy and it is defined as the part of the exergy which traverses a system without taking any part in the mechanical, thermal or chemical changes which take place in the system.

The universal efficiency offers a clear definition for a variety of systems. A disadvantage of this definition, however, is that the efficiency values obtained can be insensitive to changes in the system.

4.2.5.2 Rational Exergy Efficiency (Functional)

Rational Efficiency: rational efficiency ψ is defined by [59]. This efficiency is given by the ratio of the desired exergy output to the exergy used:

$$\psi = \frac{\Delta\dot{E}_{out}}{\Delta\dot{E}_{in}} = \varepsilon_p = \frac{\Delta\dot{E}_P}{\Delta\dot{E}_F} \tag{4-37}$$

where $\Delta\dot{E}_{out}$, is the sum of all exergy transfers making up input, and $\Delta\dot{E}_{in}$ is the sum of all exergy transfers making up output.

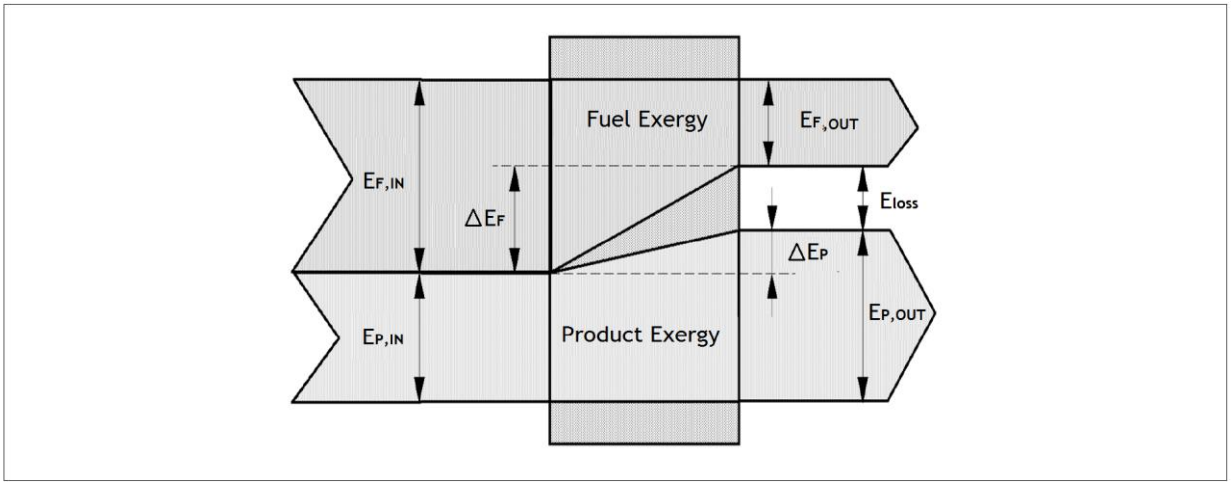

Figure 4-4 Explanation of efficiency definitions (heat exchanger)

4.3 Exergoeconomic

Exergoeconomics (exergoeconomic analysis) is defined as a branch of engineering that incorporates exergy analysis at the system component level into the economic laws, in order to provide useful information for the designer or operator to cost-effectively design or operate the system. It should be noted that this information could not be obtained using regular energy or exergy analysis, and/or economic analysis separately. Exergoeconomics rests on the notion that exergy is the only rational basis for assigning monetary costs to the interactions that a system experiences with its surroundings and to the sources of thermodynamic inefficiencies within it. Tsatsaroinis [64] calls this approach exergy costing. When exergy costing is not applied, authors should use a different term (e.g., thermoeconomics). Thermoeconomics, being a more general term and characterizing any combination of a thermodynamic and economic analysis, might also be used instead of the term exergoeconomics (but not vice versa).

The second law of thermodynamics combined with economics represents a very powerful tool for the systematic study and optimization of energy systems. This combination forms the basis of the relatively new field of thermoeconomics or exergoeconomics [2].

4.4 Exergoeconomic Analysis

Exergoeconomics combines the principles of exergy and economic analyses, at the level of system components. Through exergoeconomic analysis, the effectiveness of various energy converting systems can be compared considering unit costs of products. This comparison, however, cannot be performed considering separately exergy and economic principles. In an exergoeconomic analysis of a system, exergy is recognized as the rational basis for assigning monetary costs to the interactions between the system and its surroundings as well as to the sources of thermodynamic inefficiencies within the system. The objectives of an exergoeconomic analysis are [62]:

- To identify the location, magnitude, and sources of exergy destruction and exergy losses in an energy system
- To calculate the cost associated with the exergy destruction and exergy losses
- To assess the production costs of each product in the energy conversion system, which has more than one output
- To facilitate feasibility and optimization studies during the design phase for an energy system, as well as process improvement studies for an existing system
- To assist in decision-making procedures concerning plant operation and maintenance
- To compare technical alternatives

This exergoeconomic analysis consists of three main steps:

4.4.1.1 Quantifying of Energy and Exergy Streams

Refers to the application of the mass and energy conservation expressions as well as the exergy balance, respectively, to each component of the system (control volume) as mentioned above in section 4.1 and section 4.2

4.4.1.2 Definition of Fuel and Product for each System Component

In exergoeconomic analysis, fuel and product are defined for each component. The product is what we desire from a component, in terms of exergy, and the fuel is the required exergy to generate the product [65].

4.4.1.3 Cost Balance

Exergy costing involves cost balance usually formulated for each component separately. A cost balance applied to the k^{th} system components shows that the sum of cost rates associated with all existing exergy stream equals the sum of cost rates of all entering exergy streams, plus the appropriate charges due to capital investment and operating and maintenance expenses. The sum of the last two terms is denoted by $\dot{Z}_k$. Accordingly, for each flow line in the system, a parameter called flow cost rate $\dot{C}(\$s^{-1})$ is defined, and the cost balance equation of each component is written as [66]:

$$\sum_e \dot{C}_{e,k} + \dot{C}_{w,k} = \dot{C}_{q,k} \sum_i \dot{C}_{i,k} + \dot{Z}_k \tag{4-38}$$

where i, e, q indicate the entering, exiting, heat and work streams for component k

$$\dot{C}_j = c_j \dot{E}_j \tag{4-39}$$

where c is the specific cost per unit exergy, using equation (4-38), one can write:

$$\sum_e (c_e \dot{E}_e)_k + c_{w,k} \dot{W}_k = c_{q,k} \dot{E}_{q,k} \sum_i (c_i \dot{E}_i)_k + \dot{Z}_k \tag{4-40}$$

In the cost balance formulation, equation (4-38), there is no cost term directly associated with exergy destruction of each component. Accordingly, the cost associated with the exergy destruction in a component or process is a hidden cost. Thus, if one combines the exergy balance and exergoeconomics balance together, one can obtain the following equation:

$$\dot{E}_{D,k} = \dot{E}_{F,k} - \dot{E}_{P,k} - \dot{E}_{loss,k} \tag{4-41}$$

where $\dot{E}_{D,k}$ represents the exergy destruction rate for k^{th} component, and $\dot{E}_{loss,k}$ stands for the exergy losse of k^{th} component, $\dot{E}_{F,k}$ and $\dot{E}_{P,k}$ are the fuel exergy and the product exergy rate of k^{th} component, respectively.

Accordingly, the expression for the cost of exergy destruction is defined as:

$$\dot{C}_{D,k} = c_{F,k} \dot{E}_{D,k} \tag{4-42}$$

where $c_{F,k}$ is the the average cost per unit exergy of fuel for k^{th} component.

After applying the equations for the costing balance equation (4-40) to (4-42) there are N exergy streams exiting the component to be considered, with N_e

unknowns and only one equation, the cost balance. Therefore, we need to formulate $N_e - 1$ auxiliary equations.

This is accomplished with the aid of the F and P principles in the specific exergy costing approach [34].

F- Principle: The F principle refers to the removal of exergy from an exergy stream within the component being considered (when for this stream the exergy difference between inlet and outlet is considered in the definition of the fuel). The F principle states that the specific cost (cost per exergy unit) associated with this removal of exergy from a fuel stream must be equal to the average specific cost at which the removed exergy was supplied to the same stream in upstream components. In this way, we obtain one auxiliary equation per each removal of exergy so that the number of auxiliary equations provided by the F principle is always equal to the number $N_{e,F}$ of exiting exergy streams that are associated with the definition of the fuel for the component. It is worth noting that no auxiliary costing equation is required for an entering exergy stream for which no difference between inlet and outlet is considered in the fuel definition.

P- Principle: The P principle refers to the supply of exergy to an exergy stream within the component being considered. The P principle states that each exergy unit is supplied to any stream associated with the product at the same average cost, which is denoted with c_P. Since each stream to which exergy is supplied corresponds to an existing stream, the number of auxiliary equations provided by the P principle is always equal to $N_{e,P} - 1$ where $N_{e,P}$ is the number of exiting exergy streams that are included in the product definition. Since each exiting exergy stream is associated either with the fuel or with the product, the total number of exiting streams (N_e) is equal to the sum ($N_{e,F} + N_{e,P}$). Thus, the F and P principles together provide the required $N_e - 1$ auxiliary equations.

In addition, several methods were suggested to express the purchase cost rate $\dot{Z}_k$ of equipment in terms of design parameters in equation (4-38). For converting the capital investment into cost per time unit, one may write

$$\dot{Z}_k = \frac{Z_k CRF \varphi}{3600N} \tag{4-43}$$

where Z_k is the purchase cost of k^{th} component in dollar.

The capital recovery factor CRF depends on the interest rate as well as estimated equipment lifetime. CRF was determined using the following relation [67]:

$$CRF = \frac{i(1+i)^n}{(1+i)^n - 1} \tag{4-44}$$

here, i is the interest rate and n is the total operating period of the system in years.

In equation (4-43), N is the annual number of the operation hours of the unit, and φ is the maintenance factor.

4.4.2 Exergoeconomic Evaluation

Average cost per exergy unit of fuel and product for the component k was defined using the equations:

$$c_{F,k} = \frac{\dot{C}_{F,k}}{\dot{E}_{F,k}} \tag{4-45}$$

$$c_{P,k} = \frac{\dot{C}_{P,k}}{\dot{E}_{P,k}} \tag{4-46}$$

where $c_{F,k}$ and $c_{P,k}$ are the average unit cost of fuel and product respectively. In order to conduct exergoeconomic analysis exergoeconomic variables of the component k, such as: cost rate of exergy destruction $\dot{C}_D$, relative cost difference r_k and exergoeconomic factor f_k have to be calculated. Cost rate of exergy destruction $\dot{C}_D$ were calculated using the equation (4-42) and equation (4-34), the relative cost difference r_k and exergoeconomic factor f_k are known as the thermoeconomic variables and they were calculated using the equations (4-47) and (4-48), among which r_k and f_k are the most important two exergoeconomic variables to rank the components based on their individual performance. The relative cost difference r_k is expressed as the difference between the specific cost of the product $c_{P,k}$ and the fuel $c_{F,k}$:

$$r_k = \frac{c_{P,k} - c_{F,k}}{c_{F,k}} \tag{4-47}$$

The cost added to an exergy stream due to the thermodynamic inefficiency within one component can be evaluated by the component exergoeconomic factor

through which the monetary impact of exergy destruction and capital investment of each component can be revealed:

$$f_k = \frac{\dot{Z}_k}{\dot{Z}_k + \dot{C}_{D,k}} \tag{4-48}$$

The relative cost difference for component k represents the increase in the unit cost of exergy between product and fuel (expressed in relation to the unit cost of fuel relative cost difference) is a very good way of pointing out ineffective elements in the system, which may have serious influence on the formation of costs in the system. Together with the exergoeconomic factor, it is one of the most useful parameters in thermoeconomic optimization. The exergoeconomic factor defines what portion of the cost rate increase in considered components is caused by the destruction and loss of exergy, and which portion is due to a purchase and maintenance cost. By comparing the values obtained in calculations for typical components with the values for the particular type of component, which can be found in literature, it is possible to find the optimum balance between component efficiency and investment cost.

5 Mathematical Modeling of CCGT Optimization

5.1 System Description

A complex configuration of the combined cycle gas turbine power plant is chosen to be studied in this thesis. The triple pressure combined cycle gas turbine was selected for this research (as shown in the schematic diagram, Figure 5-1). The system consists of a gas turbine, heat recovery steam generator, feed water tank, condenser, two generators, pumps, and the high, intermediate, and low-pressure steam turbine. The fuel used is natural gas.

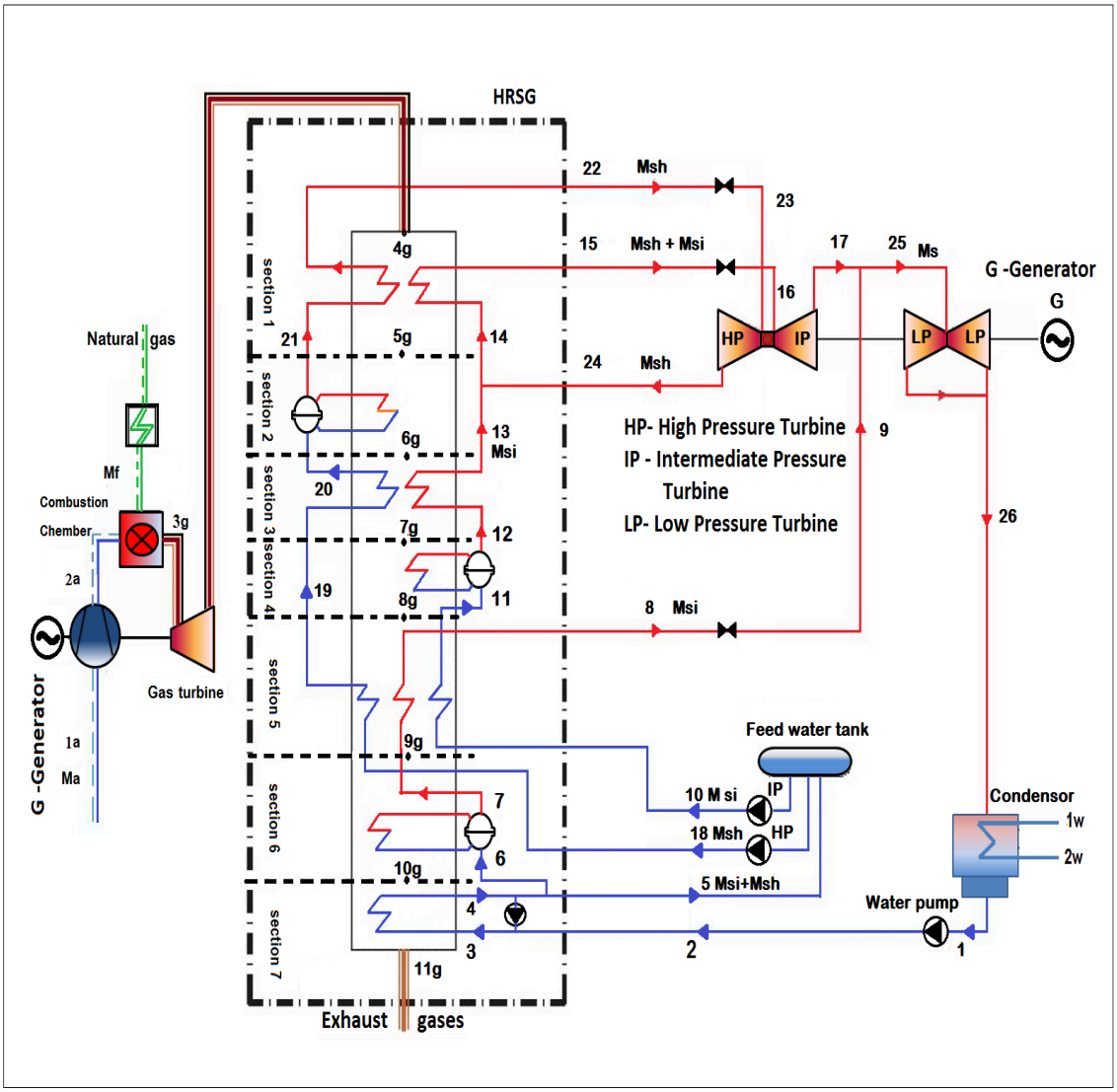

Figure 5-1 A schematic diagram of the triple pressure combined cycle power plant

5.1.1 Gas Turbine

The gas turbine model used in this study was Siemens SGT5–PAC 4000F, formerly known as V94.3A. The parameters of the Siemens V94.3A gas turbine are listed in Table 5-1 [68]. The exhaust gas parameters at the outlet of the gas turbine (mass flow rate, temperature, and chemical composition) were defined as the inlet parameters of the HRSG and they were not a subject for further consideration.

Table 5-1 Gas turbine parameters

SIEMENS GAS TURBINE PARAMETERS	Value
Ambient air pressure [bar]	1.013
Ambient air temperature [°C]	15
Net power output (P_{GT}) [MW]	288
Turbine isentropic efficiency [%]	92
Compressor isentropic efficiency [%]	82
Compression ratio [-]	18
Air mass flow rate [kgs^{-1}]	679
Fuel mass flow rate [kgs^{-1}]	19
Pressure drop in the combustion chamber [bar]	0.01
Exhaust gas mass flow [kgs^{-1}]	688
Gas turbine inlet temperature [°C]	1300
Exhaust gas temperature at the gas turbine outlet [°C]	580
The gas turbine efficiency [%]	39.5
Net heat rate [kJ/kWh]	9.114
Lower heat value of the fuel [$kJkg^{-1}$]	47141

5.1.2 Heat Recovery Steam Generator HRSG

Triple-pressure HRSG is placed after the gas turbine. Hot exhaust gases from gas turbine are conducted through the heat recovery steam generator heaters to generate steam for the steam turbine. The HRSG in this study consists of three-pressure levels

(low, intermediate, and high) where each pressure level is made up of several heat exchangers.

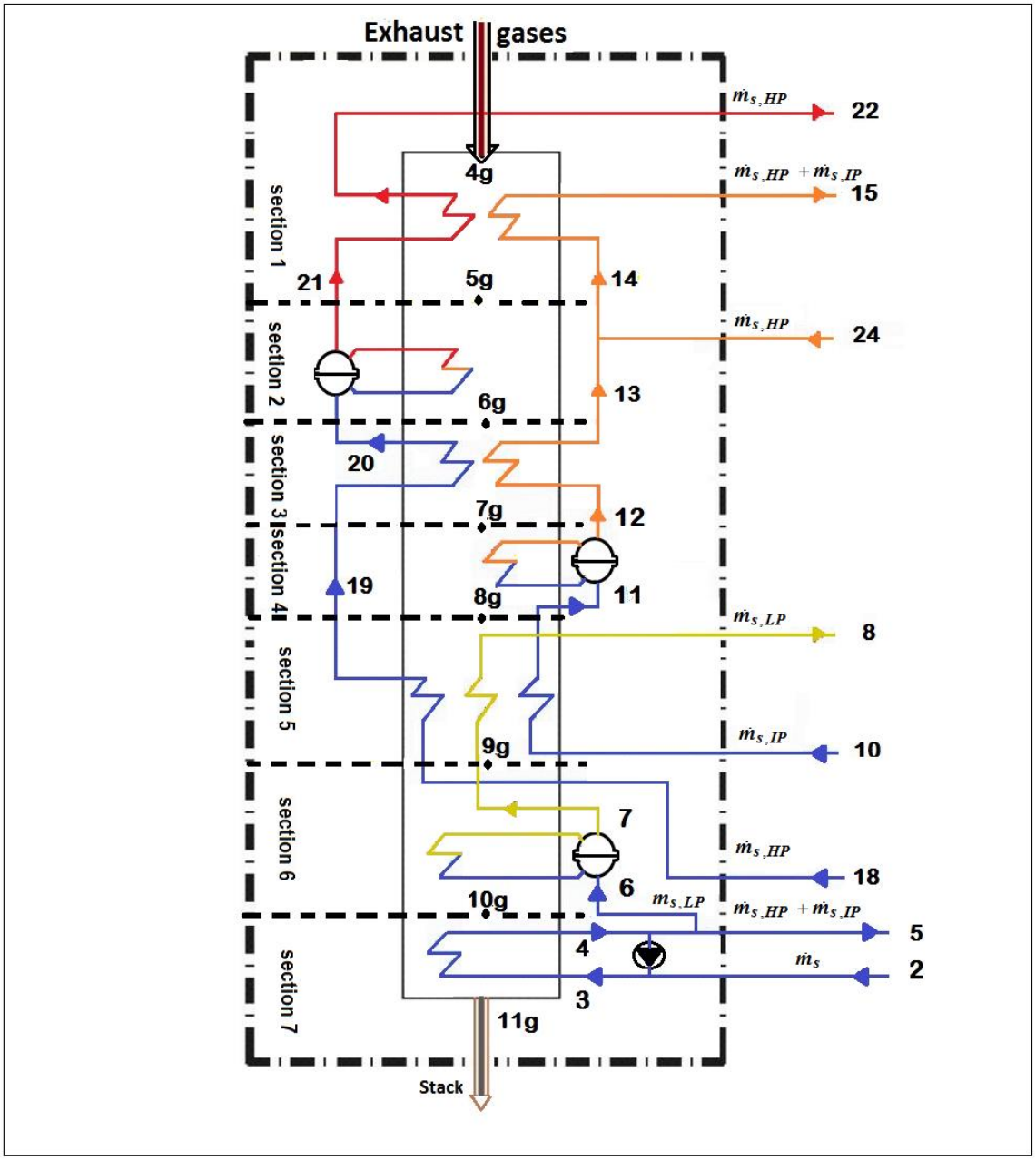

Figure 5-2 HRSG sections

The heat recovery steam generator in this work is arranged in seven sections as shown in Figure 5-2, and these sections are:

section 1. High pressure superheater and reheater

section 2. High pressure evaporator

section 3. High pressure economizer II and intermediate pressure superheater

section 4. Intermediate pressure evaporator

section 5. High pressure economizer I, intermediate pressure economizer and low pressure superheater

section 6. Low pressure evaporator

section 7. Low pressure economizer

The assumptions and parameters of the HRSG selected for the analyses are tabulated in Table 5-2.

Table 5-2 Main characteristics and assumptions of the of HRSG (initial input data)

PARAMETER	Value
The pinch point temperature difference for HP, IP, and LP [°C]	13
The minimum temperature difference between the gas turbine exhaust gases and live/reheat steam [°C]	25
Pressure in LP drum of HRSG [bar]	5
Pressure in IP drum of HRSG [bar]	36
Pressure in HP drum of HRSG [bar]	104
Live steam temperature at the inlet of low pressure steam turbine [°C]	535
Live steam temperature at the outlet of intermediate pressure superheater [°C]	325
Live steam temperature at the outlet of low pressure superheater [°C]	235
Minimum stack temperature [°C]	93
The heat recovery steam generator efficiency [1]	99.3%
The pressure drop for water in the economizers [1]	25%
The pressure drop for steam in the reheat and Superheater tubes [1]	8%
Feed water temperature at 3 [°C]	60

5.1.3 Steam Turbine

The steam turbine used in this study consisted of three turbines: high pressure ST_{HP}, intermediate pressure ST_{IP}, and low pressure ST_{LP}.

The assumptions and parameters selected for the thermodynamic analysis of the steam turbine are tabulated in Table 5-3.

Table 5-3 Main assumptions of the steam turbine

PARAMETER	Value
The isentropic efficiency of all three steam turbine parts	90%
The isentropic efficiencies of water pumps	82%
The mechanical efficiency	99.5%
The generator efficiency	98%
Minimum dryness fraction of steam at low steam turbine outlet [1]	0.88
Low-pressure steam turbine outlet (condenser pressure) [bar]	0.055
The inlet cooling water temperature in condenser [°C]	20

5.2 Methodology Steps

There have been different methods for CCGT optimization in recent history. There are numerous CCGT optimization methods based on minimization of exergy destructions and exergy losses or maximization of exergy transfer respectively on second law analysis of CCGT. The methodology developed and used in this work is based on minimizing the objective functions comprising of both the thermodynamic and thermoeconomic component. Thereby, the thermodynamic component tends to minimize the exergy losses and thermoeconomic component, and to minimize the total combined cycle power plant cost by introducing the reduction to a common monetary base of the costs of exergy losses and of CCGT investment costs.

This chapter is devoted to a description of the various steps involved in the development of thermoeconomic and exergoeconomic optimization methods to be adopted for the combined cycle gas turbine described in section 5.1. The optimization methods presented in this chapter are proposed for an application to the combined cycle gas turbine configuration in Figure 5-1; the methods are also compared to identify the best option with minimum electrical production cost, possible minimum costs, and maximum efficiency and power output, which are the objectives of this optimization. In this context, three methods are proposed. One of them is the reference method [20], and the other two are newly developed methods.

a) Energy optimization method (reference method)
b) Exergy destruction optimization method

c) Exergoeconomic optimization method

Two approaches for each method are studied in this thesis:

First approach: Six operating parameters were subjected for the optimization: drum pressures and pinch point temperatures for each pressure level of the HRSG (high, intermediate, and low-pressure).

Second approach: Four operating parameters were subjected to the optimization: pressure in the pressure drum (high, intermediate, and low-pressure) of every three-steam stream in the HRSG and one pinch point temperature.

In order to achieve the objectives previously described, the following steps are required.

5.2.1 Energy Analysis

First law of thermodynamic, briefly discussed in Section 4, is applied to the case studies to find the mass flow rate of steam generated at the drums, the thermodynamic properties of each state, the power output of the system and thermal efficiency of the cycle. In the analysis, processes are considered as a steady state flow. Additionally, kinetic and potential energy effects are ignored.

5.2.1.1 Heat Recovery Steam Generator (HRSG)

The analysis of HRSG unit is based on the pinch point. The pinch point is simply defined as the difference between the saturation temperature of water and the gas temperature prior to entry to the economizer. The pitch point is denoted as PP , as shown in Figure 5-3.

The greater the pinch point, the smaller the surface area available for thermal energy transfer from the hot exhaust gas to the steam. This results in a higher HRSG exit temperature.

The water-steam properties were derived from the standard “IAPWS” 97 [69]. The properties of the gas turbine exhaust gases, which are the combustion products of the specified fuel, were calculated according to Baehr and Diederichsen [70]. The process of heat exchange in triple pressure HRSG is explained using Figure 5-3. The flue gases enter the HRSG at temperature T_{4g} and passes through different sections in HRSG and then leaves at T_{11g} . The low pressure feed water is heated from T_3 to the saturation

temperature T_6 in the low-pressure economizer section; at this temperature T_6 the low pressure feed water enters the low-pressure evaporator to generate the steam and leaves at the same temperature T_7 where $T_7 = T_6$.

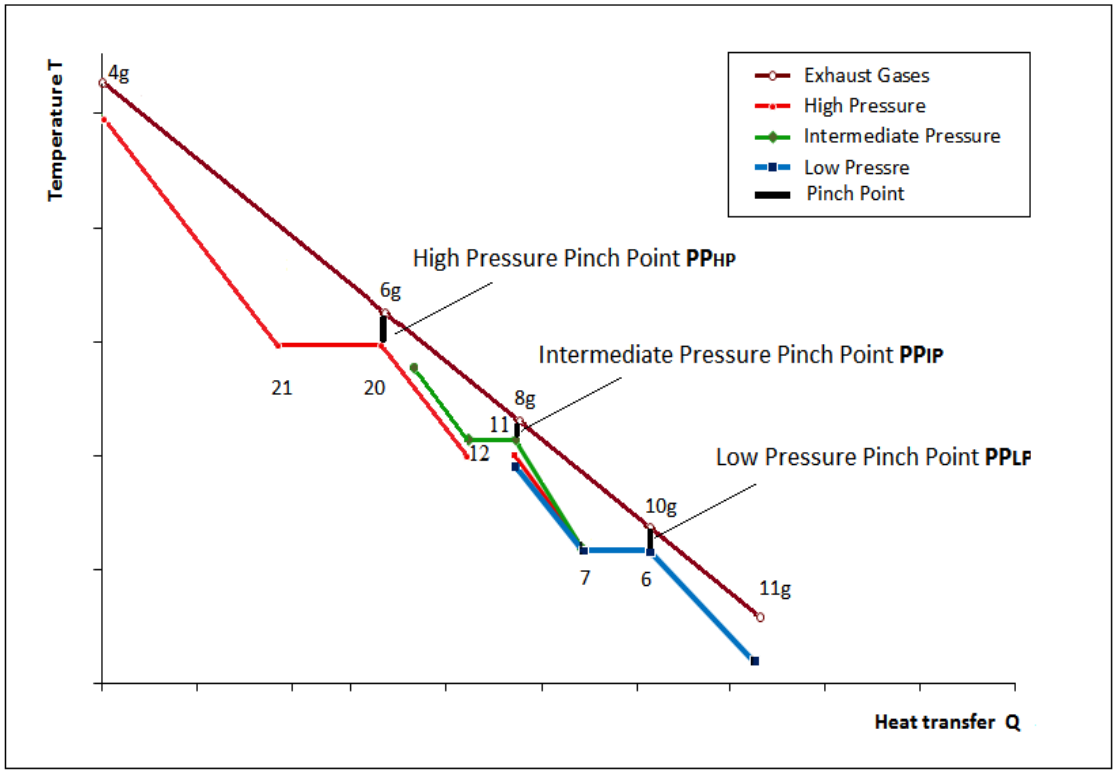

Figure 5-3 General form of T-Q diagram for triple pressure HRSG

The low-pressure steam is superheated to temperature T_8 in the superheater section. The gas temperature at the inlet of the low pressure is equal to:

$$T_{10g} = T_6 + PP_{LP}. \tag{5-1}$$

The intermediate pressure feed water is heated from temperature T_{10} to the saturation temperature T_{11} in the intermediate pressure economizer section; the feed water enters the evaporator section at this temperature T_{11} and leaves at the same temperature T_{12} where $T_{12} = T_{11}$. The intermediate pressure steam is superheated to temperature T_{13} in the intermediate pressure superheater section, and then the superheated steam is mixed with the high-pressure steam from the high-pressure turbine and reheated to temperature T_{15} in the reheater section. The gas temperature entering the intermediate pressure economizer can be written as:

$$T_{8g} = T_{11} + PP_{IP} \tag{5-2}$$

The high pressure feed water is first heated from temperature T_{18} to the saturation temperature T_{21} in two economizers (high pressure economizer 1 from temperature T_{18} to T_{19} and high pressure economizer 2 from temperature T_{19} to T_{20}), after which the feed water enters the high evaporator section at this temperature T_{20} and leaves at the same temperature T_{21} where $T_{21} = T_{20}$. The high-pressure steam is superheated to temperature T_{22} in the reheater section. The exhaust gas temperature at the inlet of the high-pressure economizer is equal to:

$$T_{6g} = T_{20} + PP_{HP} \tag{5-3}$$

Applying the first law of thermodynamics (energy balance equations) to the heat recovery steam generator parts (low-pressure intermediate pressure and high pressure), yields a system of equations. The steam mass flow rate is calculated by solving these equations.

From Figure 5-1, mass flow rate of the steam generated at the intermediate and high-pressure steam drum is calculated by applying an energy balance for the control volume around the high-pressure evaporator, high-pressure superheater, and intermediate pressure superheater (section1 and section 2 as shown in Figure 5-2)

$$\dot{m}_g \eta_h \left(h_{4g} - h_{6g}\right) = [(h_{22} - h_{20}) + (h_{15} - h_{24})]\dot{m}_{s,HP} + \dot{m}_{s,IP}.\left(h_{15} - h_{115}\right) \tag{5-4}$$

$$\dot{m}_g \eta_h \left(h_{6g} - h_{8g}\right) = (h_{20} - h_{19})\dot{m}_{s,HP} + \dot{m}_{s,IP}.\left(h_{15} - h_{115}\right) \tag{5-5}$$

where $\dot{m}_g$, $\dot{m}_{s,HP}$, $\dot{m}_{s,IP}$ and η_h are the exhaust gases mass flow rate, high-pressure steam mass flow rate , intermediate pressure mass flow, rate and HRSG efficiency.

From equation (5-4) and equation (5-5), we can get

$$\dot{m}_{s,HP} = \frac{\dot{m}_g \eta_h (h_{4g} - h_{6g}) - \dot{m}_{s,IP} (h_{15} - h_{13})}{(h_{22} - h_{20}) + (h_{15} - h_{24})} \tag{5-6}$$

and

$$\dot{m}_{s,IP} = \frac{\dot{m}_g \eta_h (h_{6g} - h_{8g}) - \dot{m}_{s,HP} (h_{19} - h_{20})}{(h_{13} - h_{11})}. \tag{5-7}$$

Substituting equation (5-6) in equation (5-7) we get:

$$m_{s,IP} = \frac{\dot{m}_g \eta_h (h_{6g} - h_{8g}) - [\frac{\dot{m}_g \eta_h (h_{4g} - h_{6g}) - m_{s,IP} (h_{15} - h_{13})}{(h_{22} - h_{20}) + (h_{15} - h_{24})}](h_{20} - h_{19})}{(h_{13} - h_{11})} \tag{5-8}$$

$$B1 = \dot{m}_g \eta_h (h_{6g} - h_{8g}) \tag{5-9}$$

$$\dot{m}_{s,IP} = \frac{B1-\left[\left(\frac{\dot{m}_g \eta_h (h_{4g} - h_{6g})(h_{20} - h_{19})}{(h_{22} - h_{20}) + (h_{15} - h_{24})}\right) - \left(\frac{\dot{m}_{s,IP} (h_{15} - h_{13})(h_{20} - h_{19})}{(h_{22} - h_{20}) + (h_{15} - h_{24})}\right)\right]}{(h_{13} - h_{11})} \quad (5\text{-}10)$$

$$\dot{m}_{s,IP} (h_{13} - h_{11}) = B1 - \left(\frac{\dot{m}_g \eta_h (h_{4g} - h_{6g})(h_{20} - h_{19})}{(h_{22} - h_{20}) + (h_{15} - h_{24})}\right) + \dot{m}_{s,IP} \frac{(h_{15} - h_{13})(h_{20} - h_{19})}{(h_{22} - h_{20}) + (h_{15} - h_{24})} \quad (5\text{-}11)$$

$$B2 = \frac{\dot{m}_g \eta_h (h_{4g} - h_{6g})(h_{20} - h_{19})}{(h_{22} - h_{20}) + (h_{15} - h_{24})} \quad (5\text{-}12)$$

$$\dot{m}_{s,IP} \left((h_{13} - h_{11}) - \frac{(h_{15} - h_{13})(h_{20} - h_{19})}{(h_{22} - h_{20}) + (h_{15} - h_{24})}\right) = B1 - B2 \quad (5\text{-}13)$$

$$B3 = \left((h_{13} - h_{11}) - \frac{(h_{15} - h_{13})(h_{20} - h_{19})}{(h_{22} - h_{20}) + (h_{15} - h_{24})}\right) \quad (5\text{-}14)$$

where B1, B2, and B3 are used in above equations in order to simplify them.

The final equation for calculating the mass flow rate for intermediate pressure level is:

$$\dot{m}_{s,IP} = \frac{B1 - B2}{B3} \quad (5\text{-}15)$$

or

$$\dot{m}_{s,IP} = \frac{\left(\dot{m}_g \eta_h (h_{6g} - h_{8g})\right) - \left(\frac{\dot{m}_g \eta_h (h_{4g} - h_{6g})(h_{20} - h_{19})}{(h_{22} - h_{20}) + (h_{15} - h_{24})}\right)}{\left((h_{13} - h_{11}) - \frac{(h_{15} - h_{13})(h_{20} - h_{19})}{(h_{22} - h_{20}) + (h_{15} - h_{24})}\right)} \quad (5\text{-}16)$$

Substituting equation (5-15) in equation (5-6), we get the equation to calculate $\dot{m}_{s,HP}$:

$$\dot{m}_{s,HP} = \frac{\dot{m}_g \eta_h (h_{4g} - h_{6g}) - \left(\frac{(B1 - B2)}{B3}\right)(h_{15} - h_{13})}{(h_{22} - h_{20}) + (h_{15} - h_{24})} \quad (5\text{-}17)$$

Similarly, by taking energy balance for the control volume around the high pressure economizer 1, intermediate pressure economizer, low pressure superheater and low pressure evaporator (section 5 and section 6 as shown in Figure 5-2), the mass flow rate of low pressure steam $\dot{m}_{s,LP}$ generated is obtained as:

$$\dot{m}_g \eta_h \left(h_{8g} - h_{10g}\right) = \dot{m}_{s,HP} (h_{19} - h_{18}) + \dot{m}_{s,IP} \left(h_{11} - h_{10}\right) + \dot{m}_{s,IP} \left(h_8 - h_6\right) \quad (5\text{-}18)$$

$\dot{m}_{s,LP}$ can be written as

$$\dot{m}_{s,LP} = \frac{\dot{m}_g \eta_h \left(h_{8g} - h_{10g}\right) - \dot{m}_{s,HP}\left(h_{19} - h_{18}\right) - \dot{m}_{s,IP}\left(h_{11} - h_{10}\right)}{\left(h_8 - h_6\right)} \quad (5\text{-}19)$$

The total feed water mass flow is obtained as:

$$\dot{m}_s = \dot{m}_{s,LP} + \dot{m}_{s,IP} + \dot{m}_{s,HP} \quad (5\text{-}20)$$

Exhaust gases properties at points 5g, 7g, 9g, and 11g can be obtained by applying the energy balance around section 1, section 3, section 5, and section 7 respectively.

$$h_{5g} = h_{4g} - \frac{(\dot{m}_{s,HP} + \dot{m}_{s,IP})(h_{15} - h_{14}) + \dot{m}_{s,HP}\left(h_{22} - h_{21}\right)}{\dot{m}_g \eta_h} \quad (5\text{-}21)$$

$$h_{7g} = h_{6g} - \frac{\dot{m}_{s,IP}\left(h_{13} - h_{12}\right) + \dot{m}_{s,HP}\left(h_{20} - h_{19}\right)}{\dot{m}_g \eta_h} \quad (5\text{-}22)$$

$$h_{9g} = h_{8g} - \frac{\dot{m}_{s,LP}\left((h_8 - h_7) + (h_{11} - h_{10})\right) + \dot{m}_{s,HP}\left(h_{19} - h_{18}\right)}{\dot{m}_g \eta_h} \quad (5\text{-}23)$$

$$h_{11g} = h_{10g} - \frac{(\dot{m}_s + \Delta\dot{m}_s)(h_4 - h_3)}{\dot{m}_g \eta_h} \quad (5\text{-}24)$$

where $\Delta\dot{m}_s$ is the part of the feed water mass flow circulated between 3 and 4 (Figure 5-4) for preheating the feed water in order to avoid condensation of water at the tube wall surface. A rule in the power plant industry requires the *HRSG* feed water to enter with a minimum temperature of 60 °C.

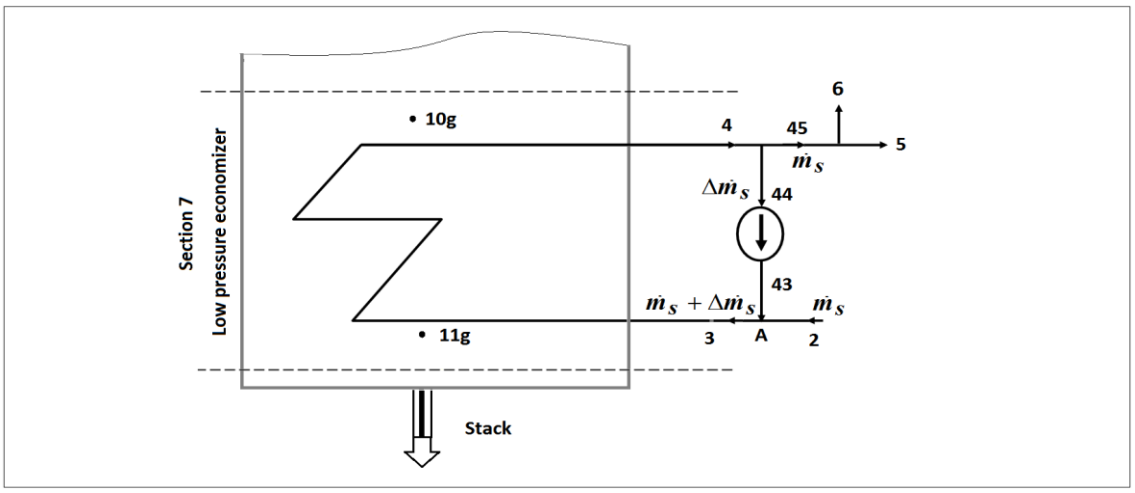

Figure 5-4 Low pressure economizer collector (A) in the preheating loop

The circulated part of the feed water $\Delta\dot{m}_s$ is calculated by applying energy balance around the collector (A), as shown in Figure 5-4.

$$\Delta \dot{m}_s = \dot{m}_s \frac{(h_3 - h_2)}{(h_{43} - h_3)} \tag{5-25}$$

5.2.1.2 Steam Turbine (ST)

By applying the energy balance for steam turbine levels, the following relation is obtained:

$$P_{G,ST,LP} = \eta_M \eta_G \dot{m}_s (h_{25} - h_{26}) \tag{5-26}$$

$$P_{G,ST,IP} = \eta_M \eta_G (\dot{m}_{s,HP} + \dot{m}_{s,IP})(h_{16} - h_{17}) \tag{5-27}$$

$$P_{G,ST,HP} = \eta_M \eta_G \dot{m}_{s,HP} (h_{23} - h_{24}) \tag{5-28}$$

$$P_{G,ST} = \eta_M \eta_G (\dot{m}_{s,HP} (h_{23} - h_{24}) + (\dot{m}_{s,HP} + \dot{m}_{s,IP})(h_{16} - h_{17}) + \dot{m}_s (h_{25} - h_{26}) \tag{5-29}$$

where $P_{G,ST}$, η_M and η_G are: steam turbine power output, mechanical efficiency, and generator efficiency respectively.

5.2.1.3 Pumps

Similarly, to the steam turbine calculations, the power needed for the pumps $P_{G,pump}$ is obtained by applying the energy balance around the pumps:

$$P_{G,pump,FW} = \dot{m}_s \frac{(h_2 - h_1)}{\eta_{pump}} \tag{5-30}$$

$$P_{G,pump,IP} = \dot{m}_{s,IP} \frac{(h_{10} - h_5)}{\eta_{pump}} \tag{5-31}$$

$$P_{G,pump,HP} = \dot{m}_{s,HP} \frac{(h_{18} - h_5)}{\eta_{pump}} \tag{5-32}$$

where η_{pump} is the isentropic efficiency of the water pump.

5.2.1.4 Performance Assessment Parameters

The performances of combined cycle power plant, including the overall combined cycle power output and the combined cycle thermal efficiency are calculated as given below:

$$P_{CCGT} = P_{G,GT} + P_{G,ST} \tag{5-33}$$

$$\eta_{CCGT} = \frac{P_{CCGT}}{Q_{add}} \tag{5-34}$$

$$Q_{add} = \frac{P_{GT}}{\eta_{GT}} \tag{5-35}$$

where Q_{add} is the heat added to the combined cycle in the combustion chamber of the gas turbine.

5.2.2 Exergy Analysis

The basic equations employed in the exergy analysis performed on the selected combined cycle power plant are presented in this section. As with the energy analysis, exergy balances for individual components are written, and exergy flows and irreversibilities for each component are found. Then, overall exergy efficiency and exergy destruction are found for the whole system.

The exergy components of each state of the bottoming cycle shown in Figure 5-1 are calculated according to equation (4-20) for physical exergy and equation (4-21) for chemical exergy.

Exergy destruction and exergy efficiency equations for each element in the bottoming cycle are calculated by applying the exergy balance around the element using equation (4-30).

For the control volume around *HRSG* (Figure 5-2), the equations for exergy destructions $\dot{E}_{D,HRSG}$, exergy wastes $\dot{E}_{Waste,HRSG}$ to the environment with exhaust gases and exergy efficiency ε_{HRSG} are listed as shown below:

$$\dot{E}_{D,HRSG} = \dot{E}_{4g} + \dot{E}_{24} + \dot{E}_{18} + \dot{E}_{10} + \dot{E}_{2} - \dot{E}_{22} - \dot{E}_{15} - \dot{E}_{8} - \dot{E}_{5} - \dot{E}_{11g} \tag{5-36}$$

Exergy rate in this study associated with stream exiting HRSG is considered as exergy wastes $\dot{E}_{Waste,HRSG}$:

$$\dot{E}_{Waste,HRSG} = \dot{E}_{11g} \tag{5-37}$$

$$\varepsilon_{HRSG} = \frac{\dot{E}_{22} + \dot{E}_{15} + \dot{E}_{8} + \dot{E}_{5} - \dot{E}_{24} - \dot{E}_{18} - \dot{E}_{10} - E_{2}}{\dot{E}_{4g}} \tag{5-38}$$

It should be noted that exergy transfer due to heat loss from HRSG is taken as zero due to assumption of ideal insulation.

For the control volume around the steam turbine Figure 5-4, the exergy destruction is:

$$\dot{E}_{D,ST} = \dot{E}_{22} + \dot{E}_{15} + \dot{E}_{8} - \dot{E}_{24} - \dot{E}_{26} - \dot{E}_{ST} \tag{5-39}$$

and the exergy efficiency:

$$\varepsilon_{ST} = \frac{\dot{E}_{ST}}{\dot{E}_{22} + \dot{E}_{15} + \dot{E}_{8} - \dot{E}_{24} - \dot{E}_{26}} \tag{5-40}$$

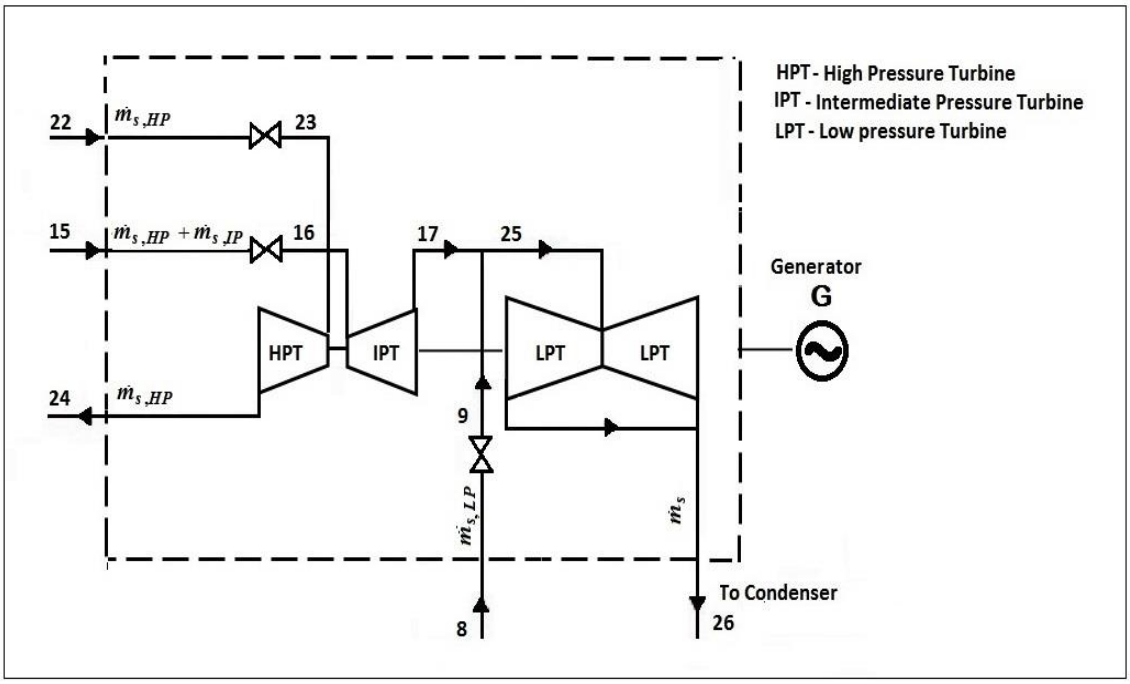

Figure 5-5 Schematic of steam turbine

The exergy rate difference of condenser cooling water at the inlet and outlet streams are considered as exergy losses $\dot{E}_{loss,Con}$. For the control volume around condenser the following equation is used:

$$\dot{E}_{loss,Con} = \dot{E}_{26} - \dot{E}_1 \tag{5-41}$$

$$\varepsilon_{Con} = 1 - \frac{\dot{E}_1}{\dot{E}_{26}} \tag{5-42}$$

And for the control volume around the feed water tank including pumps:

$$\dot{E}_{D,FW} = \dot{E}_5 + P_{G,pump,HP} + P_{G,pump,IP} - \dot{E}_{10} - \dot{E}_{18} \tag{5-43}$$

$$\varepsilon_{FW} = 1 - \frac{\dot{E}_{D,FW}}{P_{G,pump,HP} + P_{G,pump,IP}} \tag{5-44}$$

Total exergy destruction in the bottoming cycle $\dot{E}_{D,TOT}$, the total exergy losses, $\dot{E}_{loss,TOT}$, and total exergy waste $\dot{E}_{waste,TOT}$ are given as follows:

$$\dot{E}_{D,TOT} = \dot{E}_{D,HRSG} + \dot{E}_{D,ST} + \dot{E}_{D,FW} + \dot{E}_{D,Con} \tag{5-45}$$

$$\dot{E}_{loss,TOT} = \dot{E}_{loss,CON} + \dot{E}_{loss,HRSG} \tag{5-46}$$

$$\dot{E}_{waste,TOT} = \dot{E}_{D,TOT} + \dot{E}_{loss,TOT} \tag{5-47}$$

Exergetic efficiency ε_{TOT} of the bottoming cycle case studies may be given as:

$$\varepsilon_{TOT} = 1 - \frac{\dot{E}_{waste,TOT}}{\dot{E}_{4g}} \tag{5-48}$$

5.2.3 Calculation of Heat Transfer Area

The heat transfer areas of HRSG are computed by the well-known method of Logarithm Means Temperature Difference $LMTD$ as follows:

$$Q_i = U_i \cdot A_i \cdot LMTD_i \tag{5-49}$$

where U and $LMTD$ refer to the global heat transfer coefficient and Logarithm Means Temperature Difference respectively. The model assumed is counter flow heat exchanger. The $LMTD$ for each section of the HRSG was calculated using equation (5-50) as follows:

$$LMTD_i = \frac{\Delta T_{1i} - \Delta T_{2i}}{\ln\left(\frac{\Delta T_{1i}}{\Delta T_{2i}}\right)} \tag{5-50}$$

Applying equation (5-49) and equation (5-50) the heat transfer and heat transfer area are calculated for each section as shown in Figure 5-2:

- Section 1: The heat transfer for high-pressure superheater and reheater (Q_r and $Q_{HP,su}$) and heat transfer area (A_r and $A_{HP,su}$) for this section are calculated by the following equations:

$$Q_r = \left(\dot{m}_{s,HP} + \dot{m}_{s,IP}\right)\left(h_{15} - h_{14}\right) \tag{5-51}$$

$$\Delta T_{11r} = \left(T_{4g} - T_{15}\right) \tag{5-52}$$

$$\Delta T_{21r} = \left(T_{5g} - T_{14}\right) \tag{5-53}$$

$$LMTD_r = \frac{\Delta T_{11r} - \Delta T_{21r}}{\ln\left(\frac{\Delta T_{11r}}{\Delta T_{21r}}\right)} \tag{5-54}$$

$$A_r = \frac{Q_r}{U_r LMTD_r} \tag{5-55}$$

$$Q_{HP,su} = \left(\dot{m}_{s,HP}\right)\left(h_{22} - h_{21}\right) \tag{5-56}$$

$$\Delta T_{11su} = \left(T_{4g} - T_{22}\right) \tag{5-57}$$

$$\Delta T_{21su} = \left(T_{5g} - T_{21}\right) \tag{5-58}$$

$$LMTD_{HP,su} = \frac{\Delta T_{11su} - \Delta T_{21su}}{\ln\left(\frac{\Delta T_{11su}}{\Delta T_{21su}}\right)} \tag{5-59}$$

$$A_{HP,su} = \frac{Q_{HP,su}}{U_{su} LMTD_{HP,su}} \tag{5-60}$$

Similarly, the heat transfer and heat transfer areas for other sections can be calculated.

- Section 2: High pressure evaporator HP,v

$$Q_{HP,v} = \dot{m}_{s,HP}\left(h_{21} - h_{20}\right) \tag{5-61}$$

$$A_{HP,v} = \frac{Q_{HP,v}}{U_v LMTD_{HP,v}} \tag{5-62}$$

- Section 3: Intermediate pressure superheater IP,su and high pressure economizer-2 $HP,ec2$

$$Q_{IP,su} = \dot{m}_{s,IP}\left(h_{13} - h_{12}\right) \tag{5-63}$$

$$A_{IP,su} = \frac{Q_{IP,su}}{U_{su} LMTD_{IP,su}} \tag{5-64}$$

$$Q_{HP,ec2} = \dot{m}_{s,HP}\left(h_{20} - h_{19}\right) \tag{5-65}$$

$$A_{HP,ec2} = \frac{Q_{HP,ec2}}{U_{ec} LMTD_{HP,ec2}} \tag{5-66}$$

- Section 4: Intermediate pressure evaporator IP,v

$$Q_{IP,v} = \dot{m}_{s,IP}\left(h_{12} - h_{11}\right) \tag{5-67}$$

$$A_{IP,v} = \frac{Q_{IP,v}}{U_v LMTD_{IP,v}} \tag{5-68}$$

- Section 5: Intermediate pressure economizer IP,ec, low pressure superheater LP,su, and high pressure economizer-1 $HP,ec1$

$$Q_{IP,ec} = \dot{m}_{s,IP}\left(h_{11} - h_{10}\right) \tag{5-69}$$

$$A_{IP,ec} = \frac{Q_{IP,ec}}{U_{ec} LMTD_{IP,ec}} \tag{5-70}$$

$$Q_{HP,ec1} = \dot{m}_{s,HP}\left(h_{19} - h_{18}\right) \tag{5-71}$$

$$A_{HP,ec1} = \frac{Q_{HP,ec1}}{U_{ec} LMTD_{HP,ec1}} \tag{5-72}$$

$$Q_{LP,su} = \dot{m}_{s,LP} \left(h_8 - h_7 \right) \tag{5-73}$$

$$A_{LP,su} = \frac{Q_{LP,su}}{U_{su} LMTD_{LP,su}} \tag{5-74}$$

- Section 6: Low pressure evaporator LP,v

$$Q_{LP,v} = \dot{m}_{s,LP} \left(h_7 - h_6 \right) \tag{5-75}$$

$$A_{LP,v} = \frac{Q_{LP,v}}{U_v LMTD_{LP,v}} \tag{5-76}$$

- Section 7: Low pressure economizer LP,ec

$$Q_{LP,ec} = \dot{m}_{s,LP} \left(h_4 - h_3 \right) \tag{5-77}$$

$$A_{LP,ec} = \frac{Q_{LP,ec}}{U_{ec} LMTD_{LP,ec}} \tag{5-78}$$

The HRSG area A_{HRSG}, which is necessary to ensure the heat transfer at given PP was calculated as follows:

$$A_{HRSG} = \sum_{ec} A_{ec} + \sum_{v} A_v + \sum_{su} A_{su} + \sum_{re} A_{re} \tag{5-79}$$

- Heat transfer area for condenser A_{CON}

$$Q_{Con} = \dot{m}_s \left(h_{26} - h_1 \right) \tag{5-80}$$

$$TR = T_{w,out} - T_{w,in}$$

$$ITD = \left(T_{26} - T_{w1} \right) \tag{5-81}$$

$$LMTD_{Con} = \frac{TR}{\ln\left(\frac{1}{1 - \frac{TR}{ITD}} \right)} \tag{5-82}$$

$$A_{Con} = \frac{Q_{Con}}{U_{Con} LMTD_{Con}} \tag{5-83}$$

where TR is the temperature rise of cooling water in the condenser, and ITD the difference between the steam temperature and cooling water inlet temperature (the initial temperature difference).

5.2.4 Economic Analysis

The primary objective of every project is to be profitable. Therefore, a proper design for any cost-effective thermal system requires an evaluation of the project cost. Economic analysis was performed for the purpose of this objective.

The economic model takes into account the annual cost associated with owning and operating each plant component and the annual cost associated with exergy destruction. The costs of the components include amortization and maintenance, and the cost of fuel consumption. In order to define a cost function that depends on the optimization parameters of interest, component costs have to be expressed as functions of thermodynamic variables.

Table 5-4 Economic assumptions, prices and coefficients

PARAMETER		VALUE
Economic life of the plant (N) [year]		20
Price of natural gas (cf) [\$kWh^{-1}]		0.0467
Selling price of electricity (S) [\$kWh^{-1}]		0.114
Maintenance factor (φ) [-][22]		1.06
Interest rate (i) [-]		0.1
The power plant Operating hours a year [hour]		7500
The overall heat transfer coefficients for the HRSG sections [21]	Economizer (U_{ec}) [wm^{-2}k]	42.6
	Evaporator (U_v) [wm^{-2}k]	43.7
	Superheater (U_{su}) [wm^{-2}k]	50
	Reheater (U_r) [wm^{-2}k]	50
	Condenser (U_{Con}) [wm^{-2}k]	2500
Unit price of surface area of the HRSG sections [21]	Economizer [\$m^{-2}]	45.7
	Evaporator [\$m^{-2}]	34.9
	Superheater [\$m^{-2}]	96.2
	Reheater [\$m^{-2}]	56.2

5.2.4.1 Component Capital Cost Functions

A very important step for the development of the optimization model was the development of component capital cost functions. The expressions of purchase components costs and amortization factors that are accepted here are similar to Silveira and Tuna [71], Behbahani-nia et al [23] and Roosen et al [72]. The format is widely used by various authors. In Table 5-4, the economic assumption for this study is presented.

Cost function equations for the components of CCGT are presented as:

- Air Compressor: The investment capital cost Z_{AC} and investment cost per unit time Z_{AC} given by [72]:

$$Z_{AC} = 44.71 Ma \frac{1}{0.95 - \eta_{sC}} \prod_C \ln\left(\prod_C\right) \tag{5-84}$$

where Ma, η_{sC} and $\prod_C$ are inlet air mass flow rate, compressor isentropic efficiency, and compression ratio.

- Combustion Chamber [72]

$$Z_{CC} = 28.98 Ma \frac{1}{0.995 - \frac{p_{3g}}{p_{2a}}} \left(1 + e^{0.015(T_{3g} - 1540)}\right) \tag{5-85}$$

- Gas Turbine: Gas turbine cost function as equation (5-86) [72]:

$$Z_{GT} = 301.45 Mg \frac{1}{0.94 - \eta_{sT}} \ln\left(\frac{p_{3g}}{p_{4g}}\right) \left(1 + e^{0.25(T_{3g} - 1570)}\right) \tag{5-86}$$

where η_{sT}, T_{in} and $\left(\frac{p_{in}}{p_{out}}\right)$ are turbine isentropic efficiency, turbine inlet temperature, and pressure ratio respectively.

- Heat recovery steam generator HRSG: The cost of the single HRSG section must be proportional to the surface. As well as the total cost of the HRSG equal to the sum of the costs of its sections, so that the capital cost of HRSG can be estimated as follows:

$$Z_{HRSG} = 2.31(k_{ec} A_{ec} + k_v A_v + k_{su} A_{su} + k_{re} A_{re}) \tag{5-87}$$

where k_{ec}, k_v, k_{su} and k_{re} are the unit prices of surface area of the economizer, evaporator, super heater, and reheat sections of the HRSG respectively [21].

- Steam turbine [71]

$$Z_{ST} = 6000 P_{G,ST}^{0.7} \tag{5-88}$$

- Condenser pump $Z_{pump,Con}$ and feed water tank Z_{FWT}

$$Z_{pump,Con} = 3540 P_{G,pump,Con}^{0.71} \tag{5-89}$$

$$Z_{FWT} = 3540 (P_{G,pump,HP}^{0.71} + P_{G,pump,IP}^{0.71}) \tag{5-90}$$

- Generator [71]

$$Z_{GEN,ST} = 60 P_{G,ST}^{0.95} \tag{5-91}$$

- Condenser

  for stainless condenser [73].

$$Z_{CON} = 1.7(162 A_{Con}^{1.01}) \tag{5-92}$$

The total investment cost for topping cycle, bottoming cycle and the whole power plant can be written as:

$$Z_{TOP} = Z_{AC} + Z_{CC} + Z_{GT} + Z_{GEN,GT} \tag{5-93}$$

$$Z_{BOT} = Z_{HRSG} + Z_{ST} + Z_{Con} + Z_{FWT} + Z_{PUMP,Con} + Z_{GEN,ST} \tag{5-94}$$

$$Z_{TOT} = Z_{TOP} + Z_{BOT} \tag{5-95}$$

The total annualized investment costs for topping cycle, bottoming cycle and the whole power plant $Z_{a,TOP}$, $Z_{a,BOT}$, $Z_{a,TOT}$ can be calculated by:

$$Z_{a,TOP} = \frac{Z_{TOP}}{N},\ Z_{a,BOT} = \frac{Z_{BOT}}{N},\ Z_{a,TOT} = \frac{Z_{TOT}}{N} \tag{5-96}$$

Applying equations (4-43) and (4-44) to the investment cost per unit time for bottoming, topping and combined cycle are expressed by:

$$\dot{Z}_{TOP} = \frac{Z_{TOP} CRF \varphi}{3600 N} \tag{5-97}$$

$$\dot{Z}_{BOT} = \frac{Z_{BOT} CRF \varphi}{3600 N} \tag{5-98}$$

$$\dot{Z}_{TOT} = \dot{Z}_{TOP} + \dot{Z}_{BOT} \tag{5-99}$$

5.2.4.2 Cost of the Exergy Destruction and Exergy Losses

The cost of the exergy wastes can be expressed in the form

$$\dot{C}_D = c_{wast} \dot{E}_D,\ \dot{C}_{loss} = c_{wast} \dot{E}_{\text{loss}},\ \dot{C}_{wast} = c_{wast} \dot{E}_{\text{wast}} \tag{5-100}$$

$$c_{wast} = \frac{c_{fu}}{k_1} \tag{5-101}$$

where c_{wast} represents the specific cost of the exergy wastes, c_{fu} is the fuel cost, and k_1 is the correction factor.

For the definition of the specific cost of the exergy wastes c_{wast} various strategies can be assumed [21]:

1. To consider it as the cost of the fuel $k_1 = 1$.
2. To consider the cost of the exergy wastes as the cost of the fuel divided by the efficiency of the plant $k_1 = \eta_{CCGT}$.
3. Another possibility is to consider the exergy wastes equal to an average value of the selling price of the electrical energy. This last option is derived from the consideration that an exergy loss in the HRSG corresponds to a lower output of the plant and to a lower amount of energy that can be sold.

In the recent work, the specific cost of the exergy wastes c_{wast} is chosen to be equal to the fuel cost c_f .

5.2.5 Exergoeconomic Analysis

The purpose of thermoeconomics is to combine exergy analysis with economic considerations in order to find the most cost-effective design for the system. Exergy costing is an approach based on exergy as the only meaningful thermodynamic value to which costs may be assigned. In the chapter dealing with exergy analysis, all exergy flow rates in the system were calculated - including losses of exergy to the environment and exergy destruction rates. In this chapter, costs are assigned to these streams in order to identify cost-ineffective processes and show the way the system may and should be changed in order to assure the best economic performance. The exergoeconomic analysis is based on the specific exergy costing approach (as mentioned in section 4.3), which consists of the following steps.

5.2.5.1 Identification of Exergy Streams

The first step was carried out as in section 5.2.1 using the FORTRAN code. The energy and exergy streams were calculated. The total exergy was used in this study, because the use of separate forms of exergy, such as thermal, mechanical or chemical, only marginally improves calculation accuracy [35].

5.2.5.2 Definition of Exergy Fuel and Exergy Product of the System Components

Each component of the system has a particular productive function that contributes to achieving the aim of production. In order to define this function, this section will clearly indicate which flow or the combination of flows constitutes the product P, and which ones are resources or fuel F and, finally, which flows are losses $Loss$, i.e. those flows that leave the component and the plant and which are not subsequently used. The important step for the exergoeconomic analysis is a proper 'fuel-product definition' of the system to show the real production purpose of its subsystems by attributing a well-defined role (i.e. fuel or product) to each physical flow entering or leaving the subsystems. The fuel represents the resources needed to generate the product and it is not necessarily restricted to being an actual fuel such as natural gas, oil, and coal. The product represents the desired result produced by the system. Both the fuel and the product are expressed in terms of exergy. The losses represent the exergy loss from the system.

The exergy product is defined to be equal to the sum of [34]:

a) All the exergy values to be considered at the outlet (including the exergy of energy streams generated in the component) plus
b) All the exergy increases between inlet and outlet (i.e. the exergy additions to the respective material streams) that are in accord with the purpose of the component

Similarly, the exergy fuel is defined to be equal to:

a) All the exergy values to be considered at the inlet (including the exergy of energy streams supplied to the component) plus
b) All the exergy decreases between inlet and outlet (i.e. the exergy removals from the respective material streams) minus
c) All the exergy increases (between inlet and outlet) that are not in accordance with the purpose of the component.

The productive structure of the system sections and components corresponding to figures in Table 5-5 is given in Table 5-6. T ($F-P$) of a system is defined according to the role mentioned above.

Table 5-5 Control volume of the system components

	Components	Control volume
SECTION 1	High pressure superheater and reheater	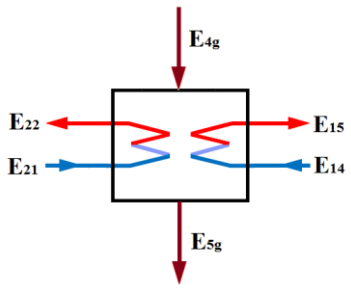
SECTION 2	High pressure evaporator	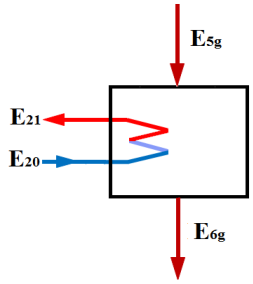
SECTION 3	High pressure economizer 2 and intermediate pressure superheater	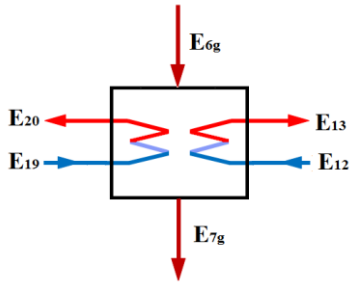
SECTION 4	Intermediate pressure evaporator	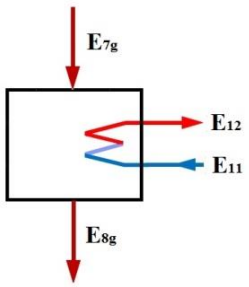
SECTION 5	High pressure Economizer 1, intermediate pressure economizer and low pressure superheater	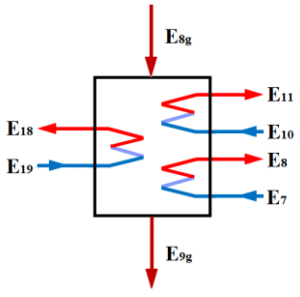

	Components	Control volume
SECTION 6	Low pressure Evaporator	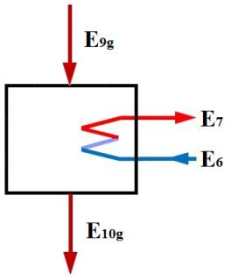
SECTION 7	Low pressure economizer	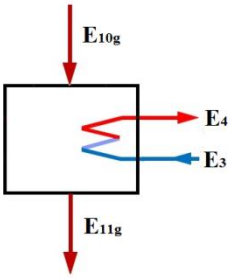
ST_{HP}	High pressure steam turbine	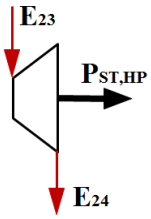
ST_{IP}	Intermediate pressure steam turbine	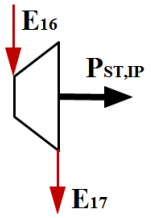
ST_{LP}	Low pressure steam turbine	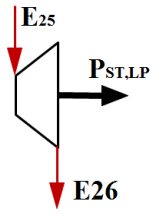
Cond.	Condenser	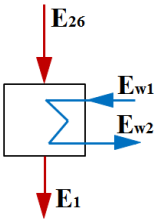

	Components	Control volume
Mix.1	Mixing of streams 2 and 43	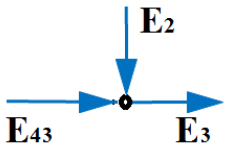
FWT	Feed water tank	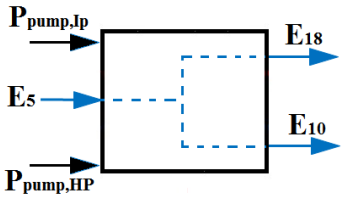
SPL.1	Splitting of streams 43 and 45	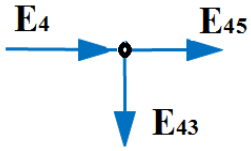
FWP	Condenser pump	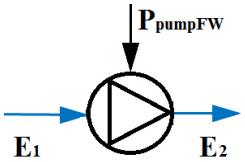
Mix.2	Mixing of streams 13 and 14	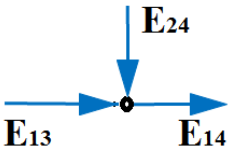
SPL.2	Splitting of streams 5 and 6	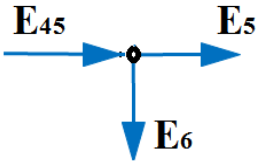
Mix.3	Mixing of streams 9 and 17	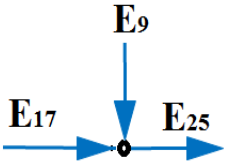

Table 5-6 Fuel–product definition of the system corresponding to Figures in Table 5-5

Component		Fuel exergy rate $\dot{E}_F$	Production exergy rate $\dot{E}_P$
HRSG	Section1	$\dot{E}_{4g} - \dot{E}_{5g}$	$\dot{E}_{22} - \dot{E}_{21} + \dot{E}_{15} - \dot{E}_{14}$
	Section2	$\dot{E}_{5g} - \dot{E}_{6g}$	$\dot{E}_{21} - \dot{E}_{20}$
	Section3	$\dot{E}_{6g} - \dot{E}_{7g}$	$\dot{E}_{20} - \dot{E}_{19} + \dot{E}_{13} - \dot{E}_{12}$
	Section4	$\dot{E}_{7g} - \dot{E}_{8g}$	$\dot{E}_{12} - \dot{E}_{11}$
	Section5	$\dot{E}_{8g} - \dot{E}_{9g}$	$\dot{E}_8 - \dot{E}_7 + \dot{E}_{11} - \dot{E}_{10} + \dot{E}_{19} - \dot{E}_{18}$
	Section6	$\dot{E}_{9g} - \dot{E}_{10g}$	$\dot{E}_7 - \dot{E}_6$
	Section7	$\dot{E}_{10g} - \dot{E}_{11g}$	$\dot{E}_4 - \dot{E}_3$
Steam turbine pressure level	High	$\dot{E}_{23} - \dot{E}_{24}$	$P_{ST,HP}$
	Intermediate	$\dot{E}_{16} - \dot{E}_{17}$	$P_{ST,IP}$
	Low	$\dot{E}_{25} - \dot{E}_{26}$	$P_{ST,LP}$
Condenser		$\dot{E}_{26} - \dot{E}_1$	$\dot{E}_{w2} - \dot{E}_{w1}$
Feed water tank		$P_{pump,HP} + P_{pump,LP}$	$\dot{E}_{18} + \dot{E}_{10} - \dot{E}_5$
Condenser pump		$P_{pump,Con}$	$\dot{E}_2 - \dot{E}_1$

5.2.5.3 Cost Balance

Exergy costing involves cost balances formulated for each system component separately. A cost balance applied to the k^{th} component shows that the sum of cost rates associated with all exiting exergy streams equals the sum of cost rates of all entering exergy streams plus the appropriate charges (cost rate) due to capital investment and operating and maintenance expenses.

In order to calculate the cost rate of each stream in the system, equation (4-41) and equation (4-45) are applied for each system component corresponding to figures in Table 5-5. Thus, the cost-balance equations and auxiliary equations may be written respectively, as in Table 5-7 and Table 5-8. This is accomplished with the aid of the F and P principles discussed previously.

Table 5-7 Exergetic cost rate balances and corresponding auxiliary equations for components of the bottoming cycle CCGT applying equation (4-38)

	Equation type	Exergetic cost rate balance equation
SECTION 1	Main eq.	$\dot{C}_{4g}+\dot{C}_{21}-\dot{C}_{22}-\dot{C}_{5g}+\dot{C}_{14}-\dot{C}_{15}=-\dot{Z}_{su,HP}-\dot{Z}_{RH}$
	P rule	$\frac{\dot{C}_{15}-\dot{C}_{14}}{\dot{E}_{15}-\dot{E}_{14}}=c_{p1}$
	P rule	$\frac{\dot{C}_{22}-\dot{C}_{21}}{\dot{E}_{22}-\dot{E}_{21}}=c_{p1}$
	F rule	$\frac{\dot{C}_{4g}}{\dot{E}_{4g}}=\frac{\dot{C}_{5g}}{\dot{E}_{5g}}$
Section 2	Main eq.	$\dot{C}_{5g}+\dot{C}_{20}-\dot{C}_{21}-\dot{C}_{6g}=-\dot{Z}_{ev,HP}$
	F rule	$\frac{\dot{C}_{5g}}{\dot{E}_{5g}}=\frac{\dot{C}_{6g}}{\dot{E}_{6g}}$
Section3	Main eq.	$\dot{C}_{6g}+\dot{C}_{19}-\dot{C}_{20}-\dot{C}_{7g}+\dot{C}_{12}-\dot{C}_{13}=-\dot{Z}_{ec2,HP}-\dot{Z}_{su,IH}$
	P rule	$\frac{\dot{C}_{20}-\dot{C}_{19}}{\dot{E}_{20}-\dot{E}_{19}}=c_{p2}$
	P rule	$\frac{\dot{C}_{13}-\dot{C}_{12}}{\dot{E}_{13}-\dot{E}_{12}}=c_{p2}$
	F rule	$\frac{\dot{C}_{6g}}{\dot{E}_{6g}}=\frac{\dot{C}_{7g}}{\dot{E}_{7g}}$
Section 4	Main eq.	$\dot{C}_{7g}+\dot{C}_{11}-\dot{C}_{12}-\dot{C}_{8g}=-\dot{Z}_{ev,IP}$
	F rule	$\frac{\dot{C}_{7g}}{\dot{E}_{7g}}=\frac{\dot{C}_{8g}}{\dot{E}_{8g}}$
Section 5	Main eq.	$\dot{C}_{8g}+\dot{C}_{18}-\dot{C}_{19}-\dot{C}_{9g}+\dot{C}_{10}-\dot{C}_{11}+\dot{C}_{7}-\dot{C}_{8}=-\dot{Z}_{ec1,HP}-\dot{Z}_{ec,IP}-\dot{Z}_{su,LP}$
	P rule	$\frac{\dot{C}_{19}-\dot{C}_{18}}{\dot{E}_{19}-\dot{E}_{18}}=c_{p3}$
	P rule	$\frac{\dot{C}_{11}-\dot{C}_{10}}{\dot{E}_{11}-\dot{E}_{10}}=c_{p3}$
	P rule	$\frac{\dot{C}_{8}-\dot{C}_{7}}{\dot{E}_{8}-\dot{E}_{7}}=c_{p3}$
	F rule	$\frac{\dot{C}_{8g}}{\dot{E}_{8g}}=\frac{\dot{C}_{9g}}{\dot{E}_{9g}}$
Section 6	Main eq.	$\dot{C}_{9g}+\dot{C}_{6}-\dot{C}_{7}-\dot{C}_{10g}=-\dot{Z}_{ev,LP}$
	F rule	$\frac{\dot{C}_{9g}}{\dot{E}_{9g}}=\frac{\dot{C}_{10g}}{\dot{E}_{10g}}$

	Equation type	Exergetic cost rate balance equation
Section 7	Main eq.	$\dot{C}_{10g} + \dot{C}_2 - \dot{C}_4 - \dot{C}_{11g} = -\dot{Z}_{ec,LP}$
	F rule	$\frac{\dot{C}_{10g}}{\dot{E}_{10g}} = \frac{\dot{C}_{11g}}{\dot{E}_{11g}}$
ST_{HP}	Main equation	$\dot{C}_{22} - \dot{C}_{24} - \dot{C}_{ST,HP} = -\dot{Z}_{ST,HP}$
	F rule	$\frac{\dot{C}_{23}}{\dot{E}_{23}} = \frac{\dot{C}_{24}}{\dot{E}_{24}}$
ST_{IP}	Main eq.	$\dot{C}_{15} - \dot{C}_{17} - \dot{C}_{ST,IP} = -\dot{Z}_{ST,IP}$
	F rule	$\frac{\dot{C}_{16}}{\dot{E}_{16}} = \frac{\dot{C}_{17}}{\dot{E}_{17}}$
ST_{LP}	Main eq.	$\dot{C}_{25} - \dot{C}_{26} - \dot{C}_{ST,LP} = -\dot{Z}_{ST,LP}$
	F rule	$c_{25} = c_{26}$
Cond.	Main eq.	$\dot{C}_{26} + \dot{C}_{w1} - \dot{C}_1 - \dot{C}_{w2} = -\dot{Z}_{CON}$
	F rule	$\frac{\dot{C}_{26}}{\dot{E}_{26}} = \frac{\dot{C}_1}{\dot{E}_1}$
Mix.1	Mixing of streams 2 and 43	$\dot{C}_2 + \dot{C}_{43} = \dot{C}_3$
FWT	Main eq.	$\dot{C}_5 + \dot{C}_{pump,IP} + \dot{C}_{pump,HP} - \dot{C}_{10} - \dot{C}_{18} = -\dot{Z}_{FWT}$
	P rule	$\frac{\dot{C}_{10}}{\dot{E}_{10}} = \frac{\dot{C}_{18}}{\dot{E}_{18}}$
SPL.1	Splitting of streams 43 and 45	$\dot{C}_4 = \dot{C}_{43} + \dot{C}_{45}$
	Additional equation	$\frac{\dot{C}_{43}}{\dot{E}_{43}} = \frac{\dot{C}_{45}}{\dot{E}_{45}}$
FWP	Feed water tank	$\dot{C}_1 + \dot{C}_{pump,CON} - \dot{C}_2 = -\dot{Z}_{pump}$
Mix.2	Mixing of streams 13 and 14	$\dot{C}_{24} + \dot{C}_{13} = \dot{C}_{14}$
SPL.2	Main eq.	$\dot{C}_{45} = \dot{C}_5 + \dot{C}_6$
	F rule	$\frac{\dot{C}_5}{\dot{E}_5} = \frac{\dot{C}_6}{\dot{E}_6}$
Mix.3	Mixing of streams 8 and 17	$\dot{C}_8 + \dot{C}_{17} = \dot{C}_{25}$

Table 5-8 Exergetic cost rate balances and corresponding auxiliary equations for components of the bottoming cycle CCGT applying equation (4-40)

	Equation type	Exergetic cost rate balance equation
SECTION 1	Main eq.	$c_{4g}\dot{E}_{4g} + c_{21}\dot{E}_{21} - c_{22}\dot{E}_{22} - c_{5g}\dot{E}_{5g} + c_{14}\dot{E}_{14} - c_{15}\dot{E}_{15} = -\dot{Z}_{su,HP} - \dot{Z}_{RH}$
	P rule	$c_{15}\dot{E}_{15} - c_{14}\dot{E}_{14} = c_{p1}(\dot{E}_{15} - \dot{E}_{14})$
	P rule	$c_{22}\dot{E}_{22} - c_{21}\dot{E}_{21} = c_{p1}(\dot{E}_{22} - \dot{E}_{21})$
	F rule	$c_{4g} = c_{5g}$
Section 2	Main eq.	$c_{5g}\dot{E}_{5g} + c_{20}\dot{E}_{20} - c_{21}\dot{E}_{21} - c_{6g}\dot{E}_{6g} = -\dot{Z}_{ev,HP}$
	F rule	$c_{5g} = c_{6g}$
Section3	Main eq.	$c_{6g}\dot{E}_{6g} + c_{19}\dot{E}_{19} - c_{20}\dot{E}_{20} - c_{7g}\dot{E}_{7g} + c_{12}\dot{E}_{12} - c_{13}\dot{E}_{13} = -\dot{Z}_{ec2,HP} - \dot{Z}_{su,IP}$
	P rule	$c_{20}\dot{E}_{20} - c_{19}\dot{E}_{19} = c_{p2}(\dot{E}_{20} - \dot{E}_{19})$
	P rule	$c_{13}\dot{E}_{13} - c_{12}\dot{E}_{12} = c_{p2}(\dot{E}_{13} - \dot{E}_{12})$
	F rule	$c_{6g} = c_{7g}$
Section 4	Main eq.	$c_{7g}\dot{E}_{7g} + c_{11}\dot{E}_{11} - c_{12}\dot{E}_{12} - c_{8g}\dot{E}_{8g} = -\dot{Z}_{ev,IP}$
	F rule	$c_{7g} = c_{8g}$
Section 5	Main eq.	$c_{8g}\dot{E}_{8g} + c_{18}\dot{E}_{18} - c_{19}\dot{E}_{19} - c_{9g}\dot{E}_{9g} + c_{10}\dot{E}_{10} - c_{11}\dot{E}_{11} + c_{7}\dot{E}_{7} - c_{8}\dot{E}_{8} = -\dot{Z}_{ec1,HP} - \dot{Z}_{ec,IP} - \dot{Z}_{su,LP}$
	P rule	$c_{19}\dot{E}_{19} - c_{18}\dot{E}_{18} = c_{p3}(\dot{E}_{19} - \dot{E}_{18})$
	P rule	$c_{11}\dot{E}_{11} - c_{10}\dot{E}_{10} = c_{p3}(\dot{E}_{11} - \dot{E}_{10})$
	P rule	$c_{8}\dot{E}_{8} - c_{7}\dot{E}_{7} = c_{p3}(\dot{E}_{8} - \dot{E}_{7})$
	F rule	$c_{8g} = c_{9g}$
Section 6	Main eq.	$c_{9g}\dot{E}_{9g} + c_{6}\dot{E}_{6} - c_{7}\dot{E}_{7} - c_{10g}\dot{E}_{10g} = -\dot{Z}_{ev,LP}$
	F rule	$c_{9g} = c_{10g}$

	Equation type	Exergetic cost rate balance equation
Section 7	Main eq.	$c_{10g}\dot{E}_{10g} + c_3\dot{E}_3 - c_4\dot{E}_4 - c_{11g}\dot{E}_{11g} = -\dot{Z}_{ec,LP}$
	F rule	$c_{10g} = c_{11g}$
ST_{HP}	Main eq.	$c_{22}\dot{E}_{22} - c_{24}\dot{E}_{24} - c_{ele}\dot{E}_{ST,HP} = -\dot{Z}_{ST,HP}$
	F rule	$c_{22} = c_{24}$
ST_{IP}	Main eq.	$c_{15}\dot{E}_{15} - c_{17}\dot{E}_{17} - c_{ele}\dot{E}_{ST,IP} = -\dot{Z}_{ST,IP}$
		$c_{15} = c_{17}$
ST_{LP}	Main eq.	$c_{25}\dot{E}_{25} - c_{26}\dot{E}_{26} - c_{ele}\dot{E}_{ST,LP} = -\dot{Z}_{ST,LP}$
	F rule	$c_{25} = c_{26}$
Cond.	Main eq.	$c_{26}\dot{E}_{26} + c_{w1}\dot{E}_{w1} - c_1\dot{E}_1 - c_{w2}\dot{E}_{w2} = -\dot{Z}_{Con}$
	F rule	$c_{26} = c_1$
Mix.1	Mixing of streams 2 and 43	$c_2\dot{E}_2 + c_{43}\dot{E}_{43} = c_3\dot{E}_3$
FWT	Main eq.	$c_5\dot{E}_5 + c_{ele}P_{pump,IP} + c_{ele}P_{pump,HP} - c_{10}\dot{E}_{10} - c_{18}\dot{E}_{18} = -\dot{Z}_{FWT}$
	P rule	$c_{10} = c_{18}$
SPL.1	Splitting of streams 43 and 45	$c_4\dot{E}_4 = c_{43}\dot{E}_{43} + c_{45}\dot{E}_{45}$
	Additional equation	$c_{43} = c_{45}$
FWP	Feed water tank	$c_1\dot{E}_1 + c_{ele}P_{pump,Con} - c_2\dot{E}_2 = -\dot{Z}_{pump}$
Mix.2	Mixing of streams 13 and 14	$c_{24}\dot{E}_{24} + c_{13}\dot{E}_{13} = c_{14}\dot{E}_{14}$
SPL.2	Main eq.	$c_{45}\dot{E}_{45} = c_5\dot{E}_5 + c_6\dot{E}_6$
	F rule	$c_5 = c_6$
Mix.3	Mixing of streams 8 and 17	$c_8\dot{E}_8 + c_{17}\dot{E}_{17} = c_{25}\dot{E}_{25}$

In order to find cost flow rates and average costs per unit exergy, a system of linear equations was constructed. Matrix formulation was used to solve the system of the equations:

$$A \times X = B \tag{5-102}$$

where A is the matrix of coefficients constructed from main and auxiliary equations, X is the unknown vector of cost flow rates ($c_k \dot{E}$), and B is the vector of capital cost flow rates ($\dot{Z}$). The systems of these linear equations were constructed and solved using the FORTRAN code.

5.2.6 Optimization Methods and Optimization Procedure

5.2.6.1 First Approach, Simple Approach with Three Optimization Methods

Optimization is the art of obtaining the best results under given circumstances. In an optimization problem one seeks to maximize or minimize a specific quantity called the objective function, where the objective function depends on a finite number of (input) variables. These variables may be independent of one another or they may be related through one or more constraints. In engineering design activities, engineers have to take many technological and managerial decisions at several stages. The objective is to maximize desired benefit or minimize the effort required. The optimization methods are also known as mathematical programming techniques. There may be more than one acceptable design and the purpose of optimization is to choose the best one out of the many acceptable design variables. An optimization problem is generally stated by specifying the constraints, objective functions, and design vectors.

5.2.6.1.1 Design Variables

An engineering system is described by a set of quantities, which are viewed as variables during the design process. Some quantities are usually fixed on the outset and they are called pre-assigned parameters. All other quantities are treated as variables in the design process and they are called design or decision vectors. The choice of the important design variables in an optimization problem that largely depends on the user and his experience. However, it is important to understand that the efficiency and speed of optimization technique depend largely on the number of chosen design variables. Thus, by selectively choosing the design variables, the efficiency of the optimization technique can be increased. In this thesis, the design variables are chosen as follows:

1. Pinch point temperatures (PP_{LP} , PP_{IP} , PP_{HP})
2. Steam pressure in low, intermediate, and high pressure drum p_{LP} , p_{IP} , p_{HP}

5.2.6.1.2 Constraints

Constraints are the limitations imposed upon the value of the design variable. There may be both equality as well as inequality constraints. The design variables are not chosen arbitrarily. They have to satisfy certain specified functional requirements, as well as other requirements. These restrictions must be met in order to produce an acceptable design called design constraints. The constraints, which represent limitations on the behavior or performance of a system, are termed as behavior or functional constraints. The constrains in this work are given as:

1. The upper limit of the steam pressure p_{HP} of the high pressure level

$$p_{HP} \leq 180 \text{ bar} \tag{5-103}$$

2. The lower limit of the exhaust gas temperature

$$T_{11g} \geq 93 \text{ °C} \tag{5-104}$$

3. Lower limit pinch point temperature PP , PP_{LP} , PP_{IP} , PP_{HP}

$$PP \geq 4 \text{ °C} \tag{5-105}$$

4. Lower limit of the feed water temperature (inlet temperature to the HRSG)

$$T_3 \geq 60 \text{ °C} \tag{5-106}$$

5.2.6.1.3 Objective Function

The criterion with respect to which design is optimized when expressed as function of design variables is known as objective function. Defining an appropriate objective function is a vital step in optimization of any thermal system. The choice of the objective function is governed by the nature of the problem. Thus, the selection of the objective function is one of the most important decisions in the whole optimum design process. In general, the objective function can be of two types: the objective function is either to be maximized or to be minimized. However, the optimization methods are usually either for minimization problems or for maximization problems. If the method (or design) is developed for solving a minimization problem, it can also be used to solve a maximization problem by simply multiplying the objective function by (minus) and vice-versa.

Considering only a single thermodynamic objective function, which can be minimizing the irreversibility within the system, might lead to an uneconomical design. Since the economic considerations have a great importance in the design of engineering systems, the designer must consider the total cost of the project alongside achieving the maximum thermodynamics efficiency. Therefore, one of the common objective functions, which simultaneously contain both capital cost and energy or exergy cost, is thermoeconomic objective function. In this work, both kinds of objective functions are used:

Thermodynamic Objective Function: A suitable objective in thermodynamic optimization is minimizing the sum of irreversibilites within the bottoming cycle. In the bottoming cycle, irreversibility is the sum of the total exergy waste and destruction in each single component of the system. By minimizing this objective function, the efficiency will be maximized.

Thermoeconomic Objective Function: Different objective functions are chosen for the thermoeconomic optimization, depending on the optimization method; the optimization procedure was performed for each objective function and the result was compared with the aim to minimize the production cost of electricity, maximize the power output, and to enhance the exergoeconomic performance. Three objective functions were used in this thesis:

a) Energy Optimization Method (Case 1). The first objective function f_1 selected on the basis of energy analysis is the generating cost of electricity C_{kWh}. The production cost of electricity C_{kWh} is the total annual investment cost $Z_{a,TOT}$ of the CCGT plant divided by mean annual energy output $W_{CCGT}H$.

$$C_{kWh} = f_1 = \frac{Z_{a,TOT}}{W_{CCGT}H} \tag{5-107}$$

b) Exergy Destruction Optimization Method (Case 2). The second objective function chosen for this method is defined as the sum of three parts: the annual capital cost that stands for the capital investment and maintenance expenses $Z_{a,BOT}$, the corresponding cost of exergy destruction $C_{D,BOT}$, and exergy losses $C_{loss,BOT}$ of the bottoming cycle. Therefore, the objective function represents the total annual cost rate of the bottoming cycle in terms of dollars per year and it is defined as [21] and [74]:

$$Ct_{BOT} = f_2 = Z_{a,BOT} + C_{D,BOT} + C_{loss,BOT} \quad (5\text{-}108)$$

The objective function f_2 is to be minimized so that the values of optimal design parameters could be obtained. The decision variables (design parameters) considered in this study are as follows: pinch points PP, PP_{LP}, PP_{IP}, PP_{HP}, and pressures p_{LP}, p_{IP}, p_{HP}, in the pressure drums.

c) Exergoeconomic Optimization Method (Case 3). In general, exergoeconomic optimization of a thermal system requires two conflicting objectives: one being increased in exergetic efficiency and the other decreased in product cost. It hopes to satisfy both objectives simultaneously. The first objective is governed by thermodynamic requirements, and the second by economic constraints. Therefore, the objective function should be defined in such a way that the optimization satisfies both requirements [75]. The objective function to be minimized in the optimization problem is the sum of the specific costs of the products, which includes the plant investment, operation and maintenance, and fuel costs. The objective function for this method is defined as the specific total cost of the products, expressed by equation (5-109),

$$c_{P,TOT} = f_3 = \frac{\sum \dot{Z}_k + \sum c_{F,k} \dot{E}_{F,k}}{\sum \dot{E}_{P,k}} \quad (5\text{-}109)$$

where c_F denotes a specific exergetic cost of fuel, and $\dot{E}_{F,k}$ is the *kth* fuel exergetic flow rate. The sum of the capital investment and the operation and maintenance costs for the k components of the plant is $\dot{Z}_k$. The specific exergetic cost of fuel c_F in equation (5-109) is calculated by solving the linear system of equations in Table 5-8.

$$c_{F,k} = c_{4g} \quad (5\text{-}110)$$

5.2.6.1.4 Optimization Procedure

In this study a procedure for optimizing six steam cycle parameters was developed, and described as follows:

First step. Optimum parameters of low pressure line PP_{LP}, and p_{LP}. It seeks the optimum low-pressure pinch point PP_{LP}, and optimum pressure p_{LP} in a low-pressure drum. In order to find the optimum values of these parameters the initial

values for steam cycle parameters PP_{IP}, PP_{HP}, p_{IP}, and p_{HP} were taken from the initial case. The values for PP_{LP}, and p_{LP} vary in the range 3-30 °C and 1-10 bar respectively. Both thermodynamic parameters and thermoeconomic parameters are calculated. The optimal value for PP_{LP}, and p_{LP} are determined based on the minimized objective function and constraint limitations (exhaust gas temperature $T_{11g} = 93$ °C and lower limit of pinch point PP_{LP}, $= 5$ °C). However, the considered PP_{LP}, and p_{LP} in the current study have to be higher than the optimum ones to maintain the exhaust gas temperature above the dew point of potentially corrosive acidic vapors.

Second step. Optimum parameters of intermediate and high pressure lines. It seeks the optimum pinch points PP_{IP}, PP_{HP} in the intermediate and high-pressure lines, and pressure p_{IP}, p_{HP} in the pressure drums of intermediate and high-pressure lines. In order to define their optimal values, PP_{IP}, PP_{HP}, p_{IP} and p_{HP} were varied, where the previously determined PP_{LP}, and p_{LP} were used. In this proposed method, the values of PP_{IP}, PP_{HP}, p_{IP} and p_{HP} were varied as follows: PP_{IP} in range 1-30 °C, p_{HP} in range 100-200 bar and p_{IP} in range 22-60 bar.

Third step. Iteration: The procedure is then repeated (as in the first step and the second step) in several iterations for new optimum parameters, until the values converge and give the optimum for this step.

5.2.6.2 Optimization Method Using MIDACO Software

To test the effectiveness of the optimization methods, a black box solver (software) named MIDACO is used, which stands for "mixed integer distributed Ant Colony Optimization." MIDACO implements the extended algorithm called Ant Colony Optimization (ACO) for mixed integer nonlinear programming MINLP [90] [91] in combination with the oracle penalty method.

MIDACO solves the general MINLP by assuming a set of lower and upper bounds (x_l, y_l and x_u, y_u) for the decision variables x and y. This additional set of constraints is also known as the box constraints. Equation (5-111) illustrates the MINLP as assumed by MIDACO. It can be noted that functions f(x; y) and g(x; y) are considered

as black box functions by MIDACO. This means that the actual function calculation is considered to happen in a virtual black box (for example, a software library) without any inside knowledge and only the function values are returned after the actual calculation is performed.

Mixed integer nonlinear programming (MINLP) problems are an important class of optimization problems with many real-world applications. A mathematical formulation of a MINLP is given in the equation (5-111).

$$\begin{aligned} &\text{Minimize } f(x,y) \qquad (\mathrm{x} \in \mathbb{R},\ \mathrm{y} \in \mathbb{N}) \\ &\text{subject to: } \mathrm{g_i}(x,y) = 0,\ \ i = 1,\ldots,m_{eq} \in \mathbb{N} \\ &\qquad\qquad \mathrm{g_i}(x,y) = 0,\ \ i = m_{eq}+1,\ldots,m \in \mathbb{N} \\ &\qquad\qquad x_l \le x \le x_u \quad (x_l, x_u \in \mathbb{R}) \\ &\qquad\qquad y_l \le y \le y_u \quad (y_l, y_u \in \mathbb{N}) \end{aligned} \tag{5-111}$$

Where $f(x,y)$ denotes the objective function to be minimized. In equation (5-111), the equality constraints are given by $\mathrm{g}_{1,\cdots,me}(x,y)$ and the inequality constraints are given by $\mathrm{g}_{me+1,\cdots,m}(x,y)$. The vector x contains the continuous decision variables and the vector y contains the discrete decision variables.

Furthermore, some box constraints as x_l, y_l (lower bounds) and x_u, y_u (upper bounds) for the decision variables x and y are considered in equation (5-111) [91].

In the MIDACO software, the distinction between continuous variables and discrete variables is not indicated by the name (x or y). Only one vector of decision variables in the software is considered and called (X). The first entries of this vector represent the continuous variables, while the last entries represent the discrete (also called integer or combinatorial) variables.

The MIDACO algorithm is based on an evolutionary metaheuristic called Ant Colony Optimization (ACO), which was extended to the mixed integer search domain in [68]. The ACO algorithm in MIDACO is based on a so-called multi-kernel Gaussian probability density functions (PDF), which generate samples of iterates (called Ants). For integer decision variables, a discretized version of the PDF is applied. Constraints are within MIDACO handled by the Oracle Penalty Method. This is an advanced method that was developed especially for heuristic search algorithms (like ACO, GA or PS). The aim of this method is finding the global optimal solution by using a parameter called Oracle [92], which corresponds directly with the objective function value $f(x,y)$. The

method is self-adaptive and therefore MIDACO can be classified as a self-adaptive algorithm.

The mathematical formulation of a problem in MIDACO consists of the objective function F(x), decision variables vector (X) and constraints g(x).

5.2.6.2.1 Objective Function

The objective function used in this method is the specific total cost of the products $c_{P,TOT}$.

5.2.6.2.2 Decision Variables

Because of the limitation of the software used in this study (with four variables), and the fact that the optimization problem in the current study deals with six decision variables, the optimization procedures consist of two steps similar to the simple optimization method: optimizing pinch point PP_{LP} of the low pressure line, and pressure p_{LP} in low pressure drum in the first step, and optimizing four variables in the second step PP_{IP} , p_{IP} , PP_{HP} , and p_{HP} .

5.2.6.2.3 Optimization Procedure

Solving the optimization problem by MIDACO software in this study is divided in two steps:

First step. Optimum parameters of low pressure line PP_{LP} and p_{LP} . To find the optimum parameters for the low-pressure line, taking into consideration the limitation of exhaust gas temperature T_{11g} , one must apply the software with two variables PP_{LP} and p_{LP} . The values for the other four variables were taken from the initial case.

Second step. Optimum parameters of Intermediate and High Pressure Lines PP_{IP} , p_{IP} , PP_{HP} , and p_{HP} . To find the optimum parameters for the intermediate and high-pressure line, one must apply software with four variables PP_{IP} , p_{IP} , PP_{HP} , and p_{HP} .

6 Results and Discussions of Analyzed Optimization Methods Applied to the CCGT Case Studies

The trends and main findings of the calculated and simulated results are presented in this chapter. A series of investigations has been performed for different combinations of objective functions and a number of operating variables. First of all, the overall system performance is investigated in terms of inlet energy and exergy flows, and the useful plant outputs. Then, the performance of individual components is explored in terms of energy and exergy losses. The effect of operating parameters on energy and exergy efficiencies of plant is also explored.

6.1 Results of Energy Analysis

This section essentially describes the results in energy analysis. Besides the energy analysis, a parametric study of the system is important to analyze how the system will perform while varying certain parameters.

Energy balances are applied to case studies for the operation data given in Table 5-2. The calculations for thermodynamic properties of ideal gases are accomplished by the FORTRAN code. Thermodynamic properties of water and steam and the thermodynamic properties of stack gases at the locations labeled with numerals in Figure 5-1 were presented in Table A-1. Other results are shown with figures in this section.

Thermodynamic parameters for each point of the system as a result of energy analysis presented in Table A-1, Figure 6-1 and Figure 6-2. Figure 6-1 presents the T-s diagram, which shows the relationship between temperature and entropy for the topping cycle and bottoming cycle. Figure 6-2 presents T-Q diagram; it shows the temperature profile of the gas side and water- steam side in the HRSG. The assumed pinch points for the three-pressure level were constant, the initial assumed input data was used in these calculations. Energy analysis is going to investigate the influences of the operating parameters (PP_{LP}, PP_{IP}, PP_{HP}, PP, p_{LP}, p_{IP}, and p_{HP}) on the live steam mass flow rates ($\dot{m}_s$, $\dot{m}_{s,LP}$, $\dot{m}_{s,IP}$, $\dot{m}_{s,HP}$), performance parameters (η_{CCGT} and $P_{G,ST}$) of the CCGT power plant and exhaust gases temperature T_{11g} from the *HRSG*.

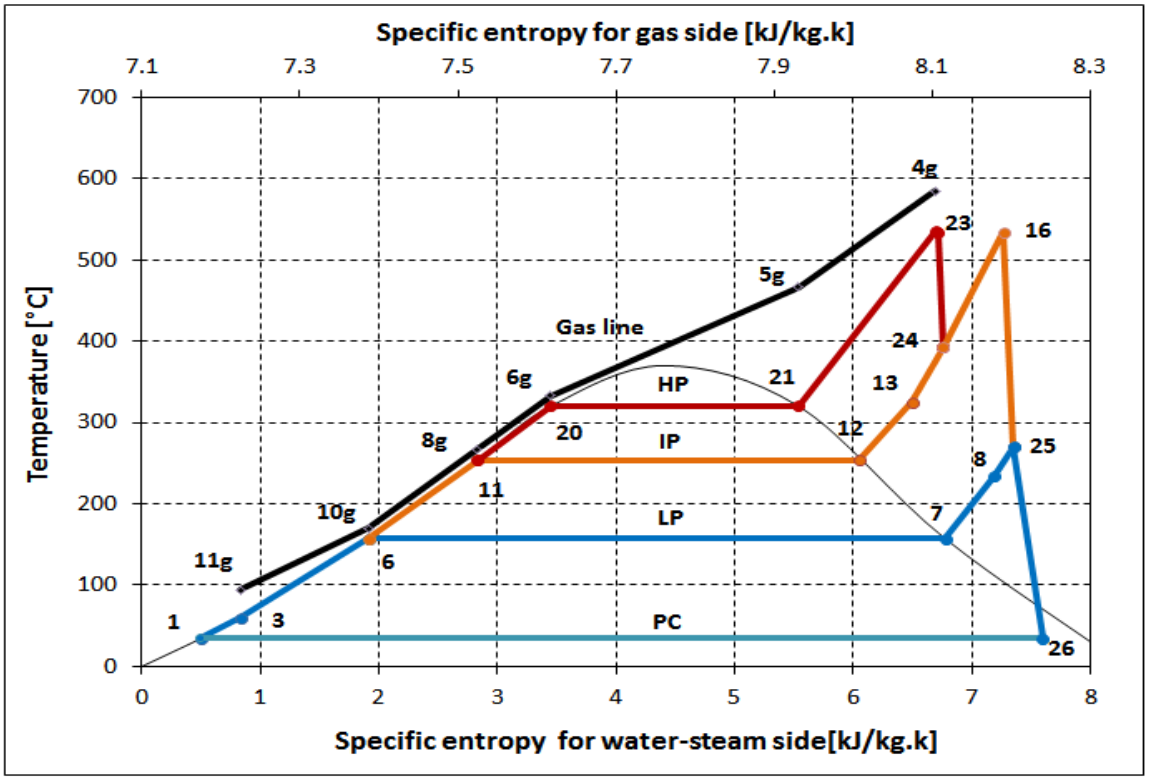

Figure 6-1 T-S diagram for triple-pressure HRSG of CCGT

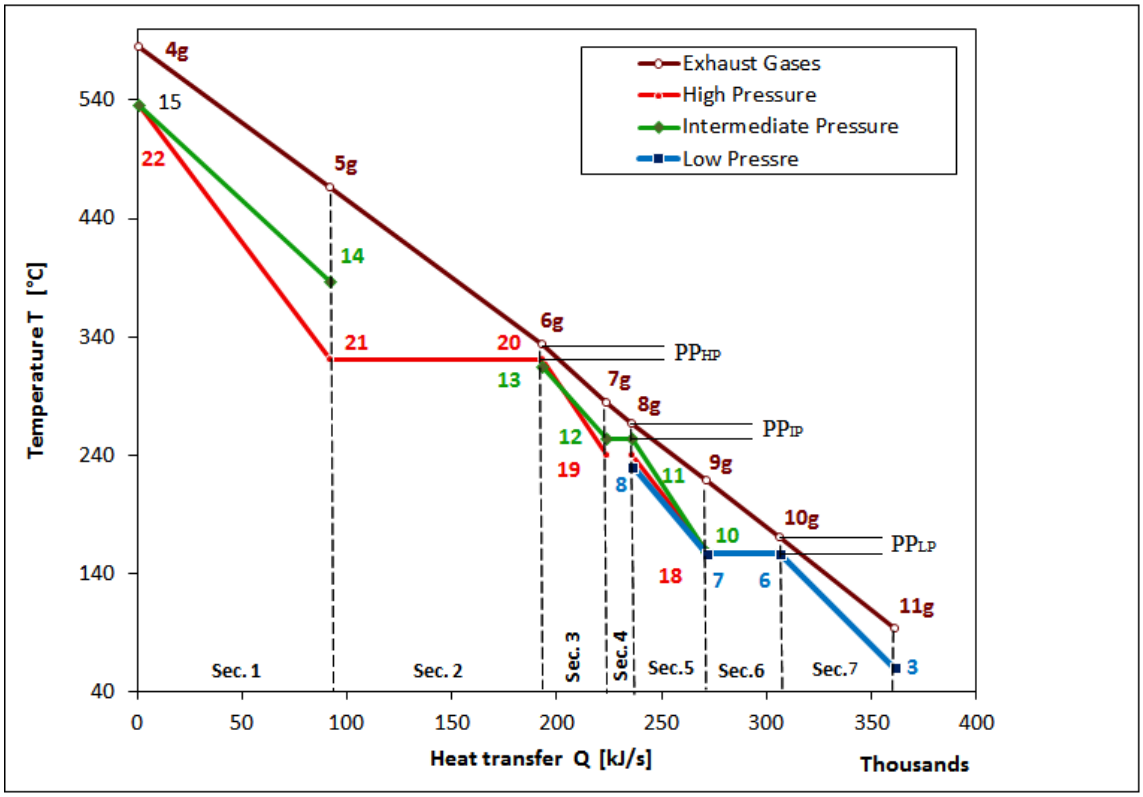

Figure 6-2 T-Q diagram for the initial case

6.1.1 Influence of Pinch Point Temperature on the Performance Parameters

In this section the effect of the pinch points on the plant performance and mass flow rate of the main plant component and sections are studied. In general, increasing the pinch point temperatures results in reduced performance of the CCGT power plant.

6.1.1.1 Steam Mass Flow Rate

Steam mass flow rate through *HRSG* pressure levels are:

1. Water-steam mass flow through low-pressure level is $\dot{m}_{s,LP,HRSG}$
2. Water-steam mass flow through intermediate-pressure level is $\dot{m}_{s,IP,HRSG}$
3. Water-steam mass flow through high-pressure level is $\dot{m}_{s,HP,HRSG}$
4. Water-steam mass flow through reheater $\dot{m}_{s,IP,HRSG}$ plus $\dot{m}_{s,HP,HRSG}$

Steam mass flow rate through steam turbine pressure level:

1. Steam mass flow through low pressure steam turbine (ST_{LP}) is $\dot{m}_{s,LP,ST}$, and equal to the total mass flow rate $\dot{m}_{s,LP,ST} = \dot{m}_s$
2. Steam mass flow through intermediate pressure steam turbine (ST_{IP}) is the $\dot{m}_{s,IP,ST}$, and equal to the summation of the $\dot{m}_{s,IP,HRSG}$ and $\dot{m}_{s,HP,HRSG}$
3. Steam mass flow through high-pressure steam turbine (ST_{HP}) is the $\dot{m}_{s,HP,ST}$, and equal to $\dot{m}_{s,HP,HRSG}$.

The relationship between the live steam mass flow rates and pinch point temperatures (PP_{LP}, PP_{IP}, PP_{HP}, and PP) is considered in this section. The results are expressed in Figure 6-3 to Figure 6-7. The variation of the low-pressure pinch point temperature PP_{LP} is represented by the blue line, the violet line for intermediate pressure pinch point PP_{IP}, the red line for high-pressure pinch point temperature PP_{HP} and the green for the three levels assumed to be an equal pinch point temperature PP.

Low Pressure Pinch Point PP_{LP} : For the HRSG, from Figure 6-3 it is clear that by increasing of PP_{LP} (blue line), the low-pressure mass flow rate $\dot{m}_{s,LP,HRSG}$ was reduced, and this is because of the point 10_g moving towards 19_g within a gas exhaust line Figure 6-2, that leads to increasing in heat transferred in section 6. On the other hand, no change happened with $\dot{m}_{s,HP,HRSG}$ and $\dot{m}_{s,IP,HRSG}$.

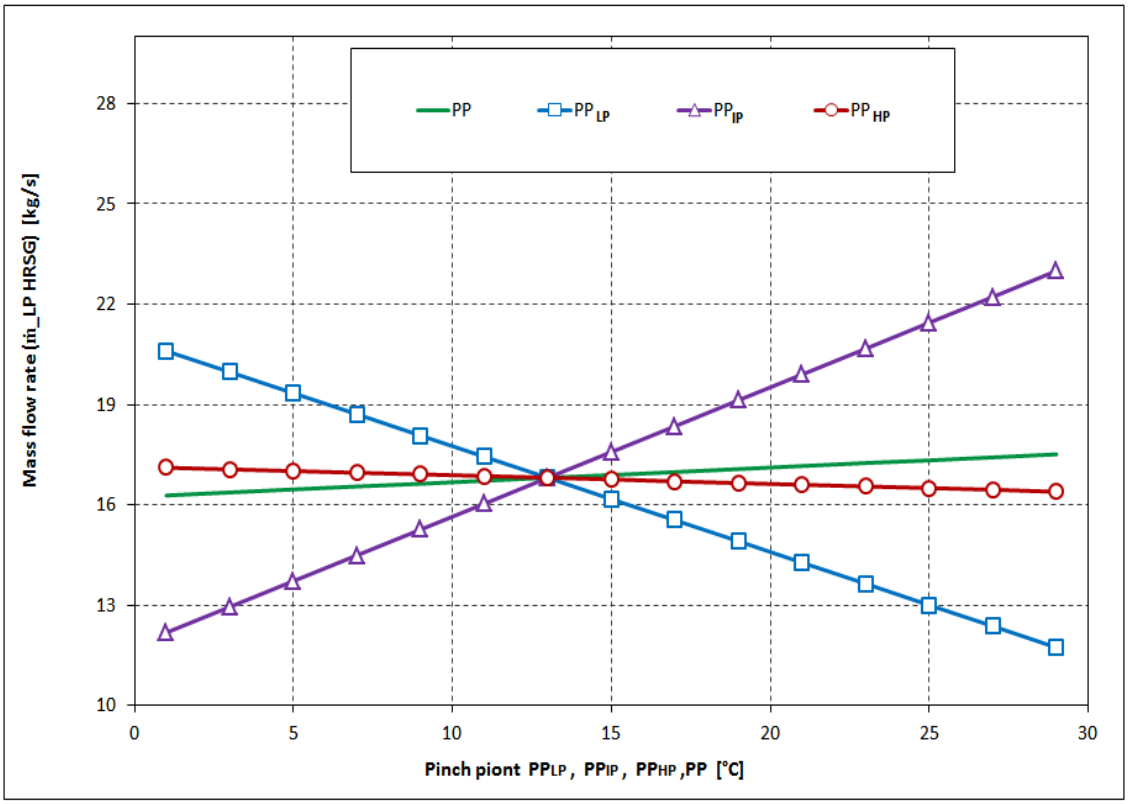

Figure 6-3 Steam mass flow rate of low pressure line of the HRSG vs. the PP

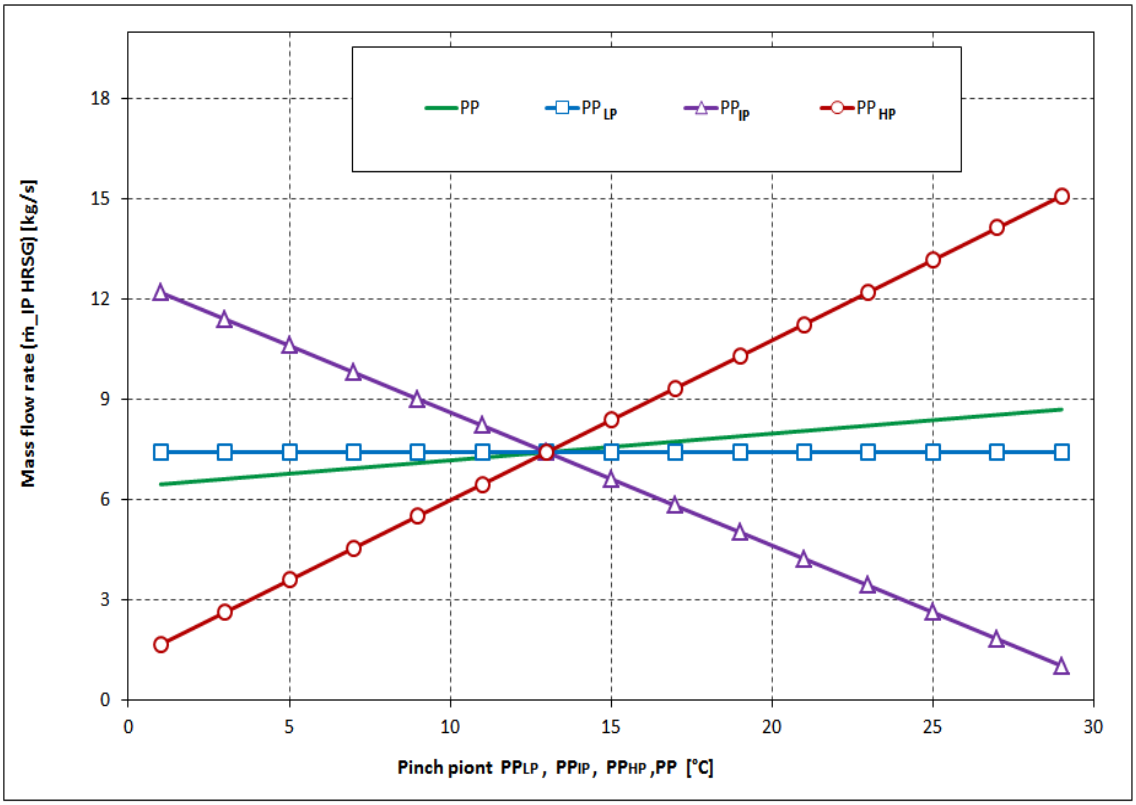

Figure 6-4 Steam mass flow rate of intermediate pressure line of the HRSG vs. the PP

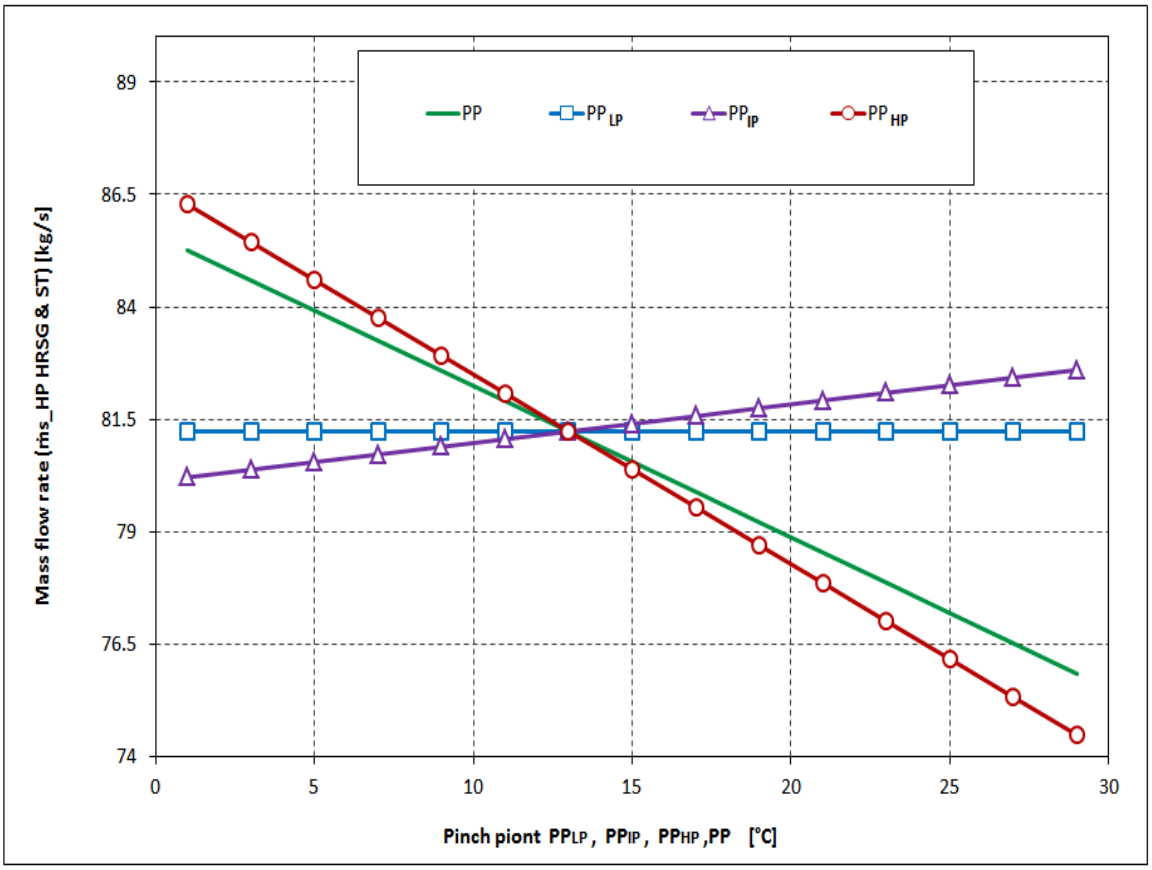

Figure 6-5 Steam mass flow rate of high pressure line of HRSG vs. PP

For the steam turbine, increasing of PP_{LP} there is no change in the high and intermediate pressure steam turbine mass flow rate as seen in (blue line) Figure 6-5 and Figure 6-6. The mass flow rate of low-pressure steam turbine $\dot{m}_{s,LP,ST}$ (blue line) Figure 6-7, is also reduced, because of the reduction in low-pressure mass flow rate of HRSG.

Intermediate Pressure Pinch Point PP_{IP} : By increasing the intermediate pressure pinch point PP_{IP} (violet line), the $\dot{m}_{s,IP,HRSG}$ was extremely reduced as a result of energy balance (low heat transfer, low mass flow rate) Figure 6-4. Because of a high inlet temperature to the low-pressure sections of the HRSG, the low-pressure mass flow rate $\dot{m}_{s,LP,HRSG}$ were extremely increased Figure 6-3, while, the $\dot{m}_{s,HP,HRSG}$ slightly increased. Mass flow rate behavior through the steam turbine sections are always connected with HRSG sections' behavior, $\dot{m}_{s,IP,ST}$ and $\dot{m}_{s,LP,ST}$ extremely increase Figure 6-6 and Figure 6-7.

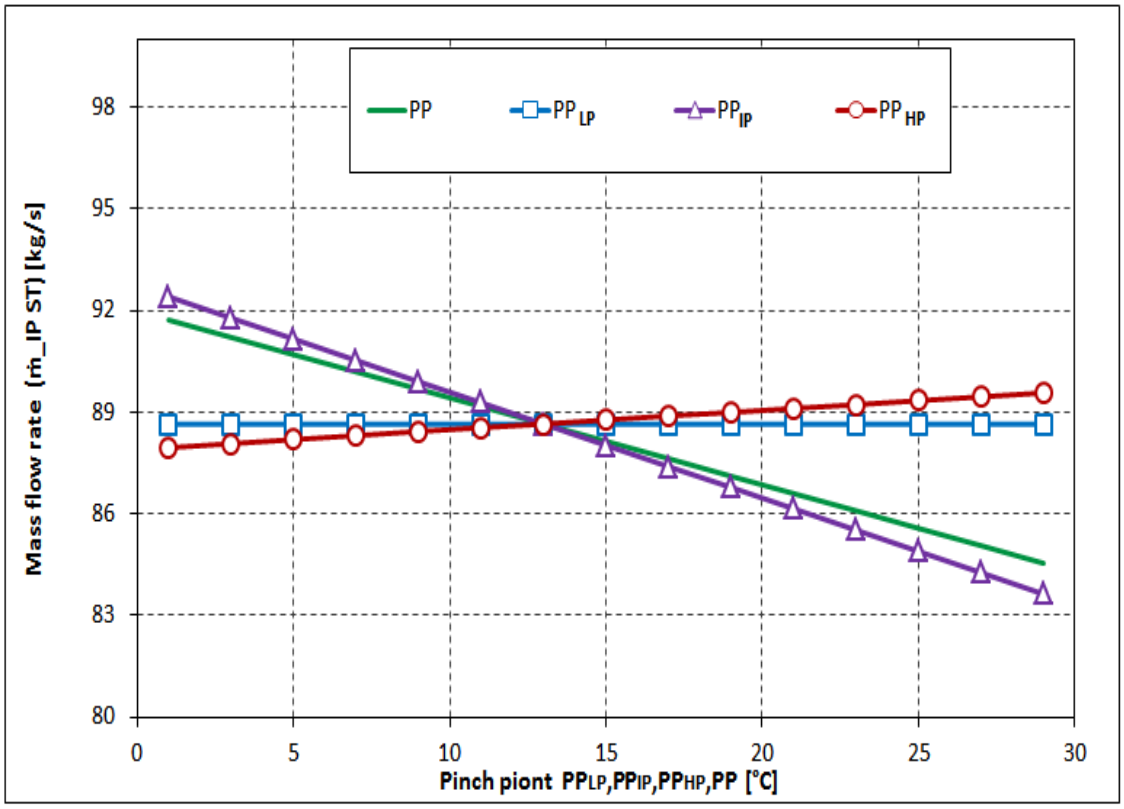

Figure 6-6 Steam mass flow rate of IP steam turbine according to variation of PP

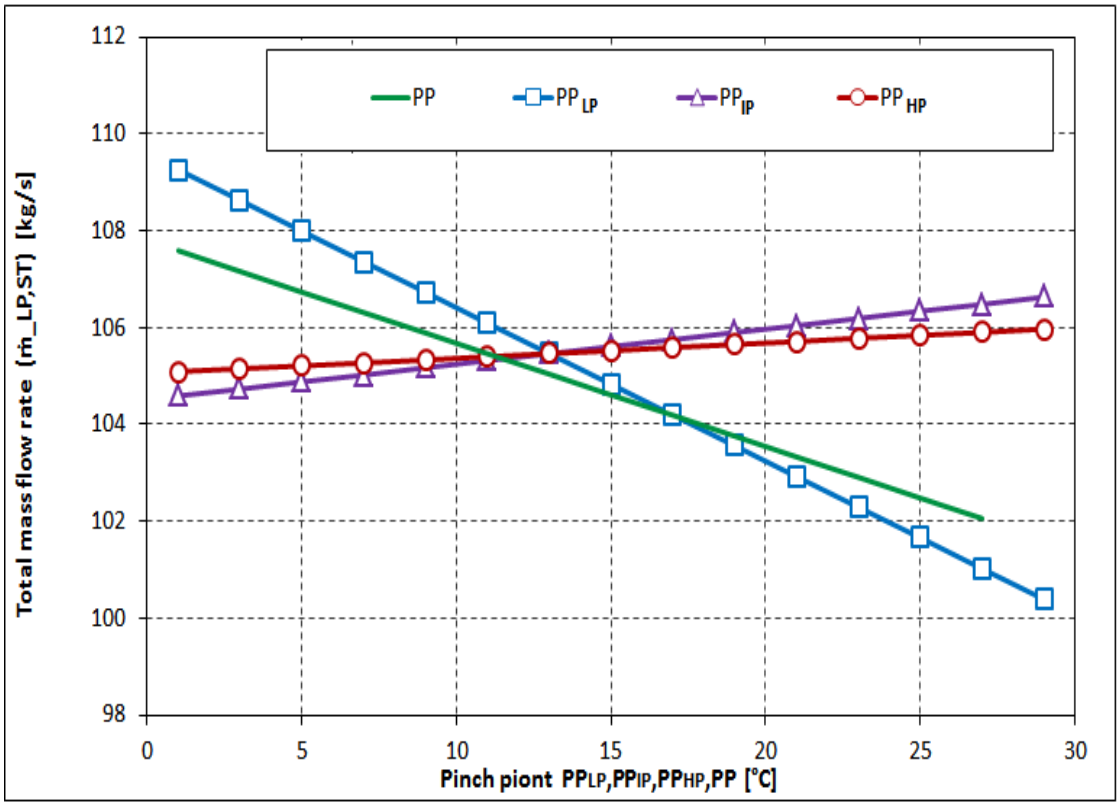

Figure 6-7 Total steam mass flow rate variation of increasing pinch point temperature

High Pressure Pinch Point PP_{HP} : Variation of high pressure pinch point PP_{HP} (red line) shows opposite behavior between intermediate pressure live steam mass flow rate $\dot{m}_{s,IP,HRSG}$ and high pressure live steam mass flow rate $\dot{m}_{s,HP,HRSG}$ as shown in Figure 6-4 and Figure 6-5.

The high pressure mass flow rate $\dot{m}_{s,HP,HRSG}$ were reduced as a result of energy balance while, the intermediate pressure mass flow rate $\dot{m}_{s,IP,HRSG}$ were increased because of a high inlet temperature to the intermediate pressure section T_{6g} . Low-pressure live steam mass flow rate $\dot{m}_{s,LP,HRSG}$ does not change with variations of PP_{HP} as shown in Figure 6-3. High-pressure steam turbine mass flow rate $\dot{m}_{s,IP,ST}$ and total mass flow rate $\dot{m}_{s,LP,ST}$ were slightly increased with variation of PP_{HP} .

6.1.1.2 Steam Turbine Power Output

With the increase of pinch point temperatures PP_{LP} , PP_{IP} , PP_{HP} , and PP the steam turbine power output $P_{G,ST}$ will be reduced with different a gradient as shown in Figure 6-8.

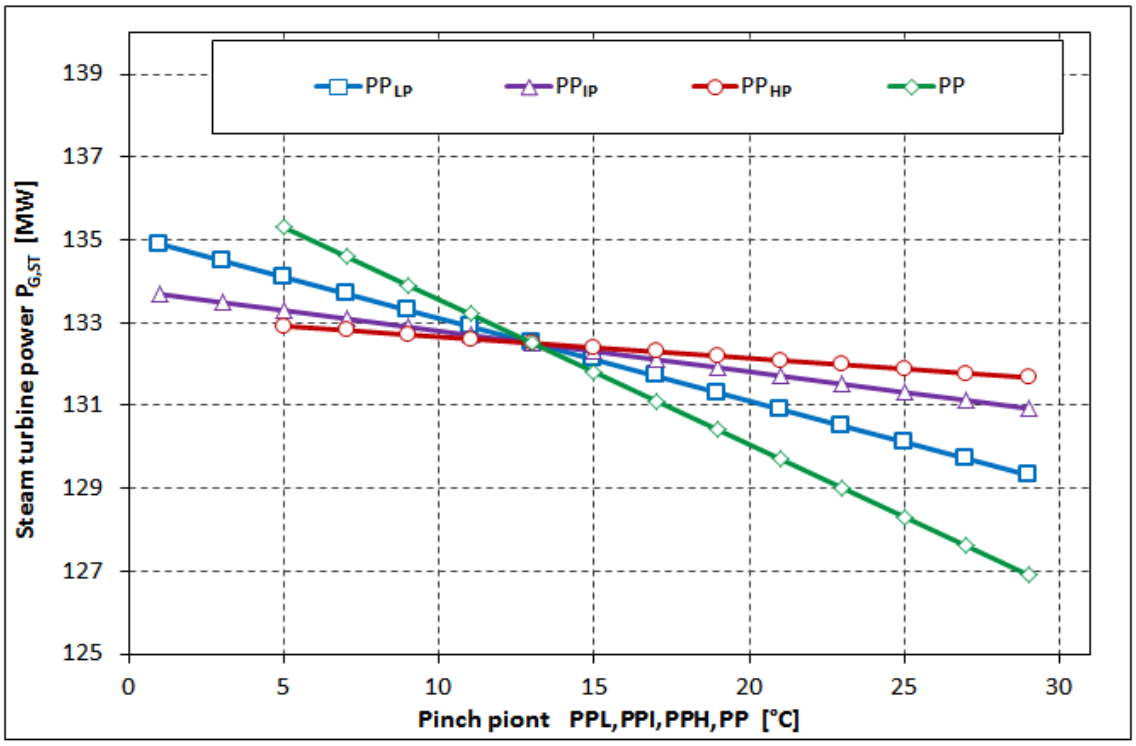

Figure 6-8 Steam turbine power variation of increasing pinch point temperature

The highest gradient of the reduction in $P_{G,ST}$ happened with variations of PP, while, lowest with variations of PP_{HP}. Figure 6-8 shows that the steam turbine power output $P_{G,ST}$ was more sensitive with variations of (PP and PP_{LP}) than with the variation of (PP_{IP} and PP_{HP}).

6.1.1.3 Combined Cycle Efficiency

Figure 6-9 shows the behavior of efficiency η_{CCGT} with the variations of pinch point temperatures PP_{LP}, PP_{IP}, PP_{HP}, and PP. It is clear from this figure that, by increasing the pinch point temperatures of each pressure level leads to decreasing in total thermal efficiency of the power plant. The low pressure pinch point PP_{LP} and PP has a significant effect on the efficiency η_{CCGT}. This behavior is similar to the behavior of the power output with variations of pinch point.

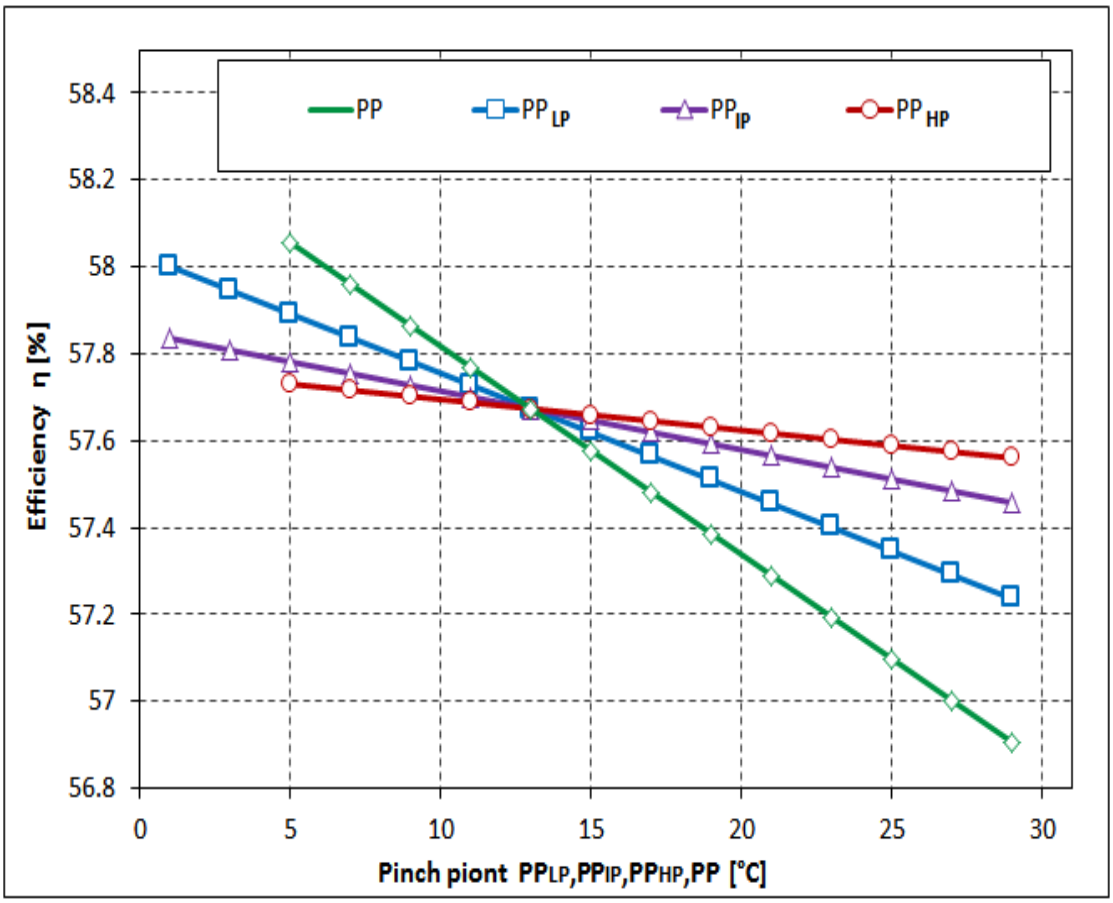

Figure 6-9 CCGT efficiency variation of increasing pinch point temperature

6.1.1.4 Exhaust Gas Temperature

From Figure 6-10, it is clear that the exhaust gas temperature increases with increase of PP_{LP} and PP while the effect of the variation of PP_{IP} and PP_{HP} on it was very small.

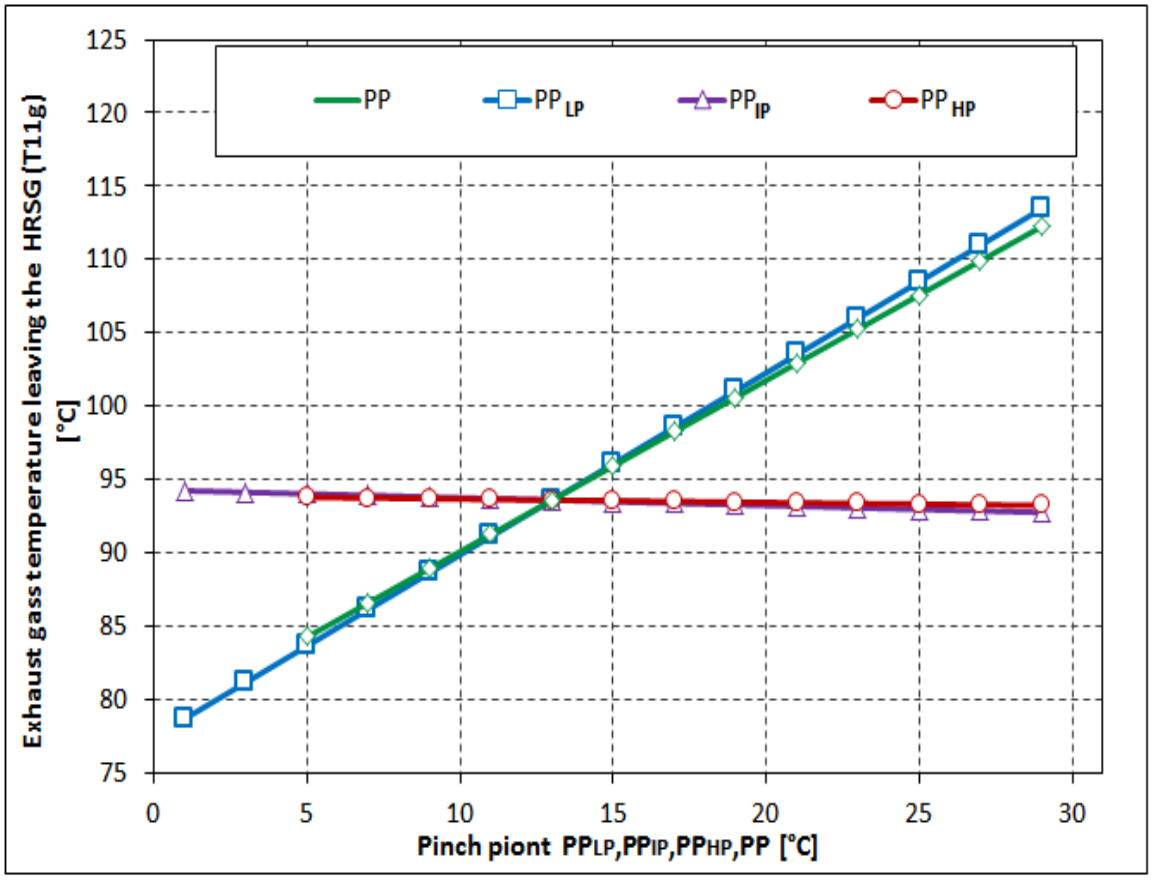

Figure 6-10 Exhaust gases temperature variation of increasing PP

6.1.1.5 Heat Transfer Area

The variations of the heart transfer area of the HRSG heaters as a function of low, intermediate, and high-pressure pinch points are shown in Figure 6-11 to Figure 6-14. By observing this representation, it is obvious that increasing the pinch point of any pressure level of the HRSG will lead to reduction in the heat transfer area of the economizer and evaporator of that pressure level. For other heaters as seen in Figure 6-11 the variation of low-pressure pinch point PP_{LP} does not lead to significant change in the heat transfer area.

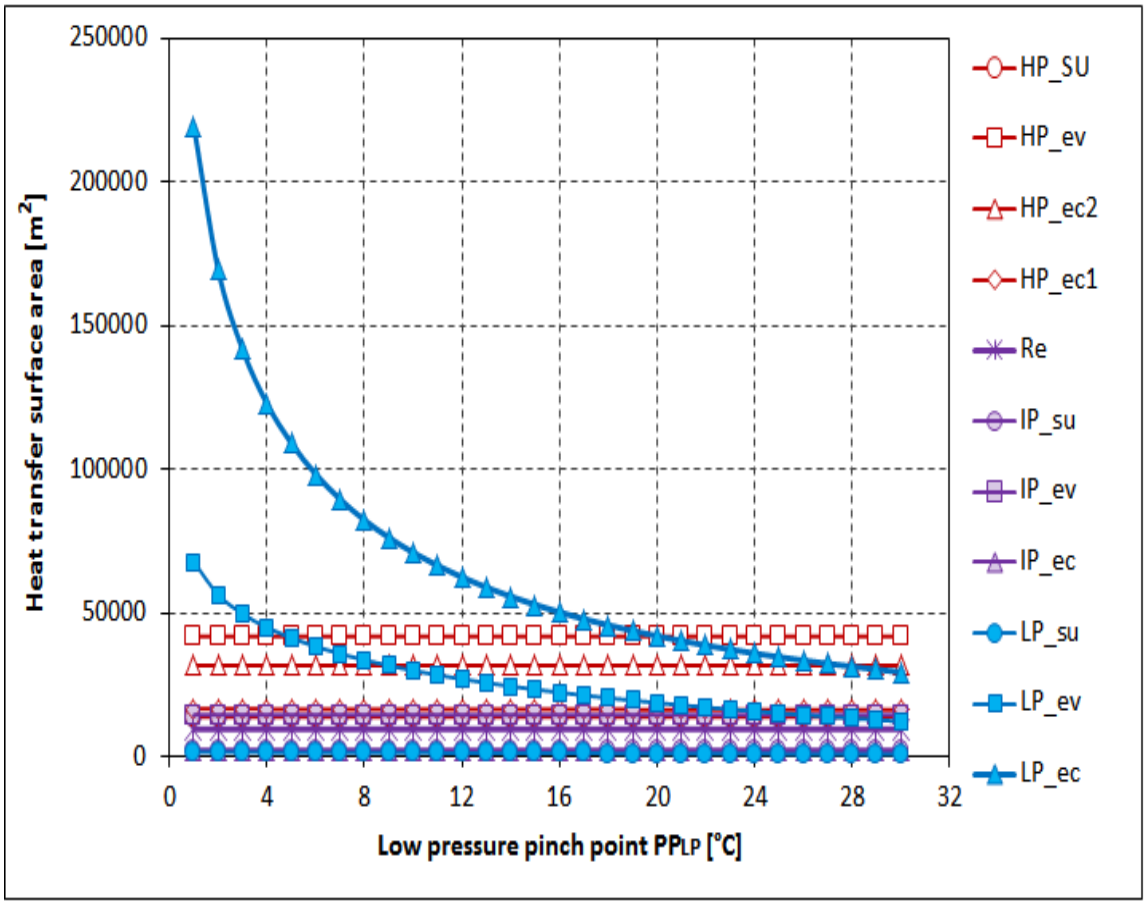

Figure 6-11 Low pressure pinch point PP_{LP} vs. heat transfer area of the HRSG

The increase of pinch points PP_{IP} and PP_{HP} caused the increase of heat transfer area of evaporators and economizers (that were positioned behind the varied pinch point level), as shown in Figure 6-12 and Figure 6-13. In Figure 6-13 low, intermediate pressure economizer, and evaporator heat transfer areas also increased. However, the heat transfer area of the pressure level before the one where the pinch point varied did not change significantly. The heat transfer area of evaporator and economizer for the same pressure level where the pinch point varied was significantly changed, as seen in Figure 6-11 to Figure 6-14.

Figure 6-14 shows the same logic as with the three previous cases; increasing the pinch point PP resulted in reduction of all the heat transfer areas with a different gradient.

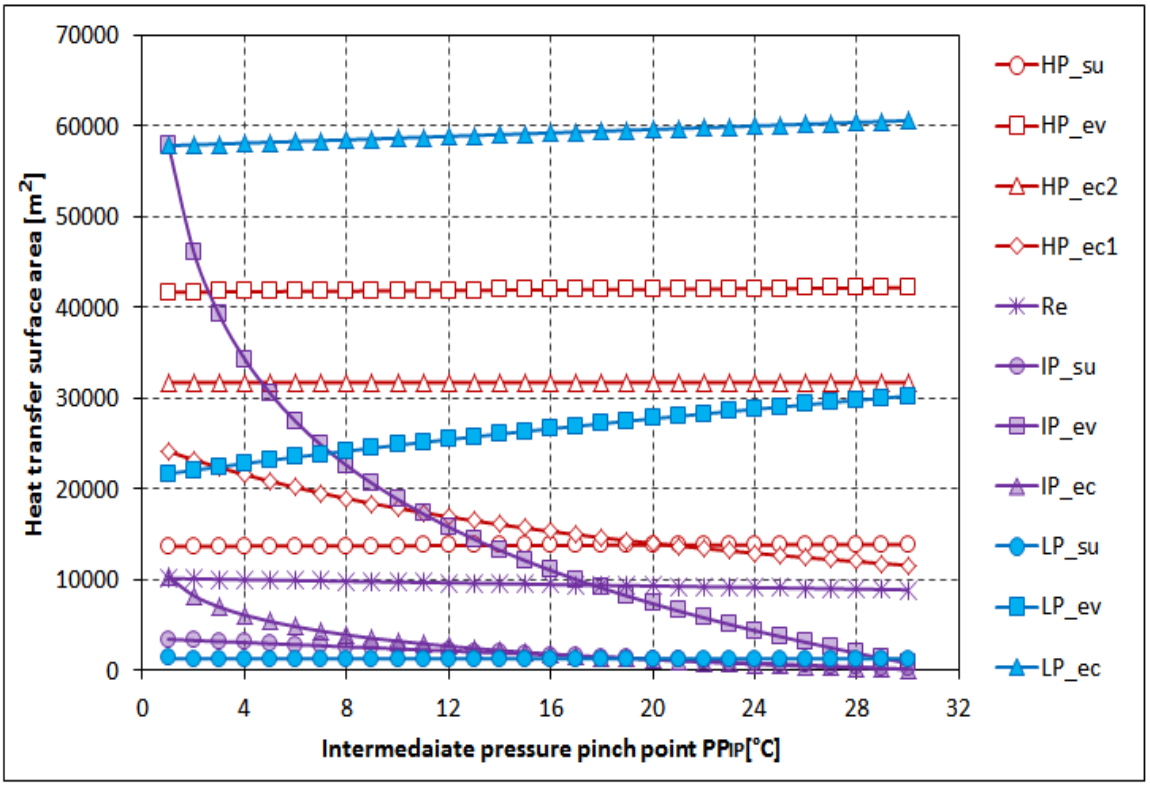

Figure 6-12 Intermediate pressure pinch point PP_{IP} vs. heat transfer area of the HRSG

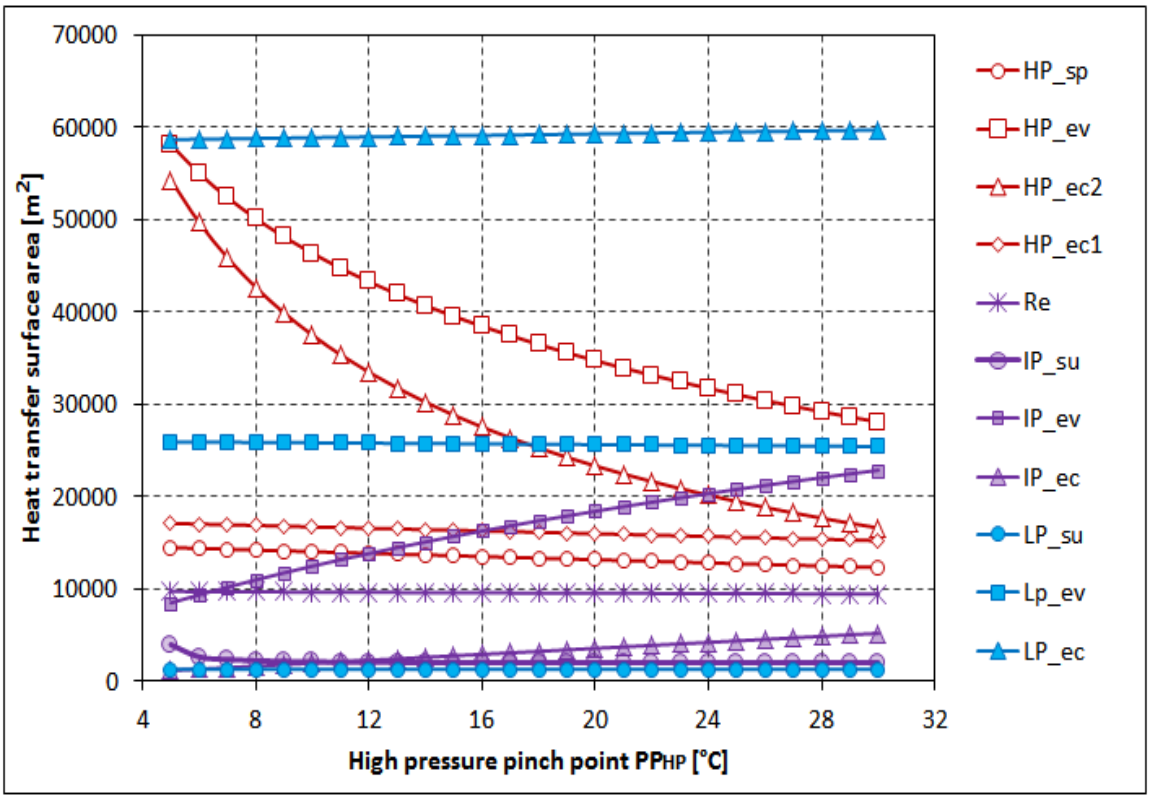

Figure 6-13 High pressure pinch point PP_{HP} vs. heat transfer area of the HRSG

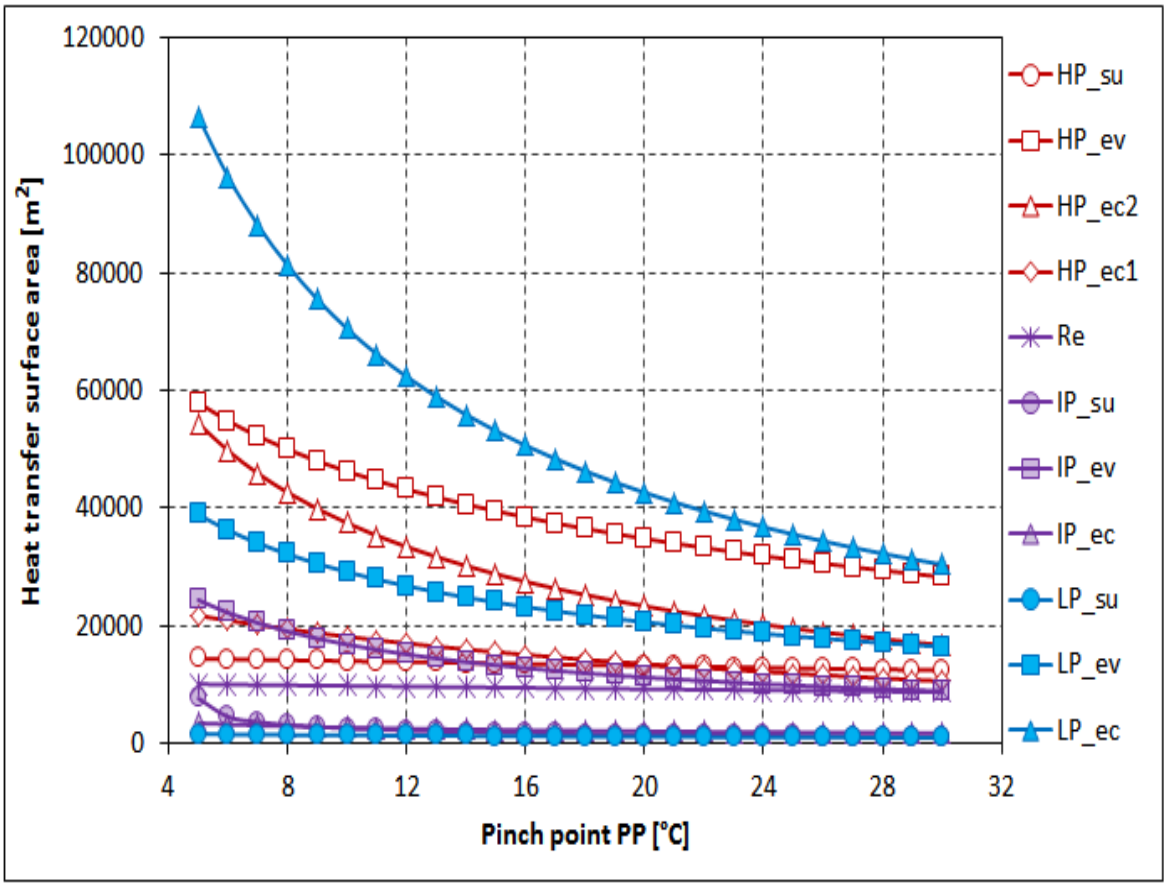

Figure 6-14 Pinch point PP vs. heat transfer area of the HRSG

6.1.2 Influence of Pressure in Drums on the Performance Parameters

6.1.2.1 Pressure p_{LP} in Low Pressure Drum

Live Steam Mass Flow Rate: Figure 6-15 presents the variation of pressure PP_{LP} in low-pressure drum with water (steam) mass flow rate. Low-pressure steam mass flow rate through $HRSG$ and low-pressure steam mass flow rate through steam turbine level are $\dot{m}_{s,LP,HRSG}$ and $\dot{m}_{s,LP,ST}$ respectively. Both are reduced with the increasing of p_{LP}. The $\dot{m}_{s,LP,HRSG}$ was reduced because of the reduction in Δh in the gas side of the low-pressure $HRSG$ section. By increasing p_{LP}, point 10_g (Figure 6-2) moved up towards point 9_g within a gas exhaust line that leads to increase in h_{10g}. Intermediate pressure live steam mass flows $\dot{m}_{s,IP,HRSG}$ and $\dot{m}_{s,IP,ST}$ are increased by increasing p_{LP}.

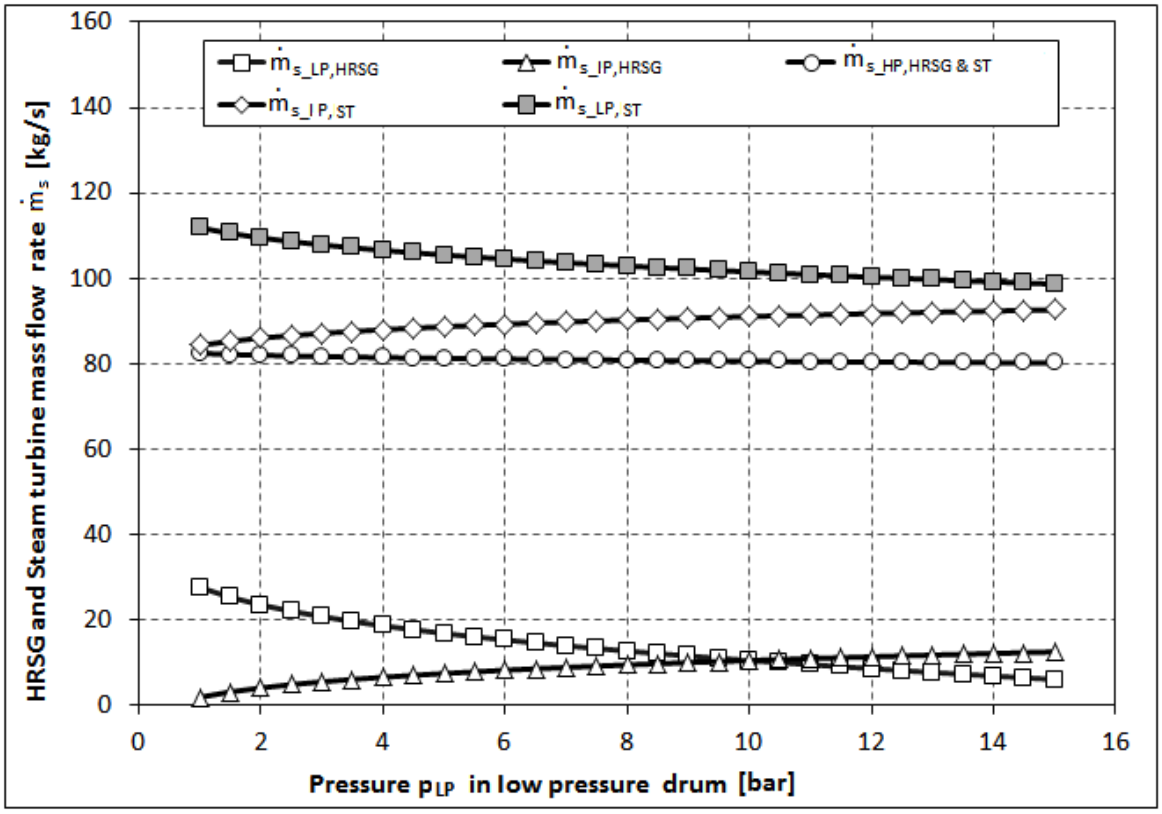

Figure 6-15 Pressure p_{LP} vs. mass flow rate through HRSG and the steam turbine

The $\dot{m}_{s,IP,HRSG}$ consists of three parts (*B1, B2, B3)* equation (5-15). With the increase of p_{LP}, B1 and B3 did not change, while B2 was reduced, which caused an increase in $\dot{m}_{s,IP,HRSG}$. High-pressure live steam mass flow rate $\dot{m}_{s,HP,HRSG}$ through *HRSG* and $\dot{m}_{s,HP,ST}$ through steam turbine were equal, and were not affected by variation of p_{LP}.

Power Output and Thermal Efficiency $P_{G,ST}$: Figure 6-16 shows the variation of the steam turbine power output when pressure p_{LP} was increased in the low-pressure drum. With the increase of p_{LP}: low pressure steam turbine power output $P_{G,ST,LP}$ will be increased (because of the increase in h_{25} equation (5-26) caused by increasing p_{25}, where p_{25} is equal to p_{LP}). Intermediate pressure steam turbine power $P_{G,ST,IP}$ will be reduced because of the increase in h_{17} as seen in the equation (5-27) because of an increase in h_{17} which equals the p_{LP} (Figure 5-1). There was a very small reduction in high-pressure steam turbine power output $P_{G,ST,HP}$ because of the increase in $\dot{m}_{s,IP}$ equation (5-17).

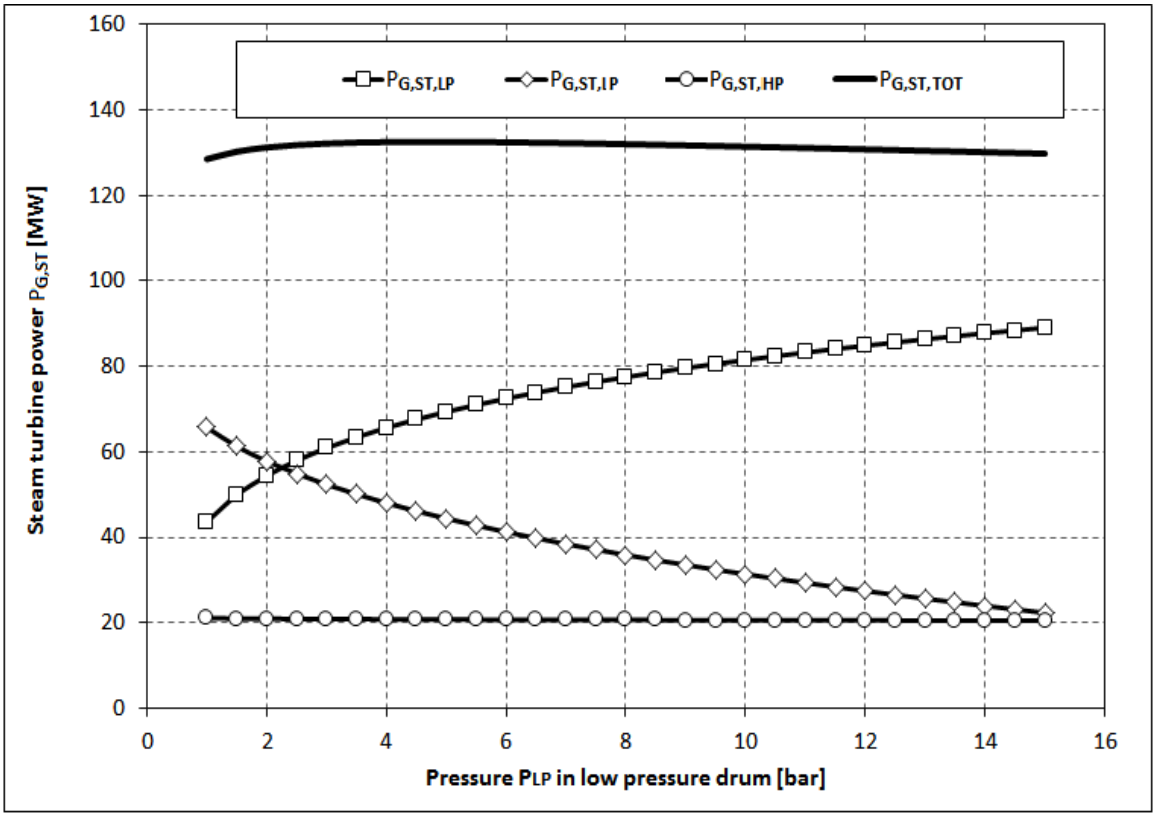

Figure 6-16 Steam turbine power $P_{G,ST}$ variation of p_{LP} increase

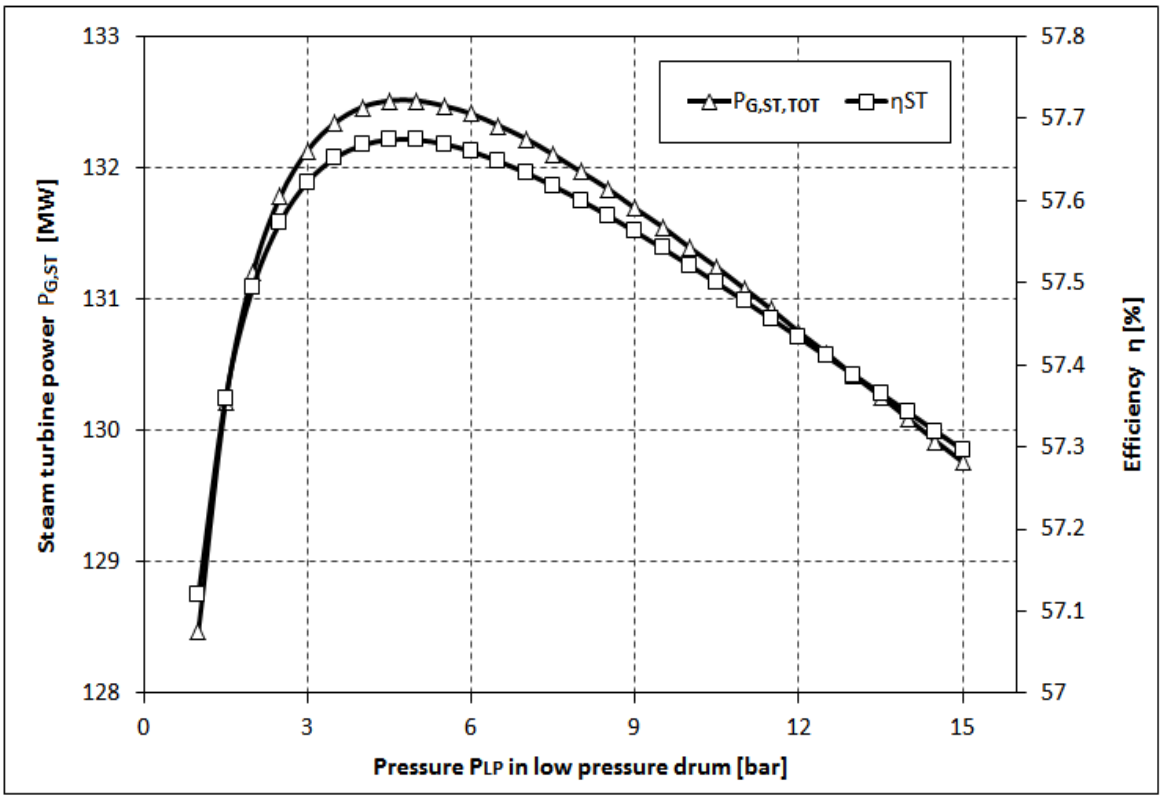

Figure 6-17 Steam turbine power $P_{G,ST}$ and efficiency η_{CCGT} variation of p_{LP} increase

Figure 6-17 shows the behavior of the total power output and efficiency with the variations of pressure p_{LP} in the low-pressure drum. It is clear from the figure that the total power output from the steam turbine $P_{G,ST}$ and total thermal efficiency η_{CCGT} of the CCGT were increased with the increase in pressure in the low pressure drum up to a maximum and then began to decrease with increase in the pressure in the low pressure drum p_{LP}.

6.1.2.2 Pressure p_{IP} in Intermediate Pressure Drum

Live Steam Mass Flow Rate: Figure 6-18 shows the variations in the steam mass flow rate through *HRSG* and steam turbine *ST* pressure levels with variations of pressure p_{IP} in the intermediate pressure drum. The mass flow rate of the low-pressure level for both $\dot{m}_{s,LP,HRSG}$ and $\dot{m}_{s,LP,ST}$ were increased with increasing p_{IP}. This happened because of the increase in Δh in the gas side of the low pressure *HRSG* section ($h_{8g} - h_{10g}$), which was caused by increasing p_{IP}. Point $8g$ Figure 6-12 moves up toward point $7g$ within the gas exhaust line that caused an increase in h_{8g}.

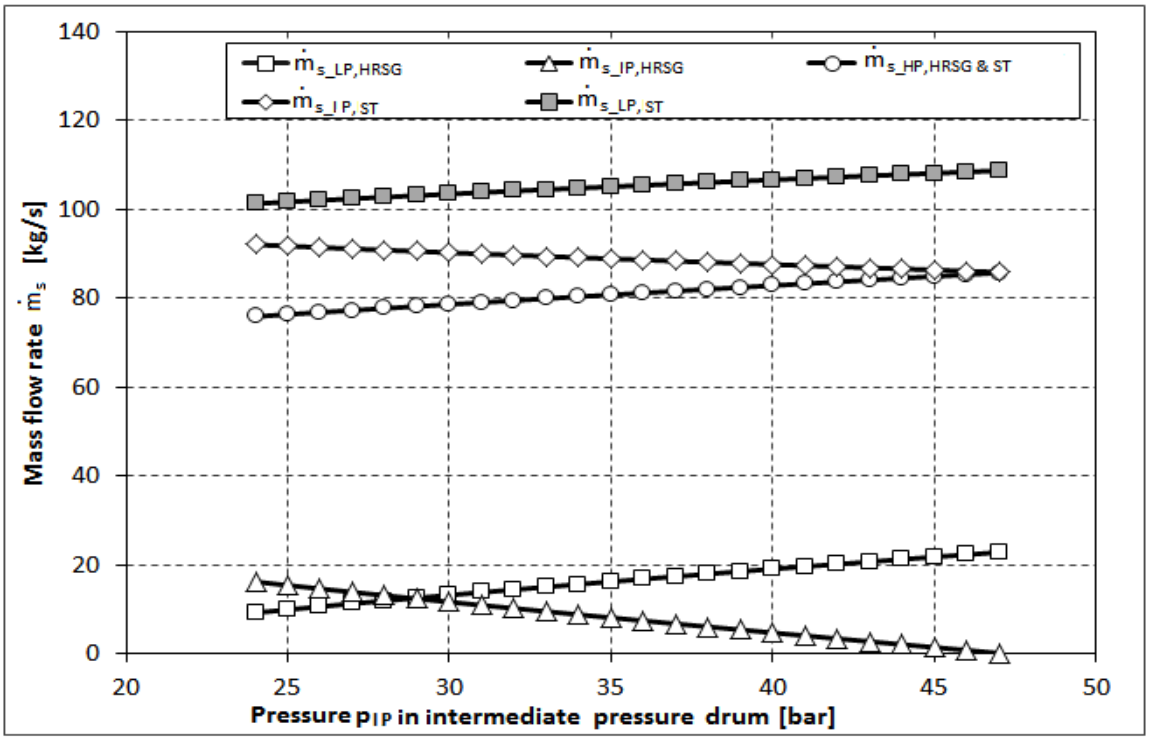

Figure 6-18 Mass flow rate through HRSG and steam turbine variation of p_{IP}

However, increasing h_{8g} resulted in reduction in Δh in the gas side of the intermediate pressure *HRSG* section ($h_{6g} - h_{8g}$) Figure 6-18, that lead to reduction in the steam mass flow rate of intermediate pressure in both $\dot{m}_{s,IP,HRSG}$ and $\dot{m}_{s,IP,ST}$. High-pressure mass flow rate through *HRSG* and steam turbine were increased with increasing p_{IP}; by increasing p_{IP} enthalpy h_{24} will be increased which, in turn, caused an increase in mass flow rate in the high-pressure steam turbine $\dot{m}_{s,HP,HRSG}$ equation (5-17).

Power and Efficiency: The effects of the variations of intermediate pressure drum p_{IP} on the steam turbine power $P_{G,ST,TOT}$ were shown in Figure 6-19.

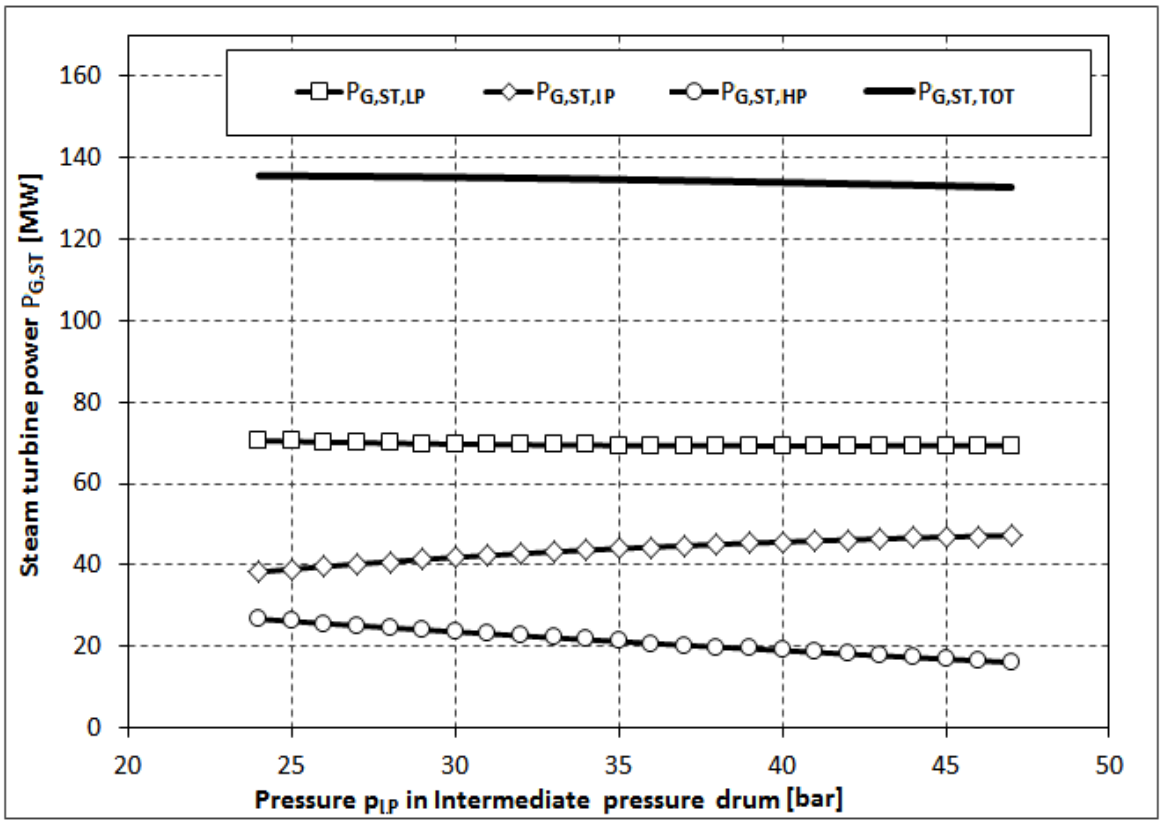

Figure 6-19 Steam turbine power $P_{G,ST}$ variation of increasing p_{IP}

Increases in the p_{IP} caused a reduction in the low pressure steam turbine power $P_{G,ST,LP}$ to the minimum point. After passing a minimum point, increasing the p_{IP} causes steam turbine power $P_{G,ST,LP}$ to increase. This happened because of the increase in mass flow rate and reduction in Δh equation (5-26). By increasing the pressure p_{IP}, pressures p_{15} and p_{24} increased as well. By increasing p_{15} the Δh for the intermediate

pressure turbine increased, which caused an increase in $P_{G,ST,IP}$ equation (5-27). By increasing p_{15}, the Δh for the high pressure turbine reduced, which led to a reduction in $P_{G,ST,HP}$ equation (5-28).

Figure 6-20 shows the variations of the efficiency η_{CCGT}, and the total power output when increasing the pressure p_{IP} in the intermediate pressure drum. The efficiency η_{CCGT} and the steam turbine power were reduced with increasing the pressure in the intermediate pressure drum.

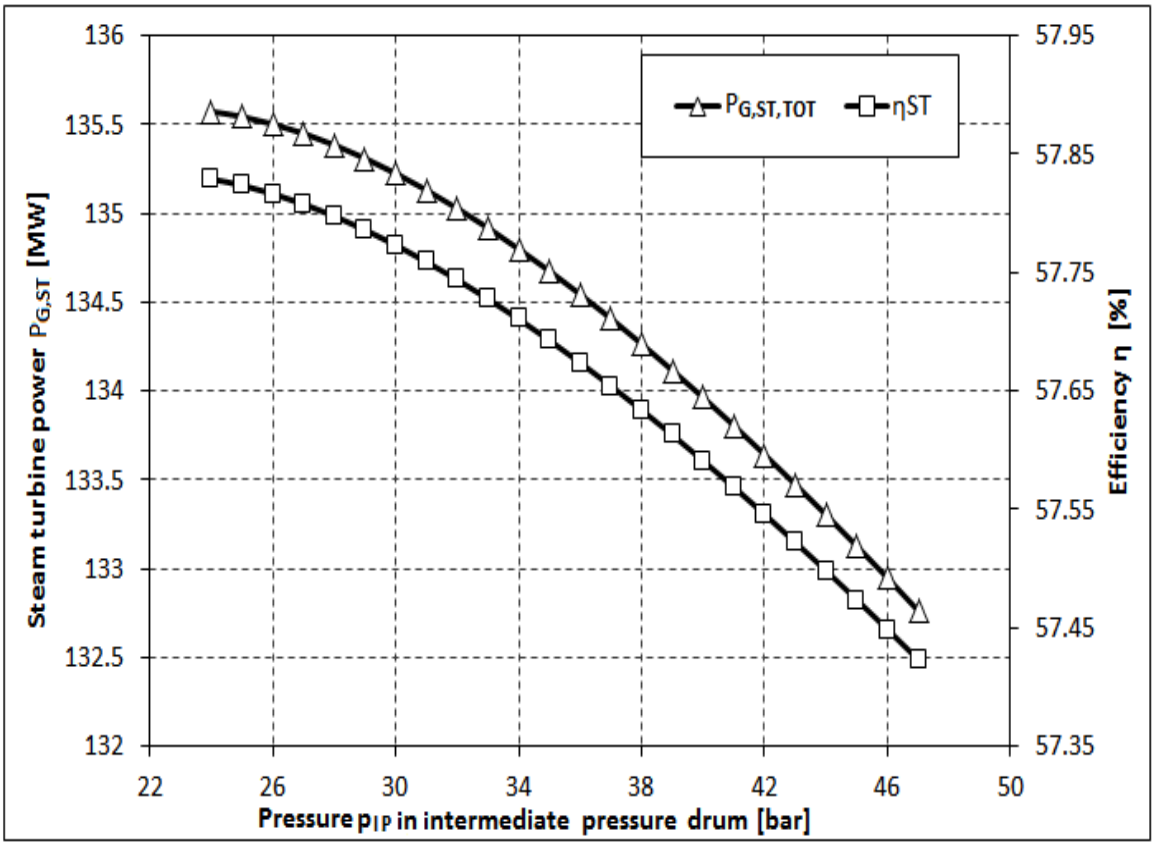

Figure 6-20 Steam turbine power $P_{G,ST}$ and efficiency η_{CCGT} variation of increasing p_{IP}

6.1.2.3 Pressure p_{HP} in High Pressure Drum

Live Steam Mass Flow Rate: Figure 6-21 shows, that the high pressure steam mass flow rate $\dot{m}_{s,HP,HRSG}$, was decreased with increasing the pressure p_{HP}.

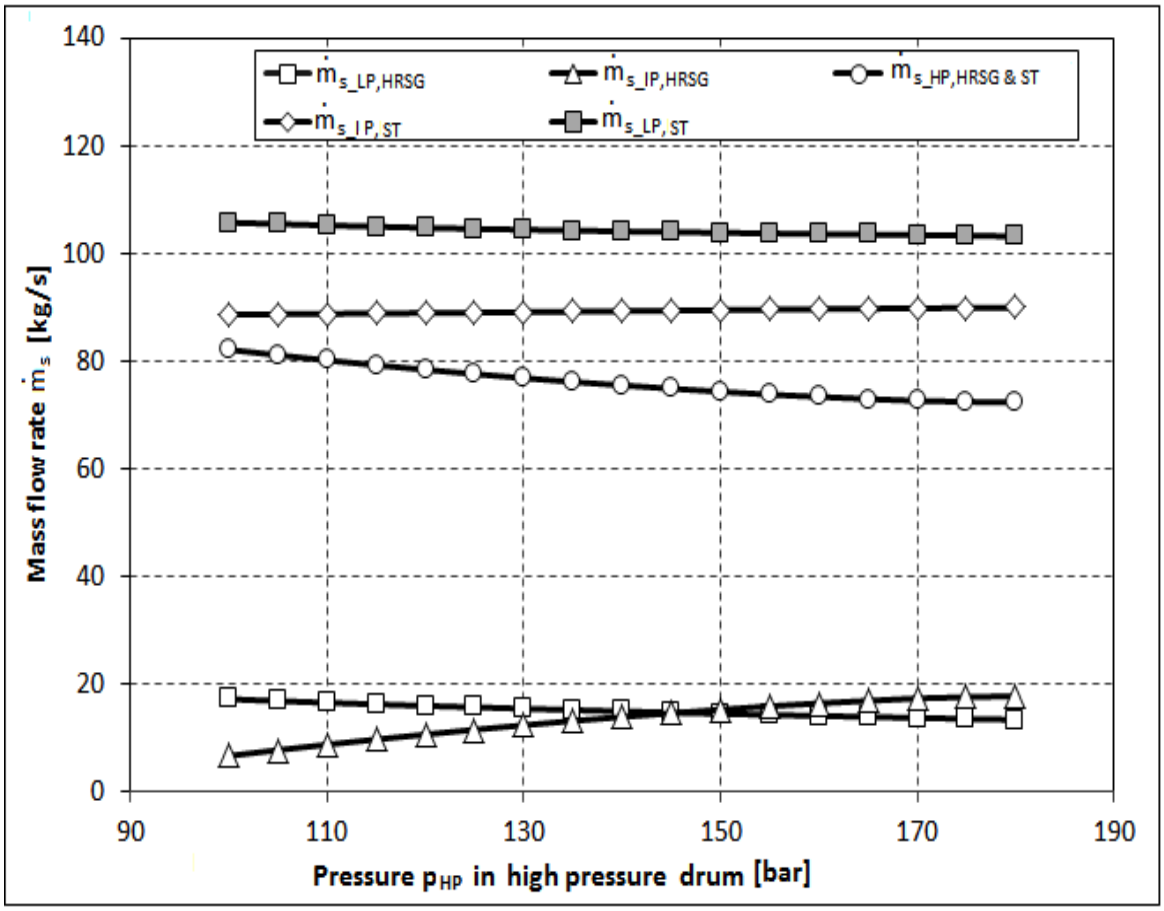

Figure 6-21 Water (steam) mass flow rate variation of increasing p_{HP}

This behavior occurred for the same reason as with intermediate and low pressure drum, because of decreasing in Δh of the gas side of the high-pressure evaporator. The intermediate pressure steam mass flow rate $\dot{m}_{s,IP,HRSG}$ was increased because of increasing Δh of the gas side of the intermediate pressure evaporator. The low pressure steam mass flow rate is more complicated. The $\dot{m}_{s,LP,HRSG}$ is a function of $\dot{m}_{s,IP,HRSG}$, $\dot{m}_{s,HP,HRSG}$ and gas temperature of the previous sections equation (5-19), therefore the resulting $\dot{m}_{s,LP,HRSG}$ decreased.

Power and Efficiency: Figure 6-22 and Figure 6-23 present the effect of the variation of p_{HP} on the steam turbine power $P_{G,ST}$ and the plant efficiency η_{CCGT}. The $P_{G,ST,HP}$ and $P_{G,ST,IP}$ were increased with the increase in p_{HP}.

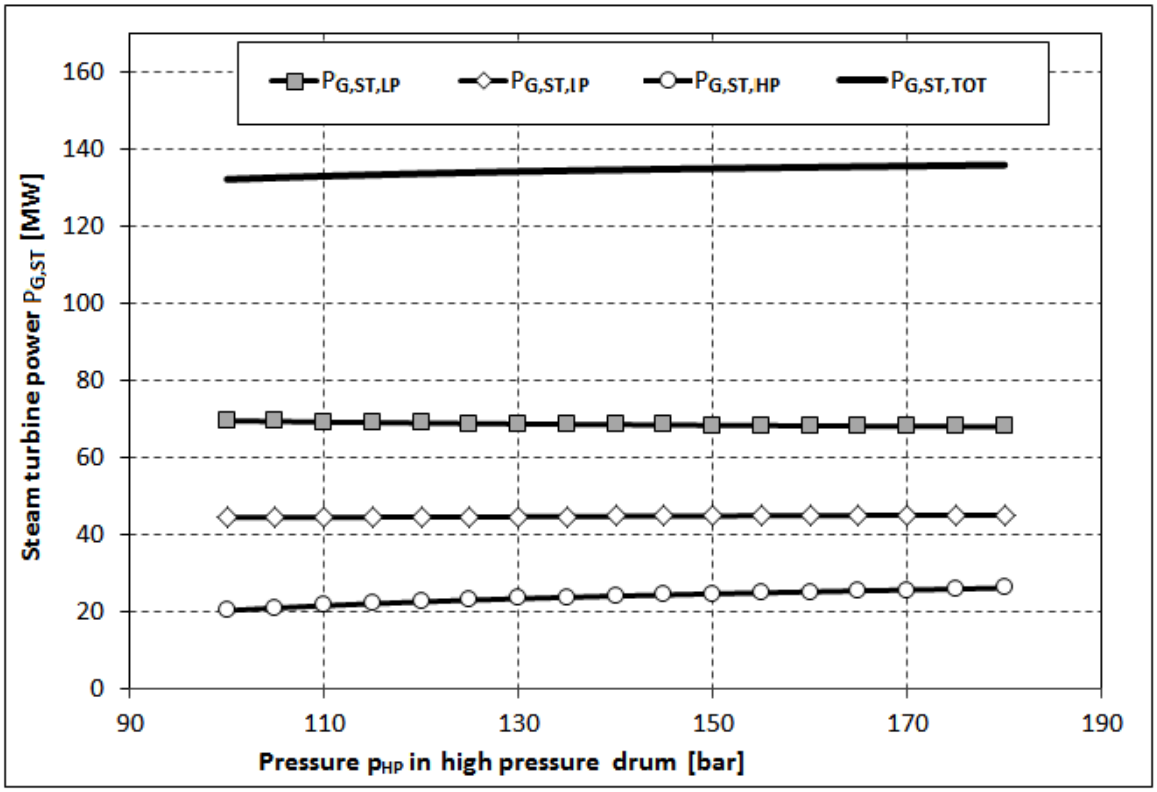

Figure 6-22 Steam turbine power $P_{G,ST}$ variation of increasing pressure p_{HP}

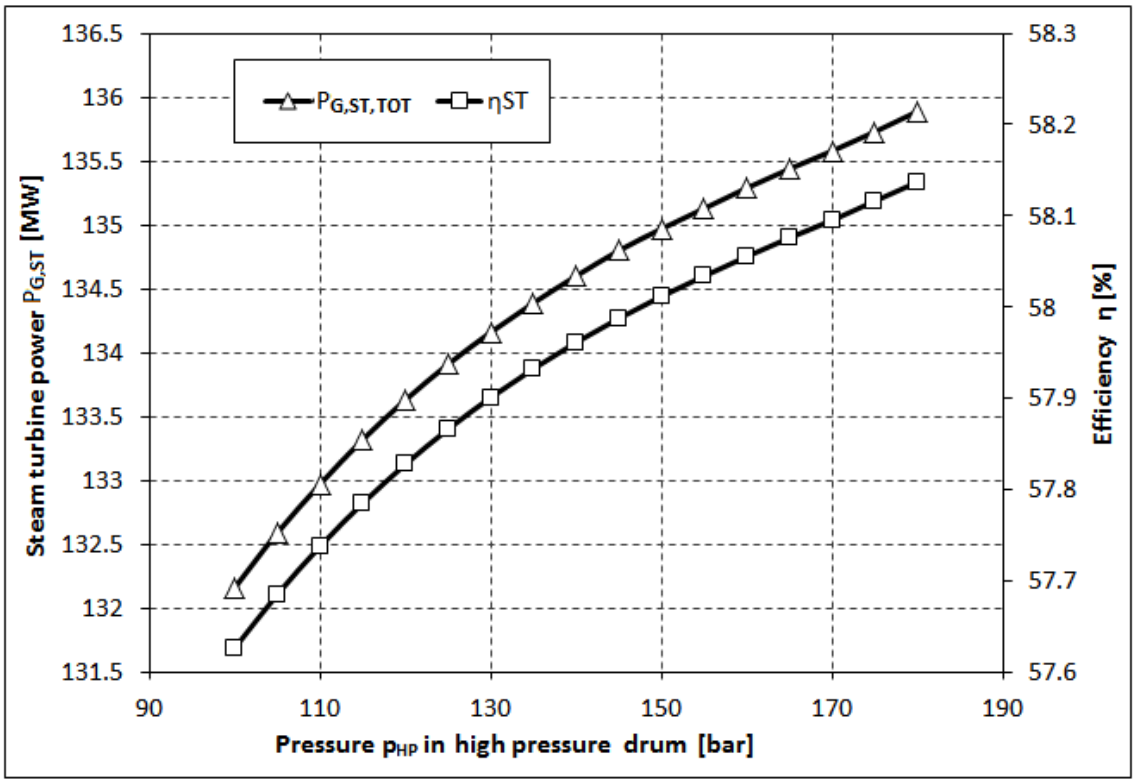

Figure 6-23 Steam turbine power $P_{G,ST}$ and efficiency η_{CCGT} variation of increasing p_{HP}

High-pressure steam turbine power output $P_{ST,HP}$ was increased because of the effect of p_{HP} on Δh (by increasing p_{HP}, Δh was increased in the high-pressure steam turbine). The $P_{G,ST,IP}$ was increased because of the increase in steam mass flow rate $\dot{m}_{s,IP,ST}$. The $P_{G,ST,LP}$ was reduced with increasing p_{HP}. This reduction was a result of the reduction in mass flow rate $\dot{m}_{s,LP,ST}$. Figure 6-23 shows the increasing of the total steam turbine power and efficiency with increasing p_{HP}.

6.1.2.4 Exhaust Gas Temperature

Sections 5.2.6 and 5.2.6.1.2 above explain the importance of the dew point and its effect on an exhaust gas temperature limitation (constraints). Therefore, it is very important to understand the behaviors of exhaust gas temperature with variation of operating parameters.

From Figure 6-24, it is clear that the low-pressure drum variation had a significant effect on the exhaust gas temperature. By increasing the pressure in the low-pressure drum, there was an extreme increase in the exhaust gas temperature in HRSG.

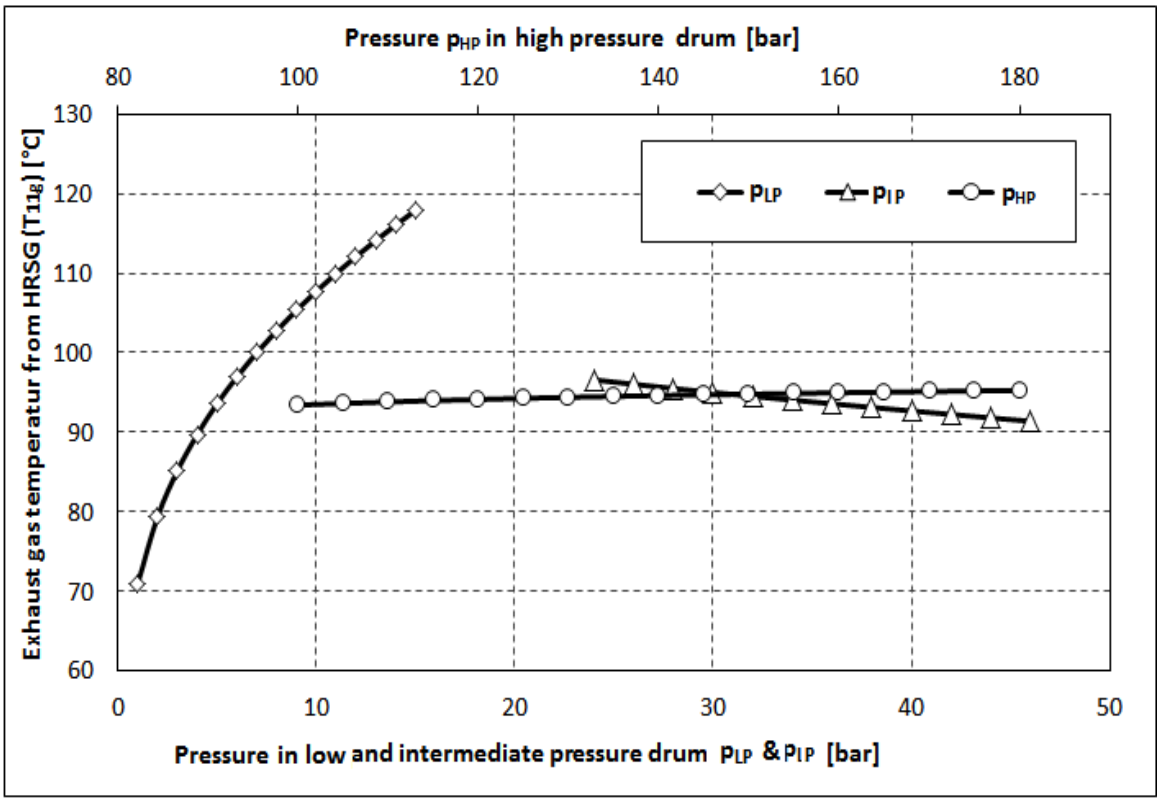

Figure 6-24 Exhaust gases temperature variation of p_{LP}, p_{IP}, and p_{HP}

Increasing the high-pressure drum leads to increases in the exhaust gas temperature, with a very small gradient. While increasing the intermediate pressure drum led to decreases in the exhaust gas temperature, also with a very small gradient. Therefore, it is very important to pay attention to this when selecting the optimal low-pressure drum.

6.1.2.5 Heat Transfer Area

The results of the effect of the pressure variations p_{LP}, p_{IP}, and p_{HP} on the heat transfer area, are shown in Figure 6-25, Figure 6-26, and Figure 6-27. Increasing the pressures p_{LP} resulted in reduction of all the heat transfer areas of low pressure levels. Increasing the pressures p_{IP} resulted in reduction of all the heat transfer areas of intermediate pressure levels. Decreasing the heat transfer areas of low and intermediate pressure evaporators ($A_{LP,v}$ and $A_{IP,v}$), low and intermediate pressure economizers ($A_{LP,ec}$ and $A_{IP,ec}$), superheaters ($A_{LP,su}$ and $A_{IP,su}$), and reheater $A_{IP,re}$, are shown in Figure 6-25 and Figure 6-26.

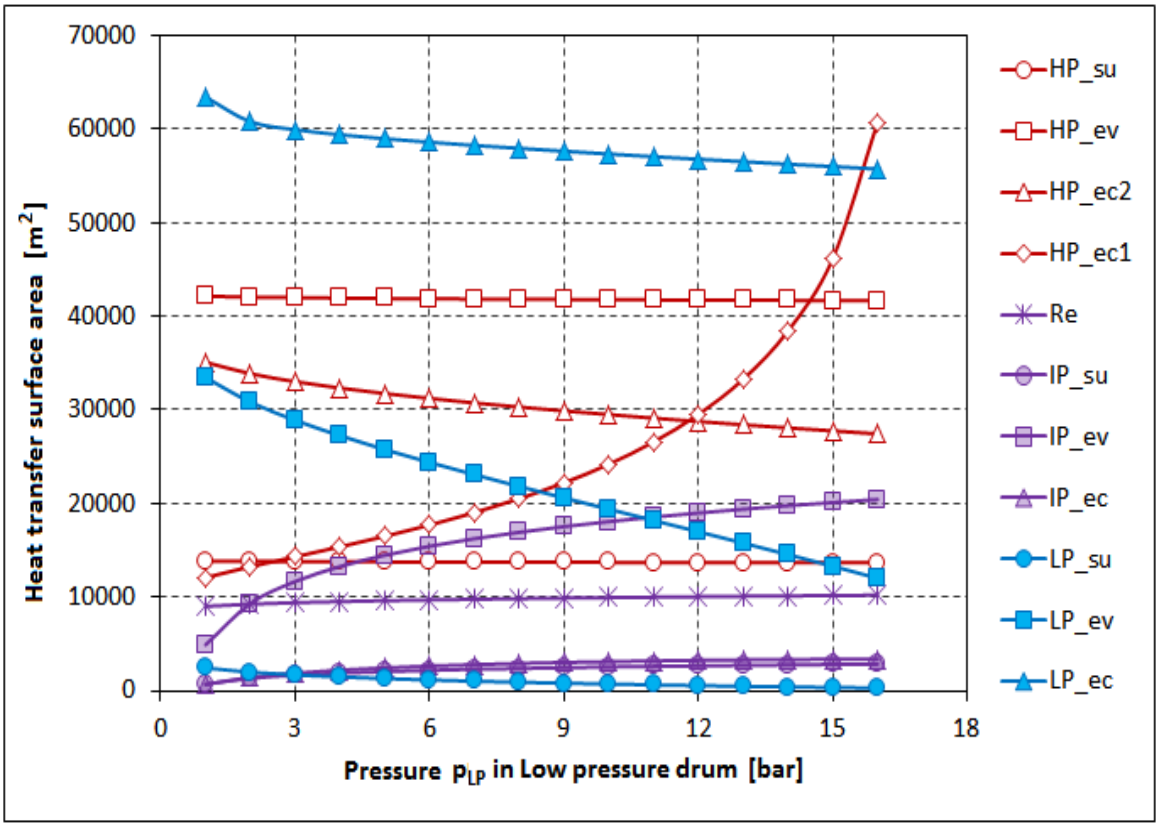

Figure 6-25 Variation of the HRSG sections area versus low pressure drum p_{LP}

By increasing p_{HP} Figure 6-27, only the $A_{HP,v}$ was reduced and the other three areas $A_{HP,ec1}$, $A_{HP,ec2}$ and $A_{HP,su}$ increased, due to the increase in heat transfers $Q_{HP,ec1}$, $Q_{HP,ec2}$ and $Q_{HP,su}$ in these sections, equations (5-56), (5-65) and (5-71). What follows is an explanation of the effects of increasing the pressure in the pressure drum of any pressure level on the heat transfer area of other pressure level. Figure 6-25 shows that with the increase of p_{LP}, intermediate pressure heat transfer areas $A_{IP,ec}$, $A_{IP,v}$, $A_{IP,su}$ and $A_{IP,re}$ increased with a different gradient, while high-pressure evaporator and superheater heat transfer areas $A_{HP,v}$ and $A_{HP,su}$ did not change. On other hand, $A_{HP,ec1}$ was increased and $A_{HP,ec2}$ was reduced.

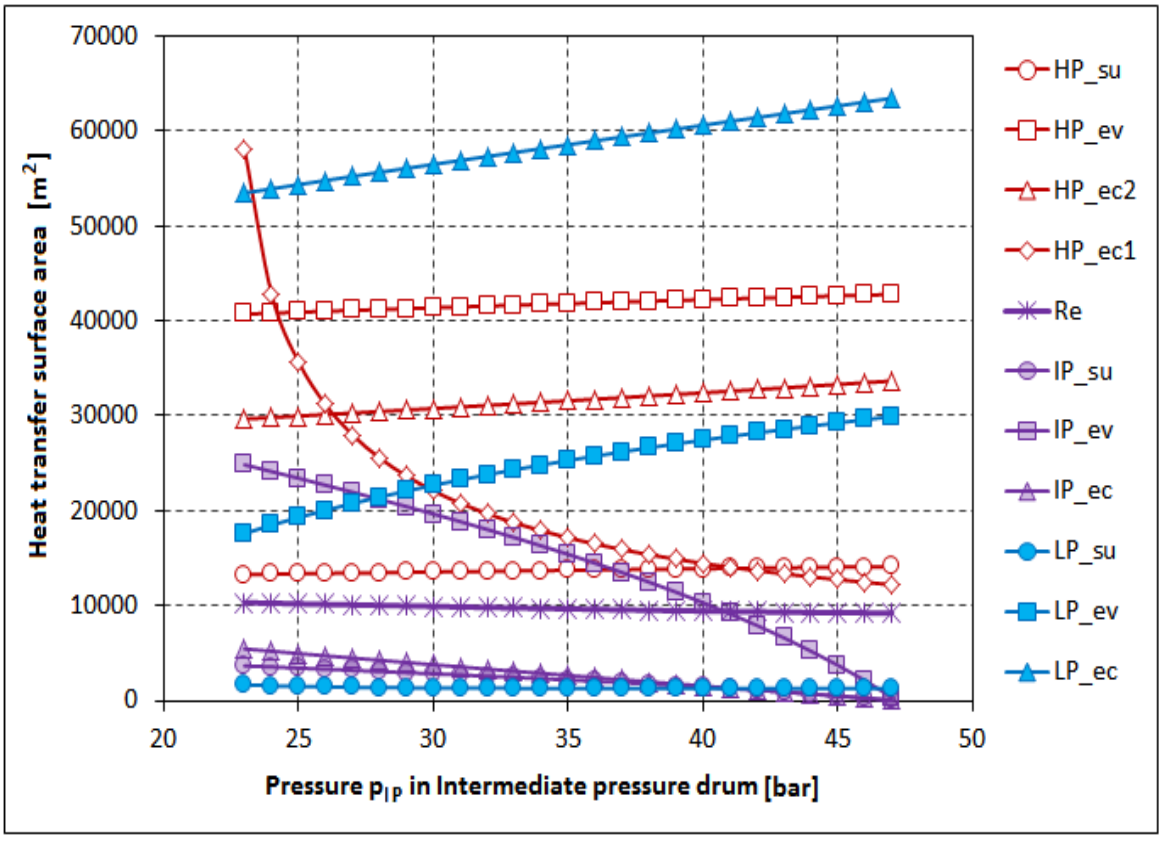

Figure 6-26 Variation of the HRSG sections area versus pressure p_{IP}

Figure 6-26 shows that by increasing p_{IP}, all heat transfer areas will also increase except $A_{IP,re}$, $A_{IP,su}$ and $A_{HP,ec1}$. By increasing p_{HP} Figure 6-27, low-pressure heat transfer areas was reduced while intermediate pressure level increased with a different gradient.

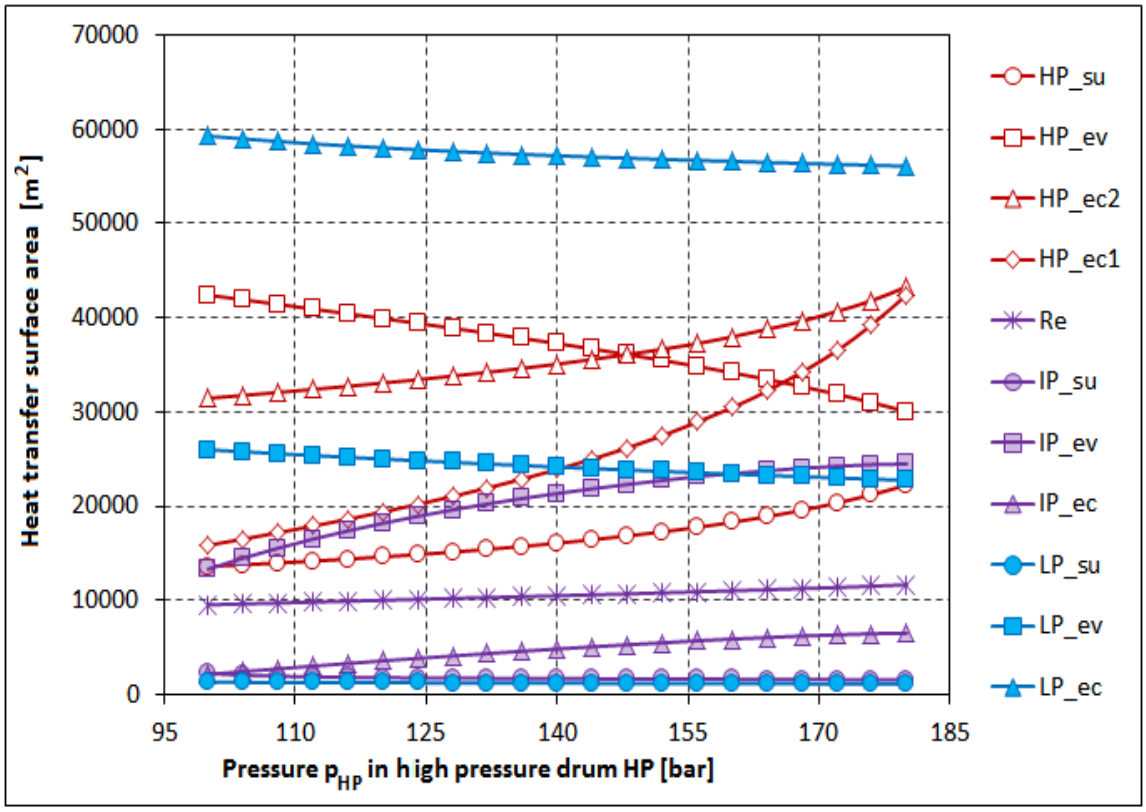

Figure 6-27 Variation of the HRSG sections area versus pressure p_{HP}

6.2 Result Exergy Analysis

To illustrate values of exergy components, exergy destructions, exergy losses and the relevant ratios for the condition, i.e. initial case for operating data given in Table 5-2, the exergy rates for the CCGT components are tabulated in Table A-1. Other results are shown within the figures in this section. The exergy destruction rates in the main components of the CCGT are given in Figure 6-28, in accordance with their state numbers as specified in Figure 5-1.

The exergy streams in the CCGT power plant as well as in the subsystems analyzed are shown in the Grassman diagram Figure 6-29. In this diagram, the distribution of the irreversibilities in the plant can be seen. The exergy curve shows a continuous decrease of the primary exergy through the process. In addition, it can be seen that the highest irreversibilities occurred in the HRSG. However, the largest exergy destruction ratio was found in the HRSG. The HRSG was responsible for the destruction of almost 49.4% of total exergy destroyed in the system. Exergy destruction ratio in other components was considerably lower compared with the HRSG.

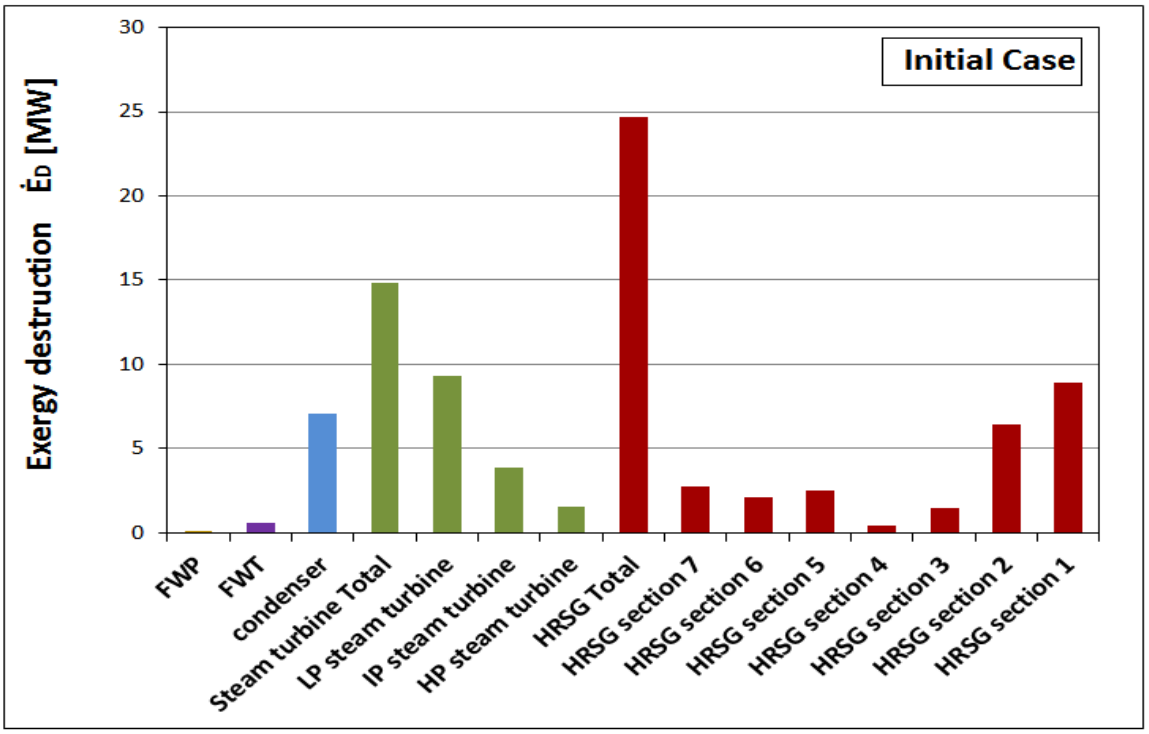

Figure 6-28 Exergy destruction in the main CCGT components

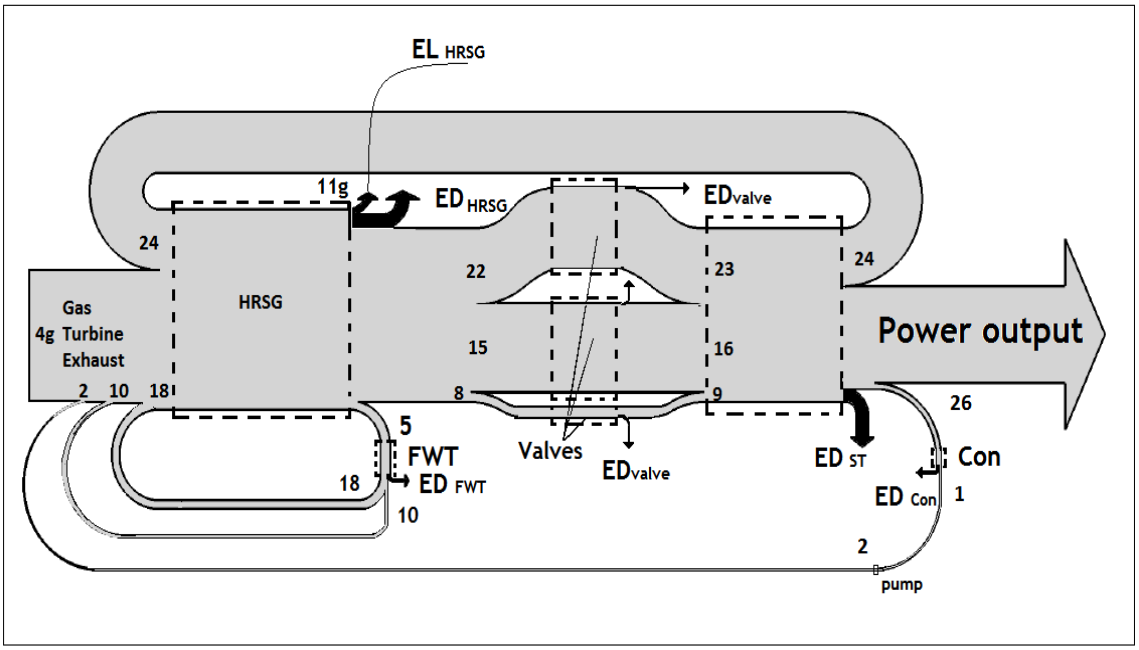

Figure 6-29 Grassman diagram

In this study, the effect of steam cycle operating parameters; pinch point temperatures (PP_{LP}, PP_{IP}, PP_{HP}, and PP) and pressures (p_{LP}, p_{IP}, and p_{HP}) in the pressure drum on the main exergetic parameters (exergy destructions $\dot{E}_D$ and exergy

efficiency ε) of bottoming cycle and other main components of the bottoming cycle were investigated.

6.2.1 Influence of Pinch Points PP, PP_{LP}, PP_{IP}, and PP_{HP} on the Exergy Efficiency and Exergy Destructions

One of the most significant operating parameters in HRSG is pinch point temperature, so the effect of variation pinch point temperatures versus exergy efficiency and exergy destructions of the bottoming cycle are presented in Figure 6-30. As it is obvious, by increasing the pinch point temperatures PP, PP_{LP}, PP_{IP}, and PP_{HP} within range 1 to 30 °C, the exergy destruction (due to irreversibility of the heat transfer process between hot gas and water) increased.

Figure 6-30 also represents the effect of the pinch point temperatures (PP PP_{LP} PP_{IP} and PP_{HP}) on the exergy efficiency.

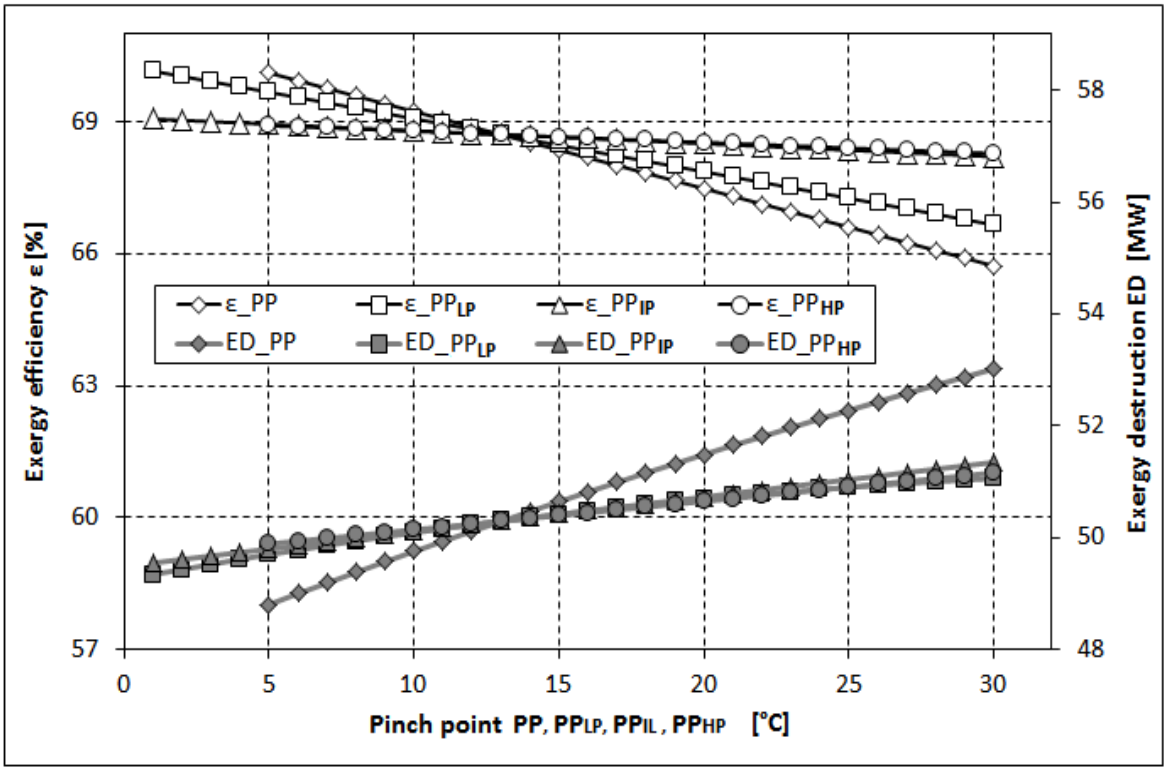

Figure 6-30 Exergy efficiency and exergy destruction as a function of pinch points

As shown, the exergy efficiency behaved with increasing of pinch point in a manner, which is completely opposite, thus contradicting the exergy destruction behaviors: as pinch point temperature increased, exergy efficiency decreased. This

indicates that large amounts of heat were dissipated into the atmosphere, without being recovered by the HRSG.

The irreversibility of the steam turbine was decreased because of low mass flow rate from steam generated in HRSG. From the previous discussion it is clear that the maximum efficiency, minimum exergy destruction and maximum steam turbine gross power will be reached at a null value of pinch points (PP, PP_{LP}, PP_{IP}, and PP_{HP}), and with an infinite heat transfer surface HRSG area.

In addition, by comparing the effect of different pinch point levels PP, PP_{LP}, PP_{IP}, and PP_{HP} on the exergy efficiency and exergy destruction, the pinch point PP (pinch point assumed constant) has the highest decrease in exergy efficiency and highest increase in exergy destructions.

6.2.2 Influence of Pressure p_{LP}, p_{IP}, and p_{HP} on the Exergy Efficiency and Exergy Destructions

Exergy efficiency and exergy destruction versus drum pressures are presented in Figure 6-31 to Figure 6-33.

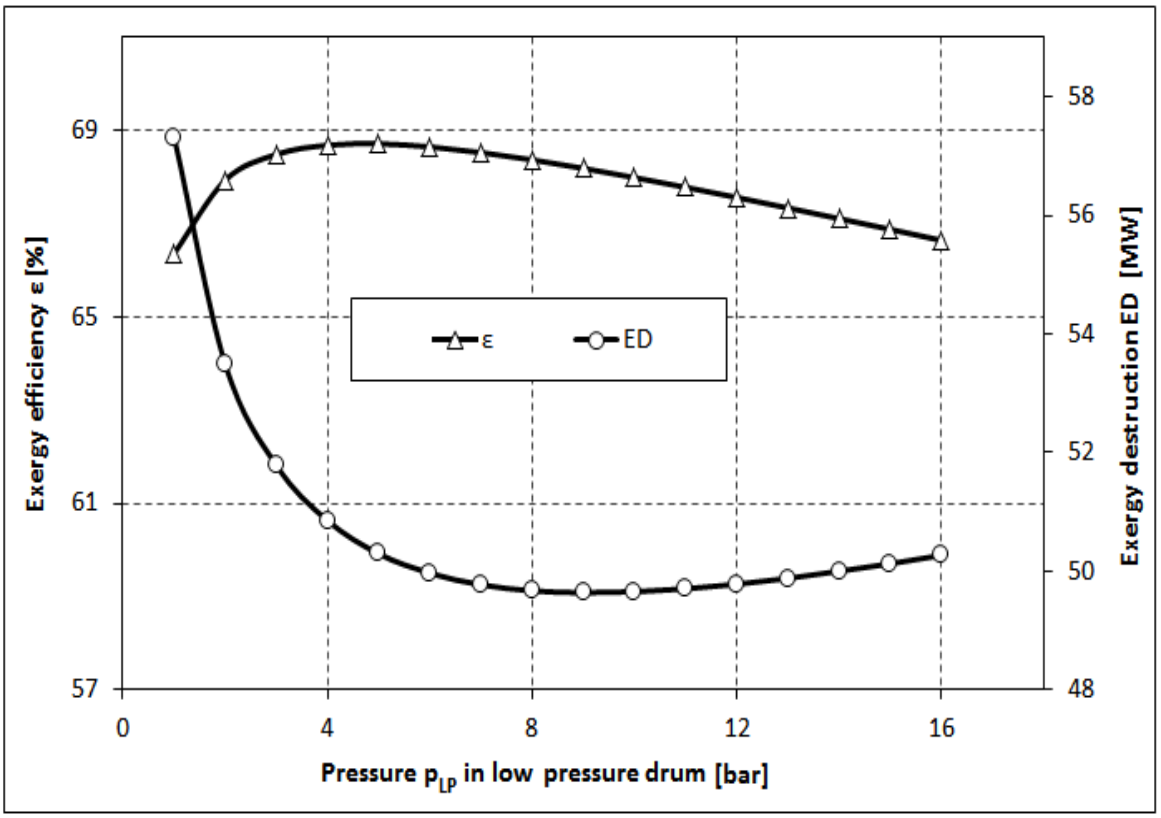

Figure 6-31 Exergy efficiency and exergy destruction as a function of p_{LP} variations

Figure 6-31 shows that the exergy efficiency increased with increasing p_{LP} to a maximum of 4 bar, and then it started to decrease, while the exergy destruction was reduced to 10 bar and then was increased.

Figure 6-32 shows that the exergy efficiency decreased and the exergy destruction increased with the increase of p_{IP}.

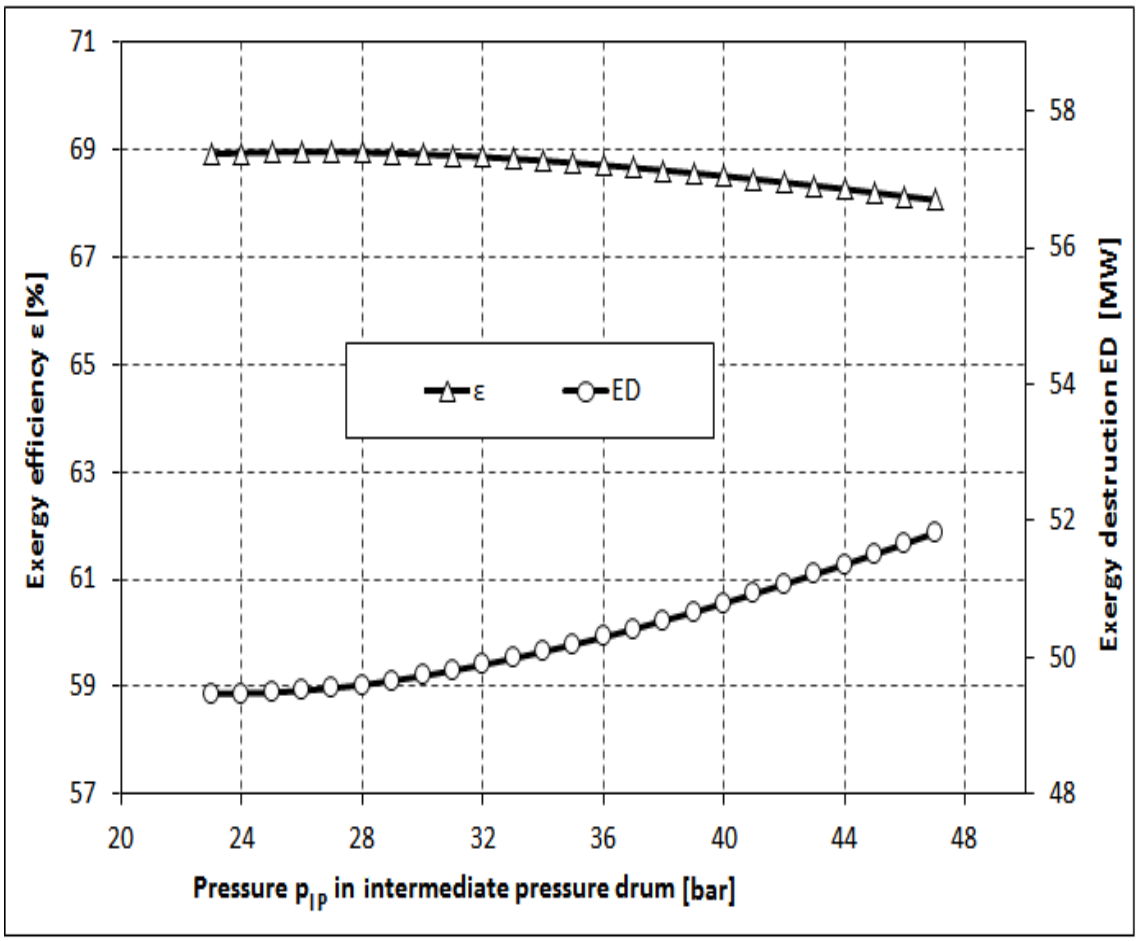

Figure 6-32 Exergy efficiency and exergy destruction as a function of p_{IP} variations

Figure 6-33 shows that the exergy efficiency increased while exergy destruction was reduced by increasing the p_{HP}. It is easy to notice from the previous explanation that the p_{HP} must be high in order to attain a good exergetic utilization of the wasted heat by generating high quality steam. This means that there is no upper limit value for the p_{HP}. Hence the p_{IP} steam pressure must be low, and the lower limit of p_{IP} is the logarithm means temperature difference ($LMTD$) should be positive.

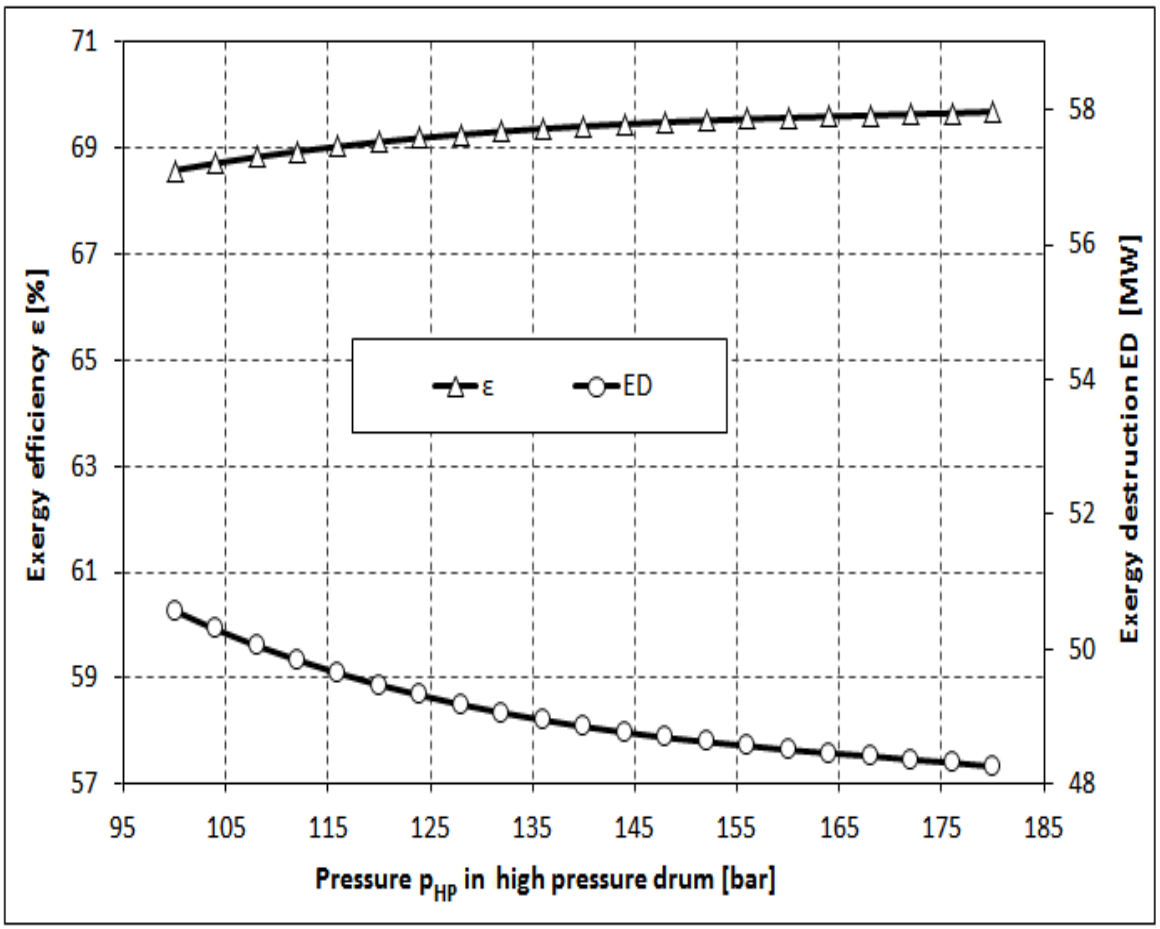

Figure 6-33 Exergy efficiency and exergy destruction as a function of p_{HP} variations

6.3 Results of Thermoeconomic Analysis

The relationship between operating parameters and some important economic parameters (economic parameters being functions of thermodynamic parameters) are considered in this section. The results are expressed in Figure 6-34 to Figure 6-44. In the CCGT power plant, the three most important economic parameters are investment cost, production cost of electricity, and annual cash flow.

6.3.1 Influence of Pinch Points PP, PP_{LP}, PP_{IP}, and PP_{HP} on Economic and Thermoeconomic Parameters

In Figure 6-34 the variation of the production cost of electricity and annual cash flow with pinch points is shown.

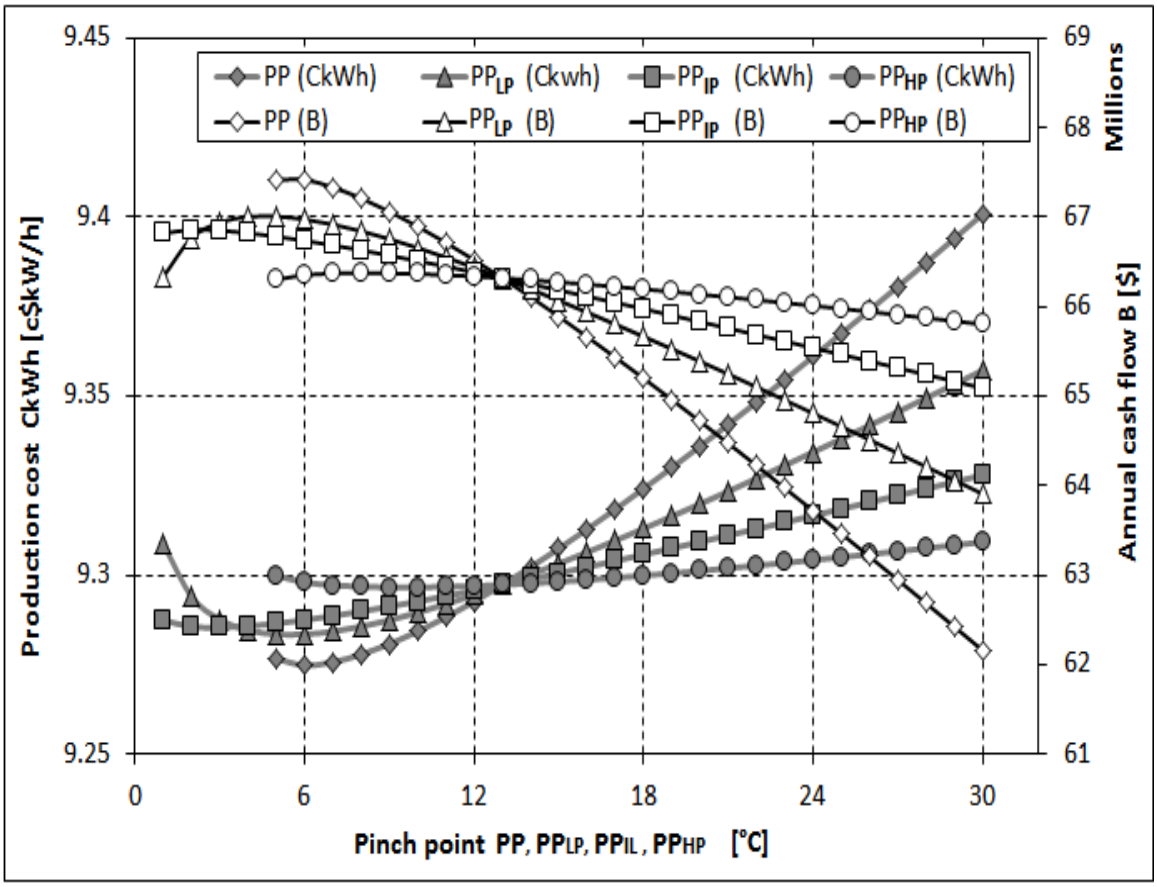

Figure 6-34 Production cost and annual cash flow vs. PP, PP_{LP}, PP_{IP}, and PP_{HP}

Here, pressures in pressure drums were constant , the production cost first decreased ,then increased with an increasing pinch point temperature for all pressure levels (PP, PP_{LP}, PP_{IP}, and PP_{HP}), while the cash flow behaved opposite to the behavior of the production cost (Figure 6-34). The result shows that C_{kWh} and B were more sensitive to the variation of PP and PP_{LP} especially with a higher pinch point temperature where their curve had a higher gradient than with PP_{IP} and PP_{HP}. The third important economic parameter is investment cost. The relationship between the investment cost and pinch points are given in Figure 6-35, the investment cost decreased with the increasing of pinch points PP_{LP}, PP_{IP}, PP_{HP}, and PP with different gradients as can be seen in Figure 6-35. The investment cost was more sensitive to PP_{LP}, and PP while there was a more gradual gradient with PP_{IP}, and PP_{HP}.

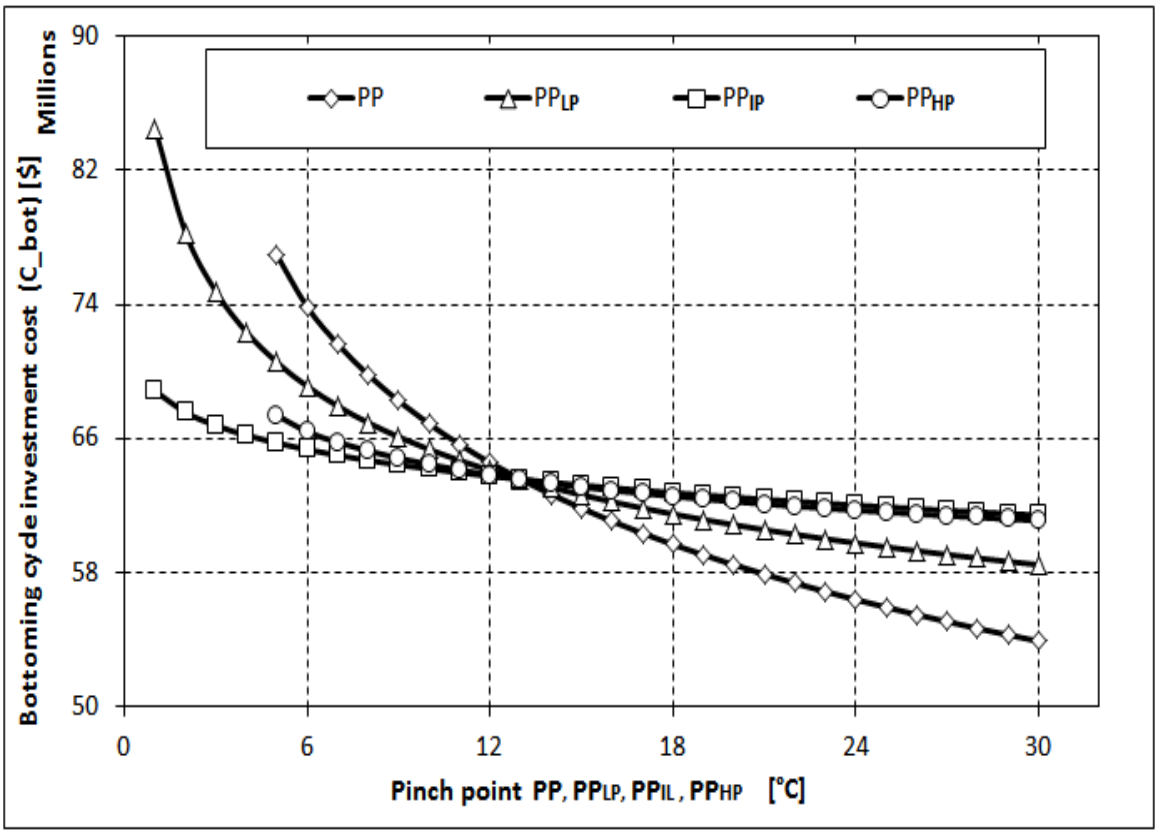

Figure 6-35 Investment cost vs. pinch point temperature PP, PP_{LP}, PP_{IP}, and PP_{HP}

6.3.2 Influence of Pressure in the Pressure Drum on Economic and Thermoeconomic Parameters

6.3.2.1 Investment Cost

The behavior of the investment cost of the combined cycle gas turbine ($CCGT$) and its main subsystems (C_{CCGT}, C_{Bott}, C_{HRSG}, $C_{Turbine}$ and C_{Con}) with variations of pressure drum were presented in this section. Figure 6-36, Figure 6-40 and Figure 6-41 show the plots of this behavior.

Pressure p_{LP} in Low Pressure Drum: Pressure p_{LP} variation did not have the same effect on the investment cost of the different subsystem of the CCGT as seen from Figure 6-36 to Figure 6-38. Figure 6-36 shows the HRSG investment variation with increasing p_{LP}. Figure 6-36 shows that the investment cost was more sensitive to the increasing pressure in low-pressure drum after 8 bar. By increasing the pressure p_{LP} from 1 to 8 bar HRSG the investment cost increased by 0.6%, while from 8 to 16 bar the HRSG investment increased by about 13%.

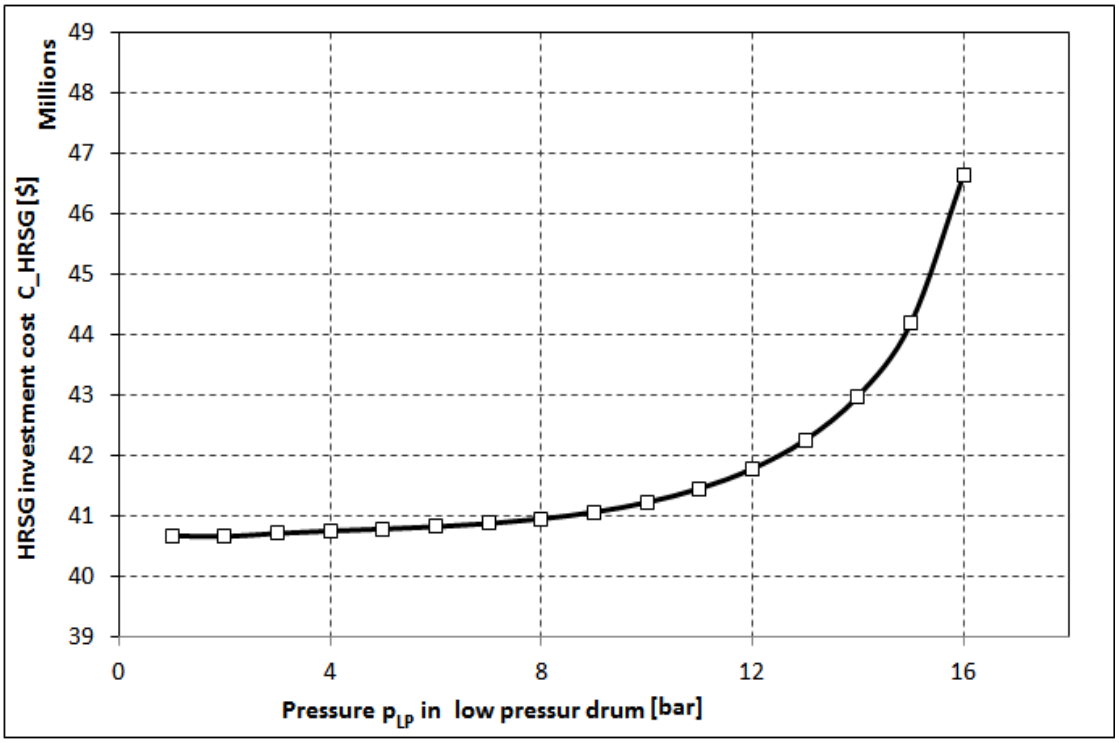

Figure 6-36 HRSG investment cost vs. pressure p_{LP} in low pressure drum

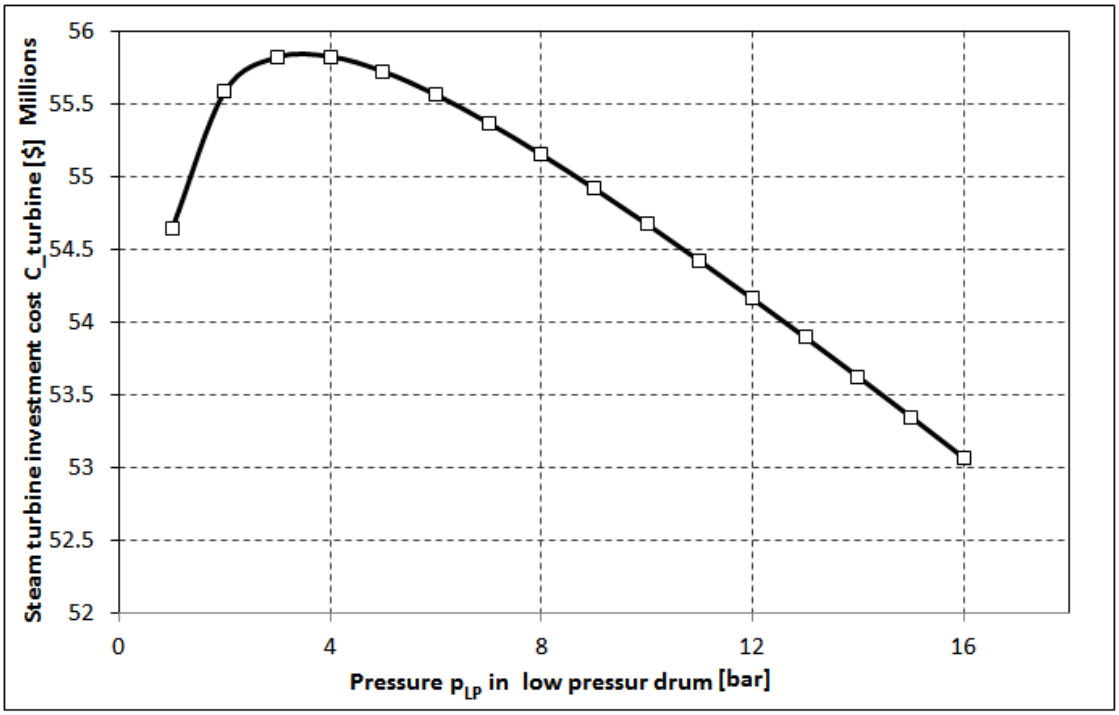

Figure 6-37 Steam turbine investment cost vs. pressure p_{LP} in low pressure drum

Figure 6-37 shows the variation of the steam turbine investment with increasing pressure p_{LP} in low-pressure drum. Steam turbine investment cost first increased by 2%

with an increase in low pressure drum from 1 to about 4 bar, then reduced by about 5% at 16 bar.

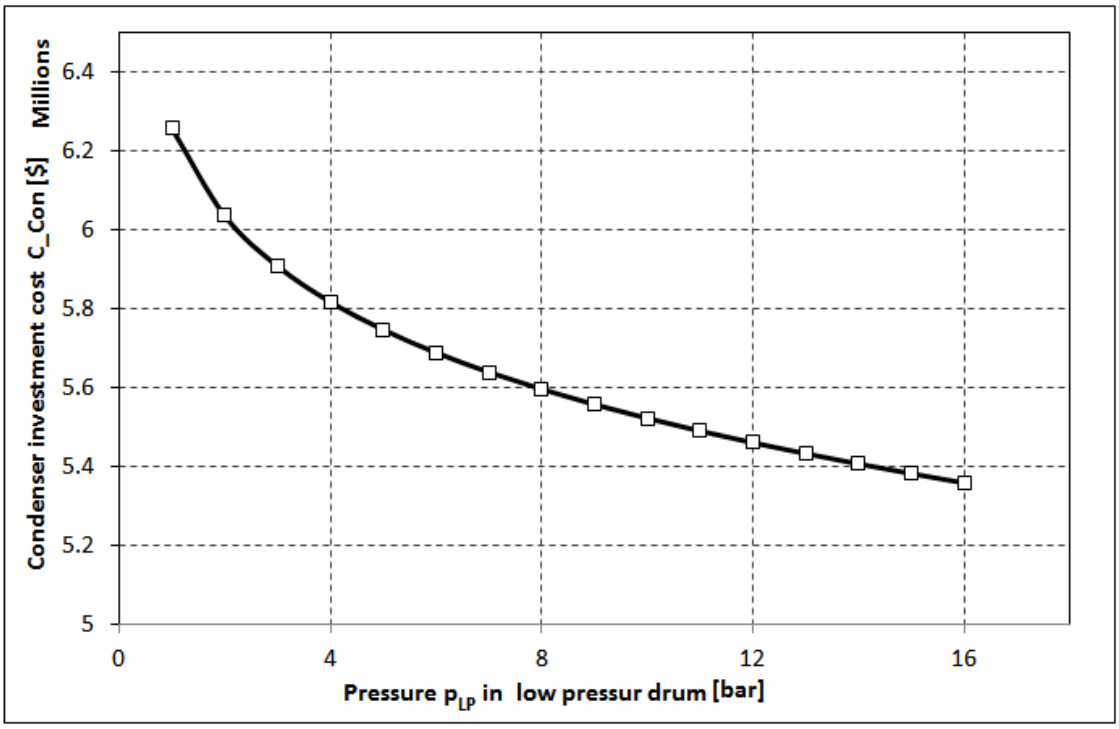

Figure 6-38 Condenser investment cost vs. pressure p_{LP} in low pressure drum

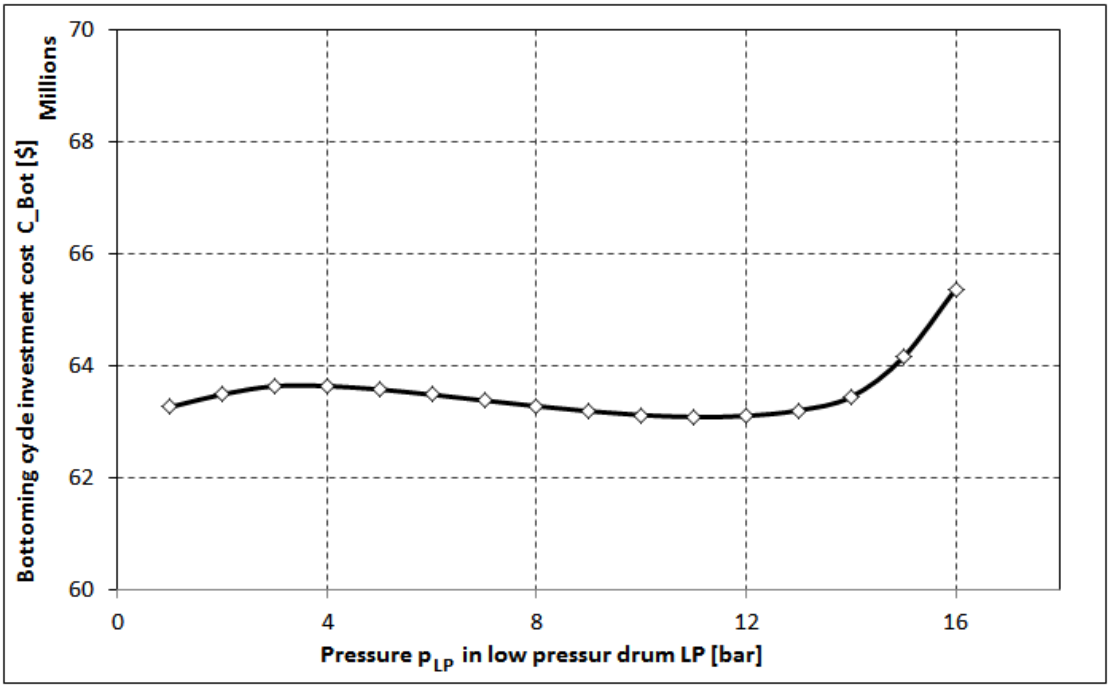

Figure 6-39 Bottoming cycle investment cost vs. pressure p_{LP} in low pressure drum

Condenser investment cost reduced with variation of pressure p_{LP} in low-pressure drum (Figure 6-38), the result shows the increase of investment cost by 16% when the pressure p_{LP} in low-pressure drum was increased from 1 to 16 bar.

Figure 6-39 presents the result of the effect of the pressure p_{LP} low-pressure drum variations on the total investment cost of the bottoming cycle.

Pressure p_{IP} in Intermediate Pressure Drum: Figure 6-40 shows that the HRSG and ST investment decreased with increasing the pressure p_{IP} in intermediate pressure drum by different gradients, while the condenser investment cost increased.

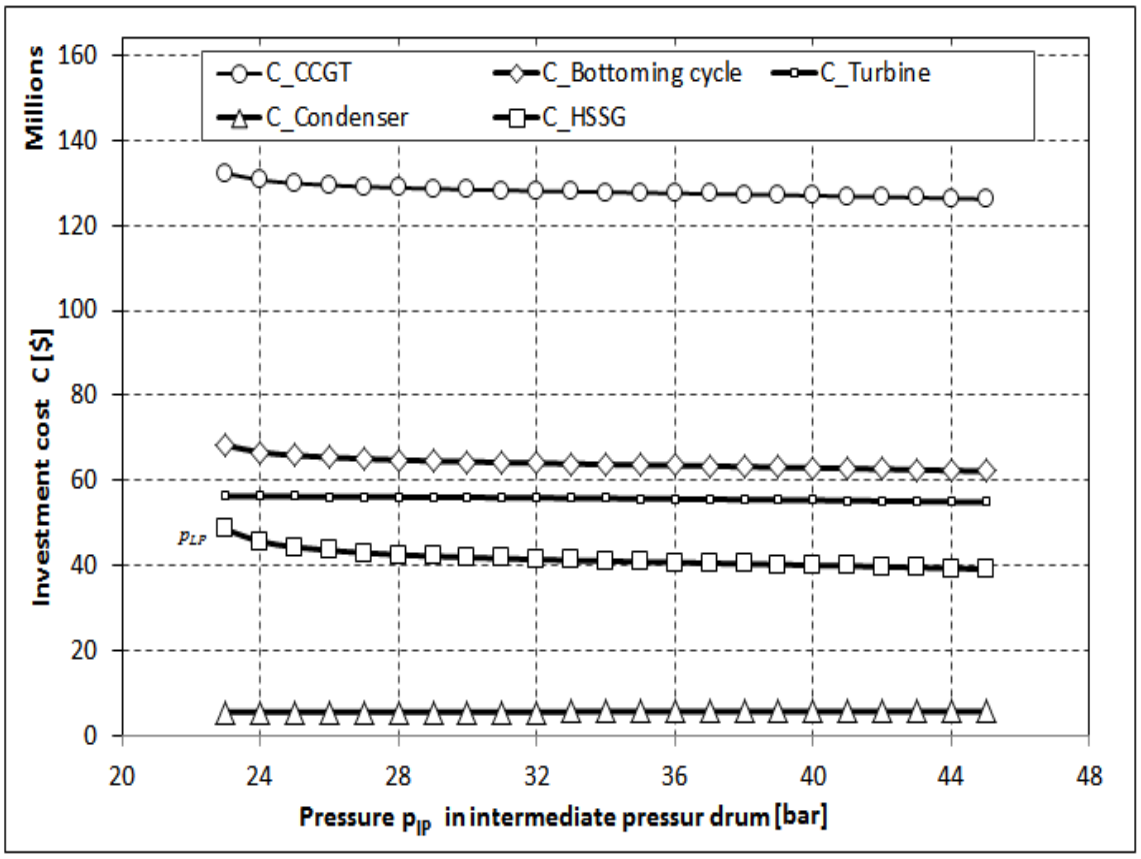

Figure 6-40 Investment cost vs. pressure p_{IP} in intermediate pressure drum

By increasing p_{IP} from 23 to 45 bar the C_{HRSG} was reduced by 25%, and the $C_{Turbine}$ was reduced by 3%. Condenser investment cost increased by 3%. The same result as with low pressure drum had a major effect on the C_{CCGT} and the C_{Bott} is the C_{HRSG}, both C_{CCGT} and C_{Bott} were decreased with reduction of p_{IP} as seen in Figure 6-40.

Pressure p_{HP} in High Pressure Drum: Investment cost for the *CCGT* and its main subsystems (C_{CCGT} ,C_{Bott} , C_{HRSG} , $C_{Turbine}$ and C_{Con}) with a variation of the pressure p_{HP} behaved in an opposite way to the behaviors of p_{HP}. Figure 6-41 shows that by increasing of p_{HP} from 100 to 180 bar, the C_{HRSG} increased by 25% and the $C_{Turbine}$ increased by 4%, while reducing the C_{Con} by about 3% for the same range of the p_{HP} variation.

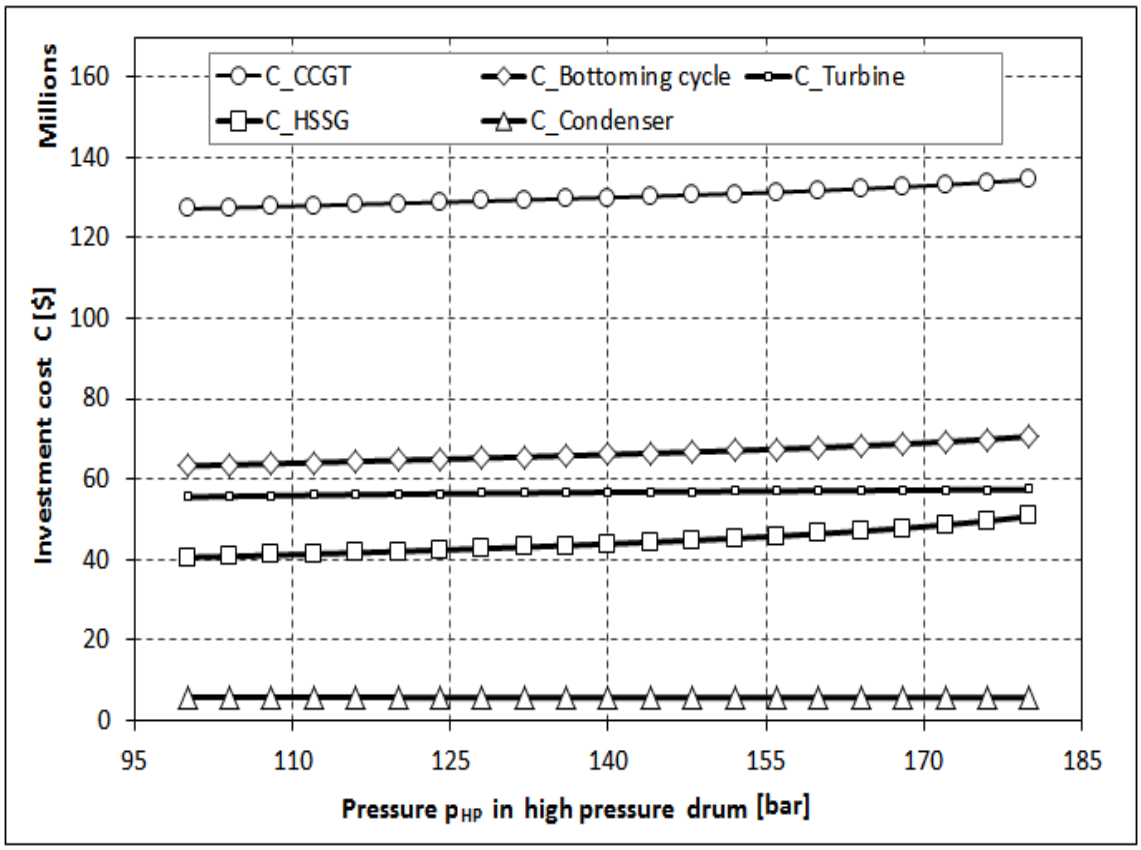

Figure 6-41 Investment cost vs. pressure p_{HP} in high pressure drum

Total investment cost for the CCGT and bottoming cycle increased (C_{CCGT} and C_{Bott}) as the result of increasing the HRSG investment cost C_{HRSG} .

6.3.2.2 Production Cost of Electricity and Annual Cash Flow

The production cost and annual cash flow are the most important thermoeconomic parameters. The effect of variations of operating parameters on production cost were completely contrary to its effect on annual cash flow as it is seen in Figure 6-42, Figure 6-43 and Figure 6-44

Figure 6-42 presents the variation of pressure p_{LP} in low-pressure drum with production cost and annual cash flow. The production cost first decreased with increasing pressure p_{LP}, which then started to increase, while the cash flow behaved in the exactly opposite way. The production cost had a minimum value at a certain value of the pressure p_{LP}, while annual cash flow had a maximum.

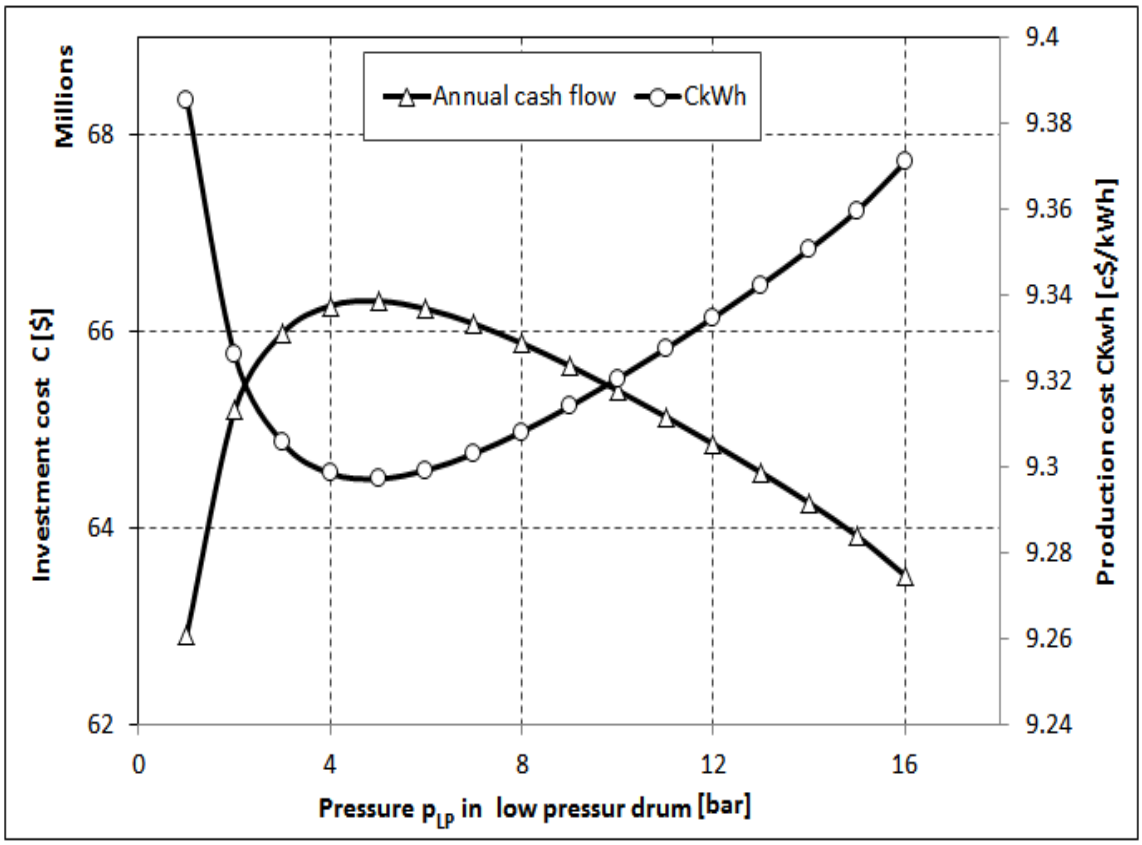

Figure 6-42 Production cost and annual cash flow vs. pressure p_{LP} in low pressure drum

Figure 6-43 illustrates the effects of the variation in the pressure p_{IP} in intermediate pressure drum with production cost and annual cash flow. The effect of variation in the pressure p_{HP} with production cost is shown in Figure 6-44. Due to the pressure limitation in the high pressure drum (its value must be less than the critical one; the limit was defined according to the professional experience at the level of 180 bar), the value of the minimal production cost and maximal annual cash flow lays out of the range of variation of p_{HP}.

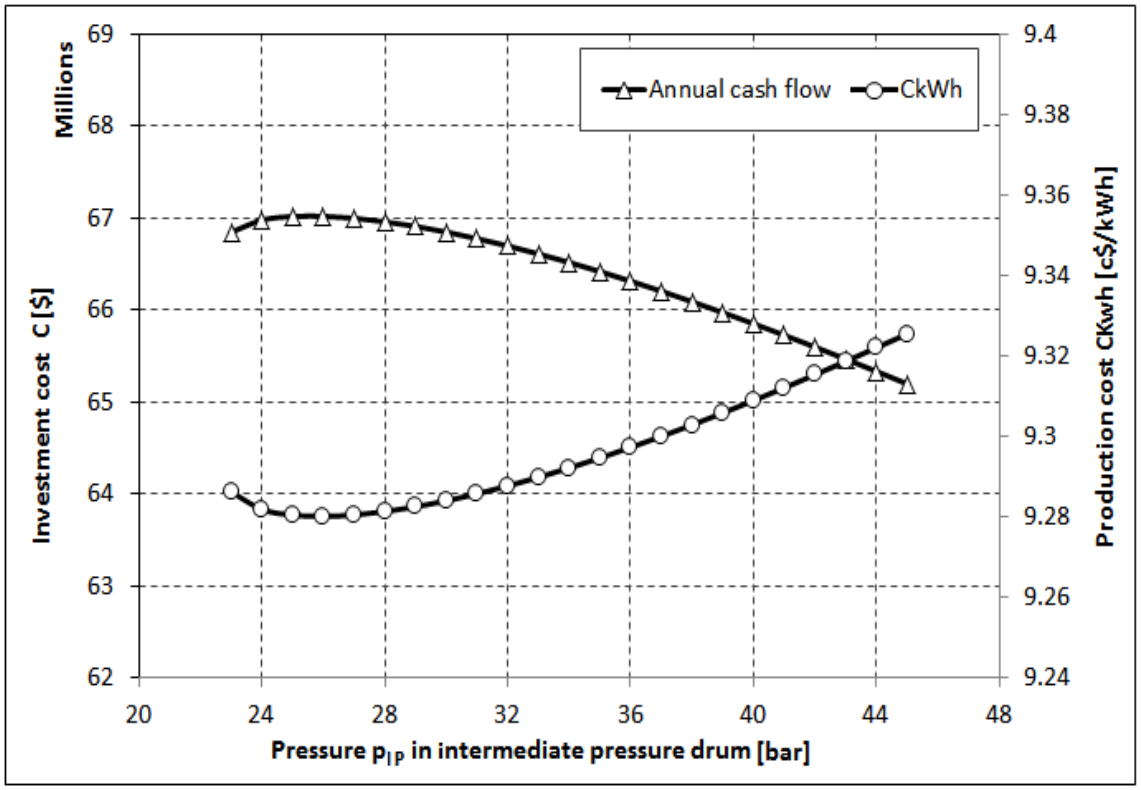

Figure 6-43 Production cost and annual cash flow vs. pressure p_{IP}

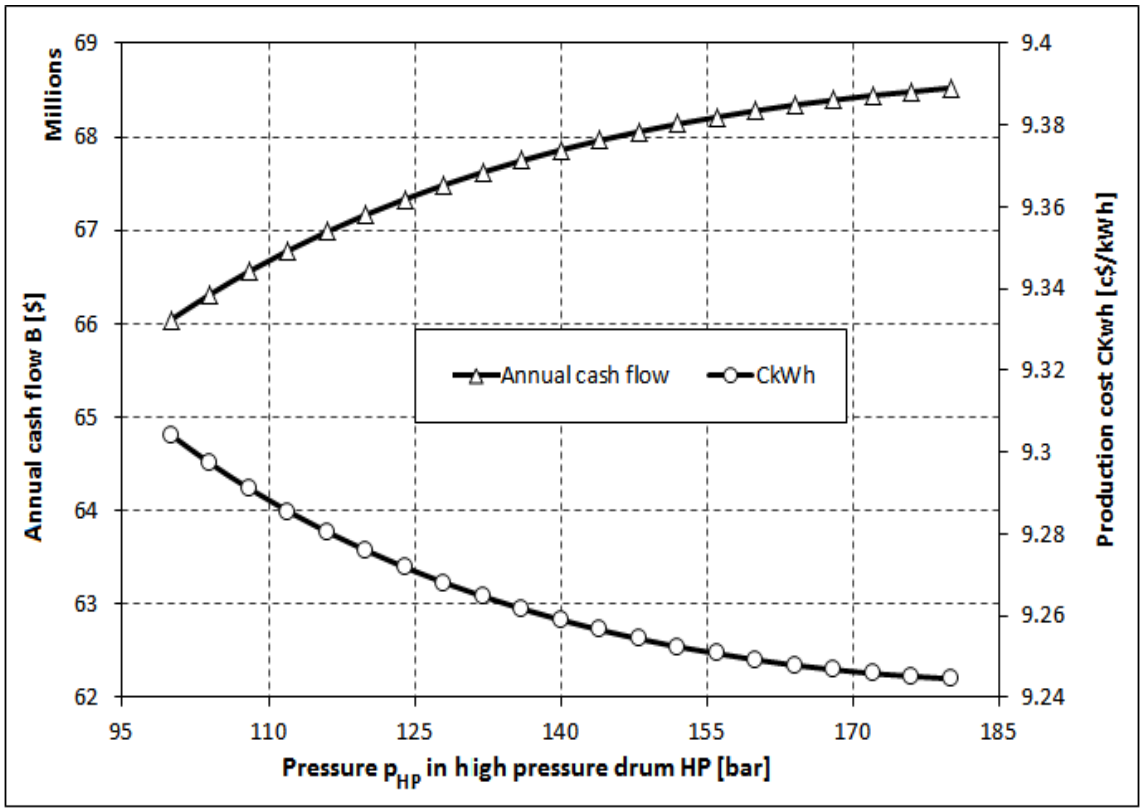

Figure 6-44 Production cost and annual cash flow vs. pressure p_{HP}

6.4 Result of Exergoeconomic Analysis

In this study, an exergoeconomic approach is used to improve the cost effectiveness according to exergy rates in a CCGT power plant at the component level. Solving the linear system consisting of related exergoeconomic equations obtained from the specific exergy costing analysis, the cost flow rates and the unit exergetic costs associated with each stream of the bottoming cycle were obtained.

Results are summarized in Figure 6-45, Figure 6-46, and Table 6-1. The Table represents important exergoeconomic parameters for the components of combined cycle power plants including the exergy destruction $\dot{E}_D$, ratio of exergy destruction to the total exergy destruction $y^*_{D,k}$ of the system, related cost of exergy destruction for each component $\dot{C}_D$, total operating cost rate $(\dot{Z}_k + \dot{C}_D)$ of components and finally the exergoeconomic factor f_k of each component. The last two factors are important thermoeconomic parameters that show the relative importance of a component cost to the associated cost of exergy destruction in that component.

Figure 6-45 illustrates the values of total operating cost rate $(\dot{Z}_k + \dot{C}_D)$ of main components CCGT.

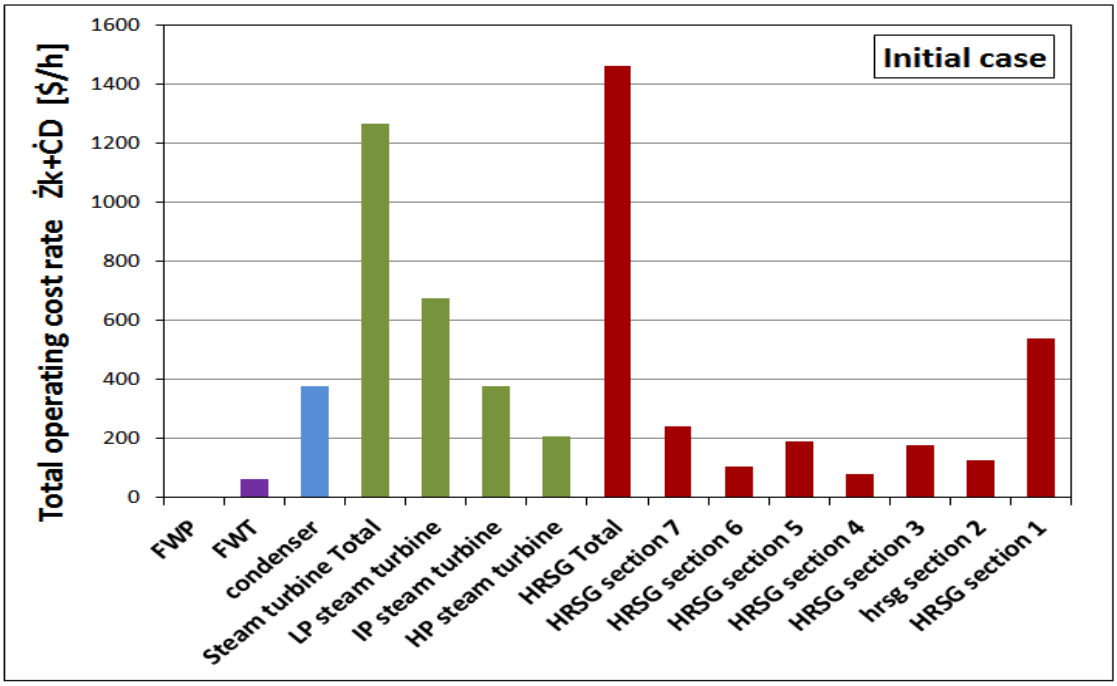

Figure 6-45 Total operating cost $\dot{Z}_k + \dot{C}_{D,k}$ for initial case

The higher the factor ($\dot{Z}_k + \dot{C}_D$), the higher the influence of the component on the overall system is, and thus, the more significant component is considered. From the figure, it is clear that the HRSG had the higher value of the total operating cost rate. The high total operating cost rate ($\dot{Z}_k + \dot{C}_D$) of the HRSG suggests that this component should be improved by reducing the exergy being destroyed within it. In addition, Figure 6-46 shows the second important factor (exergoeconomic factor f_k) in the exergoeconomic analysis; the values of exergoeconomic factor f_k for the main components are presented in this figure.

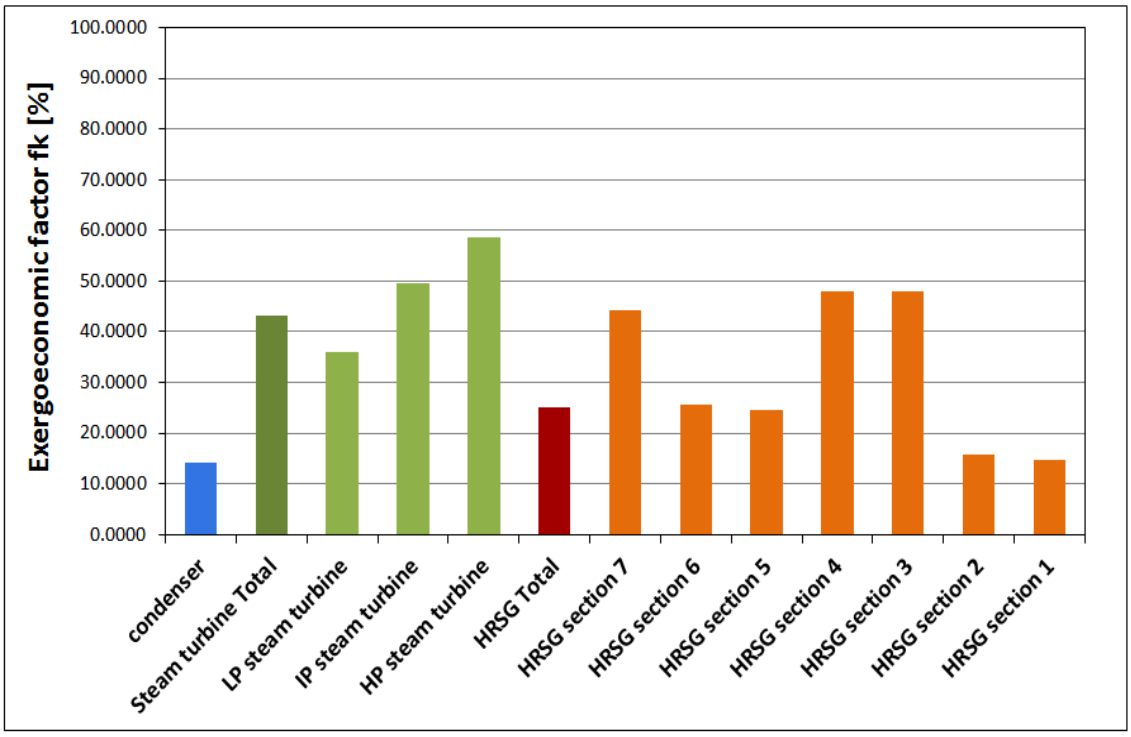

Figure 6-46 Exergoeconomic factors f_k for initial case

Higher value of exergoeconomic factor f_k implies that the major source of cost for the component under consideration was related to the capital investment and operating and maintenance costs. The lower value of exergoeconomic factor states that the associated cost of thermodynamic inefficiencies was more significant than the capital investment and operating and maintenance costs for the component under consideration. From the figure, it can be seen that the low exergoeconomic factor f_k of the HRSG components (section 1, section 2, section 5, and section 6) indicates that the associated cost of exergy destructions in these components was insignificant.

Table 6-1 Exergoeconomic parameters of the system for the initial

Component		$E_{F,k}$ [MW]	$E_{P,k}$ [MW]	$E_{D,k}$ [MW]	$C_{D,k}$ [$/h]	$E_{L,k}$ [MW]	$C_{L,k}$ [$/h]	Z_k [$/h]	$Z_k + C_{D,k}$ [$/h]	ε_k [%]	y^*_D [%]	f_k [%]
HRSG	Section 1	60.6	51.7	8.9	416.8	0	0	71.6	488.4	85	17.85	14.7
	Section 2	57.3	50.8	6.4	300.5	0	0	55.9	356.5	89	12.87	15.7
	Section 3	18.4	16.9	1.5	68.3	0	0	63.2	131.5	92	2.93	48.1
	Section 4	6	5.6	0.4	20.9	0	0	19.3	40.3	93	0.9	48
	Section 5	15.5	13	2.5	117.1	0	0	38	155.1	84	5.01	24.5
	Section 6	13.3	11.2	2.1	100.2	0	0	34.4	134.5	84	4.29	25.6
	Section 7	15.2	12.4	2.8	129.8	6.1	282.8	103.4	233.2	82	5.56	44.3
	Total	186.4	161.7	24.7	1153.6	0	0	385.8	1539.4	87	49.41	25.1
Steam turbine	LP	78.7	69.4	9.3	434.3	0	0	243.8	678.1	88	18.6	36
	IP	48.3	44.4	3.9	182.2	0	0	178.4	360.7	92	7.81	49.5
	HP	22.4	20.8	1.6	74	0	0	104.9	178.9	93	3.17	58.6
	Total	149.4	134.5	14.8	691.7	0	0	527.1	1218.8	90	29.63	43.2
Condenser		10.9	3.8	7.1	330.2	0	0	54.4	384.5	97	14.14	14.1
Feed water tank		1.9	1.4	0.5	25.5	0	0	13.5	39	72	1.09	34.6
Feed water pump		0.1	0.1	0	0.8	0	0	1.5	2.4	82	0.04	64.6
Bottoming cycle		186.4	134.5	51.8	2334.8	6.1	282.8	1055.5	3390.4	69.8	100	31.1

The capital cost of the HRSG components (section 3, section 4, and section 7), high-pressure steam turbine, and intermediate pressure steam turbine was insignificant.

As can be seen in Table 6-1, the largest sum of exergy destruction and capital cost rate ($\dot{Z}_k + \dot{C}_D$) are observed in the HRSG (1539.4 $/h). This is related to the large exergy destruction in these components.

Exergoeconomic analysis, for the improvement of the overall exergetic efficiency to the maximum possible value, suggests that exergoeconomic factor for the first group of components is increased by reducing the exergy destruction. On other hand, it suggests reducing the exergoeconomic for the second group of components.

6.5 Results of Optimization

6.5.1 First Approach, Simple Optimization Methods

6.5.1.1 Energy Optimization Method (Case 1)

Results of optimization of the energy method are presented in this section. The influence variation of PPs and drums pressures on the objective function (selected here is the production cost of electricity C_{kWh}) is presented in Figure 6-47 to Figure 6-50. Figure 6-47shows the behavior of the production cost of electricity (objective function for case 1) with variation of PPs. The minimum objective function C_{kWh} was achieved for the following values of pinch point at different pressure levels: $PP_{LP} = 7$ °C, but the lower limit of $PP_{LP} = 10$ °C was used because of the exhaust gas temperature T_{11g} constraint. Optimal intermediate and high-pressure pinch points were $PP_{HP} = 11$ °C and $PP_{LP} = 7$ °C. The production cost (objective function 1) at these optimum pinch points (PP_{LP}, PP_{IP}, and PP_{HP}) was $C_{kWh} = 9.369$ c$/hour. When the value of PP was kept constant for all three pressure levels, the optimum was achieved for $PP = 8$ °C, but for the same reason as for the low pressure level PP_{LP} the lower limit was $PP = 9.5$ °C; the minimum production cost at this optimum pinch point was $C_{kWh} = 9.371$ c$/hour.

In the case of the pressure p_{LP} in low drum pressure, the behaviors of production cost were approximately equal for both cases (first case pinch point different for each pressure level PP_{LP}, PP_{IP}, and PP_{HP}, and the second case pinch point was equal for all three pressure levels).

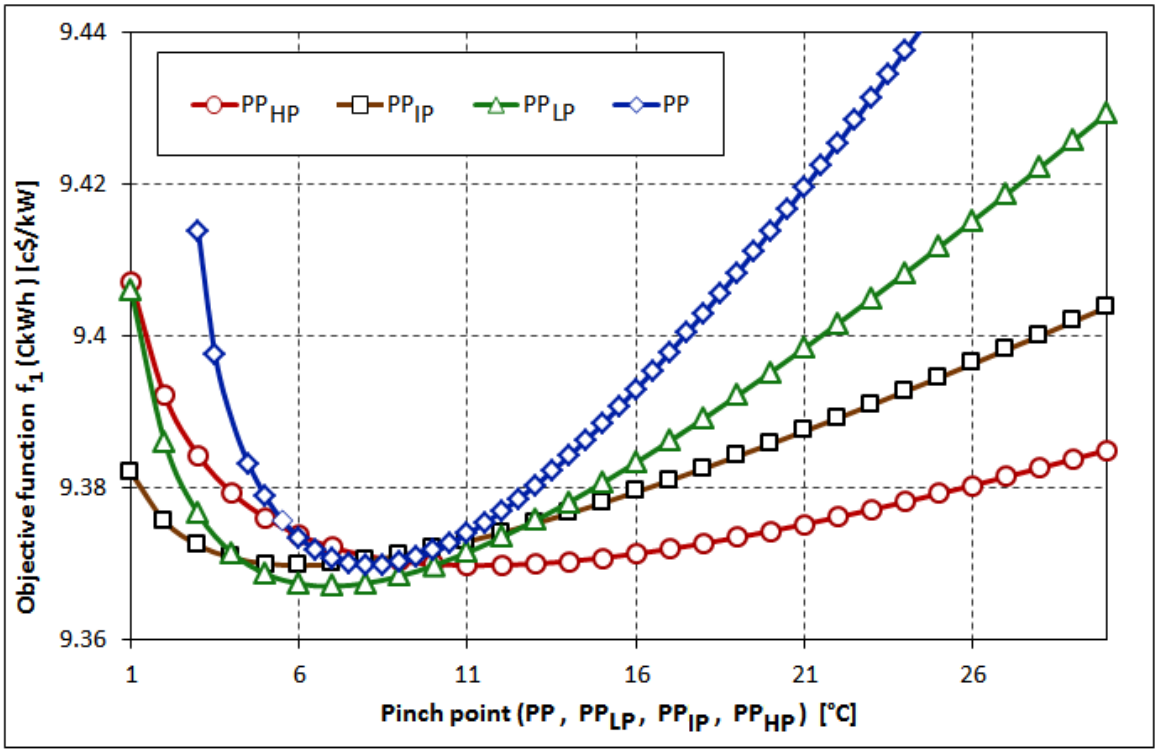

Figure 6-47 Objective function f_1 (C_{kWh}) vs. pinch point for case 1

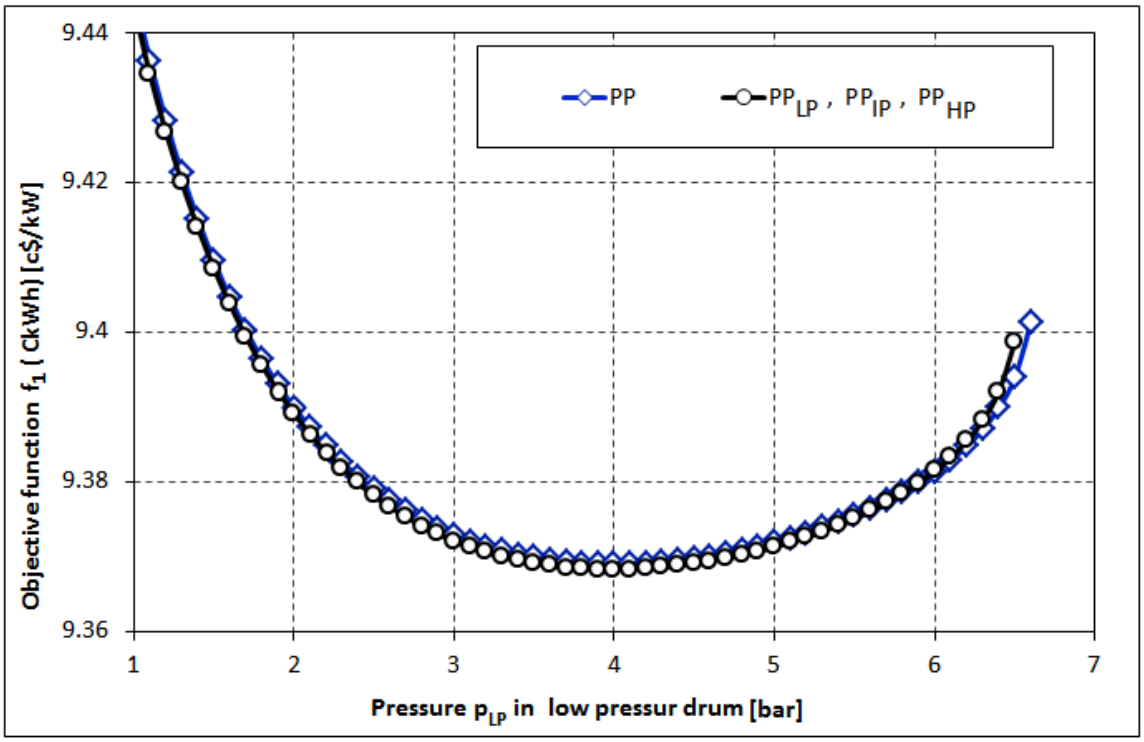

Figure 6-48 Objective function f_1 (C_{kWh}) vs. pressure p_{LP} for case 1

As seen in Figure 6-48, the minimum objective function (production cost) $C_{kWh} = 9.368$ c$/hour was achieved at $p_{LP} = 4.0$ bar .

Because the lower limit of $p_{LP} = 4.7$ bar (the exhaust gas temperature T_{11g} constraint/limitation) the production cost achieved by this optimizations was $C_{kWh} = 9.369$ c$/hour. Figure 6-48 shows the optimum pressure p_{LP} in low pressure drum for the case with constant PP for all three pressure levels; the minimum objective function C_{kWh} was also achieved in this case at $p_{LP} = 4.0$ bar, and because of the exhaust gas temperature constrain, the low limit of it was at $p_{LP} = 4.8$ bar. Figure 6-49 illustrates the effects of the variation in the pressure p_{IP} in the intermediate pressure drum with production cost.

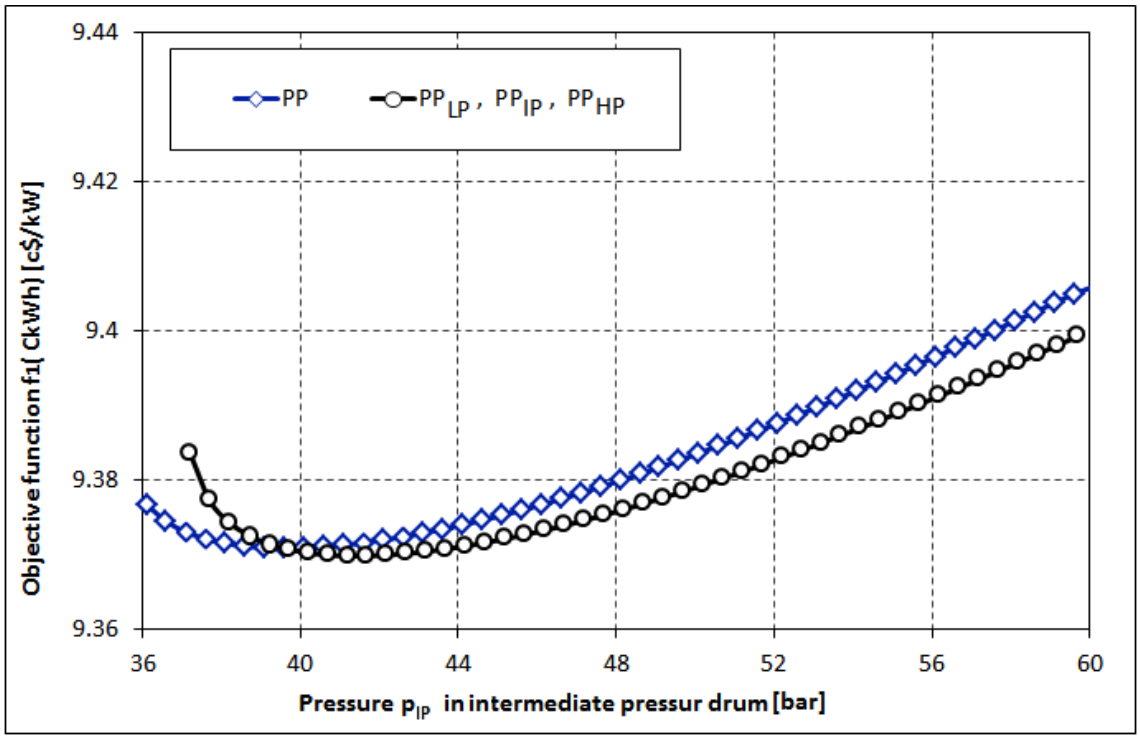

Figure 6-49 Objective function f_1 (C_{kWh}) vs. pressure p_{IP} for case 1

The figure shows that the optimum pressure was at $p_{IP} = 41.2$ bar with minimum production cost (objective function 1) $C_{kWh} = 9.369$ c$/hour. The Figure also shows the optimum pressure p_{IP} in the intermediate pressure drum was at $p_{IP} = 39.1$ bar for the case with pinch point constant for all pressure levels, and the minimum production cost in this case was $C_{kWh} = 9.37$ c$/hour.

The minimum production cost regarding pressure p_{HP} in the high-pressure drum (Figure 6-50) was achieved at $p_{HP} = 184$ bar for the case with different pinch point for

each pressure levels and at $p_{HP} = 182$ bar for the second case, but the reason was the constraint of the upper limit of pressure $f_1\ (C_{kWh})$ in the high-pressure drum (its value should be lower than critical one). According to professional experience the maximal value of p_{HP} was set here at $p_{HP} = 180$ bar. As shown in Figure 6-50 the production cost at this pressure was $C_{kWh} = 9.369$ c$/hour. For the case with constant pinch point and the same constraint (upper limit of high-pressure drum), the production cost was $C_{kWh} = 9.370$ c$/hour.

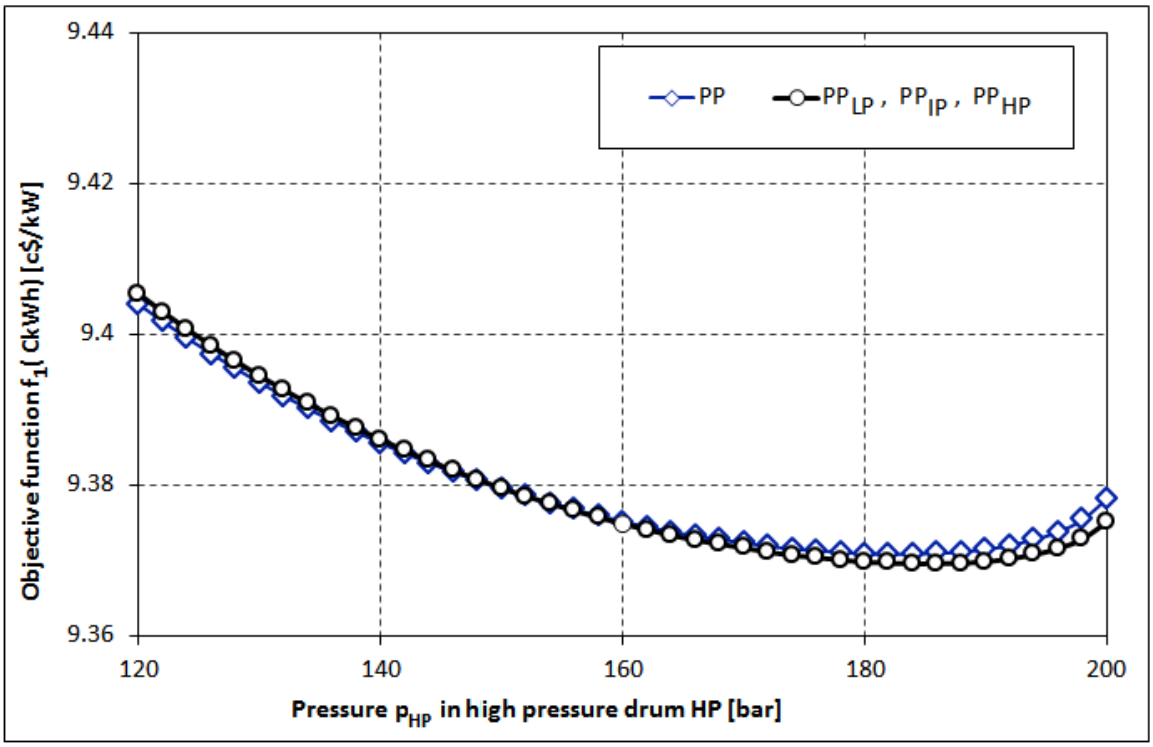

Figure 6-50 Objective function $f_1\ (C_{kWh})$ vs. pressure p_{HP} for case 1

Table 6-2 shows the result of optimization case 1. Exergoeconomic parameters of the main components of the bottoming cycle corresponding to Figure 5-1 were calculated and presented in Table 6-2. As in the table, the values of main parameters for the bottoming cycle were: the fuel exergy rate $\dot{E}_F = 186.9$ MW, the product exergy rate $\dot{E}_P = 140.4$ MW, exergy destruction rate $\dot{E}_D = 46.5$ MW, the cost rate of exergy destruction $\dot{C}_D = 2145.8$ $/hour, the cost rate of exergy losses $\dot{C}_L = 258.8$ c$/hour, the exergoeconomic factor $f_k = 36.46\%$, and the sum of destruction and capital cost rate $\dot{Z} + \dot{C}_D = 3376.9$ c$/hour.

Table 6-2 Exergoeconomic parameters of the system for the optimum case 1

Component		$E_{F,k}$ [MW]	$E_{P,k}$ [MW]	$E_{D,k}$ [MW]	$C_{D,k}$ [$/h]	$E_{L,k}$ [MW]	$C_{L,k}$ [$/h]	Z_k [$/h]	$Z_k + C_{D,k}$ [$/h]	ε_k [%]	y^*_D [%]	f_k [%]
HRSG	Section 1	73.9	64.7	9.2	431.4	0	0	110.4	541.8	88	20.1	20.38
	Section 2	27.1	25.4	1.7	80.2	0	0	43.9	124.1	94	3.74	35.39
	Section 3	28.1	26.4	1.7	81	0	0	93.1	174.1	94	3.77	53.48
	Section 4	12.7	11.8	0.8	39.5	0	0	44.6	84.1	93	1.84	53.04
	Section 5	19.2	16.9	2.3	107.6	0	0	85	192.6	88	5.01	44.15
	Section 6	11.4	9.7	1.7	77.5	0	0	36.7	114.2	85	3.61	32.12
	Section 7	14.4	12	2.4	112.3	5.5	258.8	120.3	232.6	83	5.23	51.74
	Total	186.9	167	19.9	929.3	0	0	534.1	1463.4	89	43.31	36.5
Steam turbine	LP	75.8	66.9	9	418.7	0	0	237.7	656.4	88	19.52	36.21
	IP	53.1	48.7	4.4	206.2	0	0	190.4	396.6	92	9.61	48
	HP	26.8	24.8	2	94.4	0	0	118.7	213.1	92	4.4	55.71
	Total	155.8	140.4	15.4	719.6	0	0	546.8	1266.4	90	33.54	43.18
Condenser		10.8	3.8	7	326.7	0	0	53.8	380.5	97	15.23	14.13
Feed water tank		3.2	2.3	0.9	41.7	0	0	19.5	61.1	72	1.94	31.84
Feed water pump		0.1	0.1	0	0.8	0	0	1.5	2.3	81	0.04	64.47
Bottoming cycle		186.9	140.4	46.5	2145.8	5.5	258.8	1231.2	3376.9	71.5	100	36.46

The following observations were made from the comparison of optimum case 1 in Table 6-2 and the initial case in Table 6-1 with the results tabulated in Table 6-3.

Table 6-3 Comparative results of main parameters between the optimum case 1 and the initial case

Parameter	% Variation case1 from initial case			
	HRSG	Steam turbine	Condenser	Bottoming cycle
Exergy destruction cost rate $\dot{C}_D$	-19.44	4.036	-1.05	-8.1
Purchase cost rate $\dot{Z}_k$	38.42	3.73	-1.07	16.64
$\dot{Z}_k + \dot{C}_D$	-4.94	3.90	-1.05	-0.40
Exergy efficiency ε	2.30	0.00	0.00	2.48
Exergoeconomic factor f_k	45.62	-0.17	-0.01	17.11

Exergy Destruction Cost $\dot{C}_{D,k}$; the value of the exergy destruction cost rate $\dot{C}_{D,k}$ is decreased by 19.44% and 1.05%, for the HRSG and condenser respectively, while increased for the steam turbine by 4.3%. As the result, the exergy destruction cost decreased for the whole bottoming cycle by 10.3%

Purchase Cost Rate $\dot{Z}_k$, purchase cost rate was increased for the main components of the bottoming cycle except for the condenser decrease by 1.07%. The increase of the purchase cost rate was 38.42% for HRSG, 3.73% for steam turbine and 16.46% of the total increase for the bottoming cycle.

Exergoeconomic Parameters:

a) Factor $\dot{Z}_k + \dot{C}_D$ was decreased by 4.9%, 1.05%, and 0.40% in the HRSG, condenser and bottoming cycle respectively, while increased in the steam turbine by 3.9%.

b) The exergoeconomic factor f_k increased after optimization by 45.62% for HRSG, while the effect of the optimization procedure on the steam turbine and condenser was very small, decreased by 0.17% and 0.01 for steam turbine and condenser respectively. The total increase of the bottoming cycle respectively was 17.11%

6.5.1.2 Exergy Destruction Optimization Method (Case 2)

The result of the optimization procedure using current approach adopted in the present study of the CCGT is given in Figure 6-51 to Figure 6-54 and Table 6-4. As seen in the figures, the minimum total annual cost (objective function f_2) achieved applying this optimization method was $Ct_{BOT} = 25,436,240$ \$/year for the case with different pinch point at each pressure levels, and $Ct_{BOT} = 25,446,332$ \$/year for the case with constant pinch point. Figure 6-51 shows the variations of pinch points PP_{LP}, PP_{IP}, PP_{HP}, and PP with the total annual cost of the bottoming cycle Ct_{BOT}.

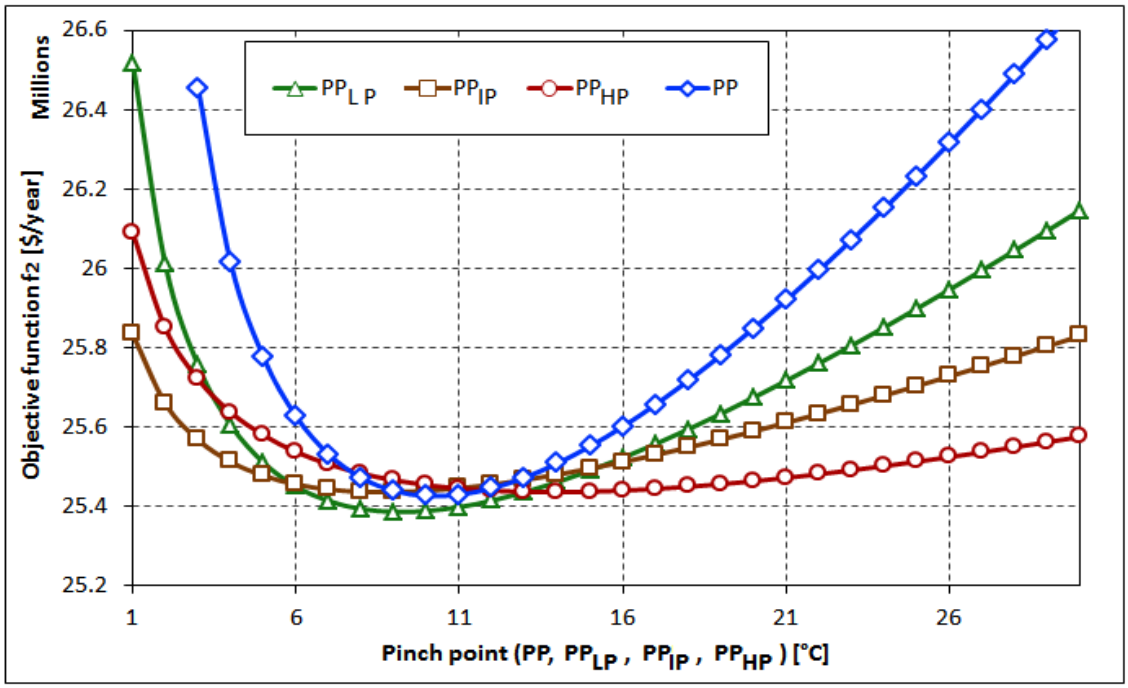

Figure 6-51 Objective function f_2 (Ct_{BOT}) vs. pinch point for case 2

Minimal objective function Ct_{BOT} was achieved for the following values of PP at different pressure levels: $PP_{LP} = 9$ °C but it was limited to 13 °C because of the lower limit of (T_{11g}) constraint; optimal intermediate and high-pressure drum were $PP_{IP} = 8.5$ °C and $PP_{HP} = 14$ °C. For the second case (PP constant), the minimum objective function Ct_{BOT} as achieved at $PP = 10$ °C, and for the same reason as with the low-pressure pinch point it was limited to $PP = 12$ °C.

The behaviors of objective function f_2 with variation of pressure p_{LP} in low-pressure drum are shown in Figure 6-52.

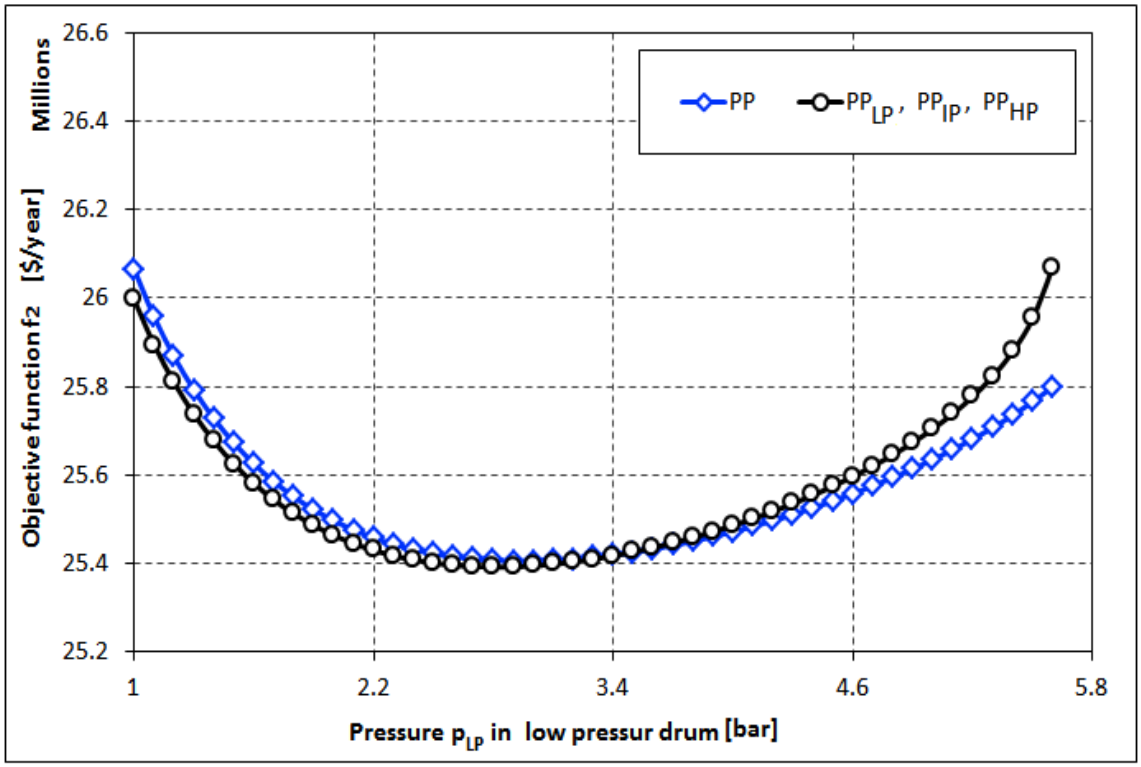

Figure 6-52 Objective function f_2 (Ct_{BOT}) vs. p_{LP} pressure for case 2

As mentioned in section 5.2 the First step: the value of exhaust gas temperature T_{11g} was determined by low-pressure drum p_{LP} and low-pressure pinch point PP_{LP}. Therefore, these two parameters were limited by the lower limit of the exhaust gas temperature of the HRSG. As shown in Figure 6-52, the minimum objective function was achieved at $p_{LP} = 2.8$ bar for the case with a different pinch point, and at $p_{LP} = 2.9$ bar for the case with the constant pinch point. However, because of T_{11g} limitation the optimum low-pressure drum for the value of the objective function mentioned above was $p_{LP} = 3.6$ bar for first case and $p_{LP} = 3.8$ bar for second case.

Figure 6-53 shows the effect of changes in the intermediate pressure p_{IP} versus objective function f_2. The results show that for a low-pressure drum of $p_{IP} = 30$ bar, the total annual cost was minimal for the case with a different pinch point temperature, and for the case with constant pinch point, the optimum intermediate pressure drum was achieved at $p_{IP} = 29$ bar.

Figure 6-54 shows that the optimum pressure drum for the high-level section was at $p_{HP} = 131$ bar for both cases.

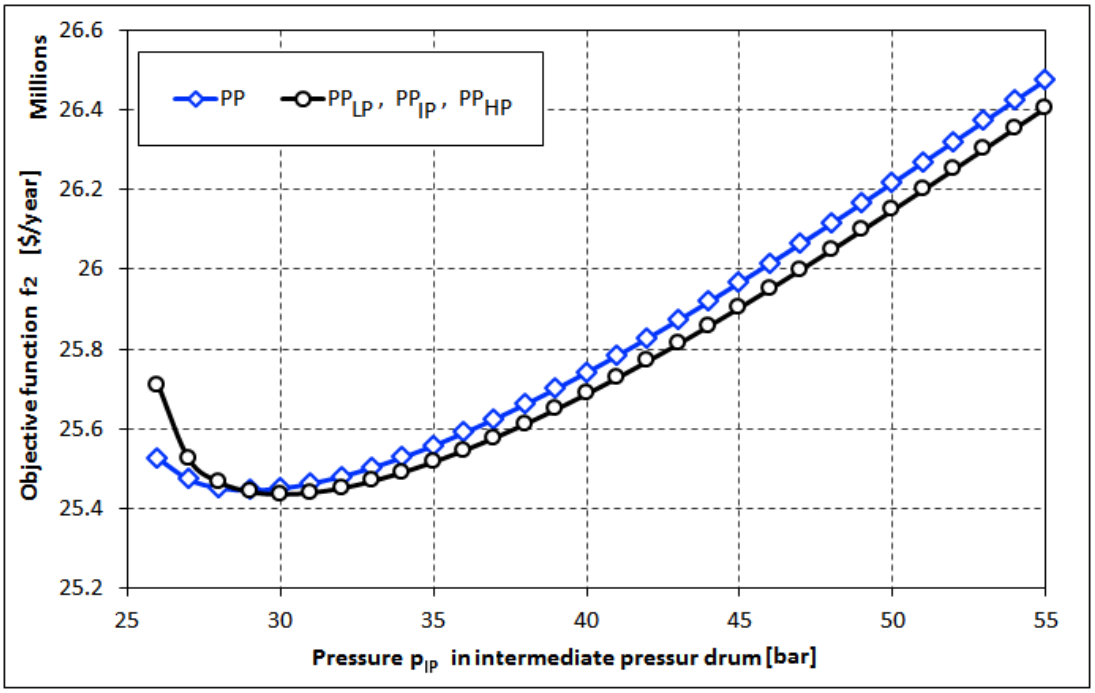

Figure 6-53 Objective function f_2 (Ct_{BOT}) vs. p_{IP} for case 2

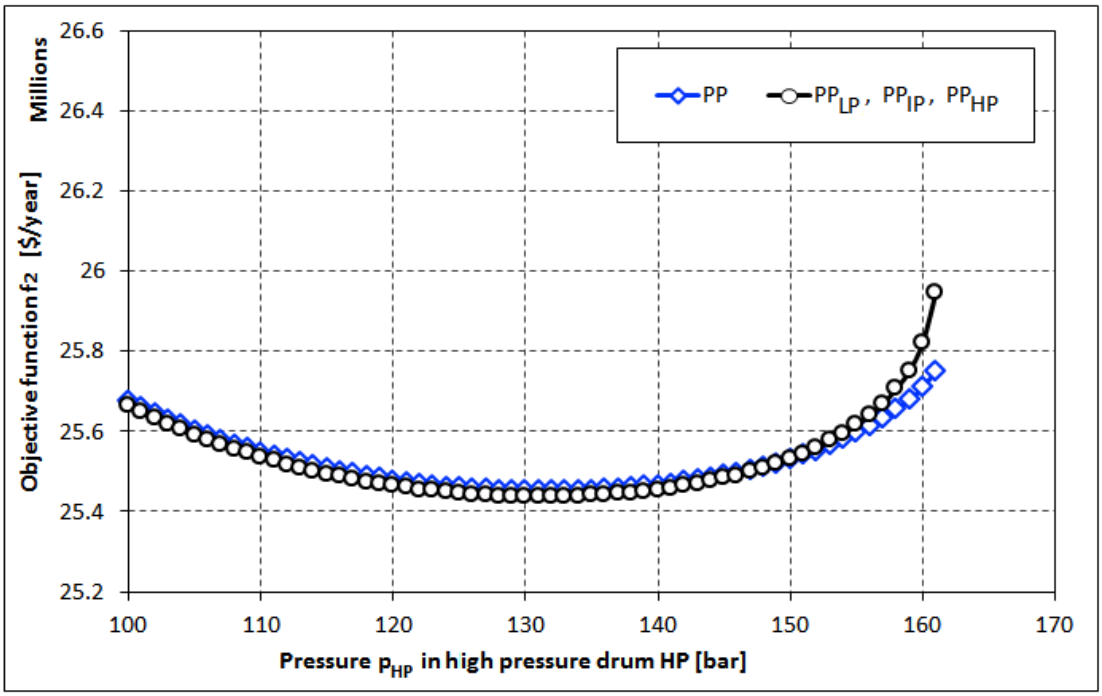

Figure 6-54 Objective function f_2 (Ct_{BOT}) vs. p_{HP} for case 2

Results of this part of the procedure (exergy destruction method) are shown in Table 6-4. The same procedure was used in this method as in the first method with the new objective function Ct_{BOT}. As illustrated in Table 6-4, the same parameters are shown as in the energy method.

Table 6-4 Exergoeconomic parameters of the system for the optimum case 2

Component		$E_{F,k}$ [MW]	$E_{P,k}$ [MW]	$E_{D,k}$ [MW]	$C_{D,k}$ [$/h]	$E_{L,k}$ [MW]	$C_{L,k}$ [$/h]	Z_k [$/h]	$Z_k + C_{D,k}$ [$/h]	ε_k [%]	y^*_D [%]	f_k [%]
HRSG	Section 1	66.03	56.76	9.27	432.68	0	0	78.03	510.72	86	19.38	15.28
	Section 2	44.41	40.32	4.09	190.9	0	0	49.03	239.92	91	8.55	20.44
	Section 3	22.41	20.51	1.9	88.69	0	0	64.52	153.21	92	3.97	42.11
	Section 4	14.5	13.31	1.19	55.78	0	0	40.92	96.7	92	2.5	42.32
	Section 5	17.19	15	2.19	102.26	0	0	74.6	176.86	87	4.58	42.18
	Section 6	9.56	8.03	1.53	71.52	0	0	29.83	101.34	84	3.2	29.44
	Section 7	12.77	10.41	2.36	110.17	5.55	259.15	97.46	207.63	82	4.93	46.94
	Total	186.87	164.34	22.53	1052	0	0	434.38	1486.38	88	47.11	29.22
Steam turbine	LP	71.87	63.37	8.5	396.84	0	0	228.89	625.73	88	17.77	36.58
	IP	53.01	48.64	4.37	204.04	0	0	190.19	394.24	92	9.14	48.24
	HP	27.62	25.55	2.07	96.82	0	0	121.17	218	92	4.34	55.58
	Total	152.51	137.56	14.95	698.11	0	0	540.26	1238.37	90	31.26	43.63
Condenser		10.89	3.83	7.06	329.71	0	0	54.29	384	97	14.77	14.14
Feed water tank		2.27	1.63	0.65	30.2	0	0	15.45	45.64	72	1.35	33.85
Feed water pump		0.07	0.06	0.02	0.73	0	0	1.23	1.96	78	0.03	62.76
Bottoming cycle		186.87	137.56	49.31	2233	5.55	259.15	1120.2	3353.29	71.04	100	33.41

The following observations are made from the comparison of optimum case 2 in Table 6-4 and with the initial case 2 in Table 6-1. The results are tabulated in Table 6-5

Table 6-5 Comparative results of main parameter between the case 2 and the initial case

Parameter	% Variation of initial case			
	HRSG	Steam turbine	Condenser	Bottoming cycle
Exergy destruction cost rate $\dot{C}_D$	-8.81	0.93	-0.14	-4.36
Purchase cost rate $\dot{Z}_k$	12.59	2.49	-0.13	6.13
$\dot{Z}_k + \dot{C}_D$	-3.44	1.60	-0.14	-1.09
Exergy efficiency ε	1.15	0.00	0.00	1.76
Exergoeconomic factor f_k	16.6	0.88	0.01	7.3

Exergy Destruction Cost $\dot{C}_{D,k}$; the value of the exergy destruction cost rate $\dot{C}_{D,k}$ was decreased by 8.8% and 0.14% for the HRSG and condenser, and in the same time increased for the steam turbine by 0.93%. As the result, the exergy destruction cost decreased for the whole bottoming cycle by 4.85%

Purchase Cost Rate $\dot{Z}_k$, purchase costs rate increased for the main components of the bottoming cycle except the condenser, which was decreased by 0.13%. The increase of the purchase cost rate was by 12.59% for HRSG, 2.49% for the steam turbine and 6.13% for the total increase for the bottoming cycle.

Exergoeconomic Parameters:

a) Total operating cost rate $\dot{Z}_k + \dot{C}_D$ decreased by 3.44% for HRSG, while, being increased by 1.6% for steam turbine and as a result decreased only by 1.1% for whole bottoming cycle.

b) The exergoeconomic factor f_k increased after optimization by 16.6%, 0.88%, 0.01%, and 7.30% for HRSG, steam turbine, condenser, and bottoming cycle respectively.

6.5.1.3 Exergoeconomic Optimization Method (Case 3)

Various data generated during the optimization procedure using current approach was adopted in the present study. The results of optimization for the minimum production cost and minimum total annual cost were reported previously.

In this part of the research, the exergoeconomic optimization was performed to minimize the specific total cost of the products $c_{P,TOT}$ as objective function f_3; the values of the specific total cost of the products $c_{P,TOT}$ were calculated using equation (5-109). In this method, the design variables were chosen in the same way as for the previous methods (low intermediate and high-pressure pinch point and pressure drum in the evaporators section of the low intermediate and high-pressure level).

The results of this method, the exergoeconomic parameters for each system components for optimum case 3, are summarized in Table 6-6. They are also outlined in Figure 6-55, Figure 6-56, Figure 6-57, and Figure 6-58.

Figure 6-55 shows specific total cost of the products versus change in pinch points (PP_{LP} , PP_{IP} , PP_{HP} , PP) of the three pressure lines of HRSG.

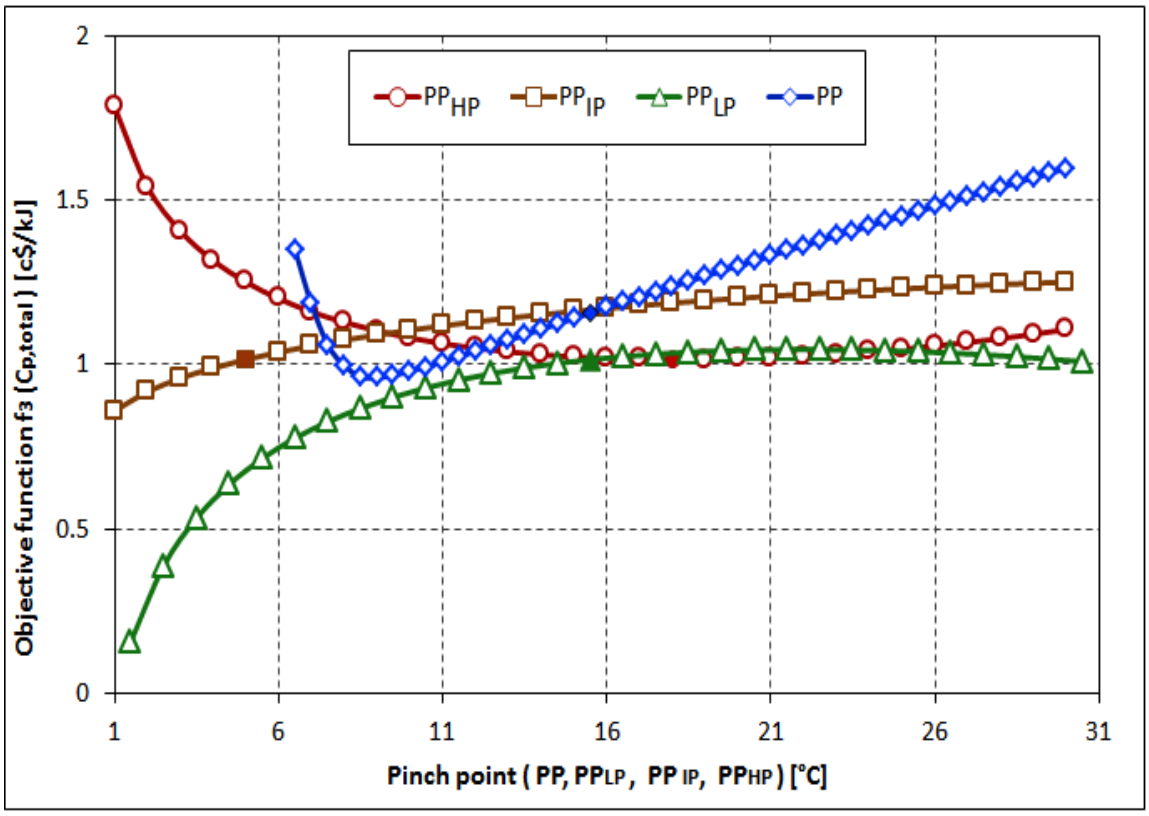

Figure 6-55 Objective function f_3 ($c_{P,TOT}$) vs. pinch point for case 3

It is observable that by decreasing low pressure pinch point PP_{LP} the objective function decreases, where the lower limit was dependent on the lower limit of the exhaust gas temperature, the minimum PP_{LP} applied here was $PP_{LP} = 15.5\ ^{\circ}\mathrm{C}$.

The case with intermediate pressure pinch point PP_{IP} is similar to the low pressure case. There was another limitation for the intermediate pressure pinch point due to the lower limit pinch point constraint (its value had to be less than acceptable in relation to the lower limit; where the limit was defined according to professional experience at the level of $5\ ^{\circ}\mathrm{C}$), and the optimum intermediate pinch point for this case was $PP_{IP} = 5\ ^{\circ}\mathrm{C}$, as seen in Figure 6-55. The minimum objective function for the high-pressure pinch point was at $PP_{HP} = 18.2\ ^{\circ}\mathrm{C}$. The behavior of objective function f_3 versus pinch point PP (case with constant pinch point) is shown in Figure 6-55. It can be seen that an optimal pinch point PP at $PP = 9.0\ ^{\circ}\mathrm{C}$ led to the minimum $c_{P,TOT}$. However, because of T_{11g} constraint, lower limit pinch point was $PP = 15.4\ ^{\circ}\mathrm{C}$.

Optimum pressure p_{LP} in low-pressure drum determined by applying current procedure depend on the exhaust gas temperature constraint. Figure 6-56 shows the variations of objective function with p_{LP}.

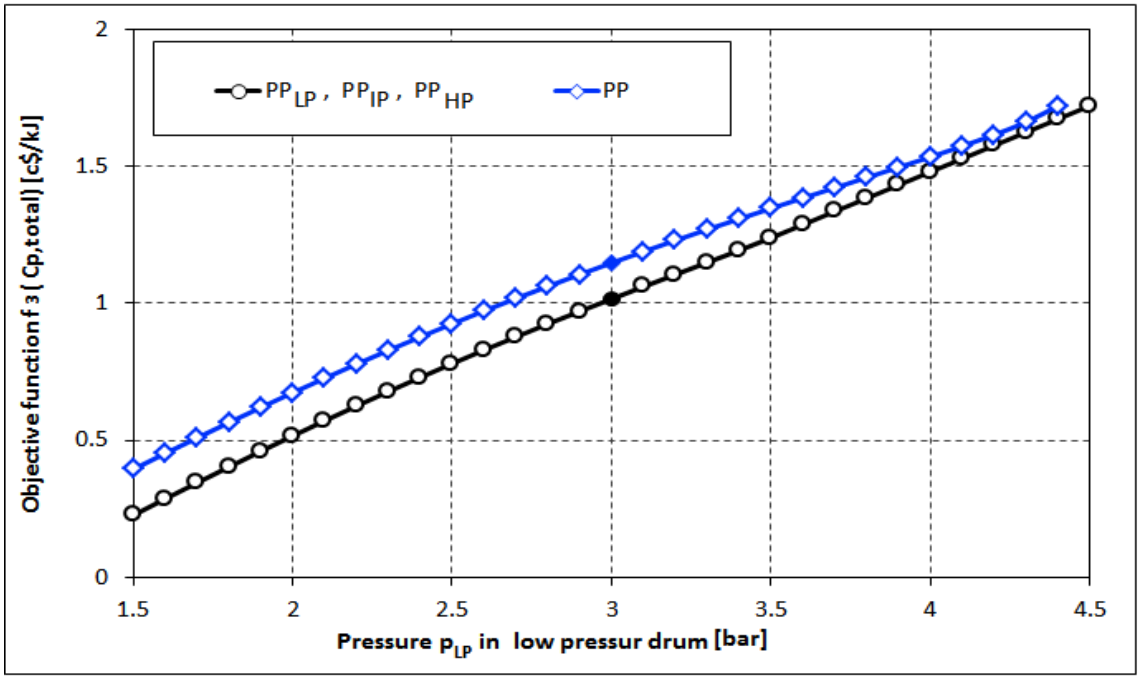

Figure 6-56 Objective function f_3 ($c_{P,TOT}$) vs. pressure p_{LP} for case 3

The figure shows that the specific total cost of the products $c_{P,TOT}$ as objective function f_3 continually increased as the pressure p_{LP} increased. The lower limit of the low-pressure drum is at $p_{LP} = 3$ bar.

Figure 6-57 plots the specific total cost of the products $c_{P,TOT}$ as a function of pressure p_{IP} in intermediate pressure drum. In Figure 6-57 the specific total cost of the products $c_{P,TOT}$ initially decreased for both cases (with different pinch points $PP_{LP}, PP_{IP}, PP_{HP}$ and constant pinch point PP) to a minimum value at $p_{IP} = 35.2$ bar for the first case, and at $p_{IP} = 31.0$ bar for the second case, and then it starts to increase.

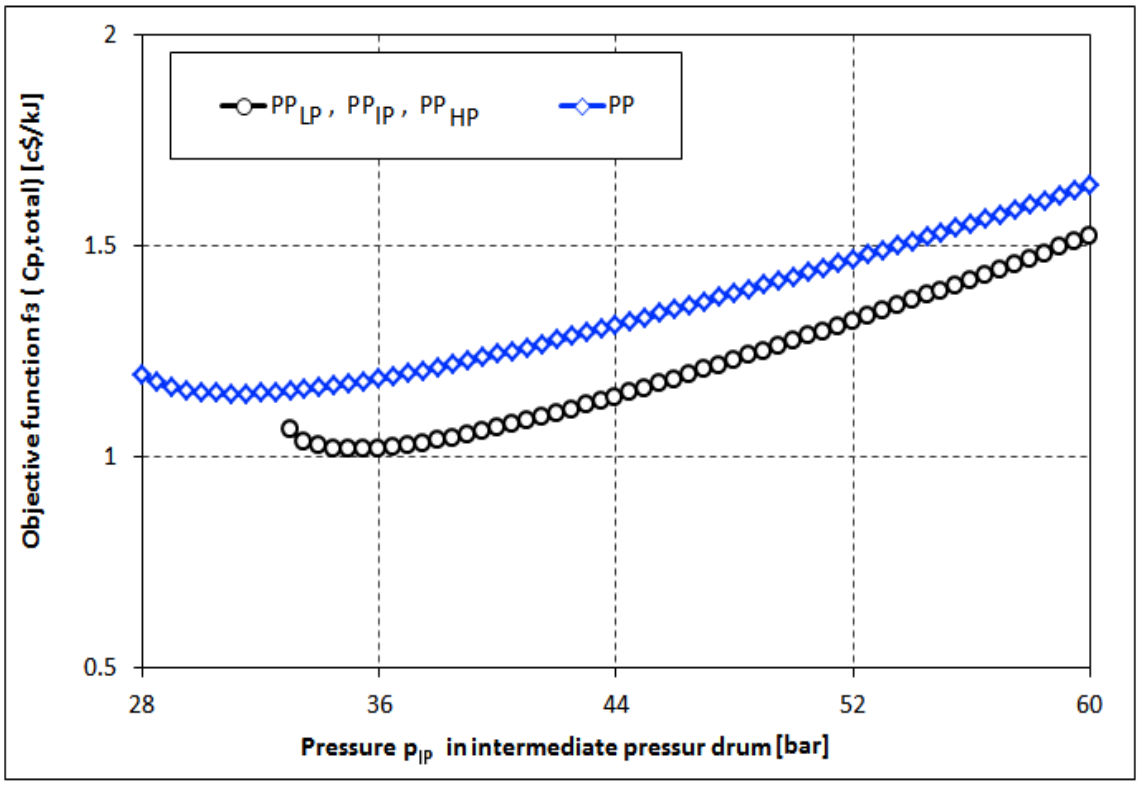

Figure 6-57 Objective function f_3 ($c_{P,TOT}$) vs. pressure p_{IP} for case 3

Figure 6-58 presents the behaviors of objective function with pressure PP_{HP} in the high-pressure drum.

This figure gives the result of variation of the pressure PP_{HP} and the specific total cost of the products $c_{P,TOT}$. Clearly, with the increase of PP_{HP}, the specific total

cost of the products $c_{P,TOT}$ decreased to minimal value for both cases (different pinch point PP_{LP}, PP_{IP}, PP_{HP} and constant pinch point PP).

As the result, the optimal value of the pressure p_{HP} for the case with different pinch point was at $p_{HP} = 184$ bar and at $p_{HP} = 182$ bar for the case with constant pinch point. On the other hand, due to the pressure limitation in the pressure p_{HP} (its value must be less than the critical one; the limit was defined according to professional experience at the level of 180 bar). Therefore, the optimal values were identical with constraint values of the pressure p_{HP} for both cases.

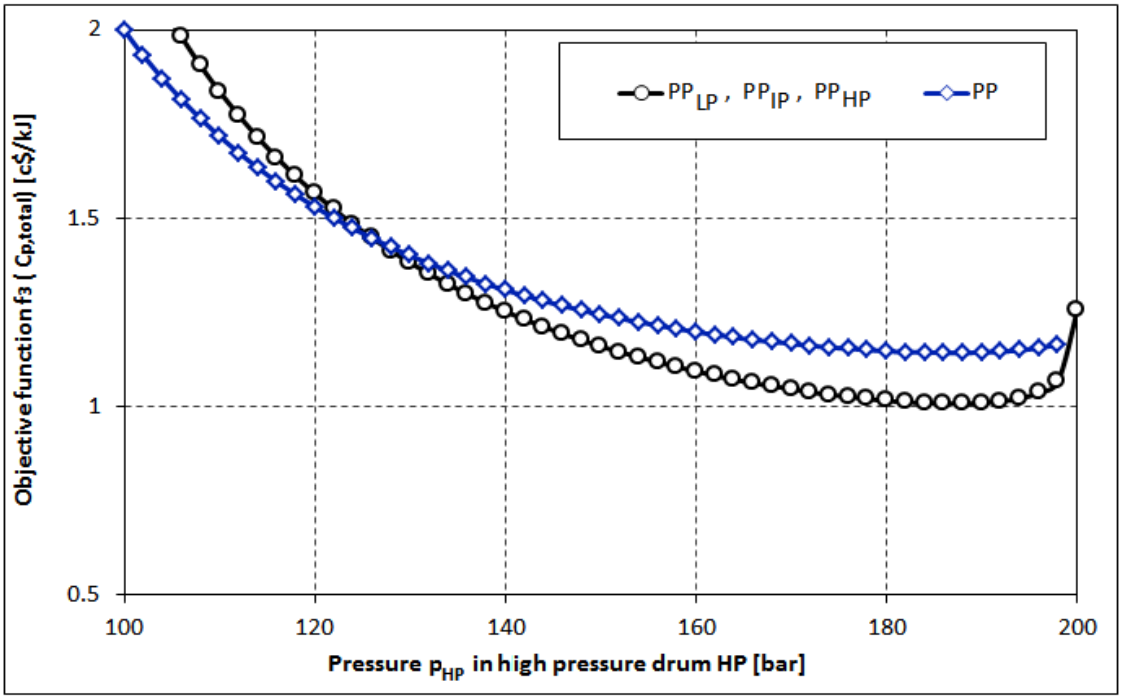

Figure 6-58 Objective function f_3 ($c_{P,TOT}$) vs. pressure p_{HP} for case 3

Table 6-6 shows the result of optimization case 3. Exergoeconomic parameters of the main components of the bottoming cycle corresponding to Figure 5-1 are calculated and presented in Table 6-6.

As shown in the table, the values of main parameters for the bottoming cycle were: the fuel exergy rate $\dot{E}_F$, the product exergy rate $\dot{E}_P$, exergy destruction rate $\dot{E}_D$, the cost rate of exergy destruction $\dot{C}_D$, the cost rate of exergy losses $\dot{C}_L$, the exergoeconomic factor f_k, and the sum of destruction and capital cost rate $\dot{Z}_k + \dot{C}_D$ for the main component of the power plant.

Table 6-6 Exergoeconomic parameters of the system for the optimum case 3

Component		$E_{F,k}$ [MW]	$E_{P,k}$ [MW]	$E_{D,k}$ [MW]	$C_{D,k}$ [$/h]	$E_{L,k}$ [MW]	$C_{L,k}$ [$/h]	Z_k [$/h]	$Z_k + C_{D,k}$ [$/h]	ε_k [%]	y^*_D [%]	f_k [%]
HRSG	Section 1	73.21	63.74	9.47	442.28	0	0	103.24	545.52	87	20.17	14.65
	Section 2	25.37	23.66	1.71	80.01	0	0	34.36	114.37	93	3.65	15.69
	Section 3	28.9	26.63	2.27	106.13	0	0	68.64	174.77	92	4.84	48.08
	Section 4	18.38	16.9	1.48	69.28	0	0	56.08	125.36	92	3.16	48.02
	Section 5	19.87	17.47	2.4	112.22	0	0	111.42	223.65	88	5.12	24.51
	Section 6	9.27	7.63	1.64	76.69	0	0	26.81	103.49	82	3.5	25.56
	Section 7	11.86	9.51	2.35	109.7	5.54	258.89	85.11	194.81	80	5	44.33
	Total	186.88	165.54	21.33	996.3	0	0	485.66	1481.96	89	45.44	25.06
Steam turbine	LP	66.93	59.02	7.91	369.56	0	0	217.76	587.31	88	16.86	35.95
	IP	59.57	54.42	5.14	240.18	0	0	205.75	445.93	91	10.96	49.47
	HP	27.85	25.7	2.15	100.45	0	0	121.69	222.14	92	4.58	58.65
	Total	154.35	139.14	15.21	710.21	0	0	545.2	1255.41	90	32.39	43.25
Condenser		10.85	3.82	7.03	328.27	0	0	54.05	382.31	97	14.97	14.14
Feed water tank		2.97	2.12	0.85	39.48	0	0	18.77	58.26	72	1.8	34.56
Feed water pump		0.06	0.05	0.01	0.69	0	0	1.1	1.79	76	0.03	64.56
Bottoming cycle		186.88	139.14	47.73	2192.5	5.54	258.89	1179.8	3372.36	71.15	100	31.13

The following observations were made from the comparison of the optimum case 3 in Table 6-6 with the initial case in Table 6-1. The result is tabulated in Table 6-7.

Table 6-7 Comparative results of the main parameters between the optimum case 3 and the initial case

Parameter	% Variation of initial case			
	HRSG	Steam turbine	Condenser	Bottoming cycle
Exergy destruction cost rate $\dot{C}_D$	-13.63	2.67	-0.58	-6.10
Purchase cost rate $\dot{Z}_k$	25.88	3.43	-0.57	11.78
$\dot{Z}_k + \dot{C}_D$	-3.73	3.00	-0.58	-0.53
Exergy efficiency ε	2.30	0.00	0.00	1.92
Exergoeconomic factor f_k	30.76	0.42	0.1	12.38

Exergy Destruction Cost $\dot{C}_{D,k}$: the value of the exergy destruction cost rate $\dot{C}_{D,k}$ was decreased by 13.63% and 0.58%, for the HRSG and condenser respectively, while being increased for the steam turbine by 2.67%. Consequently, the exergy destruction cost was decreased for the whole bottoming cycle by 6.10%

Purchase Cost Rate $\dot{Z}_k$: purchase cost rate increased for the main components of the bottoming cycle except for the condenser decrease by 0.57%. The increase of the purchase cost rate was by 25.88% for HRSG, 3.43% for steam turbine, while the total increase for the bottoming cycle was 11.78%.

Exergoeconomic Parameters:

a) Factor $\dot{Z}_k + \dot{C}_D$ was changed for the main components of the bottoming cycle as explained: for HRSG and steam turbine, the values were increased by 3.73% and 3%. For the condenser it was reduced by 0.58%. As the result, bottoming cycle factor was reduced by 0.53%.

b) The exergoeconomic factor f_k increased after the optimization by 30.76%, 0.42%, 0.01%, and 12.38% for HRSG, steam turbine, condenser, and bottoming cycle respectively.

6.5.2 Second Approach Optimization Method using MIDACO software

In order to check whether the optimization algorithm worked properly, exergoeconomic optimization method was performed by using MIDACO software. For this purpose, an objective function f_3 was chosen. In addition, the same decision variables used for the previous optimizations were selected. By determining a set of constraints, an objective function was optimized using this software algorithm. The convergence of the objective function is shown in Figure 6-59.

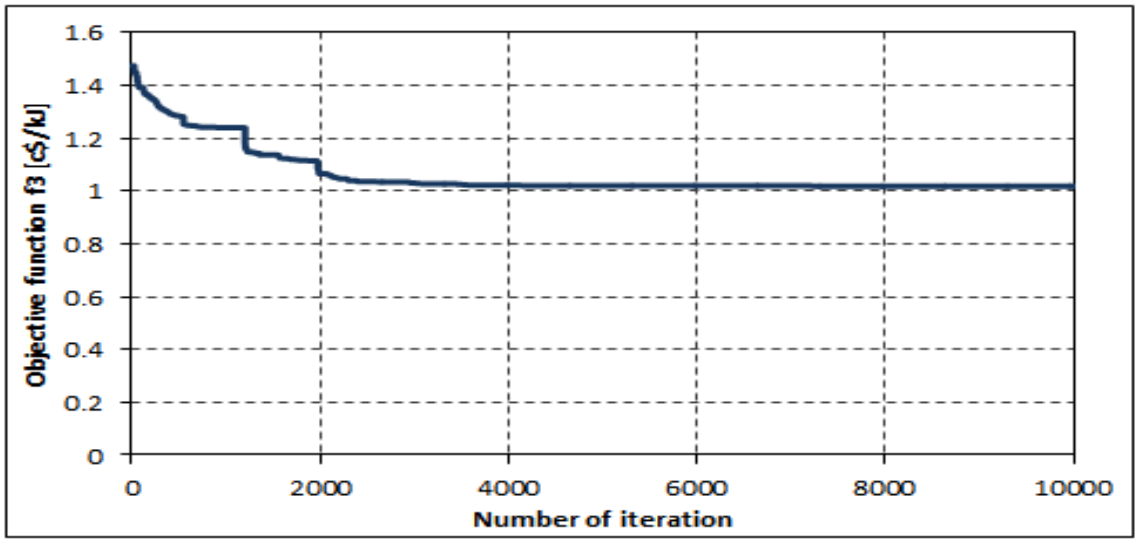

Figure 6-59 Convergence of the objective function versus generation

The convergence for the decision variables as a final result applying MIDACO software are plotted in Figure 6-60, Figure 6-61, Figure 6-62, and Figure 6-63.

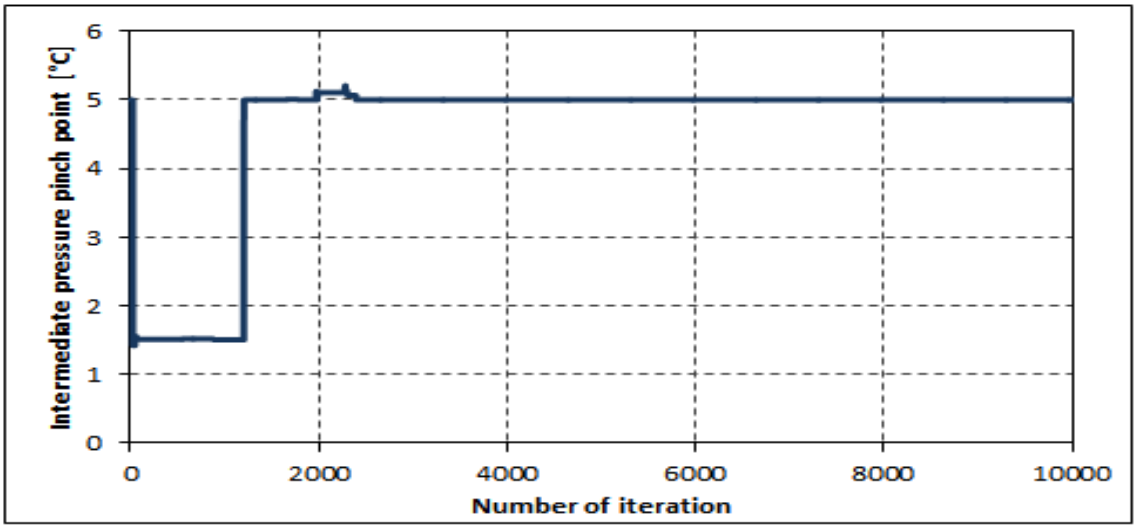

Figure 6-60 Convergence of the intermediate pressure pinch point versus generation

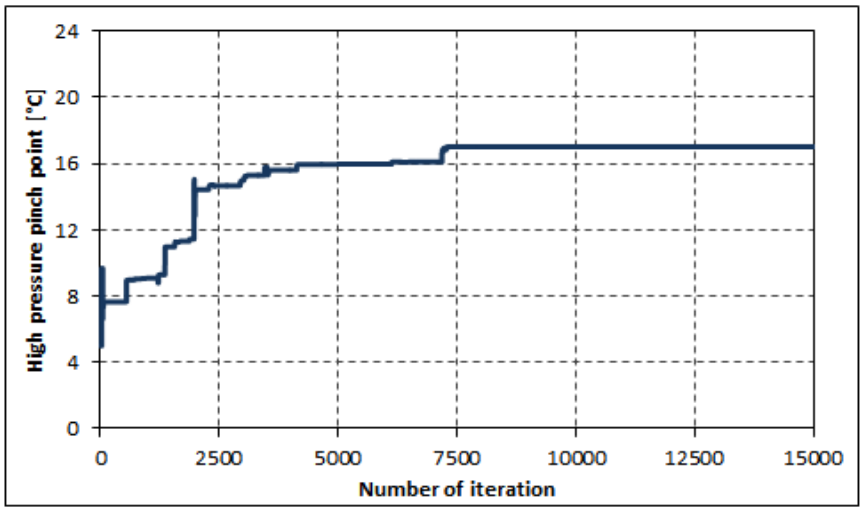

Figure 6-61 Convergence of the high pressure pinch point versus generation

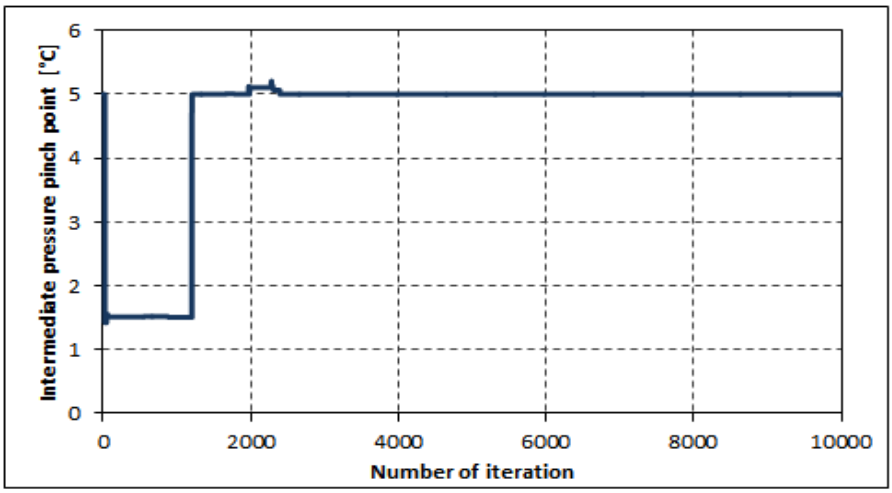

Figure 6-62 Convergence of the pressure in intermediate pressure drum versus generation

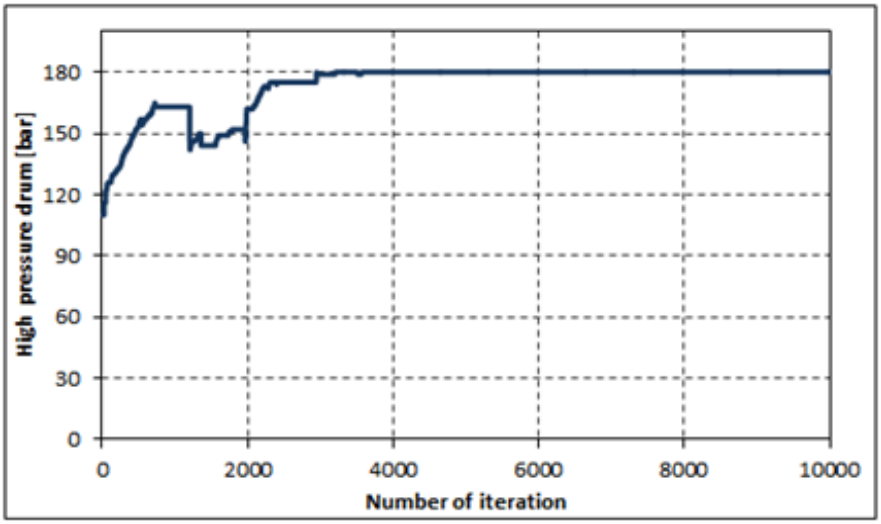

Figure 6-63 Convergence of the pressure in high pressure drum versus generation

6.5.3 Comparisons

Comparative analysis is performed to examine the impact of the optimization procedures on the CCGT performance. The measure of the enhancement in the thermodynamic performance is the values of increasing in efficiency and power output and decreasing in exergy destructions. On the other hand, the measures of the enhancement in the economic performance are minimized in costs. Comparisons of three different optimization methods (cases) with the initial case will be discussed in this section. Comparisons between the parameters shown in Table 6-2, Table 6-4, and Table 6-6 are conducted to illustrate the best method regarding thermodynamic, economic and exergoeconomic performance.

6.5.3.1 Thermodynamic Performance

Three methods were applied in this thesis to obtain the performance of the combined cycle gas turbine power plant. Applications of different methods to a given system normally yields different values of performance parameters. Thermodynamic parameters for comparison in this thesis are: exergy destruction $\dot{E}_{D,k}$, exergy efficiency ε_k, thermal efficiency η_{CCGT}, and power output P_{ST}.

It is seen from Table 6-1 that 69.9% of the exergy entering the system is converted to power from the steam turbine $\dot{E}_{P,ST} = 134.5$ MW, which is the product of the system for the initial case. The remaining exergy is either lost to the environment or destroyed due to irreversibility in the various components of the system.

The rate of exergy destruction of main components of the system as compared to total fuel exergy input and net product is given in the Grassman diagram Figure 6-29. The total exergy supplied to the system (bottoming cycle) is $\dot{E}_{4g}$ =192.420 MW. Out of total exergy supplied, 69.9% exergy is converted to a useful product, which is equivalent to 134.5 MW. For the initial case, about 26.9% exergy is destroyed (equivalent to 51.9 MW) and the remaining 3.17 % exergy is lost in the environment (equivalent to 6.1MW).

The highest exergy destruction is found in HRSG, as seen in Figure 6-64.The exergy destruction in this component is found to be about 13% of the total exergy supply or 49.4% of total exergy destruction in the system for the initial case.

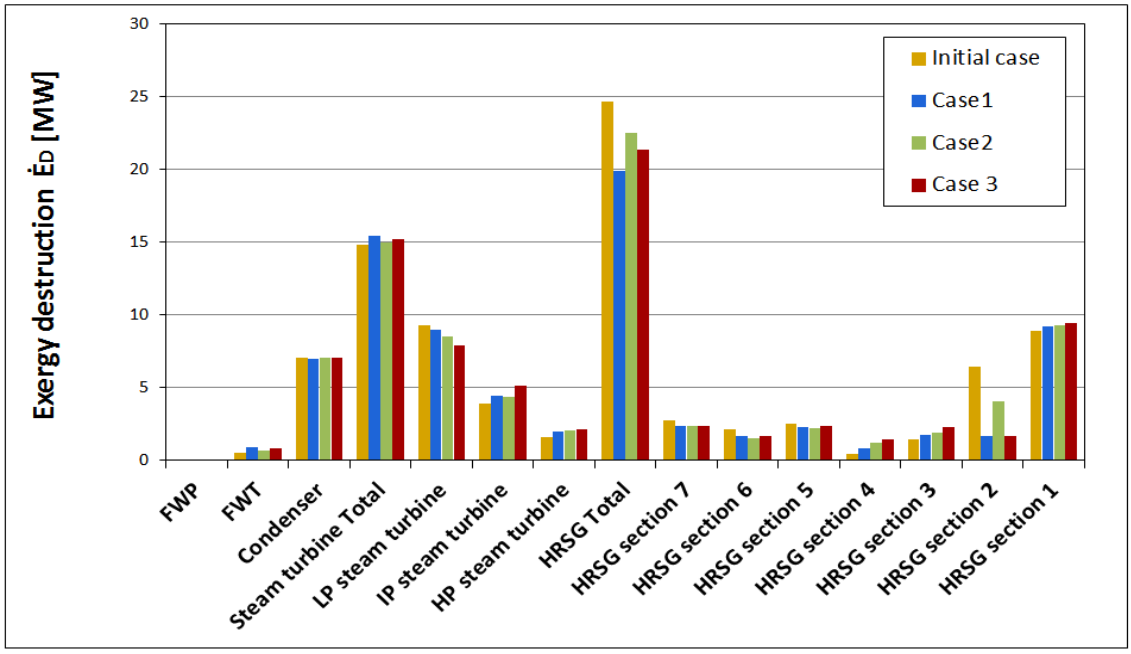

Figure 6-64 Exergy destruction in CCGT components for all cases

The reason for the highest exergy destruction is attributed to the large temperature difference between the working fluid (water or steam) and gases from the gas turbine. The second highest exergy destruction is found to be in the steam turbine, which is 14.8 MW (equivalent to 29.65% of the total exergy destruction and 7.7% of the total exergy input for the initial case).

In HRSG, in the initial case, the highest exergy destruction is found to be in section 1, followed by the exergy destruction in section 2. In the steam turbine, low-pressure steam turbine is the highest exergy destructor. However, the lowest exergy efficiency is associated with the HRSG and its components, as can be seen from Figure 6-65.

The comparison of results between the cases shows that in case 1 there is a bigger reduction in the exergy destruction compared to the case 2 and the case 3 (Figure 6-66). In addition, case 1 observed bigger enhancing in the exergy efficiency of all HRSG sections by different values, while the change in exergy efficiency of the steam turbine and condenser were less than with HRSG. The effects of the reduction of the exergy destruction of the HRSG sections on the global characteristics of the system are shown in Figure 6-66 to Figure 6-69. Figure 6-67 shows the final value of the thermal efficiency of the combined cycle gas turbine η_{CCGT} before optimization and after optimization (cases 1, 2, and 3).

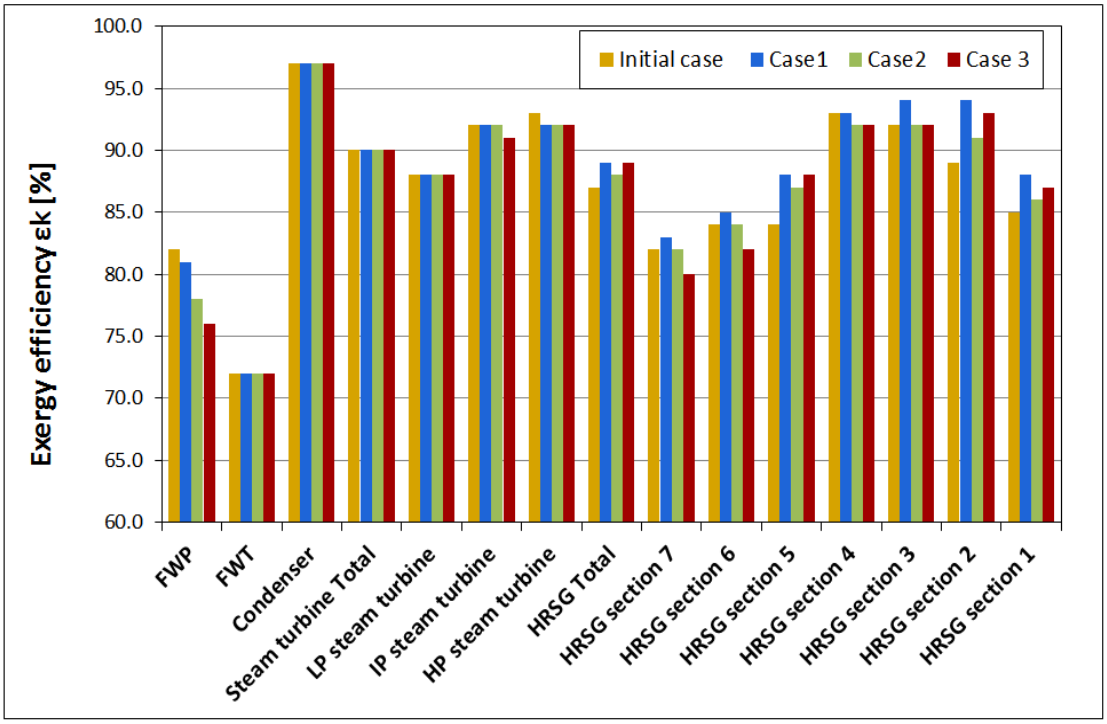

Figure 6-65 Exergy efficiency for CCGT components for all cases

It can be seen that all three optimization procedures enhanced the efficiency with the different values. The same results were achieved with power output (Figure 6-68). Case 1 is observed to be the first best result in this regard. Case 3 is the second best case from the viewpoint of thermodynamic performance.

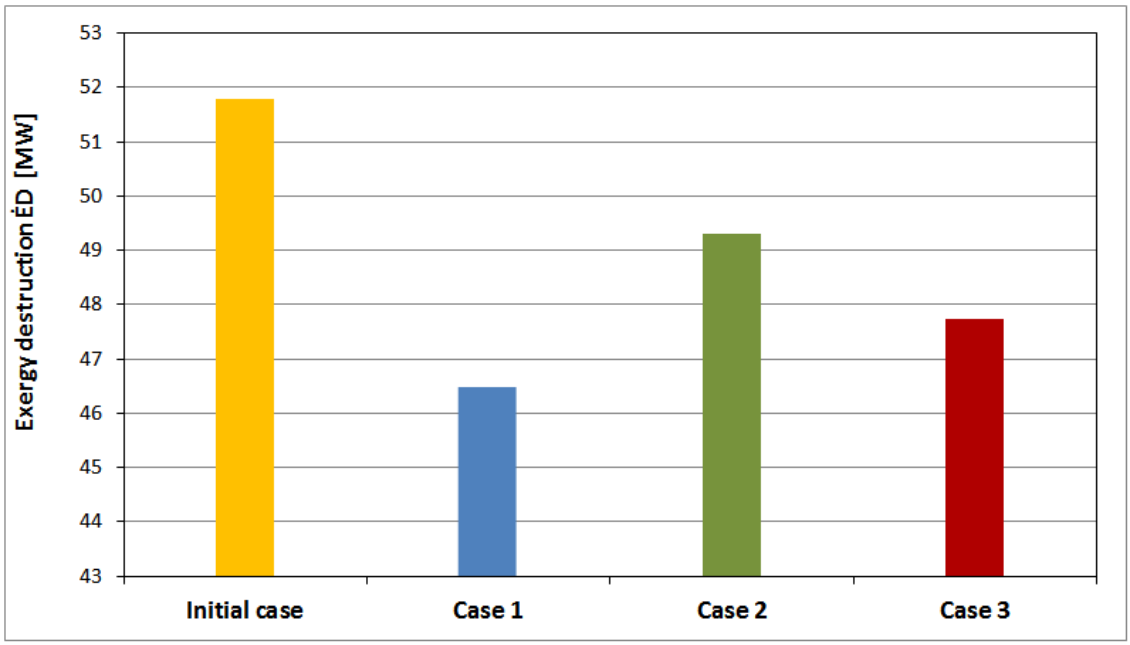

Figure 6-66 Exergy destruction in CCGT for all cases

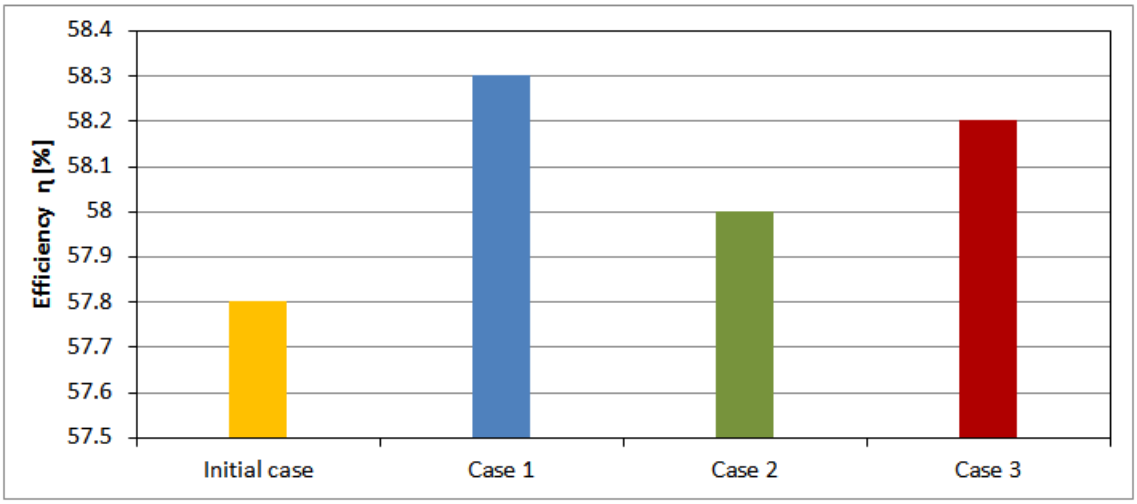

Figure 6-67 Thermal efficiency for CCGT for all cases

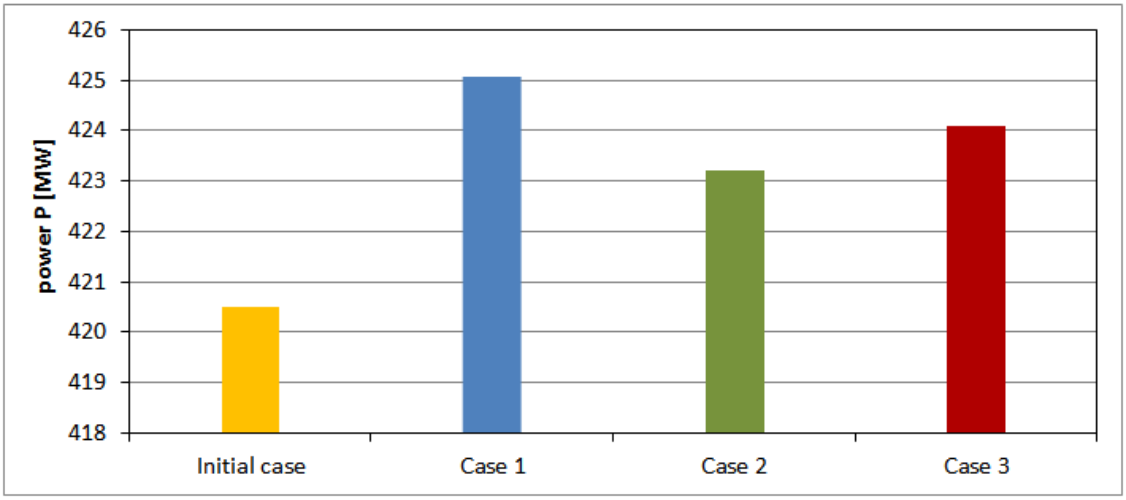

Figure 6-68 Power output for steam turbine all cases

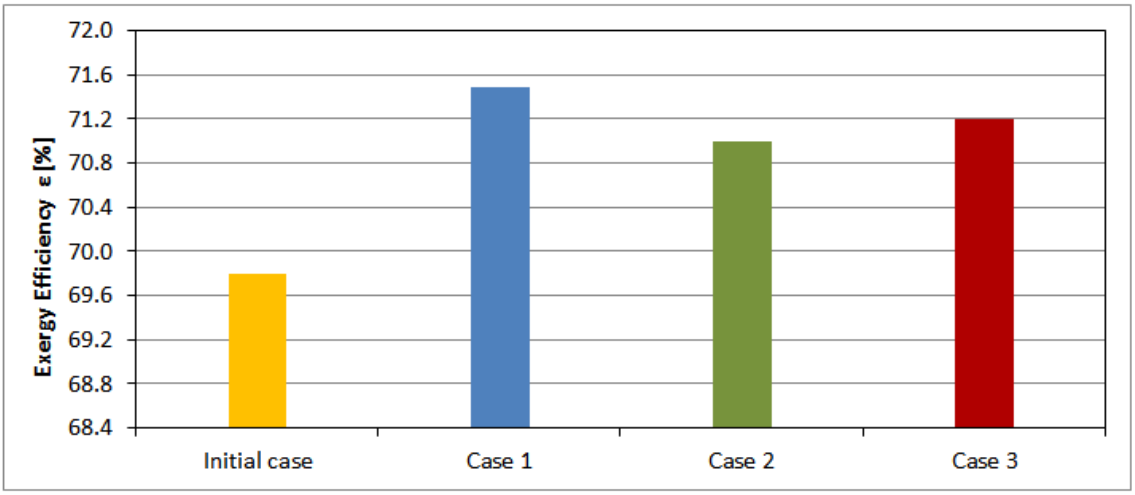

Figure 6-69 Exergy efficiency for all cases

6.5.3.2 Economic Performance

The second important performance for the optimization problem is economic performance. Investment (purchase) cost, production cost, purchase cost rate $\dot{Z}_k$, annual cash flow B and total income were considered as the important economic performance factors of the power plant. The comparison results are presented in Table 6-8, Table 6-9 and Table 6-10.

Figure 6-70 shows that the highest purchase cost rate $\dot{Z}_k$ was associated with the steam turbine. Low-pressure steam turbine had the highest purchase cost rate among the three steam turbines. The second highest purchase cost rate was associated with the HRSG. The effects of the reduction in the exergy destruction of the HRSG sections lead to reduction in the heat transfer surface area of the HRSG heaters by different values, and the effects depend on the optimization method. As it is seen from Figure 6-70 decreasing the exergy destruction (enhancing the thermodynamic performance) causes lowering of the economic performance. The effects of this lowering are the increase of purchase costs, purchase cost rate, and also the decrease in annual cash flow and total income.

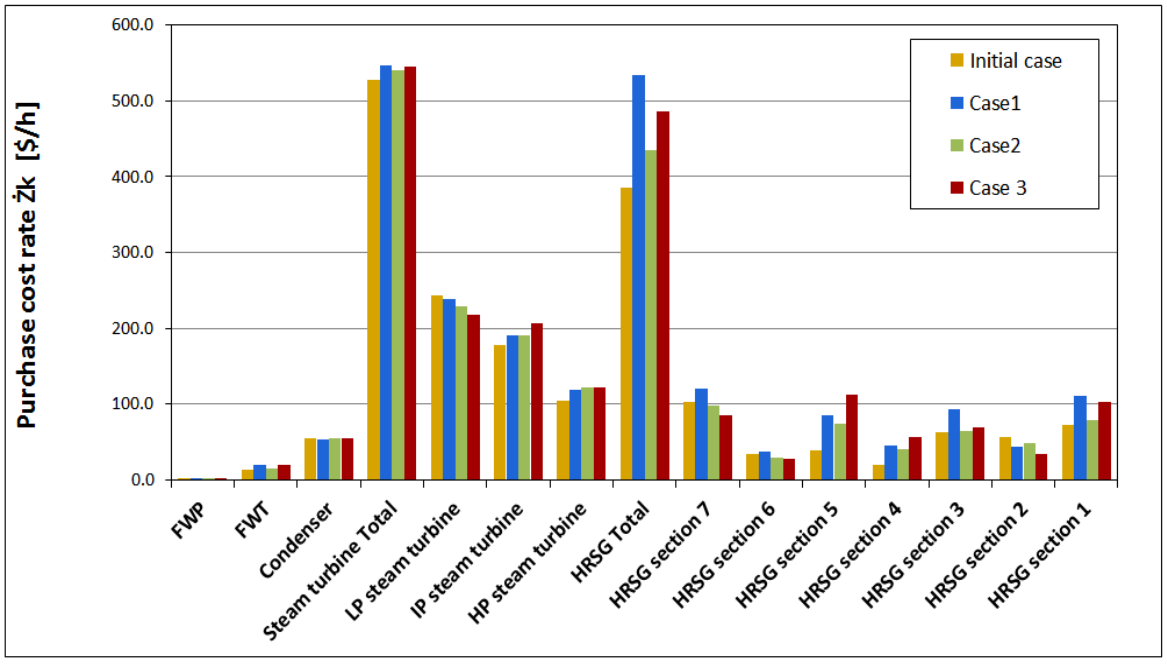

Figure 6-70 Purchase cost rate for CCGT components for all cases

Figure 6-71 shows the effect of optimization method on the purchase costs. After reviewing the results of comparison from the viewpoint of economic performance,

it is shows that Case 2 gives the best economic performance and case 3 gives the second best results.

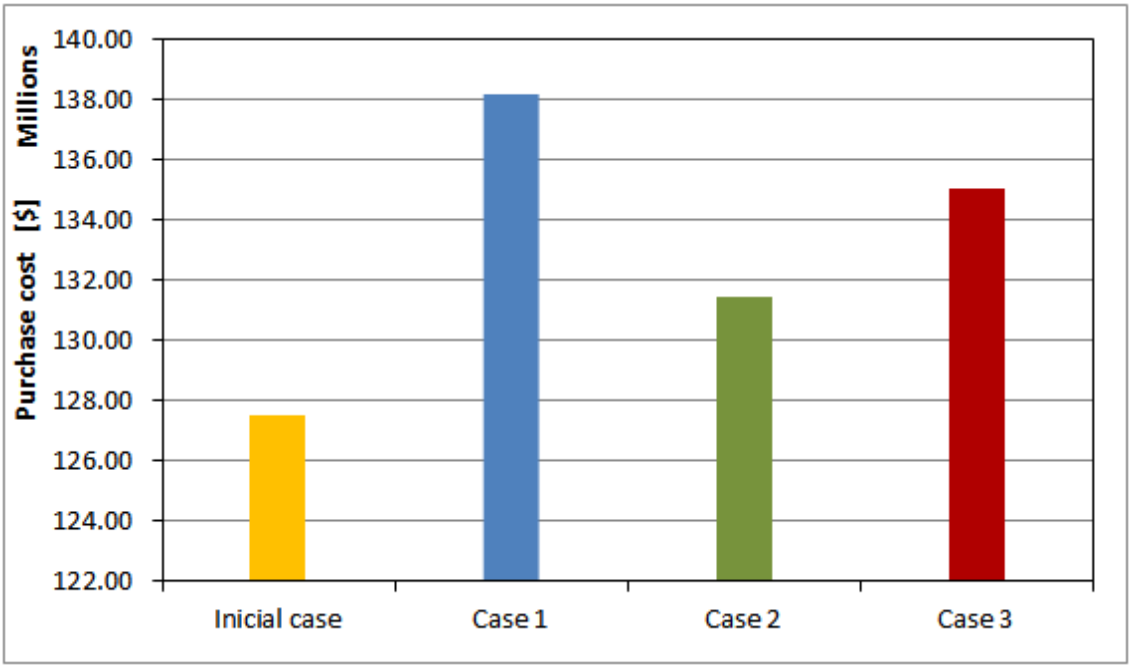

Figure 6-71 Purchase cost for CCGT all cases

6.5.3.3 Exergoeconomic Parameters

In Figure 6-72, the HRSG in the CCGT power plant is observed to be the most important component from an exergoeconomic viewpoint as it has the highest value of the total operating cost rate $\dot{Z}_k + \dot{C}_{D,k}$. The total operating cost rate, which consists of capital investment and exergy destruction cost rate. The higher this total operating cost rate, the higher the influence of the component on the overall system and thus, the more significant the component is considered. As can be seen in Figure 6-72 the largest sum of exergy destruction cost and capital cost are observed in HRSG, followed by the steam turbine and condenser.

Second important exergoeconomic parameter is the exergoeconomic factor f_k. Relative low value of exergoeconomic factor, f_k, for the section 1, 2, 5, 6, and 7, in Figure 6-74 suggests that a decrease in cost rate of exergy destruction of these components by increasing exergetic efficiency can improve the system performance. Figure 6-74 illustrates that the exergoeconomic factor f_k of all components increased after optimizations.

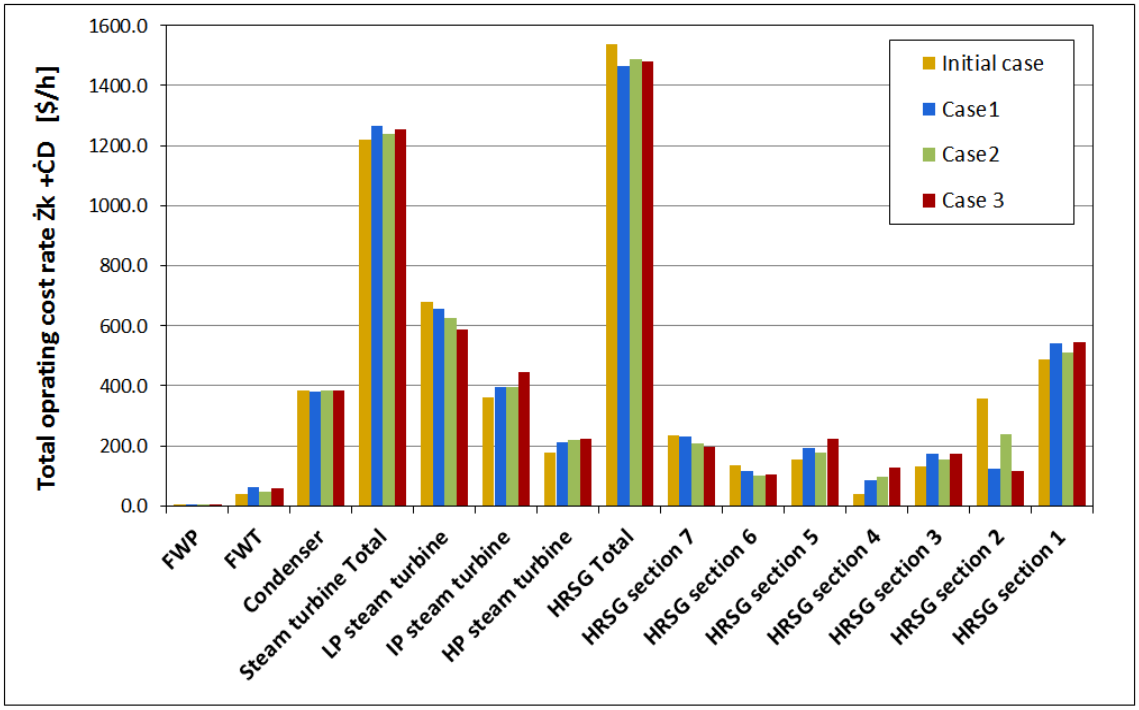

Figure 6-72 Total operating cost rate associated with CCGT components $\dot{Z}_k + \dot{C}_{D,k}$

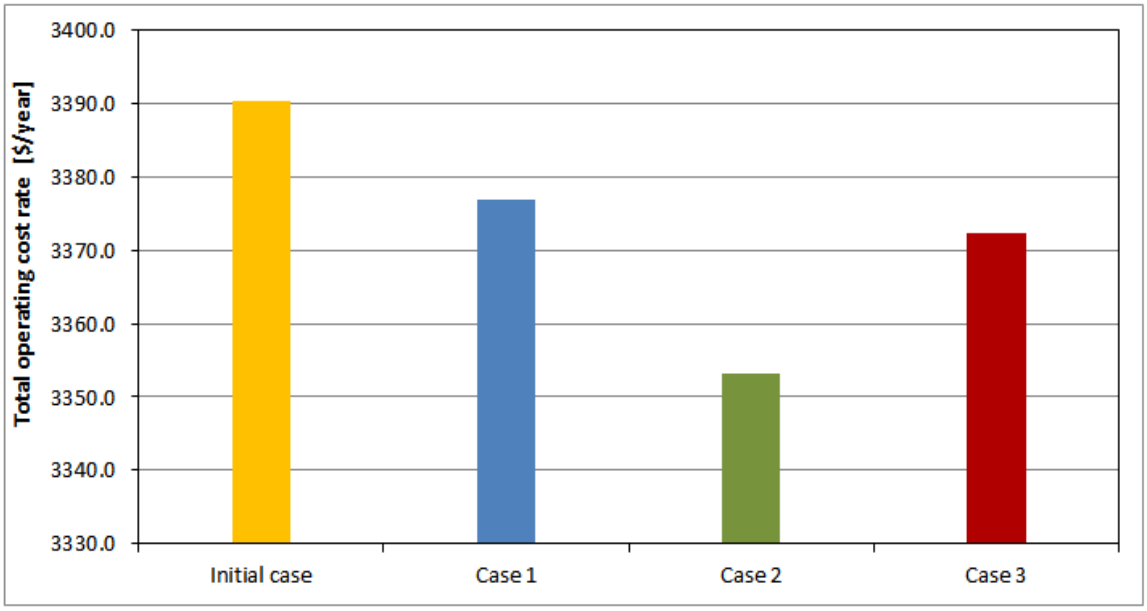

Figure 6-73 Total operating cost rate $\dot{Z} + \dot{C}_D$ associated with CCGT for all cases

The comparison results of the total operating cost rate $\dot{Z} + \dot{C}_D$ and exergoeconomic factor f_k for the whole system are illustrated in Figure 6-72 to Figure 6-75. The result of comparison between three cases shows that after optimization case 3 gave a lower total operating cost rate $\dot{Z} + \dot{C}_D$, which means that this method

caused a decrease in cost rate of exergy destruction. Case 3 also gave the highest exergy economic factor f_k .

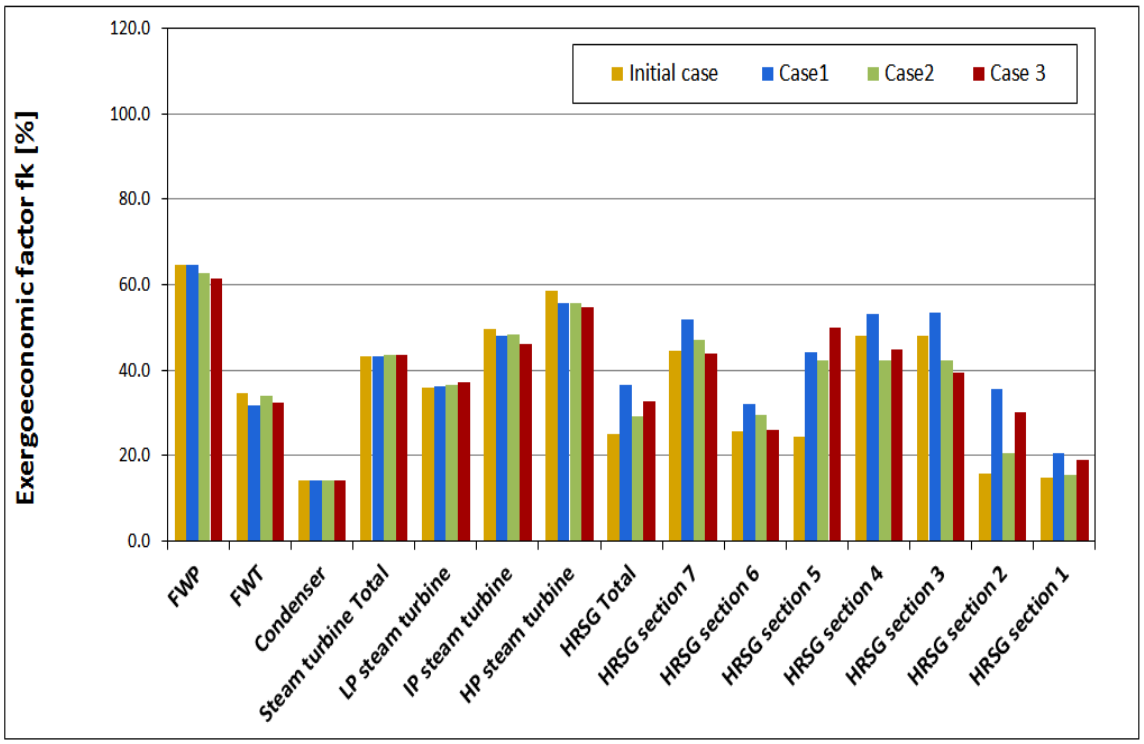

Figure 6-74 Exergoeconomic factor f_k for CCGT component for all cases

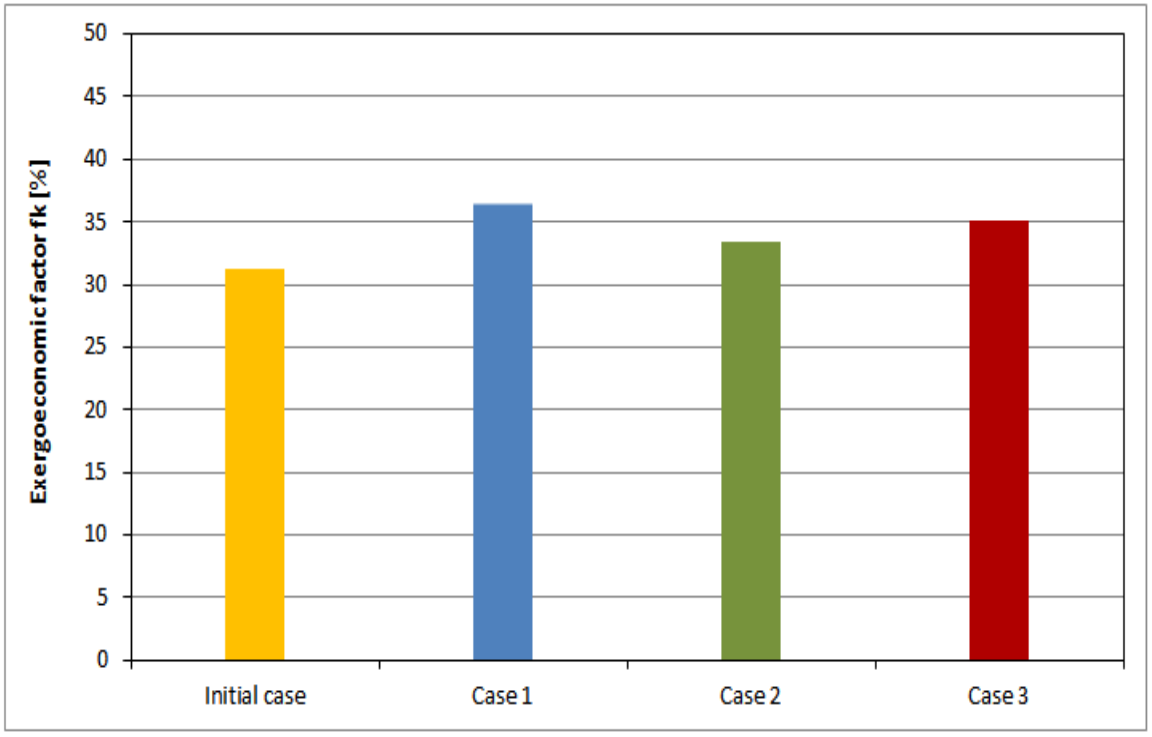

Figure 6-75 Exergoeconomic factor for the CCGT for all cases

The comparative result of the optimization cases presented in Table 6-8 denotes that each of the optimization approaches improves some of the total performance by different values.

Table 6-8 Comparison results between optimum cases and initial case

Parameter		Initial case	Case 1	Case 2	Case 3
Pinch point [° C]	PP_{LP}	13	10	13	15.5
	PP_{IP}	13	6	8.5	5
	PP_{HP}	13	11	14	17
Pressure in pressure drum [bar]	p_{LP}	5	4.7	3.6	3
	p_{IP}	36	41.2	30	34.4
	p_{HP}	104	180	131	180
CCGT efficiency [%]		57. 7	58.3	58.0	58.2
CCGT gross power [MW]		420.5	425.1	423.2	424.1
Exergy efficiency ε [%]		69.8	71.5	71.0	71.2
Exergy destruction cost [$/h]		2335	2146	2233	2196
Production cost f_1 [c$/kWh]		9.429	9.370	9.385	9.379
Total annual investment cost bottoming cycle f_2 [$/year]		25,922,894	25,685,324	25,436,240	25,680,441
Specific total cost of the products f_3 [c$/kJ]		2.588	1.56	1.450	1.019
Total annual income [$/year]		359,534,172	363,487,806	361,849,467	362,618,209
CCGT annual investment cost [$/year]		297,386,056	298,753,106	297,889,615	298,353,899
The annual cash flow [$/year]		62,148,117	64,734,700	63,959,852	64,264,309
Total purchase cost for CCGT [$]		127,523,036	138,103,463	131,420,384	135,013,763

One more comparison was made between two optimization cases Table 6-9; the first case with PP assumed to be the same for all evaporators, and another (second case) having different PPs for every pressure level. Comparing the plotted curves of these two cases (pinch point variable $PP_{LP}, PP_{IP}, PP_{HP}$ and pinch point constant PP), it can be observed that the change of obtained gradient of objective functions in the second case (constant pinch point) for all cases (case 1, case 2, case 3) is significantly greater than in the first case. This provides a wider range for the increment of one of PP pressure levels while maintaining the other two within the optimum values, which results in relatively lower amount of objective functions increase compared to the second procedure. This can be applied especially with the high-pressure level PP_{HP}, because the investment cost of the heater for the high-pressure level is 4.0 times greater than for the intermediate pressure level and 2.4 times greater than for the low-pressure level.

Table 6-9 Comparison between two cases, (one with pinch points same for all evaporators and another having different pinch points)

Parameter		Case 1		Case 2		Case 3	
		PP constant	PP different	PP constant	PP different	PP constant	PP different
Pinch point [° C]	PP_{LP}	9.5	10	12	13	15.4	15.5
	PP_{IP}		6		8.5		5
	PP_{HP}		11		14		17
Pressure in pressure drum [bar]	p_{LP}	4.8	4.7	3.8	3.6	3	3
	p_{IP}	39.1	41.2	29	30	31	34.4
	p_{HP}	180	180	131	131	180	180
CCGT efficiency [%]		58.30	58.31	58.042	58.054	58.059	58.2
CCGT gross power output [MW]		425.10	425.13	423.21	423.261	423.315	424.13
Exergy efficiency ε [%]		71.53	71.55	71.0	71.06	70.75	71.2
Production cost f_1 [c$/kWh]		9.371	9.368	9.384	9.380	9.384	9.37

Table 6-10 shows the comparison between exergoeconomic optimization using simple method case 3 and exergoeconomic optimization using MIDACO software. The result of comparison shows very good agreement between the both applied methods. However, there were very small differences, which can be neglected.

Table 6-10 Comparison between simple procedure optimization and MIDACO optimization

Parameter		Case 3	
		Simple optimization method	MIDACO optimization method
Pinch point [° C]	PP_{LP}	15.5	15.5
	PP_{IP}	5	5
	PP_{HP}	17	17.034
Pressure in pressure drum [bar]	p_{LP}	3	3.1
	p_{IP}	34.4	34.47
	p_{HP}	180	180

7 Conclusion

In this thesis, a triple pressure combined cycle gas turbine is studied thermoeconomically, based on energy, exergy, economic, and exergoeconomic analysis, with the aim to improve the cost effectiveness of the system. For this objective, an exergoeconomic optimization method was developed (case 3: the specific total cost of the products as the objective function $c_{P,TOT}$). In addition, two more optimization methods were performed (case 1: production cost of electricity as the objective function C_{kWh} and case 2: the objective function is the total cost rate Ct_{BOT}). In order to check whether the optimization algorithm works well, the exergoeconomic optimization method has been done using MIDACO software.

The developed method in this work, demonstrates the application of exergoeconomic concept to optimize combined cycle gas turbine with complex configuration. An exergoeconomic analysis by mean of specific exergy costing analysis was performed. The objective is to calculate the cost flow rates, the unit exergetic costs associated with each stream of the bottoming cycle, to evaluate and locate the exergy destruction and exergy losses in the system, and also to point out the component that needs more improvement. Based on that purpose, the cost balance and auxiliary equations were formulated for each component of the system. By solving these equations through a computer program in FORTRAN, the average costs per unit exergy at different state points were determined. The values of exergoeconomic variables for the main components of the plant were also calculated. Nevertheless, the effects of the operating parameters on the thermodynamic, economic, and thermoeconomic performances were studied in detail.

The exergy analysis indicates that the HRSG has the highest influenced component on the overall system, and thus, this more significant component is taken into consideration. Therefore, this thesis focuses on the HRSG parameters in optimization and suggests that a decrease in exergy destruction (increases exergetic efficiency) of HRSG components can improve the system performance. The lower exergoeconomic factor f_k of the HRSG in the exergoeconomic analysis, indicate that the associated cost of exergy destruction in section 1, section 2, section 5, and section 6 of HRSG are insignificant in the cost formation, while the capital cost of the

components in the others (section 3, section4, section 7, *HP* steam turbine, and *IP* steam turbine) are significant. The exergoeconomic analysis suggests that a decrease in cost rate of exergy destruction of the components with low exergoeconomic factor by increasing exergetic efficiency, and can therefore improve the system performance.

The following conclusions are derived from the study pertaining to the possible overall improvement in the CCGT power plant performance (thermodynamic and economic):

1. All three optimization procedures improved the system performance with different values:
    a) Case1is the best option from a thermodynamic point of view; the efficiency was increased by 0.86%, and the power output increased by 1.1%. However, it has the highest purchase cost. The purchase cost was increased by10,580,427 $.Annual cash flow increased by 2,586,583 $/year, production cost of electricity decreased by 0.62%
    b) Case 2 is the best option from the purchase cost point of view. Purchase cost increased only by3,897,348$. In addition, this case is the worst case from the thermodynamic point of view, since the thermodynamic performance was improved: efficiency was increased by 0.35%, and power output was increased by 0.64%. Annual cash flow increased by1,811,735$/year, production cost of electricity decreased by 0.47%
    c) Case 3 is a compromise between these two cases, since the result shows that this case gives good improvements in the thermodynamic performance, as well as a good performance on the economic side; Efficiency was increased by 0.7% and power output by 0.86%. Annual cash flow was increased by 2,116,192 $/year, production cost of electricity decreased by 0.53%, while purchase cost increased by 7,490,727$
2. From the comparison between the simple exergoeconomic procedure and optimization using MIDACO software, it can be seen that the two results were identical.

Finally, it can be concluded that the best option of the optimization gives compromise between the contradictory disciplines of the system is the exergoeconomic optimization case 3.

Reference

[1] Kaviri A. G., Jaafar M. N., Lazim T. M., Barzegaravval, H., Exergoenvironmental optimization of Heat Recovery Steam Generators in combined cycle power plant through energy and exergy analysis. *Energy Conversion and Management*, 6(2013),pp.27–33.

[2] Ahmadi P., Dincer I., Exergoenvironmental Analysis and Optimization of a Cogeneration Plant System using Multimodal Genetic Algorithm (MGA). *Energy*, 35(2010), pp. 5161-72.

[3] Boyano A., Blanco-Marigorta A. M., Morosuk T., Tsatsaronis G., Exergoenvironmental Analysis of a Steam Methane Reforming Process for Hydrogen Production. *Energy*, 36(2011), pp. 2202-2214.

[4] Petrakopoulou F., Boyano A., Cabrera M., Tsatsaronis G., Exergoeconomic and Exergoenvironmental Analyses of a Combined Cycle Power Plant with Chemical Looping Technology. *International Journal of Greenhouse Gas Control*, 5(2011),pp. 475-482.

[5] Ibrahim K. T., Rahman M. M., Abdalla N. A., Optimum Gas Turbine Configuration for Improving the Performance of Combined Cycle Power Plant. *Procedia Engineering*,15(2011), pp.4216-4223.

[6] Ameri M., Hejazi H. S., The Study of Capacity Enhancement of the Chabahar Gas Turbine Installation using an Absorption Chiller. *Applied Thermal Engineering*, 24(2004), pp.59–68.

[7] Boonnasa S., Namprakai P., Muangnapoh T., Performance Improvement of the Combined Cycle Power Plant by Intake Air Cooling using an Absorption Chiller,*Energy*,31(2006), pp. 2036–2046.

[8] Hosseini R., BeshkanI. A., Soltani M., Performance Improvement of Gas Turbines of Fars (Iran) Combined Cycle Power Plant by Intake Air Cooling using a Media Evaporative Cooler. *Energy Conversion and Management*, 48(2007), pp. 1055–1064.

[9] Ibrahim T. K., Rahman M. M., Effect of Compression Ratio on Performance of Combined Cycle Gas Turbine. *International Journal of Energy Engineering*,2(2012)1, pp. 9-14.

[10] Khaliq A., Kaushik S., Thermodynamic Performance Evaluation of Combustion Gas Turbine Cogeneration System with Reheat. *Applied Thermal Engineering*, 24(2004), pp. 1785–1795.

[11] Sanjay, Investigation of Effect of Variation of Cycle Parameters on Thermodynamic Performance of Gas-Steam Combined Cycle. *Energy*, 36(2011), pp. 157-167.

[12] Khaliq A., Exergy Analysis of Gas Turbine Trigeneration System for Combined Production of Power Heat and Refrigeration. *International Journal of Refrigeration*, 32(2009), pp. 534-545.

[13] Kaviri A. G., Jaafar M. N., Lazim, T. M., Modeling and Multi-Objective Exergy Based Optimization of a Combined Cycle Power Plant using a Genetic Algorithm. *Energy Convers Manage*, 58(2012), pp. 94-103.

[14] Mohagheghi M., Shayegan J., Thermodynamic Optimization of Design Variables and Heat Exchangers Layout in HRSGs for CCGT, using Genetic Algorithm. *Applied Thermal Engineering*, 29(2009), pp. 290–299.

[15] Bracco S., Silvia S., Exergetic Optimization of Single Level Combined Gas Steam Power Plants Considering Different Objective Functions. *Energy*, 35(2010), pp. 5365-5373.

[16] Woudstra N., Woudstra T., Pirone A., Van der Stelt T., Thermodynamic Evaluation of Combined Cycle Plants. *Energy Conversion and Management*, 51(2010)5, pp. 1099–1110.

[17] Mansouri M. T., Ahmadi P., Kaviri A. G., Exergetic and Economic Evaluation of the Effect of HRSG Configurations on the Performance of Combined Cycle Power Plants. *Energy Conversion and Management*, 58(2012), pp. 47–58.

[18] Kamate S., Gangavati P., Exergy Analysis of Cogeneration Power Plants in Sugar Industries. *Applied Thermal Engineering*, 29(2009), pp. 1187–1194.

[19] Kehlihofer R.,Combined Cycle Gas Turbine Power PLants. Tulsa: Penn Well Publishing Company (1997).

[20] Alus M., Petrović M. V., Optimization of the Triple Pressure Combined Cycle Power Plant. *Thermal Science*, 16(2012)3, pp. 901-914.

[21] Casarosa C., Donatini F., Franco A., Thermoeconomic Optimization of Heat Recovery Steam Generators Operating Parameters for Combined Plants. *Energy*, 29(2004), pp. 389–414.

[22] Ahmadi P., Dincer I., Thermodynamic Analysis and Thermoeconomic Optimization of a Dual Pressure Combined Cycle Power Plant with a Supplementary Firing Unit. *Energy Conversion and Management*, 52(2011), pp. 2296–2308.

[23] Behbahani-nia A., Sayadi S., Soleymani M., Thermoeconomic Optimization of the Pinch Point and Gas-Side Velocity in Heat Recovery Steam Generators. *Journal of Power and Energy*, (2010), pp.761-771.

[24] Ghazi M., Ahmadi P., Sotoodeh A., Taherkhani A., Modeling and Thermo-Economic Optimization of Heat Recovery Heat Exchangers using a Multimodal Genetic Algorithm. *Energy Conversion and Management*, 58(2012), pp. 149–156.

[25] Hajabdollahi H., Ahmadi P., Ibrahim D., An Exergy-Based Multi-Objective Optimization of a Heat Recovery Steam Generator (HRSG) in a Combined Cycle Power Plant (CCPP) using Evolutionary Algorithm. *International Journal of Green Energy*, 8(2011), pp. 44–64.

[26] Naemi S., Saffar-Avval M., Kalhori S. B., Mansoori Z., Optimum Design of Dual Pressure Heat Recovery Steam Generator using Non-Dimensional Parameters Based on Thermodynamic and Thermoeconomic Approaches. *Applied Thermal Engineering*,(2013), pp. 371-384.

[27] Najjar, Y. S., Efficient use of Energy by Utilizing Gas Turbine Combined Systems. *Applied Thermal Engineering*, 21(2001),pp . 407-438.

[28] Tyagi K. P., Khan M. N., Effect of Gas Turbine Exhaust Temperature, Stack Temperature and Ambient Temperature on Overall Efficiency of Combine Cycle Power Plant. *International Journal of Engineering and Technology*, 2(2010)6, pp. 427-429.

[29] Valdés M., Durán D. M., Antonio R., Thermoeconomic Optimization of Combined Cycle Gas Turbine Power Plants using Genetic Algorithms. *Applied Thermal Engineering*, 23(2003)17, pp. 2169-2182.

[30] Franco A., Casarosa C., Thermoeconomic Evaluation of the Feasibility of Highly Efficient Combined Cycle Power Plants. *Energy*, 29 (2004), pp. 1963–1982.

[31] Valdés M., Rapun J. L., Optimization of Heat Recovery Steam Generators for Combined Cycle Gas Turbine Power Plants. *Applied Thermal Engineering*, 11(2001)21, pp. 1149–1159.

[32] Bassily A., Modeling and Numerical Optomization, and Irreversibility Reduction of a Dual Pressure Reheat Combined Cycle. *Applied Energy*, 81(2005), pp. 127-151.

[33] Bassily A., Modeling Numerical Optimization, and Irreversibility Reduction of a Triple Pressure Reheat Combined Cycle. *Energy*, 32 (2007), pp. 778-794.

[34] Lozano M. A., Valero A., Theory of the Exergetic Cost. *Energy*, 18(1993)9, pp. 939–960.

[35] Lazzaretto A., Tsatsaronis G., SPECO: A Systematic and General Methodology for Calculating Efficiencies and Costs in Thermal Systems. *Energy*, 31(2006)12, pp. 1257–1289.

[36] Kwak H., Kim D., Jeon J., Exergetic and Thermoeconomic Analyses of Power Plants. *Energy*, 28(2003), pp. 343-360.

[37] Fiasch D., ManfridaG., Exergy Analysis of Semi-Closed Gas Turbine Combined Cycle (SCG/CC). *Energy Convers,* 39(1998)16, pp. 1643-1652.

[38] Cihan A., Oktay H., Kamil K., Energy–Exergy Analysis and Modernization Suggestions for a Combined-Cycle Power Plant. *International Journal of Energy Research,* 30(2006), pp. 115–126.

[39] Mousafarash A., Ameri M., Exergy and Exergo-Economic Based Analysis of a Gas Turbine Power. *Journal of Power Technologies,* 93(2013)1, pp. 44-51.

[40] Butcher C., Reddy B., Second Law Analysis of a Waste Heat Recovery Based Power Generation System. *International Journal of Heat and Mass Transfe,* 50(2007), pp. 2355–2363.

[41] Aljundi I. H., Energy and Exergy Analysis of a Steam Power Plant in Jordan. *Applied Thermal Engineering,* 29(2009), pp. 324–328.

[42] Abusoglu A., Kanoglu M., First and Second Law Analysis of Diesel Engine Powered Cogeneration Systems. *Energy Conversion and Management,* 49(2008), pp. 2026–2031.

[43] Kanoglu M., Ayanoglu A., Abusoglu A., Exergoeconomic Assessment of Ageothermal Assisted High Temperature Steam Electrolysis System. *Energy,* 36(2011), pp. 4422-4433.

[44] Orhan F. M., Dincer I., Exergoeconomic Analysis of a Thermochemical Copper–Chlorine Cycle for Hydrogen Production using Specific Exergy Cost (SPECO) Method. *Thermochimica Acta,* 497(2010), pp. 60-66.

[45] Chase D. L.,Combined-Cycle Development Evolution and Future. Schenectady, NY: GE Power SystemsGER-4206,(2006)

[46] Kim S.M., Oh S. D., Kwon Y. H., Kwak H.Y.,Exergoeconomic Analysis of Thermal Systems,*Energy*,23(1998), pp.393-406

[47] Kwon Y. H., Kwak H. Y., Oh S. D., Exergoeconomic Analysis of Gas Turbine Cogeneration Systems. *ExergyInt J.,* 1(2001), pp. 31–40.

[48] Shin H., Kim D. h., Ahn H., Choi S., Gichul, M., Thermal Stress Analysis in Structural Elements of HRSG,*International Journal of Energy Engineer,* 5(2012)2, pp. 202-209.

[49] El-Sayed Y. M., Gaggioli R. A., A Critical Review of Second Law Costing Methods— I: Background and Algebraic, *ASME J Energy Resour Technol*,111(1989), pp. 1-7

[50] Gaggioli R. A., El-Sayed Y. M., A Critical Review of Second Law Costing Methods—II: Calculus Procedures. *ASME J Energy Resour Technol*, 111(1989), pp. 8–15.

[51] Tsatsaronis G., Exergoeconomics: Is it only a New Name?,*Chem Eng Technol*,19(1996), pp. 163–169.

[52] Kowalski C.,Advanced Power Generation Technology,Advanced Technology in Electrical Power Generation. Wrocław, www.printpap.pl.(2011).

[53] Frangopoulos C. A., Application of the Thermoeconomic Functional Approach to the CGAM Problem,*Energy*, 19(1993), pp. 323-342

[54] Jonshagen K., Modern thermal power plants. Sweden: Doctoral thesis, Lund University,(2011).

[55] Horlock J., Advanced Gas Turbine Cycles, Cambridge: Elsevier Science Ltd.(2003).

[56] Dincer I., Rosen M. A.,Exergy: Energy, Environment and Sustainable Development(2nd ed.). Elsevier,(2013).

[57] Baehr H. D., Bosnjakovic F., Grassmann P., Van Lier J., Rant Z., Rogener K. R., Schmidt K. R., Energie und Exergie. Die Anwendung des Exergiebegriffs in der Energietechnik. *VDI-Verlag*, (1965), pp. 5-20.

[58] Gundersen G., The Concept of Exergy and Energy Quality,*Energy and Process Engineering*,(2011), pp. 1-26.

[59] Kotas T.,The Exergy Method of Thermal Plant Analysis. London: Exergon Publishing Company.(2012).

[60] Szargut J., Morris D. R., Steward F. R., Exergy Analysis of Thermal, Chemical, and Metallurgical Processes. *Springer-Verlag*.(1988).

[61] Moran M. J., Shapiro H. N., Fundamentals of Engineering Thermodaynamics (5th ed.). London: John Wiley & Sons Ltd., (2006).

[62] Tsatsaronis G., Thermoeconomic Analysis and Optimization of Energy Systems. *Prog. Energy Combust. Sci, 19*(1993), pp. 227 -257.

[63] Gong M., Goran W., On Exergetics, Economics and Optimization of Technical Processes to meet Environmental Conditions,. *International Conference on Thermodynamic Analysis and Improvement of Energy Systems*,Beijing: Ruixian Cai, (1997), pp. 453-460

[64] Tsatsaronis G., Definitions and Nomenclature in Exergy Analysis and Exergoeconomics. *Energy*, 32(2007), pp. 249–253.

[65] Baghernejad A., Yaghoubi M., Exergoeconomic Analysis and Optimization of an Integrated Solar Combined Cycle System (ISCCS) using genetic algorithm. *Energy Conversion and Management, 52*(2011), pp. 2193–2203.

[66] Sayyaadi H., Sabzaligol T., Exergoeconomic Optimization of a 1000 MW Light Water Reactor Power. *International Journal of Energy Research,* 33(2009), pp. 378-395.

[67] Bejan A., Tsatsaronis G., Moran M.,*Thermal Design and Optimization.* New York: Wiley,(1996).

[68] Siemens,Siemens Gas Turbine SGT5-PAC 4000F, Advance performance. Erlangen, Germany: Simenes AG energy sector.(2009).

[69] Wagner W., Kruse A.,Properties of Water and Steam, *IAPWS-IF97*. Berlin: Springer,(1998).

[70] Baehr H. D., Diederichsen C., Equations for Calculation of Enthalpy and Entropy of the Components of Air and Combustion Gases. *BWK,* 40(1988), pp. 30-33.

[71] Silveira J., Tuna C., Thermoeconomic Analysis Method for Optimization of Combined Heat and Power Systems. Part I. *Progress in Energy and Combustion Science,* 29(2003), pp. 479–485.

[72] Roosen P., Uhlenbruck S., Klaus L., Pareto Optimization of a Combined Cycle Power System as a Decision Support Tool for Trading off Investment vs. Operating Costs. *International Journal of Thermal Sciences*, 42(2003), pp. 553–560.

[73] Attala L., Facchini G. B., Ferrara G., Thermoeconomic Optimization Method as Design Tool in Gas Steam Combined Plant Realization. *Energy Vonversion and management, 42*(2001), pp. 2163-2172.

[74] Mohammed M. S., Petrovic M. V., Thermoeconomic Optimization of Triple Pressure HRSG Operating Parameters for Combined Cycle Power Plants. *Thermal science*.17(2015)2, pp 447-460.

[75] Vieira L. S., Donatelli J. L., Cruz M. E., Exergoeconomic Improvement of a Complex Cogeneration System Integrated with a Professional Process Simulator. *Energy Convers Manage,* 50(2009), pp. 1955-1967.

[76] Xiang W., Chen Y., Performance Improvement of Combined CyclePower Plant Based on theOptimization of the Bottom Cycle and Heat, Recuperation, *Thermal science,16(2007),* pp. 84-89

[77] Raja A., Srivastava A., Dwivedi M.,Power Plant Engineering,New Age International Limitd. New Delhi (2006).

[78] Bolland O., Thermal power generation,. Trondheim: Department of Energy and Process Engineering – NTNU,(2010).

[79] Martin S., Hihgly efficient plant. Retrieved February 08, 2014, from SIEMENS; http://www.siemens.com/innovation/apps/pof_microsite/_pof-spring-2013/_html_en/combined-cycle-power-plants.html,(2013).

[80] Blood D., Simpson S., Harries R., Dillon D., Weekes A., Heat Recovery Steam Generators for Power Generation and other Industrial Applications. Powergen UK plc, Mitsui Babcock Energy Ltd, ME Engineering Ltd. Crown Copyright (2003).

[81] Rosen A. M., Dincer I., Exergy as the Confluence of Energy, Environment and Sustainable Development., Exergy an International Journal, 1(2001), pp. 1-13.

[82] Aerospace students. Gas turbine. Retrieved 01 15, 2014, from Aerospace students: http://www.aerostudents.com/info/aboutThisWebsite.php, (2014).

[83] Li W., Priddy P., Power Plant System Design, John Wiley & Sons, Canada 1985.

[84] Weston C. K., Energy Conversion, Book on the web; http://www.personal.utulsa.edu/~kenneth-weston/(2000).

[85] Abusoglu A., Kanoglu M., Exergoeconomic analysis and optimization of combined heat and power. *Renewable and Sustainable Energy Reviews*, 13(2009), pp. 2295–2308.

[86] Tsatsaronis G,, Park M. H., On Avoidable and Unavoidable Exergy Destructions and Investment Costs in Thermal Systems. *Energy Conversion and Management*. 43 (2002), pp. 1259–1270.

[87] Petrović M., V., Steam Turbine: Calculation and Design, Belegrade, University of Belgrade – Faculity of Mechanical Engineering,(2009)

[88] Shukuya M., Hammache A., Introduction to the Concept of Exergy - for a Better Understanding of Low-Temperature-Heating and High-Temperature-Cooling Systems.web site http://virtual.vtt.fi/virtual/proj6/annex37/ presentation_of_ annex_37/introduction_to_exergy.pdf, (2014)

[89] Ghannadzadeh A., Exergetic Balances and Analysis in a Process Simulator: A Way to Enhance Process Energy Integration. Doctoral thesis, Institut National Polytechnique de Toulouse, (2012)

[90] Schlueter M., Rueckmann J., Gerdts M., A Numerical Study of MIDACO on 100 MINLP Benchmarks, Optimization: *A Journal of Mathematical Programming and Operations Research*, 61(2012)7, pp. 873-900.

[91] Schlueter M., Erb O., Gerdts M.,Rueckmann J., MIDACO on MINLP Space Applications, *Optimization*, 51(2013), pp. 1116-1131

[92] Schlueter M.,Gerdts M., The Oracle Penalty Method,*Global Optimization*, 47 (2010), pp. 293-325.

APPENDIX A: Thermodynamic properties for CCGT sections

Table A-1 Mass flow rates, pressures, temperatures, exergy rates of the CCGT initial case

State	Substance	$\dot{m}$ [kg/s]	P[bar]	T[°C]	$\dot{E}$ [kW]
1	Water	105.5	0.055	34.5	141.2
2	Water	105.5	7.628	34.6	251.1
3	Water	132.7	7.628	60.0	1442.6
4	Water	132.7	5.721	157.0	12788.5
5	Water	88.7	5.721	157.0	10977.3
6	Water	16.8	5.721	157.0	1811.3
7	Water	16.8	5.721	157.0	11936.4
8	Water	16.8	5.263	235.0	12626.3
9	Water	16.8	5	234.5	12528.1
10	Water	7.4	56.628	157.9	1897.1
11	Water	7.4	42.471	253.9	4550.4
12	Water	7.4	42.471	253.9	15154.4
13	Water	7.4	39.073	325.0	16466.8
14	Water	88.7	39.073	386.4	104669.2
16	Water	88.7	34.2	534.2	127701.2
17	Water	88.7	5	276.6	80695.0
15	Water	88.7	36	535.0	128297.3
18	Water	81.2	147.649	159.4	11371.7
19	Water	81.2	129.193	239.8	24017.1
20	Water	81.2	113.044	320.1	47381.7
21	Water	81.2	113.044	320.1	72639.7
22	Water	81.2	104	535.0	113482.3
23	Water	81.2	98.8	532.8	113027.8
24	Water	81.2	39.073	392.2	88215.5
25	Water	105.5	5	269.8	93181.0
26	Water	105.5	0.055	34.6	10646.5
4g	Combustion Products	688.0	1.064	585.0	189029.4
5g	Combustion Products	688.0	1.036	466.2	116958.4
6g	Combustion Products	688.0	1.034	333.1	90990.8
7g	Combustion Products	688.0	1.03	284.1	63961.1
8g	Combustion Products	688.0	1.028	266.9	53942.6
9g	Combustion Products	688.0	1.024	218.7	34769.7
10g	Combustion Products	688.0	1.022	170.0	24831.5
11g	Combustion Products	688.0	1.02	93.6	6258.4

APPENDIX B: T-S diagram for triple pressure HRSG, optimize case 3 and case 2

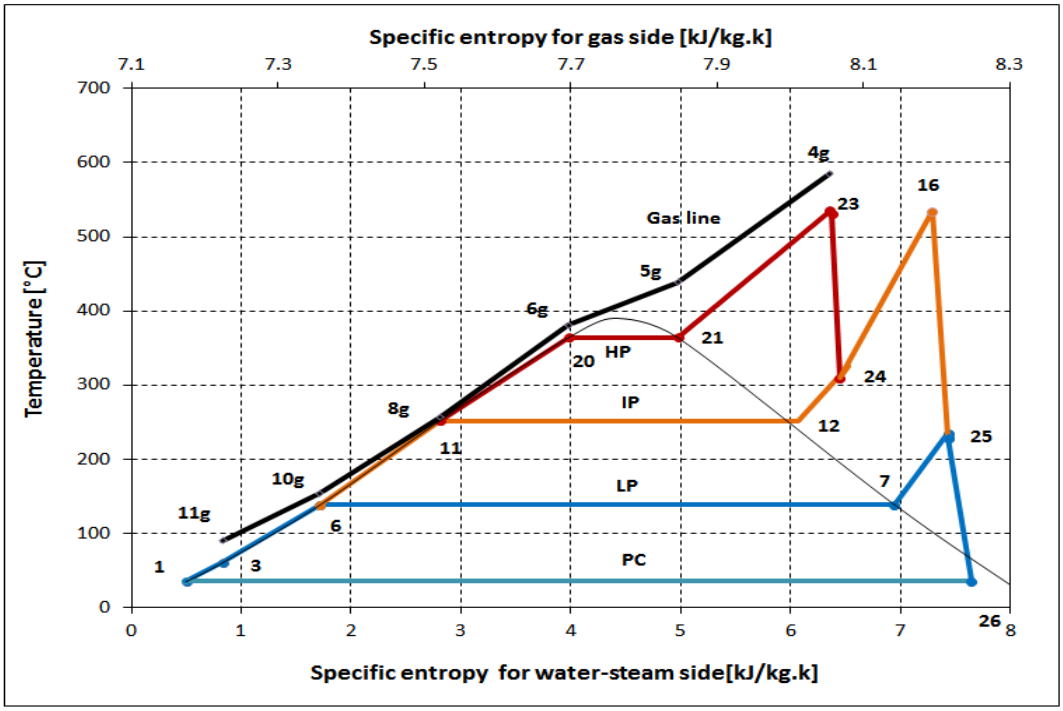

Figure B-1 T-S diagram for triple-pressure HRSG of CCGT for optimize case 3

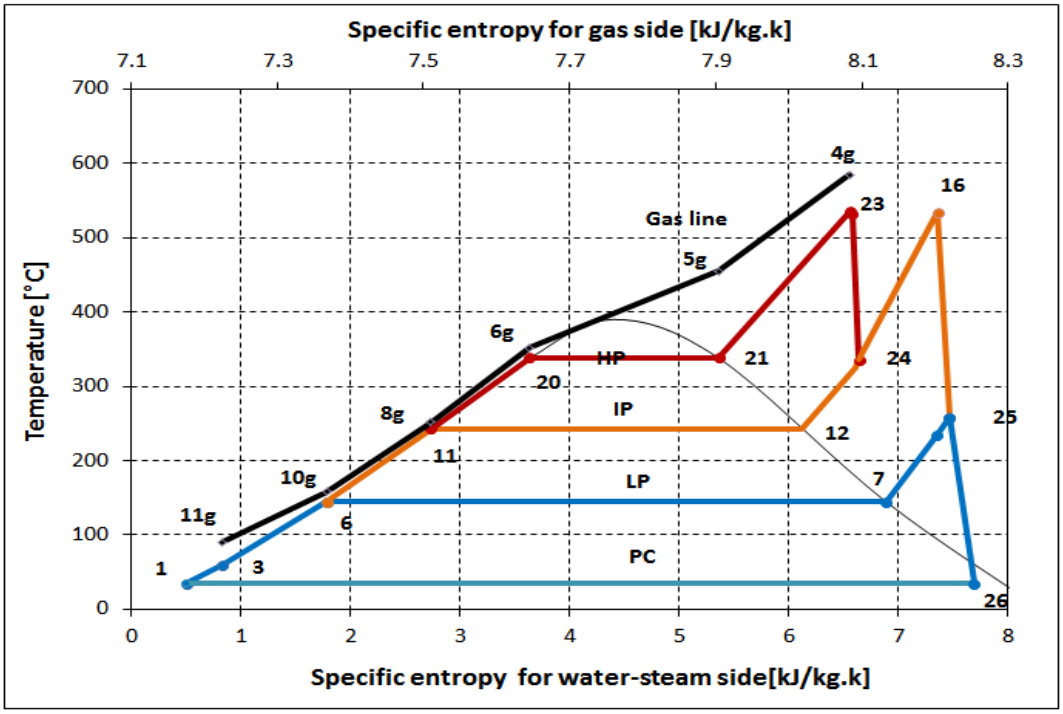

Figure B-2 T-S diagram for triple-pressure HRSG of CCGT for optimize case 2

Appendix C: Block Diagram for CCGT Optimization Computer Code

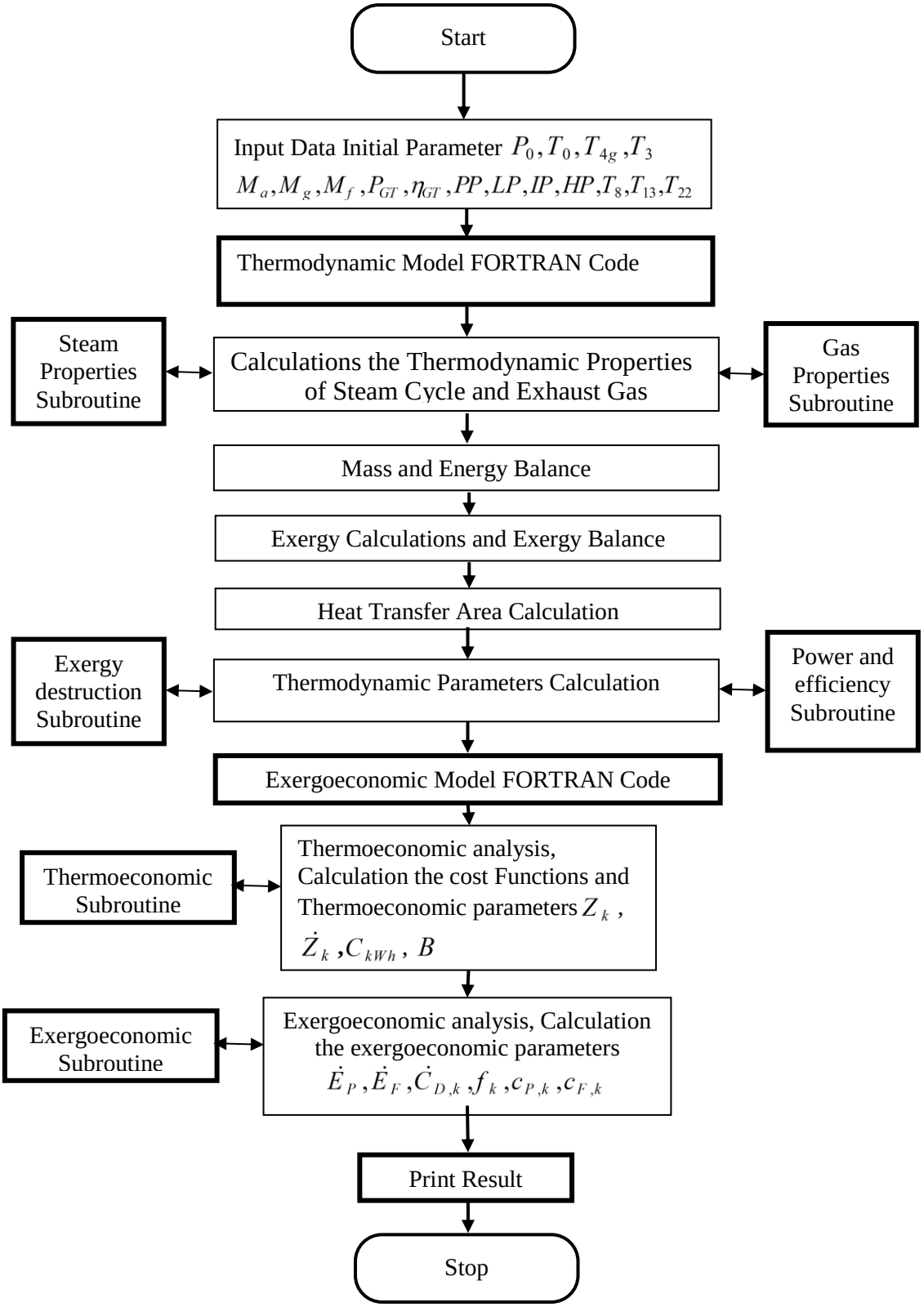

Figure C-3 Block Diagram of Main Program for Combined Cycle Power Plant

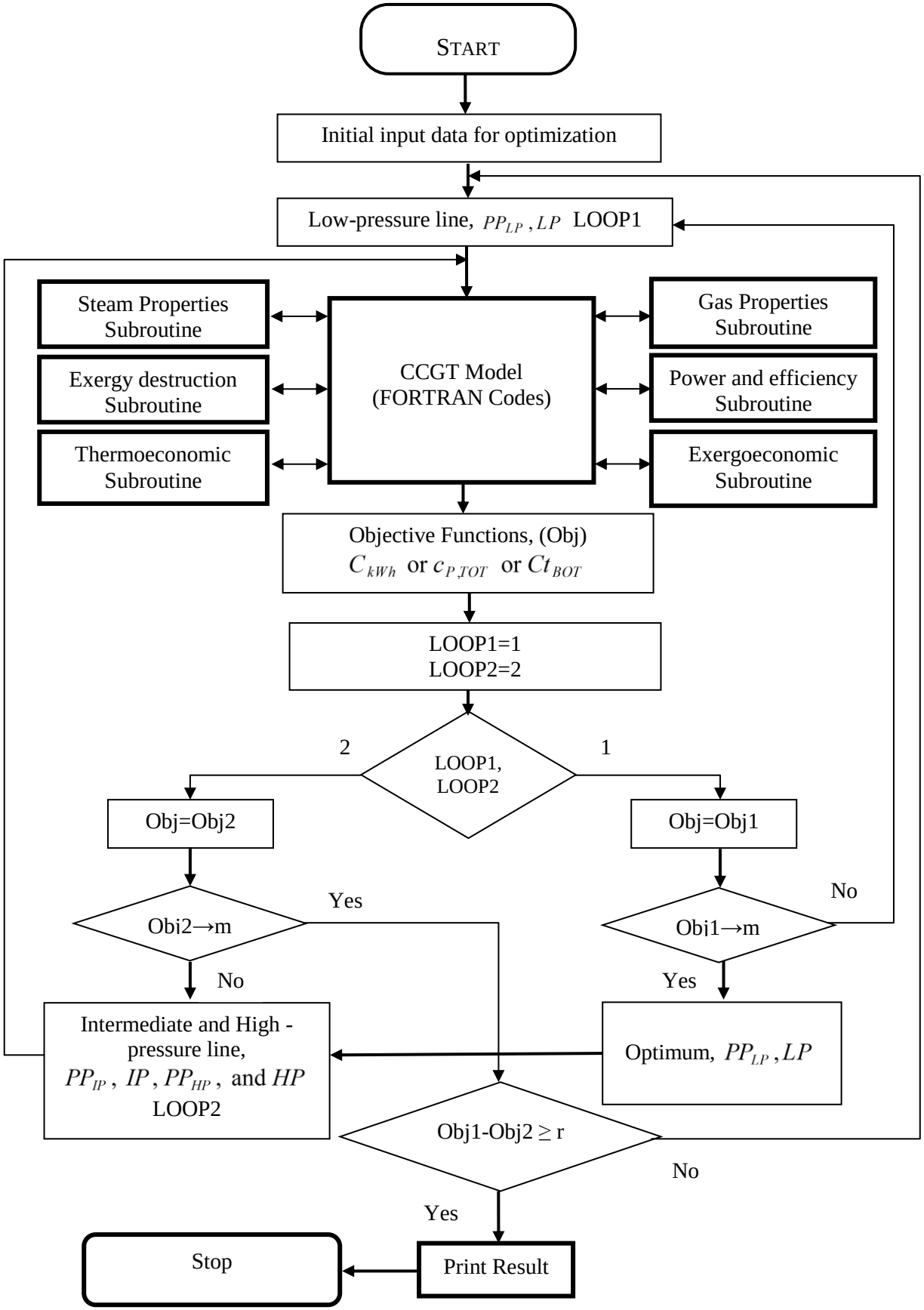

Figure C-4 Flow Chart of Simple optimization Procedure for CCGT Power Plant

Biography of the Author

Mohammed Saleh Mohammed was born on 27 July 1962 in Mosul, Iraq. He attended primary and secondary school (1968-1980) in the same city. He continued his education by taking a Serbian language course in Sarajevo, from January 1981 to July 1981. In July 1984, Mohammed completed an undergraduate study in Air Force Military Academy VTVA (Rajlovac – Sarajevo, Yugoslavia). From 1984-1986 he studied at the Faculty of Mechanical Engineering (University of Belgrade, Yugoslavia), where he obtained Dipl. Ing. (M. Sc.) in December 1986. From 1988 to 2003, he worked as an air force engineer at the Iraqi army. Mohammed was as an assistant lecturer at Mechanical Engineering Department, Faculty of Engineering at Mosul University, Iraq (subjects: Thermodynamic, Laboratory), from 2006 to 2011.

The author continued his academic training at the Faculty of Mechanical Engineering, University of Belgrade. In 2011, he engaged in Ph.D. program at Faculty of Mechanical Engineering, University of Belgrade, where he successfully completed the coursework and passed all the exams required by the doctoral program study. He started the application for doctoral dissertation in 2013, and he plans to defend it in June 2015.

Прилог 1.

Изјава о ауторству

Потписани-а Mohammed Saleh Mohammed M. Sc.

број индекса D68/10

Изјављујем

да је докторска дисертација под насловом

EXERGOECONOMIC ANALYSIS AND OPTIMIZATION OF COMBINED CYCLE POWER PLANTS WITH COMPLEX CONFIGURATION. (Ексергоекономска анализа и оптимизација комбинованих постројења гасне и парне турбине комплексне конфигурације)

- резултат сопственог истраживачког рада,
- да предложена дисертација у целини ни у деловима није била предложена за добијање било које дипломе према студијским програмима других високошколских установа,
- да су резултати коректно наведени и
- да нисам кршио/ла ауторска права и користио интелектуалну својину других лица.

Потпис докторанда

У Београду, _____

_____

Прилог 2.

Изјава о истоветности штампане и електронске верзије докторског рада

Име и презиме аутора Mohammed Saleh Mohammed

Број индекса D68/10

Студијски програм Doktorske Studije

Наслов рада EXERGOECONOMIC ANALYSIS AND OPTIMIZATION OF COMBINED CYCLE POWER PLANTS WITH COMPLEX CONFIGURATION. (Ексергоекономска анализа и оптимизација комбинованих постројења гасне и парне турбине комплексне конфигурације)

Ментор Prof. Dr. Ing. Milan V. Petrović

Потписани/а _____

Изјављујем да је штампана верзија мог докторског рада истоветна електронској верзији коју сам предао/ла за објављивање на порталу **Дигиталног репозиторијума Универзитета у Београду.**

Дозвољавам да се објаве моји лични подаци везани за добијање академског звања доктора наука, као што су име и презиме, година и место рођења и датум одбране рада.

Ови лични подаци могу се објавити на мрежним страницама дигиталне библиотеке, у електронском каталогу и у публикацијама Универзитета у Београду.

Потпис докторанда

У Београду, _____

_____

Прилог 3.

Изјава о коришћењу

Овлашћујем Универзитетску библиотеку „Светозар Марковић“ да у Дигитални репозиторијум Универзитета у Београду унесе моју докторску дисертацију под насловом:

EXERGOECONOMIC ANALYSIS AND OPTIMIZATION OF COMBINED CYCLE POWER PLANTS WITH COMPLEX CONFIGURATION. (Ексергоекономска анализа и оптимизација комбинованих постројења гасне и парне турбине комплексне конфигурације)

која је моје ауторско дело.

Дисертацију са свим прилозима предао/ла сам у електронском формату погодном за трајно архивирање.

Моју докторску дисертацију похрањену у Дигитални репозиторијум Универзитета у Београду могу да користе сви који поштују одредбе садржане у одабраном типу лиценце Креативне заједнице (Creative Commons) за коју сам се одлучио/ла.

1. Ауторство

2. Ауторство - некомерцијално

3. Ауторство – некомерцијално – без прераде

4. Ауторство – некомерцијално – делити под истим условима

5. Ауторство – без прераде

6. Ауторство – делити под истим условима

(Молимо да заокружите само једну од шест понуђених лиценци, кратак опис лиценци дат је на полеђини листа).

Потпис докторанда

У Београду, _____

_____

1. Ауторство - Дозвољавате умножавање, дистрибуцију и јавно саопштавање дела, и прераде, ако се наведе име аутора на начин одређен од стране аутора или даваоца лиценце, чак и у комерцијалне сврхе. Ово је најслободнија од свих лиценци.

2. Ауторство – некомерцијално. Дозвољавате умножавање, дистрибуцију и јавно саопштавање дела, и прераде, ако се наведе име аутора на начин одређен од стране аутора или даваоца лиценце. Ова лиценца не дозвољава комерцијалну употребу дела.

3. Ауторство - некомерцијално – без прераде. Дозвољавате умножавање, дистрибуцију и јавно саопштавање дела, без промена, преобликовања или употребе дела у свом делу, ако се наведе име аутора на начин одређен од стране аутора или даваоца лиценце. Ова лиценца не дозвољава комерцијалну употребу дела. У односу на све остале лиценце, овом лиценцом се ограничава највећи обим права коришћења дела.

4. Ауторство - некомерцијално – делити под истим условима. Дозвољавате умножавање, дистрибуцију и јавно саопштавање дела, и прераде, ако се наведе име аутора на начин одређен од стране аутора или даваоца лиценце и ако се прерада дистрибуира под истом или сличном лиценцом. Ова лиценца не дозвољава комерцијалну употребу дела и прерада.

5. Ауторство – без прераде. Дозвољавате умножавање, дистрибуцију и јавно саопштавање дела, без промена, преобликовања или употребе дела у свом делу, ако се наведе име аутора на начин одређен од стране аутора или даваоца лиценце. Ова лиценца дозвољава комерцијалну употребу дела.

6. Ауторство - делити под истим условима. Дозвољавате умножавање, дистрибуцију и јавно саопштавање дела, и прераде, ако се наведе име аутора на начин одређен од стране аутора или даваоца лиценце и ако се прерада дистрибуира под истом или сличном лиценцом. Ова лиценца дозвољава комерцијалну употребу дела и прерада. Слична је софтверским лиценцама, односно лиценцама отвореног кода.